



**Universitat Autònoma  
de Barcelona**

**ESCOLA D'ENGINYERIA**

**DEPARTAMENT D'ENGINYERIA QUÍMICA**

**Doctorat en Ciència i Tecnologia Ambientals**

***IMPROVING EBPR STABILITY IN WWTPS AIMING AT  
SIMULTANEOUS CARBON AND NUTRIENT REMOVAL:  
FROM MODELLING STUDIES TO EXPERIMENTAL VALIDATION***

**- PhD Thesis -**

**Francisco Javier Guerrero Camacho**

Supervised by

Dr. Juan Antonio Baeza Labat and Dr. Albert Guisasola i Canudas

Bellaterra, Cerdanyola de Vallès, Barcelona

July, 2014



**GENOCOV**

Departament d'Enginyeria Química  
Escola d'Enginyeria  
Universitat Autònoma de Barcelona  
Tel: 93 5811587



ALBERT GUIASOLA I CANUDAS i JUAN ANTONIO BAEZA LABAT, Professors Agregats, del Departament d'Enginyeria Química de la Universitat Autònoma de Barcelona,

**CERTIFIQUEM:**

Que l'enginyer químic FRANCISCO JAVIER GUERRERO CAMACHO ha realitzat sota la nostra direcció, el treball que amb títol "Improving EBPR stability in WWTPs aiming at simultaneous carbon and nutrient removal: from modelling studies to experimental validation" es presenta en aquesta memòria, i que constitueix la seva Tesi per optar al Grau de Doctor per la Universitat Autònoma de Barcelona.

I per a què se'n prengui coneixement i consti als afectes oportuns, presentem a l'Escola de Postgrau de la Universitat Autònoma de Barcelona l'esmentada Tesi, signant el present certificat.

Bellaterra, 3 de juliol de 2014

Dr. Albert Guisasola i Canudas

Dr. Juan Antonio Baeza Labat





*Esta tesis está dedicada  
a mis padres, Paco y Ana M<sup>a</sup>,  
a Ana, Albert y Alex.  
Sois el mejor espejo en el que reflejarme.*

*A quien en sólo 9 días regaló más felicidad que otros en toda una vida...*

*J.L.G*



## Agradecimientos / Acknowledgements

Durante estos años me he preguntado muchas veces cómo deberían ser los agradecimientos de este trabajo. Llegados a este punto, tengo muy claro que deben ser un reflejo de lo que significa una tesis: un documento aparentemente de carácter individual pero que no sería posible sin el trabajo duro y apoyo de mucha gente. A nivel personal, todo este tiempo dentro del grupo DEPURADORAS (GENOCOV) del Departament d'Enginyeria Química ha sido una de las mejores etapas vividas hasta el momento y los responsables de ello son muchas de las personas que enumero a continuación.

Sin ninguna duda, debo y quiero empezar agradeciendo a mis directores, Juan y Albert, todo el tiempo y esfuerzo que han invertido en esta tesis. Sin vuestro apoyo y confianza en todo momento nada habría sido lo mismo. Quiero resaltar sobretudo vuestra manera, tan personal, de investigar y dirigir: con libertad para probar las nuevas ideas que os plateaba y con criticidad ante los resultados obtenidos. De vosotros he aprendido muchas cosas pero sobretudo la importancia que tiene ser riguroso en lo que uno hace. He intentado empaparme de vuestro perfil investigador y sin ninguna duda de las grandes personas que hay detrás.

En segundo lugar, Carlota, la mejor compañera de P-Team que podría haber deseado. Aún recuerdo el primer día que me enseñaste a seguir tus SBRs. Muchas gracias por todo el trabajo realizado (que ha sido mucho) durante este tiempo, sin tu ayuda esta tesis estaría incompleta. Contigo, no sólo he disfrutado investigando el mundo PAO, sino que también he encontrado una gran amiga con la que he vivido congresos, horas de laboratorio, clases de esquí y largas conversaciones. ¡Espero seguir viviendo muuuchos momentos más!

Quiero también agradecer al líder del grupo, Javier Lafuente, todo el apoyo recibido. Me sigue sorprendiendo que, pese a no tener siempre contacto directo con el laboratorio, en todo momento sabe en lo que andas metido. Por su parte, siempre he recibido palabras de ánimo o buenos consejos. Gracias por hacer malabarismos con tu tiempo y para atendernos cuando te pedimos ayuda.

I would also like to thank Professor Krist V. Gernaey and PhD. Xavier Flores Alsina for the opportunity they gave me to spend four month at DTU (Denmark). I learnt a lot from both of you and I felt very comfortable working under your supervision. Albert, Natalia y Paloma, muchas gracias por acogerme durante esos meses y hacerme disfrutar tanto de Copenhagen.

També m'agradaria agrair als doctors Joaquim Comas i Ignasi Rodríguez-Roda del Lequia, la seva col·laboració i esforç durant la simulació dels riscos microbiològics, i a en Ramon Vilanova pel seu suport en el món dels controladors i l'optimització de consignes.

Me gustaría también agradecer a mis compañeros de grupo "Vichy-Català": los Rollings (Torà, Marc F., Albert B. y Jero), Mariàngel, Carlos, Zulk, Isaac, los MECs (Núria, Yolanda, Laura, Ana y Edgar) y los Jefazos (MariE, Julio, Julian y David), por los buenos momentos vividos, las conversaciones científicas, y las que no lo eran tanto, y por echarme una mano cuando la he necesitado. Destacar a los Gaseosos (Mabel y Luís, el King) y las risas, reflexiones sobre modelos matemáticos (de una sola ecuación) o los Kms corridos junto a ellos. Por último, a Edu, que puedo decir de ti..., me vienen a la cabeza tantos momentos que hemos vivido. Sin nuestras divagaciones científicas ("Círculo de la

muerte”), las fast-food apuestas o las tardes escribiendo la tesis - de verdad que se acaba - estos años no habrían sido lo mismo. Eres un gran amigo.

A los alumnos de máster, prácticas o proyecto de final de carrera, de los cuales he supervisado su trabajo, gran parte de él se ve reflejado en esta tesis. He aprendido mucho de vosotros.

He pasado grandes momentos en la QC-1083 y eso es gracias a: Joel, Michele, Ana, Rim, Juliana, Caterina, Erasmo y Tahseen. Con vosotros, el buen clima en el despacho estaba siempre asegurado.

También mencionar a otros doctorandos del departamento, los cuales se han convertido en grandes amigos. Belén “Castillito” por la complicidad y las locuras varias que servían para romper con la rutina. Has hecho que hayan sido unos años muy divertidos. Jose y Carles, vosotros ya veníais de atrás, pero durante la tesis he podido descubrir a dos grandes personas. Espero que esto dure mucho más tiempo. A todos los aldolaseros, lipaseros, compostajeros, tóxicos,..., gracias a muchos de vosotros la ayuda prestada. Lucía D., Sergio, Marcel, Belén P., Marcel·la, Elena (y las conversaciones Vetustas), Carol (2da profesora en esquí), Andrea (x2), Marina, Cesc,... Agradecer también a los “nuevos” investigadores y las risas a la hora de comer. ..y en general a todo el departamento, ha sido un placer compartir este tiempo en tan buen ambiente.

No me gustaría olvidarme de dar las gracias a las personas que me han hecho más fácil el trabajo en el laboratorio. A Pilar por su alegría y energía, a Lorena por su amabilidad y disposición a ayudarnos (y muchos otros momentos frikis), y a Manuel por su ayuda en especial con el irritante cromatógrafo de gases. A la muy trabajadora Margot, aunque sólo coincidiéramos un año, para mí siempre serás de Depuradoras. Gracias a las siempre sonrientes Miriam, Montse, Rosa y Nati por ayudarnos con los trámites burocráticos y administrativos, nunca simples.

Fuera del entorno UAB, tengo la gran suerte de tener amigos que me han apoyado día a día durante este tiempo, pese a no entender en muchas ocasiones mi obsesión por unos bichos llamados PAO. Ana P, Manel, Amanda y Mireia, sois los de siempre y sois especiales. A las chicas NST, Cristina (tantos años juntos y espero que muchos más) y Olaia (¡Suerte con la nueva etapa! Te echaré de menos), gracias por seguir manteniendo vivo todo lo que construimos durante el proyecto. A Alba, por dar alegría a raudales. Me siento afortunado de teneros a todos.

Por último, como no podía ser de otra forma, dar las gracias a mi familia por soportarme a mí y a esta tesis. Cualquier logro conseguido, ahora o en el futuro, siempre será parte de vosotros. Agradecer a mis padres, Ana M<sup>a</sup> y Paco, todo el amor y cariño con el que me han inculcado grandes valores y a luchar por mis sueños siempre con respecto y tenacidad. A Ana, por el apoyo diario, por ser el mejor ejemplo de fortaleza, aun cuando parecía imposible, y porque con una mirada tuya...ya no hace falta más. Daros las gracias a ti y a Alberto por haberme hecho “Tito” de dos sobrinos maravillosos, Javi y Albert. Junto con Inés y María, disfruto como un enano todo el tiempo que paso con ellos. A Alex, por hacerme simplemente feliz sin pedir nada a cambio.

*The author thanks Spanish Government and Universitat Autònoma de Barcelona for the FPU (AP2009-1632) and the PIF PhD grants that allowed to conduct his research and to participate in academic tasks.*

## **Abstract**

Wastewater treatment plants (WWTPs) do not only remove pollutants from wastewater but also they help to maintain healthy ecosystems. In the last decades, water shortage is forcing the governments to become stricter with WWTP effluent discharge as it is reflected in Urban Water Directive (91/271/EC), where a decrease of WWTP effluent pollution arriving to surface waters is pointed out. As a result, research on upgrading of current WWTP by implementing advanced and more efficient treatments is still required. In this sense, considering biological nutrient removal (BNR) in WWTP seems nowadays an obligated short-term aim because it is the most economical and environmental alternative to prevent eutrophication of water bodies meeting simultaneously the increasingly stricter discharge limits. For the case of biological nitrogen (N) removal, it has been widely studied and successfully implemented in numerous WWTPs treating both urban and industrial wastewater. On the other side, the so called Enhanced Biological Phosphorus (P) Removal (EBPR) process is a current topic of interest in wastewater research. However, its full-scale implementation is not widely applied yet in many developed areas. Among other reasons, unpredictable EBPR failures have been reported when is integrated with biological N removal. Most of the reported WWTP configurations for simultaneous C/N/P removal have an aerobic zone before the settler which may result in some nitrate (or nitrite) in the external recycle and consequently, in the anaerobic phase. This presence is one of the most reported causes of EBPR failure in real WWTP and, despite its importance, the causes have not been fully understood yet. A commonly accepted hypothesis is that nitrate presence under anaerobic conditions triggers the competition for the electron donor (i.e. carbon source) between denitrifying ordinary heterotrophic organisms (OHO) and Polyphosphate Accumulating Organisms (PAO). However, the experience in real systems shows that this hypothesis fails to describe the magnitude of EBPR deterioration when the amount of nitrate entering the anaerobic zone is considered.

This thesis aims at understating the underlying mechanisms of such EBPR deterioration due to nitrate presence in the anaerobic phase and studying alternatives to minimise its causes. The research of this thesis has been focused in two different approaches within this framework. On the one hand, the role of the nature of the carbon source and the effect of the operational configuration on EBPR and N-removal interactions have been studied. On the other hand, different control strategies have been assessed to reduce the negative effect of the nitrate recycle to the anaerobic reactor. The use of alternative and economic carbon sources (crude glycerol from biodiesel production) and the optimisation of the control strategies have been deeply evaluated in this part. The utilization of different tools has enabled to approach this problem from different points of view: modelling, microbial analysis, multi-criteria optimisation, multivariate analysis, pilot plant operation and process control. The main achievements of this thesis are next summarised.

Firstly, an anaerobic/anoxic/aerobic (A<sup>2</sup>/O) pilot WWTP (146L) for simultaneous biological N and P removal was operated using different carbon sources that resulted in a PAO-enriched sludge. In this system, nitrate entered in the anaerobic phase through the external recycle and its deleterious effect on EBPR was extensively studied. When the influent was mainly composed by volatile fatty acids (VFA), PAO outcompeted OHO for the carbon source and thus, EBPR did not fail even when treating wastewaters with carbon shortage. Contrary, when more complex carbon sources were used (e.g. sucrose), denitrification in the anaerobic phase was favoured against EBPR because nitrate presence prevented VFA formation from complex substrate fermentation. Different batch test with biomass from the A<sup>2</sup>/O pilot plant and from an anaerobic/aerobic sequential batch reactor (SBR) were performed to study the effect of the operational conditions on EBPR failure. The biomass from this latter plant was never in contact with nitrate. The results from such batch tests concluded that nitrate could be inhibitory for EBPR process, even when VFA were used as a sole carbon source, if PAO sludge has not been previously acclimated to coexist with nitrate.

In the second part of the thesis, different approaches to minimise the nitrate inlet in the anaerobic phase were developed and analysed. On this context, it was studied how the setpoint optimisation of the conventional control loops implemented in a WWTP (ammonium control in aerobic reactors or anoxic nitrate concentration) can improve the operation in terms of not only reducing the running costs but also ensuring low effluent discharges and low risks of developing microbiology-related failures (bulking or rising sludge). Two different objective functions were used for setpoint optimisation: a single cost function that translates the effluent quality into monetary units and a multi-criteria function that analyses the different parameters separately. The optimised setpoints favoured P-removal process by reducing the recycled nitrate load to the anaerobic reactor.

Additionally, it was demonstrated that the crude-glycerol (biodiesel byproduct) dosage governed by a simple PI feed-back control could be very useful to prevent nitrate-driven EBPR failure and control effluent P concentration. The added crude-glycerol was, in part, likely fermented to VFA favouring EBPR and the rest was also used by denitrifying organisms (OHO and DPAO) to remove the nitrate recycled. This dual effect of crude glycerol provided a stable EBPR process. A biochemical model was developed for describing experimental data and to design a control strategy based on crude-glycerol addition, which was afterwards experimentally validated. In addition, this model was also used to test new control modifications to correct some weaknesses observed during the experimental validation (e.g. control actuation delay). Thus, a feedforward control or controlling anaerobic P concentration were also proved as good alternatives to also reduce nitrate presence. However, it is known that the use of external carbon sources can not be cost-effective at full-scale and thus, a novel control strategy aiming at improving P-removal in a WWTP with carbon-limitation was *in-silico* developed and evaluated. The principle behind this novel approach is that lowering the nitrate entrance to the anoxic reactor would result in more

organic matter available for EBPR. As a result, P-removal was enhanced at expenses of increasing nitrate in the influent (but always below the discharge limits). This novel control strategy was also compared with other control strategies based on carbon or metal (P-precipitation) dosage resulting in similar operational costs and effluent discharges.

Finally, it is presented a modelling study with five new benchmark plant design configurations for BNR ( $A^2/O$ , Bardenpho 5-stage, UCT, Modified UCT and Johannesburg) and under different model assumptions (single or two-step nitrification/denitrification and different reactive settler types). This study analysed the importance of these new model extensions to correctly describe the carbon source competition between OHO and PAO. In addition, it was assessed the efficiency of eight control strategies using a multivariate statistical method, the discriminant analysis (DA). This method has the capacity of finding correlations between different treatment alternatives according to different criteria. The outcome of DA was that the plant configuration highly affected the N removal efficiency, while EBPR processes were mostly influenced by the type of control strategy. This study was mostly conducted during a research stay at the Technical University of Denmark (DTU).





## Resum

Les estacions depuradores d'aigües residuals (EDARs) no es troben concebudes tan sols per a eliminar els contaminants presents en les aigües residuals, sinó que també permeten mantenir la bona salut dels ecosistemes en general. En les darreres dècades, la manca d'aigua corrent està forçant a l'Administració a establir límits d'abocament cada cop més restrictius en les EDARs. Aquesta tendència es veu reflectida en la Directiva sobre el Tractament de les Aigües Residuals Urbanes (91/271/EC), en la qual s'estableixen uns valors bastant baixos de contaminants per aquells efluents d'EDARs que són abocats en aigües superficials. Com a resultat, la recerca aplicada a obtenir una millor i més eficient operació a les EDARs actuals continua sent un punt clau. En aquest sentit, la implantació del procés d'eliminació biològica de nutrients (nitrogen i fòsfor) en aquestes instal·lacions és un objectiu a curt termini ja que es considera el procés més rentable i mediambientalment més respectuós per prevenir el procés d'eutrofització dels sistemes aquàtics i per complir, simultàniament, els cada cop més estrictes límits d'abocament. L'eliminació biològica de nitrogen (N) ha estat àmpliament estudiada i implementada en nombroses EDARs, tant urbanes com industrials. Contràriament, per a l'eliminació biològica de fòsfor, P, (procés EBPR) no existeixen encara molts exemples de la seva aplicació a escala real, principalment degut a l'aparició de fallades no esperades quan s'integrà amb l'eliminació biològica de N. Per aquesta raó, el procés EBPR continua sent un tema d'interès en la recerca realitzada actualment. La major part de les configuracions d'EDAR conegudes per a l'eliminació biològica de matèria orgànica (DQO), N i P tenen una zona aeròbia abans del decantador, la qual dona lloc a la presència de nitrat en la recirculació externa i per tant, a la zona anaeròbia. Aquest nitrat a la zona anaeròbia es considera la principal causa d'aquestes fallades i, tot i la seva importància, els motius que les provoquen no es coneixen en profunditat. La hipòtesi més estesa assenyala que la presència de nitrat en condicions anaeròbies provoca la competència per la font de carboni (DQO) entre els organismes desnitrificants i els acumuladors de P (PAO). No obstant això, l'experiència en plantes reals indica que aquesta hipòtesi no és capaç de descriure l'elevada pèrdua real de EBPR, tenint en compte la quantitat de nitrat present a la fase anaeròbia.

Aquesta tesis té com a objectiu entendre els motius subjacents a aquesta perduda d'activitat EBPR i proposar alternatives per tal de minimitzar les seves causes. La recerca s'ha dut mitjançant dos visions diferents. Per una banda, s'ha estudiat el paper que juga la naturalesa de la font de carboni i l'efecte de la configuració de planta en les interaccions entre el processos d'eliminació de P i N. Per una altra banda, s'han avaluat diferents estratègies de control per reduir l'efecte negatiu produït per la recirculació de nitrat a la fase anaeròbia. L'ús de fonts de carboni alternatives i de baix cost (glicerol cru, subproducte de la producció de biodiesel) i la optimització de les estratègies de control van ser aspectes analitzats en profunditat en aquesta part. Per abordar aquesta problemàtica des de diferents punts de vista, s'han utilitzat diferents eines: modelització, anàlisi multi-criteri, anàlisi multivariable,

operació a planta pilot i control de processos. Les principals fites assolides en aquest treball es resumeixen a continuació.

A la primera part de la tesi, es va operar una EDAR pilot (146L) amb configuració anaeròbia/anòxica/aeròbia ( $A^2/O$ ) per a l'eliminació biològica simultània de DQO/N/P, que va donar lloc a un llot altament enriquit en PAO. En aquest sistema, el nitrat arribava a la fase anaeròbia a través de la recirculació externa, de manera que l'efecte negatiu en el procés EBPR es va poder estudiar àmpliament. A partir dels resultats experimentals es va concloure que quan l'afluent era format principalment per àcids grassos volàtils, els PAO van ser capaços de guanyar la competència per la font de carboni. Per l'altra banda, els organismes desnitrificants van ser afavorits quan es tractaren fonts de carboni més complexes (ex. sacarosa). També es varen realitzar diferents experiments en discontinu amb la biomassa del pilot  $A^2/O$  i a partir de la que es va extreure d'un reactor discontinu seqüencial (SBR, 10L), que operava alternant fases anaeròbies/aeròbies, per estudiar com podia afectar la forma d'operació en la pèrdua d'activitat EBPR. La biomassa del SBR mai va estar exposada a nitrat fins que es van realitzar aquest experiment. Els resultats obtinguts concloueren que el nitrat pot tenir un efecte inhibidor en el procés EBPR, tot i que la font de carboni estigui formada únicament per àcids grassos volàtils, si els PAO no han estat prèviament aclimatats a coexistir amb nitrat.

En la segona part de la tesi, es varen estudiar i analitzar diferents propostes per tal de minimitzar l'entrada de nitrat a la fase anaeròbia. Sota aquest context, al es va estudiar com l'optimització de consignes de les estratègies de control aplicades normalment en EDARs (control de la concentració d'amoni als reactors aerobis o control de nitrat a la fase anòxica) podia millorar la seva operació, no només reduint els costos d'explotació, sinó també obtenint un efluent altament clarificat i un baix risc de desenvolupar problemes d'origen microbiològic (creixement excessiu de bacteris filamentosos o desnitrificació al sedimentador secundari). Per a l'optimització de les consignes es varen utilitzar dues funcions objectiu diferents: una funció única que traduïa la qualitat de l'efluent a unitats monetàries i una funció multi-criteri que analitzava diferents paràmetres de manera separada. Com a resultat es va observar que les consignes optimitzades afavorien el procés EBPR reduint la càrrega de nitrat al reactor anaerobi.

D'altra banda, també es va demostrar que la dosificació controlada de glicerol cru (subproducte del biodiesel) a través d'un controlador PI és una alternativa molt útil per a prevenir la pèrdua d'EBPR per presència de nitrat i per a controlar la concentració de P a l'efluent. Part del glicerol cru afegit en la fase anaeròbia va ser, presumiblement, fermentat cap a àcids grassos volàtils afavorint el procés EBPR, mentre que la resta va permetre la desnitrificació del nitrat portat per la recirculació externa. Aquest doble efecte del glicerol cru esdevingué en un procés estable i amb una alta activitat EBPR. Durant aquest estudi, també es va desenvolupar un model bioquímic per a descriure les dades experimentals i per

poder dissenyar el sistema de control de dosificació de glicerol, que va ser posteriorment validat experimentalment. Aquest model també va permetre plantejar algunes modificacions de l'estratègia de control per corregir algunes mancances que es van observar durant la seva validació al pilot (ex. retard en l'actuació del controlador). D'aquesta manera, es va avaluar satisfactòriament la utilització d'un controlador anticipatiu o l'ús de la concentració de P al reactor anaerobi com a variable controlada. Malauradament, l'adició de fonts de carboni externes no és rentable a escala real i, per tant, també es va desenvolupar i avaluar *in-silico* una nova estratègia de control per tal de millorar l'eliminació de P en aigües amb un baix contingut de matèria orgànica. El principi bàsic d'aquesta nova estratègia va ser desviar la DQO disponible cap al procés EBPR, en detriment de la desnitrificació (major concentració de nitrat a l'efluent), però respectant sempre els límits d'abocament. Aquesta estratègia de control també es va comparar amb d'altres basades en l'adició de fonts de carboni o agents precipitants, resultant en uns costos d'operació i una eficiència d'eliminació de nutrients semblants.

Finalment, es va estudiar la importància d'ampliar els models bioquímics existents per millorar la simulació dels processos d'eliminació biològica de nutrients i evitar la predicció de fallades irrealistes del procés EBPR. D'aquesta manera, es va incloure i estudiar conceptes com la nitrificació/desnitrificació en dos passos o la inclusió de sedimentadors reactius. Per aquest estudi, es van utilitzar cinc configuracions estàndard de planta ( $A^2/O$ , Bardenpho 5-etapes, UCT, UCT modificada i Johannesburg). Així mateix, també es va avaluar l'eficiència de vuit estratègies de control aplicant un mètode estadístic multivariable, l'anàlisi discriminant (DA). Aquest mètode va permetre trobar de manera senzilla les correlacions entre diferents estratègies d'operació tenint en compte un gran nombre de criteris. Com a resultat principal d'utilitzar el DA, es va obtenir que la configuració de planta afectava de manera notable en la eficiència de l'eliminació de N, mentre que el procés EBPR estava governat per la estratègia de control implementada. La major part d'aquest treball es va realitzar principalment durant una estància en la Technical University of Denmark (DTU).



## Resumen

Las estaciones depuradoras de aguas residuales (EDARs) no sólo están concebidas para eliminar los contaminantes presentes en las aguas residuales, sino que también permiten mantener la buena salud de los ecosistemas en general. En las últimas décadas, la escasez de agua corriente está forzando a la Administración a establecer límites de vertidos cada vez más restrictivos en las EDARs. Esta tendencia se refleja en la Directiva sobre el Tratamiento de las Aguas Residuales Urbanas (91/271/EC), en la cual se fijan unos valores bastante bajos de contaminantes para aquellos efluentes de EDAR que son vertidos en aguas superficiales. Como resultado, la investigación aplicada a obtener una mejor y más eficiente operación en las EDARs actuales sigue siendo muy necesaria. En este sentido, la implantación del proceso de eliminación biológica de nutrientes (nitrógeno y fósforo) en estas instalaciones es un objetivo a corto plazo ya que se considera el proceso más rentable y medioambientalmente más respetuoso para prevenir la eutrofización de los ecosistemas acuáticos y cumplir, simultáneamente, con los cada vez más estrictos límites de vertido. La eliminación biológica de nitrógeno (N) ha sido ampliamente estudiada e implementada con éxito en numerosas EDARs, tanto urbanas como industriales. Contrariamente, para la eliminación biológica de fósforo, P, (proceso EBPR) no existen aun muchos ejemplos de su aplicación a escala real, principalmente debido a la aparición de fallos inesperados cuando se integra con la eliminación biológica de N. Por esta razón, el proceso EBPR sigue centrando el interés de parte de la investigación realizada actualmente. La mayoría de las configuraciones de EDAR conocidas para la eliminación de materia orgánica (DQO), N y P tienen una zona aerobia antes del decantador, lo cual da lugar a la presencia de nitrato en la recirculación externa y por tanto, en la zona anaerobia. Este nitrato en la fase anaerobia se considera la principal causa de estos fallos y, a pesar de su importancia, los motivos que los desencadenan no se conocen perfectamente. La hipótesis más extendida apunta que la presencia de nitrato en condiciones anaerobias provoca la competencia por la fuente de carbono entre los organismos desnitrificantes y los acumuladores de P (PAO). Sin embargo, la experiencia en plantas reales indica que esta hipótesis no es capaz de describir la elevada pérdida real de EBPR, considerando la cantidad de nitrato en la fase anaerobia.

Esta tesis pretende estudiar los motivos subyacentes a esta pérdida de actividad EBPR y proponer alternativas para minimizar sus causas. La investigación realizada se ha llevado a cabo mediante dos enfoques diferentes. Por un lado, se ha estudiado el papel que juega la naturaleza de la fuente de carbono y el efecto la configuración de planta en las interacciones entre los procesos de eliminación de P y N. Por otro lado, se evaluaron diferentes estrategias de control para reducir el efecto negativo producido por la recirculación de nitrato a la fase anaerobia. El uso de fuentes de carbono alternativas y de bajo coste (glicerol crudo, subproducto de la producción de biodiesel) y la optimización de las estrategias de control fueron aspectos evaluados en profundidad en esta parte. Para abordar esta problemática desde diferentes puntos de vista, se han utilizado diferentes herramientas: modelización,

análisis microbiológicos, optimización multi-criterio, análisis multivariable, operación en planta piloto y control de procesos. Los mayores logros conseguidos se resumen a continuación.

En la primera parte de la tesis, se operó una EDAR piloto (146L) con configuración anaerobia/anóxica/aerobia ( $A^2/O$ ) para la eliminación biológica simultánea de DQO/N/P, que resultó en un lodo altamente enriquecido en PAO. En este sistema, el nitrato llegaba a la fase anaerobia por medio de la recirculación externa, de modo que su efecto negativo en el proceso EBPR pudo ser ampliamente estudiado. A partir de los datos experimentales se concluyó que cuando el afluente estaba formado principalmente por ácidos grasos volátiles, los PAO eran capaces de ganar la competencia por la fuente de carbono. Por el contrario, los organismos desnitrificantes eran favorecidos cuando se trataban fuentes de carbono más complejas (ej. sacarosa). Además, se realizaron diferentes experimentos en discontinuo con biomasa del piloto  $A^2/O$  y la extraída de un reactor discontinuo secuencial (SBR, 10L), que operaba alternando fases anaerobias/aerobias, para estudiar cómo podía afectar el modo de operación en la pérdida de actividad EBPR. La biomasa del SBR nunca estuvo previamente expuesta a nitrato, hasta los ensayos en discontinuo. Los resultados obtenidos concluyeron que el nitrato puede tener un efecto inhibitorio en el proceso EBPR, incluso utilizando ácidos grasos volátiles como única fuente de carbono, si los PAO no han sido previamente aclimatados a coexistir con nitrato.

En la segunda parte de la tesis, se estudiaron y analizaron diferentes propuestas para minimizar la entrada de nitrato en la fase anaerobia. Bajo este contexto, se estudió cómo la optimización consigna de las estrategias de control aplicadas comúnmente en EDARs (control de la concentración de amonio en los reactores aerobios o control de nitrato en la fase anóxica) podía mejorar su operación, no sólo reduciendo los costes de explotación, sino también obteniendo un efluente altamente clarificado y un bajo riesgo de desarrollar problemas de origen microbiológico (crecimiento excesivo de bacterias filamentosas o desnitrificación en el decantador secundario). Para la optimización de dichas consignas se utilizaron dos funciones objetivo diferentes: una función única que traducía la calidad del efluente a unidades monetarias y una función multi-criterio que analizaba diferentes parámetros de manera separada. Como resultado se observó que las consignas optimizadas favorecían el proceso EBPR reduciendo la carga de nitrato al reactor anaerobio.

Por otra parte, se demostró que la dosificación controlada de glicerol crudo (subproducto del biodiesel) mediante un controlador PI es una alternativa muy útil para prevenir la pérdida de EBPR por presencia de nitrato y para controlar la concentración de P en el efluente. Parte del glicerol crudo añadido en la fase anaerobia fue, presumiblemente, fermentado hacia ácidos grasos volátiles favoreciendo el proceso EBPR, mientras que el resto permitió desnitrificar el nitrato aportado por la recirculación externa. Este efecto doble del glicerol crudo hizo posible obtener un proceso estable con una elevada actividad EBPR.

Durante este estudio, también se desarrolló un modelo bioquímico para describir los datos experimentales y para poder diseñar el sistema de control para la adición de glicerol, el cual fue posteriormente validado experimentalmente. Este modelo también permitió plantear algunas modificaciones de la estrategia de control para corregir algunos puntos débiles observados durante su aplicación a escala piloto (ej. retardo en la actuación de controlador). De esta manera, se evaluó satisfactoriamente la utilización de un controlador anticipativo o el uso de la concentración de P en el reactor anaerobio como variable controlada. Desgraciadamente, la dosificación de fuentes de carbono externas no es rentable a escala real y, por tanto, también se desarrolló y evaluó *in-silico* una nueva estrategia de control para mejorar la eliminación de P en aguas con un bajo contenido en materia orgánica. El principio básico de la estrategia de control fue desviar la DQO disponible hacia el proceso EBPR, en detrimento de la desnitrificación (mayor concentración de nitrato en el efluente), pero respetando los límites de vertido. Esta estrategia de control también se comparó con otras estrategias basadas en la adición de fuentes de carbono o agentes precipitantes, dando lugar a unos costes de operación y eficiencia de eliminación de nutrientes similares.

Finalmente, se estudió la importancia de extender los modelos bioquímicos existentes para mejorar la simulación de procesos de eliminación biológica nutrientes y evitar la predicción de fallos irreales en el proceso EBPR. De este modo, se incluyeron y estudiaron conceptos como la nitrificación/desnitrificación en dos pasos o la inclusión de sedimentadores reactivos. Para ello se utilizaron cinco configuraciones estándar de planta ( $A^2/O$ , Bardenpho 5-etapas, UCT, UCT modificada y Johannesburgo). Asimismo, también se evaluó la eficiencia de ocho estrategias de control mediante el uso de un método estadístico multivariable, el análisis discriminante (DA). Este método permitió encontrar de manera sencilla las correlaciones entre diferentes modos de operación teniendo en cuenta gran cantidad de criterios. Como resultado principal de utilizar el DA, se obtuvo que la configuración de planta afectaba de manera notable en la eficiencia de eliminación de N, mientras que el proceso EBPR estaba gobernado por la estrategia de control implementada. La mayor parte de este estudio fue realizado principalmente durante una estancia en la Technical University of Denmark (DTU).





## **LIST OF PUBLICATIONS AND AUTHOR'S CONTRIBUTIONS**

1. Guerrero, J., Guisasola, A., Vilanova, R., Baeza, J.A., 2011. **Improving the performance of a WWTP control system by model-based setpoint optimisation.** Environmental Modelling and Software 26, 492-497.

*Author's contribution:* Control strategies and evaluation criteria analysis implementation, optimisation process, simulation campaigns, writing research paper and preparation of the oral presentation. The original model was developed by Baeza, J.A. Research supervision, discussion of experimental design and results, writing and editing contribution from other authors. A preliminary version of this paper was presented in 10<sup>th</sup> IWA conference on instrumentation, control and automation (ICA), 14-17 June 2009, Cairns, Australia.

2. Guerrero, J., Guisasola, A., Baeza, J.A., 2011. **The nature of the carbon source rules the competition between PAO and denitrifiers in systems for simultaneous biological nitrogen and phosphorus removal.** Water Research 45, 4793-4802.

*Author's contribution:* Experimental design, experimental work, model extension/calibration/validation and writing research paper. Research supervision, discussion of experimental design and results, writing and editing contribution from other authors.

3. Guerrero, J., Guisasola, A., Comas, J., Rodríguez-Roda, I., Baeza, J.A., 2012. **Multi-criteria selection of optimum WWTP control setpoints based on microbiology-related failures, effluent quality and operating costs.** Chemical Engineering Journal 188, 23-29.

*Author's contribution:* EBPR and nitrite inclusion in the model, optimisation process, simulation campaigns, writing research paper and preparation of the oral presentation. Comas, J. and Rodríguez-Roda, I. provided the MATLAB script for microbiology-related failures analysis. Research supervision, discussion of experimental design and results, writing and editing contribution from other authors. A preliminary version of this paper was presented in IWA WaterMatex 2011 Symposium, 20-21 June 2011, San Sebastian, Spain.

4. Guerrero, J., Tayà, C., Guisasola, A., Baeza, J.A., 2012. **Understanding the detrimental effect of nitrate presence on EBPR systems: effect of the plant configuration.** Journal of Chemical Technology and Biotechnology, 1508-1511.

*Author's contribution:* Experimental design, experimental work, writing research paper and preparation of the oral presentation. Equal contribution with Tayà, C. in experimental tasks and in the results discussion. Research supervision, discussion of experimental design and results, writing and editing contribution from other authors. A preliminary version of this paper was presented in Small Water and Wastewater Systems and 4<sup>th</sup> Conference on Decentralized Water and Wastewater International Network, 18-22 April 2011, Venice, Italy.

5. Guerrero, J., Tayà, C., Guisasola, A., Baeza, J.A., 2012. **Glycerol as a sole carbon source for enhanced biological phosphorus removal.** Water Research 46 (9), 2983-2991.

*Author's contribution:* Experimental design, experimental work and writing full paper. Equal contribution with Tayà, C. in experimental tasks and in the results discussion. Research supervision, discussion of experimental design and results, writing and editing contribution from other authors. Part of this paper was presented in Nutrient Removal and Recovery (NRR), 23-25 September 2012, Harbin, China.

6. Tayà, C., Guerrero, J., Guisasola, A., Baeza, J.A., 2013. **Methanol-driven enhanced biological phosphorus removal with a syntrophic consortium.** Biotechnology and Bioengineering 110(2), 391-400.

*Author's contribution:* Experimental design, experimental work and writing full paper. Equal contribution with Tayà, C. in experimental tasks and in the results discussion. Research supervision, discussion of experimental design and results, writing and editing contribution from other authors. Part of this paper was presented in Nutrient Removal and Recovery (NRR), 23-25 September 2012, Harbin, China.

7. Ostace, G.S., Baeza, J.A., Guerrero, J., Guisasola, A., Cristea, V.M., Agachi, P.S., Lafuente, J., 2013. **Development and economic assessment of different WWTP control strategies for optimal simultaneous removal of carbon, nitrogen and phosphorus.** Computers and Chemical Engineering 53, 164-177.

*Author's contribution:* The development of the model to include different control strategies, the optimisation process, the evaluation criteria calculations and the simulation campaigns were carried out by Ostace, G.S., as well as the full paper preparation. My main contribution was related to the results discussion and full-paper editing.

8. Guerrero, J., Flores-Alsina, X., Guisasola, A., Baeza, J.A., Gernaey, K.V., 2013. **Effect of nitrite, limited reactive settler and plant design configuration of the predicted performance of simultaneous C/N/P removal WWTPs.** Bioresource Technology 136, 680-688.

*Author's contribution:* Model extension to include nitrite and new benchmarking configurations, simulation campaigns and writing research paper. Flores-Alsina, X. and Gernaey, K.V. provided the original model MATLAB/Simulink® script. Research supervision, discussion of experimental design and results, writing and editing contribution from other authors.

9. Guerrero, J., Tayà, C., Guisasola, A., Baeza, J.A., 2014. **Eliminación biológica de fósforo: avances en el estudio de su deterioro por recirculación de nitrato.** *TecnoAqua* 6, 58-65.

*Author's contribution:* Experimental design, experimental work, model extension/calibration /validation, writing research paper and preparation of the oral presentation. Equal contribution with Tayà, C. in experimental tasks and in the results discussion. Research supervision, discussion of experimental design and results, writing and editing contribution from other authors. A preliminary version of this paper was presented in X Reunión de la Mesa Española de Tratamiento de Aguas (META 2012), 4-6 October, Almeria, Spain.

10. Guerrero, J., Guisasola, A., Baeza, J.A., 2014. **A novel control strategy for an efficient biological phosphorus removal with carbon-limited wastewaters.** *Water Science and Technology*, *In press*.

*Author's contribution:* Model extension, control strategy programming, simulation campaigns and writing research paper. Research supervision, discussion of experimental design and results, writing and editing contribution from other authors. A preliminary version of this paper was presented as an oral presentation in 11<sup>th</sup> IWA conference on instrumentation, control and automation (ICA), 18-20 September 2013, Narbonne, France.

11. Guerrero, J., Guisasola, A., Baeza, J.A., 2014. **Controlled crude glycerol dosage to prevent EBPR failures due to nitrate external recycle.** *Water Research*. *In preparation*.

*Author's contribution:* Experimental design, experimental work, model calibration/validation, control design and implementation, writing research paper and poster preparation. Research supervision, discussion of experimental design and results, writing and editing contribution from other authors. Part of this paper was presented in 4<sup>th</sup> Water Treatment Modelling Seminar (WWTmod), 30 March-2 April 2014, Spa, Belgium.

12. Tayà, C., Guerrero, J., Guisasola, A., Suárez-Ojeda, M.E., Baeza, J.A., 2014. **Assessment of crude glycerol for enhanced biological phosphorus removal: Stability and role of LCFA.** *Water Research*. *In preparation*.

*Author's contribution:* Equal contribution with Tayà, C. in the experimental design, experimental work and in the results discussion. Research supervision, discussion of experimental design and results, writing and editing contribution from other authors. A preliminary version of this paper was presented in 2<sup>nd</sup> IWA Specialist Conference on Eco Technologies for Sewage Treatment Plants (EcoSTP2014), 23-25 June 2014, Verona, Italy.



## Contents

<b>CHAPTER I</b>	<b><i>General Introduction</i></b>	<b>1</b>
1.1.	WATER AND WASTEWATER	3
1.1.1.	Water and human activity: The Blue Gold versus Wastewater	3
1.1.2.	Nutrients in the environment	3
1.2.	ACTIVATED SLUDGE PROCESS FOR BIOLOGICAL NUTRIENT REMOVAL	5
1.2.1.	Biological nitrogen removal	5
1.2.1.1.	Nitrification	6
1.2.1.2.	Denitrification	7
1.2.1.3.	Advanced N removal processes	8
1.2.2.	Biological phosphorus removal	10
1.2.2.1.	Enhanced biological phosphorus removal (EBPR) process	10
1.2.2.2.	The role of the nature of the carbon source in EBPR	12
1.2.2.3.	Glycerol Accumulating Organisms (GAO)	13
1.2.3.	Phosphorus precipitation: Nutrient Recovery	14
1.3.	SIMULTANEOUS N & P BIOLOGICAL REMOVAL: INTERACTIONS ON EBPR	15
1.3.1.	Alternative plant configuration to reduce anaerobic nitrate presence	16
1.3.2.	External carbon addition in the anaerobic phase	17
1.4.	CONTROL & BENCHMARKING FOR PLANT PERFORMANCE EVALUATION	18
1.5.	RESEARCH MOTIVATION AND THESIS OVERVIEW	22
1.5.1.	EBPR background on the group	22
1.5.2.	Research motivations	23
1.5.3.	Thesis overview	24
<b>CHAPTER II</b>	<b><i>Objectives</i></b>	<b>25</b>
<b>CHAPTER III</b>	<b><i>Material and Methods</i></b>	<b>29</b>
3.1.	PILOT PLANT DESCRIPTION	31
3.2.	CHEMICAL AND BIOCHEMICAL ANALYSES	33
3.2.1.	Mixed liquor total suspended solids and volatile suspended solids	33
3.2.2.	Orthophosphate phosphorus	33
3.2.3.	Ammonium nitrogen	33
3.2.4.	Nitrate and nitrite nitrogen	33
3.2.5.	Chemical oxygen demand	33
3.2.6.	Volatile fatty acids	33
3.3.	MICROBIAL ANALYSES	34
3.3.1.	Fluorescence in situ hybridisation (FISH)	34

3.3.1.1. Sample fixation	34
3.3.1.2. Application of samples to slides	35
3.3.1.3. Probe hybridization	35
3.3.1.4. Washing	35
3.3.1.5. Embedding	35
3.3.1.6. Visualisation and quantification	35
3.3.1.7. Probes for FISH analysis	36
<b>CHAPTER IV <i>Improving the performance of a biological nutrient removal WWTP by model-based setpoint optimisation</i></b>	<b>37</b>
4.1. MOTIVATIONS	39
4.2. MATERIAL AND METHODS	40
4.2.1. Plants description	40
4.2.2. Description of the simulated control strategies	43
4.2.3. Plant performance function development	44
4.2.3.1. Operating costs function (OCF)	44
4.2.3.2. Multi-criteria function (MCF)	46
4.2.4. Simulation and optimisation	52
4.3. RESULTS AND DISCUSSION	53
4.3.1. Evaluation of different optimisation methods – Pilot plant I	53
4.3.2. Operational costs function – Pilot plant I	54
4.3.3. Operational costs function versus Multi-criteria function – Pilot Plant II	62
4.4. PRACTICAL IMPLICATIONS	68
4.5. CONCLUSIONS	69
<b>CHAPTER V <i>Elucidating the role of the carbon source nature and the plant configuration on the EBPR failure due to anaerobic nitrate presence</i></b>	<b>71</b>
5.1. MOTIVATIONS	73
5.2. MATERIAL AND METHODS	74
5.2.1. Pilot plant description	74
5.2.2. Batch experiments	77
5.2.3. Model description	78
5.3. RESULTS AND DISCUSSION	79
5.3.1. Feasibility of P-removal in a MLE system	79
5.3.2. Model calibration and validation	82
5.3.3. Simulated case studies: PAO and OHO competition	85
5.3.4. Batch experiments results	87
5.4. CONCLUSIONS	90

<b>CHAPTER VI</b>	<b><i>Reducing EBPR failure due to external nitrate recycling by controlled crude glycerol addition</i></b>	<b>93</b>
6.1.	MOTIVATIONS	95
6.2.	MATERIAL AND METHODS	97
6.2.1.	Pilot plants description	97
6.2.2.	Synthetic wastewater and disturbances	98
6.2.3.	Model description	99
6.2.4.	Confidence interval determination of calibrated parameters	99
6.2.5.	Control loop design	100
6.3.	RESULTS AND DISCUSSION	101
6.3.1.	Pilot plant configuration versus nitrogen disturbances	101
6.3.1.1.	A <sup>2</sup> /O pilot plant	101
6.3.1.2.	Johannesburg pilot plant	104
6.3.2.	Model calibration and validation I	106
6.3.3.	Crude glycerol control loop (CGCL)	108
6.3.4.	CGCL versus nitrogen disturbances: Experimental validation	110
6.3.5.	Model calibration and validation II	115
6.3.6.	Simulation case study I: P-release as controlled variable – CGCL <sub>P-R1</sub>	117
6.3.7.	Simulation case study II: Feedforward improvement	120
6.4.	PRACTICAL IMPLICATIONS	123
6.5.	CONCLUSIONS	124
<b>CHAPTER VII</b>	<b><i>Effect of different model assumptions, plant configurations and control strategies on the C/N/P removal WWTP performance: Benchmark studies I</i></b>	<b>127</b>
7.1.	MOTIVATIONS	129
7.2.	MATERIAL AND METHODS	131
7.2.1.	Wastewater treatment plants configurations under study	131
7.2.2.	Mathematical models	133
7.2.3.	Description of plant performance	134
7.2.3.1.	Operational cost index (OCI)	134
7.2.3.2.	Influent and effluent quality indexes (IQI and EQI)	136
7.2.4.	Control strategies description	136
7.2.5.	Discriminant analysis (DA)	137
7.3.	RESULTS AND DISCUSSION	138
7.3.1.	N removal and EBPR performance under different model assumptions	138
7.3.1.1.	Nitrite as state variable	138
7.3.1.2.	Importance of including nitrite to describe certain scenarios	140
7.3.1.3.	Biological reactions in the secondary settler	142

7.3.1.4. Importance of considering reactive settler under certain operation conditions	144
7.3.2. EBPR behaviour under different plant configurations	150
7.3.3. Effect of carbon addition for the different WWTP configurations	154
7.3.4. Analysis of design configurations/control strategies using discriminant analysis	155
7.3.4.1. Analysis of plant configurations (DA1)	156
7.3.4.2. Analysis of control strategies (DA2)	157
7.4. PRACTICAL IMPLICATIONS	160
7.5. CONCLUSIONS	161
<b>CHAPTER VIII <i>A novel control strategy for efficient biological phosphorus removal with carbon-limited wastewaters: Benchmarking studies II</i></b>	<b>163</b>
8.1. MOTIVATIONS	165
8.2. MATERIAL AND METHODS	166
8.2.1. Wastewater treatment plant configuration and mathematical model	166
8.2.2. Description of plant performance	167
8.2.3. Principle of the cascade and override P control strategy (COPCS)	167
8.2.4. Conventional control loops on benchmarking studies for P removal	168
8.3. RESULTS AND DISCUSSION	169
8.3.1. COPCS tuning	169
8.3.2. COPCS performance	170
8.4. PRACTICAL IMPLICATIONS	173
8.5. CONCLUSIONS	174
<b>CHAPTER IX <i>General conclusions</i></b>	<b>175</b>
<b>REFERENCES</b>	<b>179</b>
<b>LIST OF FIGURES</b>	<b>198</b>
<b>LIST OF TABLES</b>	<b>204</b>
<b>LIST OF ACRONYMS AND ABBREVIATIONS</b>	<b>206</b>
<b>ANNEX I <i>Activated Sludge Models for simulating biological C/N/P removal</i></b>	<b>209</b>
A.1. BIOLOGICAL MODELS DESCRIPTION	211
A.2. MATLAB-SIMULINK® SIMULATION ENVIRONMENT	225
<b>ANNEX II <i>Glycerol as a sole carbon source for EBPR</i></b>	<b>227</b>
<b>CURRICULUM VITAE</b>	<b>247</b>



# **CHAPTER I**

## General Introduction



## **1.1. Water and Wastewater**

---

### **1.1.1 WATER AND HUMAN ACTIVITY: THE BLUE GOLD versus WASTEWATER**

Water is a vital resource for human life and, in the last years, its availability is extremely low in our planet. Although about 70.0% of the Earth is covered by water, only 3.0% of that is considered freshwater (97.0% is salt water). This freshwater has a volume of 35.2 million cubic kilometres: 69.5% glaciers, 30.1% groundwater, 0.3% surface (directly accessible for humans) and 0.1% atmospheric water (UNESCO 2006). In addition to this, it is important to consider that 12% of the world population consumes 85% of human accessible water due to water resources are deficiently distributed among human population. A billion of people has no access to clean drinking water. Hence, water is considered one of the most important causes of poverty and it has been defined in many cases as the “Blue Gold” (UNESCO 2012).

The human activity and its effects on environment also contribute to unbalance even more such water distribution. For example, the global climate change is favouring the combination of lower precipitation and higher evaporation in many regions reducing water quantities in rivers, lakes and groundwater while water pollution increases (Alley *et al.*, 2007). As a result, the wise use of water, the water recycle and the wastewater treatment are becoming more and more critical points on water management.

Regarding wastewater, it can be defined as a combination of the liquid or water-carried wastes removed from residences, institutions and commercial or industrial establishments, together with groundwater, surface water and storm water (Metcalf and Eddy, 2003). The main pollutants are pathogens and microbial contaminants, organic matter, nutrients (nitrogen and phosphorus), salinization, acidification, heavy metals, toxic organic compounds or micro-organic pollutants and inorganic suspended particles. It is known that natural systems have high intrinsic capacity for removing some of these species, which was more than enough to avoid pollution by human rejections in the past. Nevertheless, the current increasing water demand due to population growth and the high load of contaminants going to the environment may exhaust freshwater resources in the next century (UNESCO, 2005). Consequently, research on developing new and more efficient wastewater treatments to improve water quality before its discharge on natural ecosystems is constantly conducted.

### **1.1.2 NUTRIENTS IN THE ENVIRONMENT**

The availability of nutrients in aquatic ecosystems is essential for life. Among all nutrients, nitrogen (N) and phosphorus (P) are by far the most limiting factors. Their presence in water is usually balanced through natural cycles between their organic and inorganic sources and their accessible mass is theoretically closed to the requirements of the ecosystem. Unfortunately, anthropogenic activity also unbalances this natural equilibrium by introducing large inputs of both N and P in the ecosystem. The main nutrient loading to

surface water in Europe comes from households (food, detergents, urine or human excreta) and industrial activities (Petersen and Werner, 2005). Moreover, agriculture (soil erosion, mineral fertilizers and animal manure) also contributes significantly. The outcome of this unbalanced equilibrium in the nutrient cycles is known as eutrophication of the water bodies. The eutrophication is defined as the excessive growth of plants and algae due to high concentration of nutrients in the water, which generates numerous changes in the water ecosystems with negative effects, i.e. loss of plant and animal species because the dissolved oxygen depletion and transparency reduction, toxins production by some algae species and impossibility to use water for human consumption. For solving this problem, efforts must be focused in reducing the pollution in origin, developing new removal treatments processes to diminish wastewater nutrient content and in applying stricter discharge limits polices. In the last decades, industrial and sewages discharges in sensitive areas are regulated by legislation in order to control nutrient pollution in water ecosystems: Urban Wastewater Treatment Directive (Council Directive 91/271/EEC) and Nitrate Directive (Council Directive 91/676/EEC). Table 1.1 summarizes the maximum discharge limits for urban wastewater treatment plants (WWTP) to sensitive areas. Based on this limits, Real Decreto 509/1996 fixed N restrictions in Spanish urban WWTP.

**Table 1.1** Discharge requirements for N and P in urban WWTP to eutrophication sensitive areas by Council Directive 91/271/EEC. One or both parameters may be applied depending on local situation. Total nitrogen = total Kjeldahl nitrogen (organic and ammonium nitrogen), nitrate nitrogen and nitrite nitrogen. \* p.e. population equivalent

Parameter	Population (p.e.*)	Concentration (mg·L <sup>-1</sup> )	Minimum reduction (%)
Total nitrogen	10 000-100 000	15,0	70-80
	>100 000	10,0	
Total phosphorus	10 000-100 000	2,0	80
	>100 000	1,0	

For industrial wastewater, Decret 130/2003 (Generalitat de Catalunya) set the nutrient discharge limits in Catalonia at:

**Table 1.2** Discharge limits for industrial wastewater by Decret 130/2003.

	Parameter	Concentration (mg·L <sup>-1</sup> )
N	Ammonium nitrogen	60
	Total Kjeldahl nitrogen	90
	Nitrate nitrogen	100
P	Total phosphorus	50

Moreover, the Water Framework Directive 2000/60/EC fixed an ambitious plan to protect and restore aquatic ecosystems as a basis for ensuring the long-term sustainable use of water for people, business and nature. The key objective fixed was to achieve “good status” for all water bodies by 2015. Nowadays in Spain, only the plan of the river basin district of Catalonia has adopted and reported such “good status” (COM 2012/670).

## 1.2. Activated sludge process for biological nutrient removal

The activated sludge (AS) process is the best documented and most widely used process for biological wastewater treatment. Since its development by Arden and Lockett in 1914, it has gained more and more importance for the treatment of municipal and industrial wastewater. This is mainly due to the high versatility of the process to treat different influent compositions ensuring stringent effluent criteria.

The typical AS system consists of at least one aerobic reactor for biological organic matter oxidation, followed by a solid separation stage (sedimentation tank or filtration units) where the sludge is separated from the treated water. The AS is a suspended growth process that maintains a high population of microorganisms (biomass) in biological reactors by means of sludge recycling from the solid separation step. The inclusion of non-aerobic parts has increase the adaptability of these systems by performing biological nutrient removal (BNR) processes what in turns has allowed meeting increasingly discharge limits. Anoxic phases led the system to perform denitrification of nitrate or nitrite aerobically generated and anaerobic phases enable biological P removal. Further information about AS systems and their implementation in real WWTP can be found in general books as Grady *et al.* (1999), Metcalf and Eddy (2003), Henze *et al.* (2008) or EPA (2010).

### 1.2.1. BIOLOGICAL NITROGEN REMOVAL

Biological N removal in AS systems is conventionally based on two main separated but complementary processes called nitrification and denitrification (Figure 1.1).

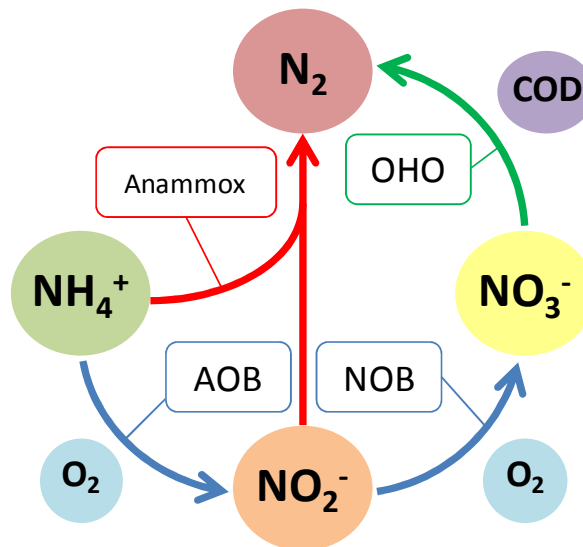
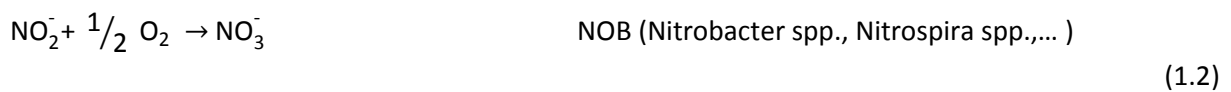
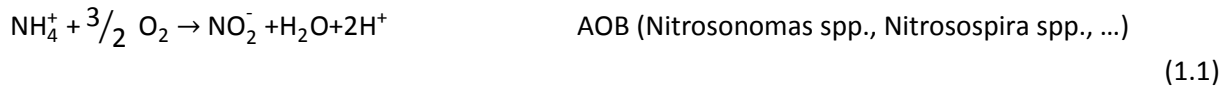


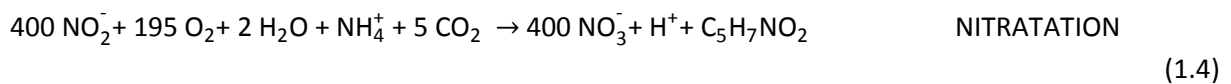
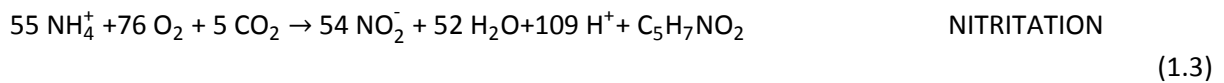
**Figure 1.1** Biological transformations in the N cycle. Blue and green arrows represent the conventional nitrification and heterotrophic denitrification process, respectively. The Anammox process is presented in red arrows.

### 1.2.1.1. Nitrification

Nitrification in AS systems is defined as the biological oxidation of the ammonium present in wastewater to its most oxidized form (nitrate). In AS systems, this process is performed by two different nitrifying bacteria communities and thus, nitrification is generally considered as a two-step process. Ammonia Oxidizing Bacteria (AOB) firstly oxidise ammonium to nitrite (nitritation, Equation 1.1) and Nitrite Oxidizing Bacteria (NOB) perform nitrate formation (nitrataion, Equation 1.2). The nitrification process has the following stoichiometric equations (Wiesmann, 1994):



If the synthesis of new bacteria is considered (assuming that the empirical formulation of bacterial cells is  $\text{C}_5\text{H}_7\text{NO}_2$ ), the above equations are modified as follows (Haug and McCarty, 1972):



It is important to take into account that nitrification is a process highly affected by different environmental factors: temperature (Metcalf and Eddy, 2003), pH (Metcalf and Eddy, 2003), free ammonia (FA) and free nitrous acid (FNA) concentration (Anthonisen *et al.*, 1976; Kim *et al.*, 2006; Torà *et al.*, 2010) or the lack of inorganic carbon presence (Wett and Rauch, 2002; Guisasola *et al.*, 2007a; Torà *et al.*, 2010; Ganigué *et al.*, 2012).

Current knowledge on nitrification process has attributed to the nitritation step the majority of nitrous oxide ( $\text{N}_2\text{O}$ ) and nitric oxide (NO) emissions detected in WWTP (Kim *et al.*, 2010; Wunderlin *et al.*, 2012). Both compounds have received increasing attention due to the detrimental effects that they can cause as green house gases (GHG) and as a toxic to living organisms. Different studies (Shaw *et al.*, 2006; Rodriguez-Caballero and Pijuan, 2013) reported that AOB is able to denitrify the nitrite produced during nitritation by using ammonium or hydroxylamine ( $\text{NH}_2\text{OH}$ ) as electron donor and resulting in NO and  $\text{N}_2\text{O}$  production. This process is called nitrifier-denitrification and it is a well known mechanism to explain nitrogen oxides emissions especially under low oxygen conditions and at high nitrite concentrations. However, other proposed pathways related with hydroxylamine oxidation

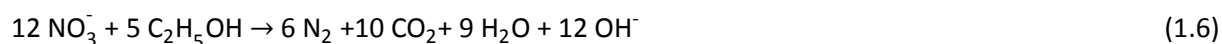
(Schmidt *et al.*, 2004) need further exploration and the combined dynamics/interactions between NO and N<sub>2</sub>O released during nitrification are still unknown. A deeper knowledge of all pathways responsible for nitrogen oxides emissions is then the key to modify, if necessary, the widespread two-step nitrification concept to a multi-step process.

### 1.2.1.2. Denitrification

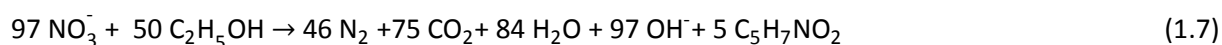
Denitrification is based on nitrate reduction to gaseous nitrogen (N<sub>2</sub>), which is removed from the system leading to wastewater N removal. This process, as also occurred in nitrification, is composed by different steps starting with nitrate reduction to nitrite, followed by nitrite reduction to nitric oxide to nitrous oxide and finally to gaseous nitrogen (Gujer *et al.*, 1999).



The stoichiometry of total denitrification to N<sub>2</sub> when using ethanol as carbon source is (Wiesmann, 1994):



If the synthesis of new bacteria is again considered, the stoichiometry is (Liu *et al.*, 2007):



Conventional denitrification in AS (i.e. heterotrophic denitrification) is mainly performed by one biomass group called ordinary heterotrophic organisms (OHO). Under anoxic conditions, OHO are able to use nitrate or nitrite for organic matter (organic electron donor) oxidation to CO<sub>2</sub> and H<sub>2</sub>O. Although the amount of organic carbon present in urban wastewaters is commonly enough for total N denitrification, some industrial influents have low COD/N ratios limiting this process. Among other possible solutions, a biodegradable external carbon source can be used for these cases (see Section 1.3). As an example, in the north of Europe the addition of methanol is a widespread practice to enhance the denitrification capacity of urban WWTP (Purtschert *et al.*, 1996).

The most implemented WWTP configuration for biological organic matter and N removal is named Modified Ludzack-Ettinger (Figure 1.2). This configuration is composed by an aerobic phase where nitrification takes place and an anoxic phase to perform the denitrification. Two recycling streams are necessary: i) the internal recycle (Q<sub>RINT</sub>), which transports nitrate formed during nitrification to the anoxic phase to be denitrified and ii) the external recycle (Q<sub>REXT</sub>) that allows to maintain biomass levels in the system by recycling the concentrated sludge obtained after settling process.

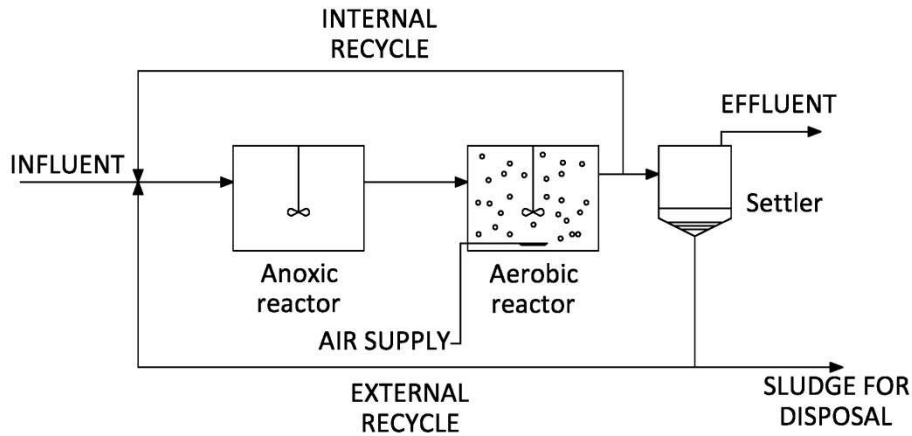
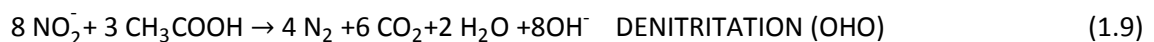


Figure 1.2 Scheme of Modified Ludzack-Ettinger process.

The denitrification process can also contribute to  $N_2O$  and  $NO$  emissions because they are intermediate compounds of nitrate or nitrite reduction to gas nitrogen (Equation 1.5). Although low emissions are related to denitrification for normal WWTP operation in comparison with nitrification due to the absence of active stripping (Ahn *et al.*, 2010), some specific conditions have been pointed out as possible factors to favour  $N_2O$  and  $NO$  accumulation under anoxic conditions. Carbon source limitations, low pH or high nitrite presence are some examples (Thörn and Sörenson, 1996; Itokawa *et al.*, 2007; Zhoue *et al.*, 2008). At present, there is still a lack of studies about understanding the influence of environmental factors and operational configurations on  $N_2O$  and  $NO$  emissions, being then current hot research topics.

### 1.2.1.3. Advanced N removal processes

Novel advanced N removal processes have been developed in the recent years mainly focused in reducing organic carbon necessities for denitrification step. Most of them are based on nitrification and denitrification via nitrite pathway (i.e. shortcut biological N removal). This process has the following stoichiometry (Henze *et al.*, 2008):



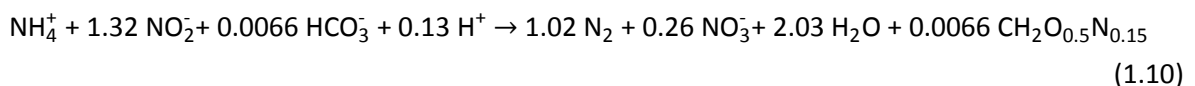
The first step consists in a partial nitrification where ammonium is oxidised to nitrite (nitritation) but not to nitrate. Consequently, total NOB washout is mandatory to ensure nitratation suppression. Several methods have been proposed so far for selecting AOB against NOB, which are based on decreasing growth rate of the NOB over AOB under some specific operational conditions: temperature above  $30^\circ C$  (Bougard *et al.*, 2006), low oxygen aerating conditions (Kuai *et al.*, 1998; Jianlong and Ning, 2004) or higher inhibitory effect for NOB under FA presence (Anthonisen *et al.*, 1976). Although more research is deserved on partial nitrification topic, nowadays it is a well-known process that has been fully studied for



different configurations in our research group: suspended biomass, granular or immobilized biomass systems (Jubany *et al.*, 2008; Bartrolí *et al.*, 2010; Marcelino *et al.*, 2011; Torà *et al.*, 2012; Isanta *et al.*, 2013, Jemaat *et al.*, 2013).

For complete biological N removal through nitrite, a second step for nitrite reduction, autotrophically or heterotrophically, has to be included. Comparing with conventional nitrification/denitrification process, heterotrophic denitrification in combination with nitritation (Equations 1.8 and 1.9) has some advantages since it results in a decrease of 25% on oxygen requirements, around 30-40% less of carbon source for denitrification step and a reduction of 40% in biomass production (Turk and Mavinic, 1987; Van Hulle *et al.*, 2010). In addition, anoxic volume can be reduced because it has been reported that denitrification rates from nitrite are around 1.5-2 times faster than denitrification from nitrate (Peng and Zhu, 2006; Aslan and Dahab, 2008).

Regarding autotrophic denitrification, the anaerobic ammonium oxidation (Anammox) is the most innovative N removal process. Under anoxic conditions, Anammox microorganisms oxidize ammonium to gaseous nitrogen by using nitrite as electron acceptor. Hence, differently to heterotrophic denitrification, for Anammox process only 50% of the ammonium entering in the system has to be previously oxidized to nitrite. The limitation of the alkalinity incoming (Van Dongen *et al.*, 2001; Okabe *et al.*, 2011) or the implementation of a control strategy to control nitrite and ammonium concentrations (Tora *et al.*, 2013) have been reported as suitable methods to generate a stable inlet for Anammox process. As can be observed in Anammox stoichiometry (Equation 1.10), no carbon source is needed during this process and around a 10% of the N treated is converted to nitrate (Strous *et al.*, 1998).



This process presents different advantages (Liu *et al.*, 2008a): i) overall energy savings around 40-50% related to low oxygen requirements, ii) there is no need for carbon source supply and iii) the amount of sludge produced is lower due to low biomass substrate yield of Anammox bacteria. On the contrary, the slow growth rate of such microorganisms, the inhibitory effect of oxygen presence and the complexity to find a proper inoculum enriched in Anammox results in long-term start-up periods. In spite of this, several treatment processes that combine nitritation and Anammox have been already developed: SHARON/Anammox (two sludge system; Hwang *et al.*, 2005), CANON (complete autotrophic N removal over nitrite; Vázquez-Padin *et al.*, 2009), OLAND (oxygen limited autotrophic nitrification and denitrification; Vlaeminck *et al.*, 2010) or NAS (floc-based partial nitritation and Anammox process; Desloover *et al.*, 2011).

Some other autotrophic denitrification processes have been also studied during last decade not based on Anammox bacteria. In these cases, autotrophic denitrification is carried out by using hydrogen ( $H_2$ ) as electron donor (Lee and Rittman, 2002; Rezaia *et al.*, 2007) or sulphur compounds such as  $H_2S$ ,  $S$ ,  $S_2O_3^{2-}$  or  $SO_3^{2-}$  (Batchelor and Lawrence, 1978; Sierra-Alvarez *et al.*, 2007; Fajardo *et al.*, 2012, Mora *et al.*, 2014). As also occurred with Anammox microorganisms, organic carbon source is not needed during denitrification. This process presents the same advantages as Anammox systems over heterotrophic denitrification, however the high alkalinity required during the process and the sulphate production due to the oxidation of sulphur compounds constitute the main drawbacks. Recent studies have developed two-steps systems that combine heterotrophic and autotrophic denitrification (Liu *et al.*, 2009). In such systems, part of the nitrate is initially reduced by heterotrophic denitrification and the rest is afterwards autotrophically denitrified using sulphur components. Thereby, high denitrification efficiency is obtained with a lower external alkalinity demand.

## 1.2.2. BIOLOGICAL PHOSPHORUS REMOVAL

### 1.2.2.1. Enhanced biological phosphorus removal (EBPR) process

P is a key nutrient to trigger off the eutrophication of aquatic systems because its presence stimulates the growth of algae and other photosynthetic microorganism such as toxic cyanobacteria (blue-green algae). Thus, P removal is mandatory to preserve the health of the aquatic ecosystems (Oehmen *et al.*, 2007). The importance of controlling P emissions has been reflected in increasingly stringent regulations that have raised the need of a more efficient WWTP operation by including P removal processes. In this sense, EBPR is considered one of the most efficient, economical and sustainable way to remove P from wastewater (Metcalf and Eddy, 2003; Broughton *et al.*, 2008) since, among other aspects, any chemical addition is necessary. EBPR is based on the AS enrichment with polyphosphate Accumulating Organisms (PAO) by alternating anaerobic and aerobic/anoxic conditions (Figure 1.3).

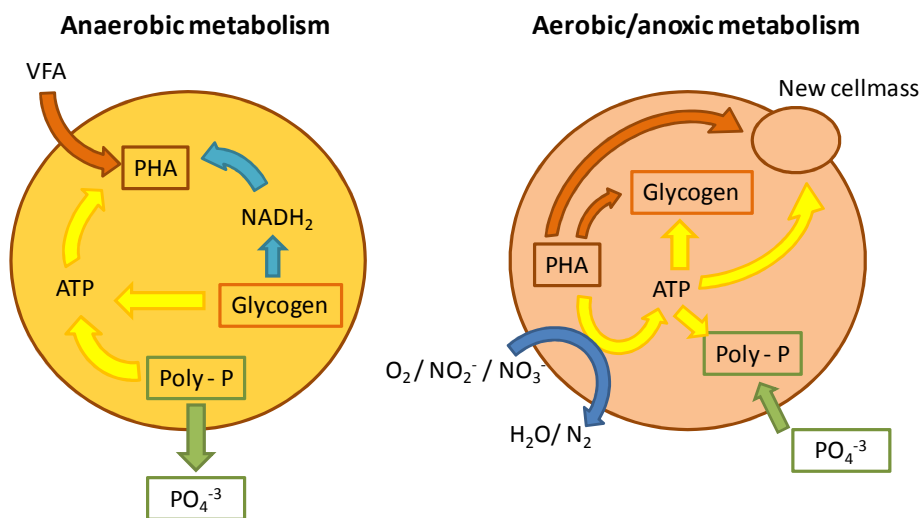


**Figure 1.3** Schematic representation of PAO metabolism.

Under anaerobic conditions, PAOs are able to store fermentation products (i.e. mainly volatile fatty acids, VFA) in form of intracellular poly- $\beta$ -hydroxyalkanoates (PHA). The energy for this process is mostly obtained from the hydrolysis of intracellular stored poly-phosphate (poly-P), resulting in an orthophosphate release to the bulk liquid (Pereira *et al.*, 1996; Yagci *et al.*, 2003). According to some studies, the catabolism of intracellular glycogen also takes place in this process by producing the reduction power (Mino *et al.*, 1987; Smolders *et al.*, 1994; Brdjanovic *et al.*, 1998). This capacity to effectively uptake organic substrate under anaerobic conditions is a selective advantage for PAOs with respect to other microorganisms, which are unable to perform this uptake in the absence of an electron acceptor (e.g. oxygen, nitrate or nitrite). Under aerobic conditions, PAOs use PHA as carbon and energy source for growing and to recover intracellular poly-P and glycerol levels (Arun *et al.*, 1988; Mino *et al.*, 1998). During this aerobic phase, orthophosphate is therefore taken up from the liquid compensating anaerobic P-release. The wasting of sludge after aerobic step ensures net P removal because biomass contains the highest level of poly-P.

Similar performance as under aerobic conditions can be observed under anoxic conditions. When the electron acceptor is nitrate or nitrite instead of oxygen, a fraction of PAOs called denitrifying PAOs (DPAOs) was demonstrated to uptake effectively P linked to denitrification phenomenon (Hascoet *et al.*, 1985 and Comeau *et al.*, 1987). In the recent years, several authors found that PAOs can be divided into two types with different denitrifying capabilities (Flowers *et al.*, 2009). One type (named IA or nitrate-DPAO) was able to couple nitrate and nitrite reduction with P uptake, but the other (named IIA or nitrite D-PAO) could only use nitrite instead of oxygen. Guisasola *et al.* (2009) demonstrated that an enriched nitrite-DPAO sludge failed at using nitrate as electron acceptor even after a long acclimation period. The results of that study were in agreement with the metagenomic analysis that concluded that two DPAO types are physiologically different (Carvalho *et al.*, 2007; He *et al.*, 2007). Most of the research conducted on DPAO metabolism was firstly focussed on using nitrate as electron acceptor (Kuba *et al.*, 1996; Yilmaz *et al.*, 2007; Tayà *et al.*, 2011), while the use of nitrite as potential electron acceptor has been a recurrent research topic in the last years. The recent results obtained have allowed a better knowledge about DPAO metabolism linked to nitrite denitrification and hence, the development of novel treatment processes. For example, a two sludge nitrite-based system for simultaneous C/N/P removal (Marcelino *et al.*, 2011) or the use of nitrite to favour PAO enrichment (Tayà *et al.*, 2013).

From the discovery of the process, finding the bacteria community responsible for EBPR has also been an important research item. *Acinetobacter* was the first organism proposed as responsible for P removal in EBPR (Fuhs and Chen, 1975) and it was believed so until the use of microbial techniques (e.g. fluorescence in situ hybridisation, FISH) showed that a high diversity of phylogenetic groups were involved in EBPR (Wagner *et al.*, 1994; Bond *et al.*, 1999). In fact, Bond *et al.* (1995; 1999) observed that *Rhodocyclus* group from subclass 2 of the *Betaproteobacteria* had a higher significance in phosphate-removing community in

comparison with *Acinetobacter*. Hesselmann *et al.* (1999) named this subclass of *Betaproteobacteria* as “*Candidatus Accumulibacter phosphatis*” (named *Accumulibacter* hereafter). This finding was very useful since it allowed the development of several FISH probes for *Accumulibacter* detection (Hesselmann *et al.*, 1999; Crocetti *et al.*, 2000), which in turn were used in many surveys in full-scale plants from different countries to study PAO presence (Zilles *et al.*, 2002; Kong *et al.*, 2004; He *et al.*, 2005; Wong *et al.*, 2005). In all of these studies, *Accumulibacter* was present in a large abundance (4-22% of all bacteria) concluding that it is an important organism contributing to EBPR in lab and full-scale plants. In the recent years, other species have been also reported to be involved in EBPR process in full-scale EBPR, as *Tetrasphaera*-PAO. Nguyen *et al.* (2011) reported that three clades of *Tetrasphaera*-PAO constituted 18-30% of the total bacterial biomass present in five well-working EBPR plants by using four FISH probe-defined groups. In some of these plants, their abundance was often greater than that of *Accumulibacter*, indicating that *Tetrasphaera*-PAO may also play an important role in full-scale EBPR. Differently to *Accumulibacter*, *Tetrasphaera*-PAO are able to uptake more diverse substrates, such as glucose, and it is believed that they are able to ferment under anaerobic conditions. In addition, no PHA formation has been observed linked to organic carbon uptake under anaerobic conditions (Nguyen *et al.*, 2011). This is a very new research topic that could be very useful for understanding EBPR in full-scale WWTP but more research should be conducted, for example FISH probes still need more experimental validation.

In terms of full-scale EBPR application, it is not fully successful yet although it is a widely studied and mostly understood technology. The main reason is that some bottlenecks have been identified and while these issues do not prevent the technology from being feasible, in many cases they result in reported failures that are very difficult to predict and to solve. Among others, two examples of bottlenecks, which have been studied in this thesis, are next summarised.

#### **1.2.2.2. The role of the nature of the carbon source in EBPR**

The EBPR response to different carbon sources is a research topic that has gained the interest of high amount of the previous research. The EBPR feasibility or deterioration in AS has been related to the nature of the carbon source available during anaerobic phase. Randall *et al.* (1997) proved that the presence of VFA was imperative to obtain high P-removal capacity. The most common VFA present in municipal wastewater are acetic and propionic acid (Chen *et al.*, 2004). Acetic acid initially focused most of the attention due to its positive effect on P-removal (Hood and Randall, 2001) but more recent studies (Pijuan *et al.*, 2004; Oehmen *et al.*, 2006; Vargas *et al.*, 2011) reported that propionic acid could be more suitable substrate for favouring EBPR (i.e. PAO enrichment).

The occurrence of EBPR when using some other organic substrates, different to acetic and propionic acid, has been also highly studied. Glucose, butyrate, ethanol, lactate or sewage

are examples that also resulted in EBPR activity (Satoh *et al.*, 1996; Jeon and Park, 2000; Puig *et al.*, 2008; Pijuan *et al.*, 2009). On the contrary, unsatisfying results have been reported so far when more complex carbon sources, such as waste sludge, starch or glycerol, are directly fed in enriched PAO sludge. For these cases, the use of pre-fermentation units to produce VFA is necessary (Tong and Chen, 2007; Yuan *et al.*, 2010a). However, this solution entails some drawbacks: i) an increase on the investment cost due to a new reaction unit (digester) is required and ii) a more complex operation because of the implementation of a two sludge system. More recently, a promising approach has been proposed in our research group: the use of one sludge syntrophic consortium able to ferment complex carbon sources to VFA, which in turn can be consumed by PAO for EBPR. Hence, suitable EBPR activity was observed by applying this new concept when using glycerol (Guerrero *et al.*, 2012; see Annex II) and methanol (Tayà *et al.*, 2013) as a sole carbon source. It is important to note that both substrates were initially considered inappropriate to be directly used for performing EBPR (Puig *et al.*, 2008; Yuan *et al.*, 2010).

### **1.2.2.3. Glycogen Accumulating Organisms (GAO)**

One of the large known EBPR failures under favourable operation for PAO growth is related to the presence of other organisms that can potentially compete with PAO for the substrate (Liu *et al.*, 1994; Nielsen *et al.*, 1999; Wong *et al.*, 2004). These microorganisms are called Glycogen Accumulating Organisms (GAO) and they also have the capacity to uptake VFA under anaerobic conditions and stored them as PHA (Mino *et al.*, 1995). Differently to PAO, GAO obtain the energy for PHA storage through glycogen hydrolysis which is their sole energy source. Poly-P is not used as energy source in this case (i.e. no P-release) and consequently, no more than the required P for growth is uptaken under aerobic conditions. Hence, the advantages of PAO above other microorganisms are compromised since GAOs can use the same substrate (VFA) anaerobically but without contributing to P removal (Cech and Hartman, 1993; Mino *et al.*, 1998; Liu *et al.*, 1994; Wong *et al.*, 2004). High GAO diversity have been detected, being the *Gammaproteobacteria Candidatus Competibacter phosphatis* (called *Competibacter* hereafter) and the *Alfaproteobacteria Defluviicoccus Vanus* (called *Defluviicoccus* hereafter), the most abundant in full-scale plants. The main difference among them is their affinity for propionic, preferred by *Defluviicoccus*, and for acetic acid, preferred by *Competibacter*.

The selection of PAO over GAO has been fully reported and so, different operational parameters have been indentified to play an important role on this topic. Hence, to favour PAO growth is recommended low COD/P ratio (Mino *et al.*, 1998), high pH (Oehmen *et al.*, 2005), propionic acid instead of acetic acid as VFA source (Pijuan *et al.*, 2004; Oehmen *et al.*, 2006), low dissolved oxygen concentration (Griffiths *et al.*, 2002), low temperature (Brdjanovic *et al.*, 1998), top sludge blanket removal when settling segregation is observed (Winkler *et al.*, 2011) and low sludge age (Whang and Park, 2006). Most recently, the presence of nitrate or nitrite has been also proposed as selecting factor in the PAO-GAO

competition, based on the different denitrifying capabilities of PAO and GAO (Zeng *et al.*, 2003; Carvalho *et al.*, 2007; Wang *et al.*, 2008; Oehmen *et al.*, 2010). As also occurred with PAO (see above), the subgroups of GAO also display varying denitrifying capabilities. Wang *et al.*, (2008) proved that some GAO (*Defluvicoccus* cluster I) are able to reduce nitrate, but not nitrite, while Burow *et al.* (2007) showed that some others (*Defluviicoccus* cluster II) are unable to denitrify. Taking into account such GAO denitrifying capabilities and the fact that *Defluvicoccus* preferred propionic acid as carbon source, Taya *et al.*, (2013) recently demonstrated that a system fed with propionic acid as a sole carbon source and nitrite as a sole electron acceptor led to the GAO washout favouring PAO growth.

### 1.2.3. PHOSPHORUS PRECIPITATION: NUTRIENT RECOVERY

P is a valuable and limited resource that, according to some studies, will be exhausted within 100 years if the current increase rate of demand is not changed (Smith *et al.*, 2009). This fact has raised the need to search new P sources and wastewater seems to be a promising alternative. In particular, some industrial wastewaters, such as swine or cattle wastewater, contain high P and N levels that could be used as an alternative nutrient source. New processes have been proposed not only to remove nutrients from wastewater but also to recover them as raw material that will benefit industry and society. Among others, struvite ( $\text{MgNH}_4\text{PO}_4 \cdot 6\text{H}_2\text{O}$ ) precipitation (Equation 1.11) has been shown as a feasible and cost-effective process for P recovery (Shu *et al.*, 2006) due to it can be directly applied as substitute for agricultural fertilizers. Struvite precipitation occurs naturally, which causes many operational problems in WWTP (Liu *et al.*, 2008b). Fortunately, such properties also provided the pathway for P and N removal together with recovery (Yetilmezsoy and Sapci-Zengin, 2009). Depending on the composition of the wastewater struvite precipitation can be used for N removal (Yetilmezsoy and Sapci-Zengin, 2009), P removal (Jordaan *et al.*, 2010) or both (Huang *et al.*, 2011).



Early studies were focused on the optimisation of solution characteristics, the struvite crystal growth or thermodynamics and kinetics analysis (Battistoni *et al.*, 2002; Hirasawa *et al.*, 2002; Michalowski and Pietrzyk, 2006; Wang *et al.*, 2006) being a high pH and the molar ratios of  $\text{Mg}^{2+}$ ,  $\text{NH}_4^+$  and  $\text{PO}_4^{-3}$  the most important parameters during struvite precipitation (Nelson *et al.*, 2003; Pastor *et al.*, 2008). Williams (1999) showed that pH could be easily increased by  $\text{CO}_2$  stripping, which reduces the purchase cost of adding a base for this aim. Regarding struvite species, high levels of N and P can be easily found in industrial wastewater and only  $\text{Mg}^{2+}$  has to be added, in most of the cases, at the expense of increasing the overall costs. Different studies focused on testing alternative magnesium sources have shown that the use bittern, a waste stream from salt production, is a practical and cheap alternative (Etter *et al.*, 2011; Ye *et al.*, 2011).

All the research conducted on struvite until now have laid a good knowledge about it, which have made this process a more and more widely used treatment in WWTP (Ueno and Fujii, 2001; Yetilmezsoy and Sapci-Zengin, 2009). Nevertheless, there is still some lack of information about the benefits of struvite as a fertilizer, its value on the market or the possible interferences when combined with biological processes, so further research is necessary. In fact, our research group is starting a new line based on combining EBPR together with P recovery as struvite.

### **1.3. Simultaneous N & P biological removal: Interactions on EBPR**

In real WWTP, EBPR has to coexist with biological N removal based on aerobic nitrification and anoxic denitrification processes. Coupling N removal and EBPR is not just as simple as adding an extra anaerobic zone before the anoxic reactor, as in A<sup>2</sup>/O (anaerobic/anoxic/aerobic) configuration (Figure 1.4), to favour PAO growth, since some detrimental interactions between both processes can appear.

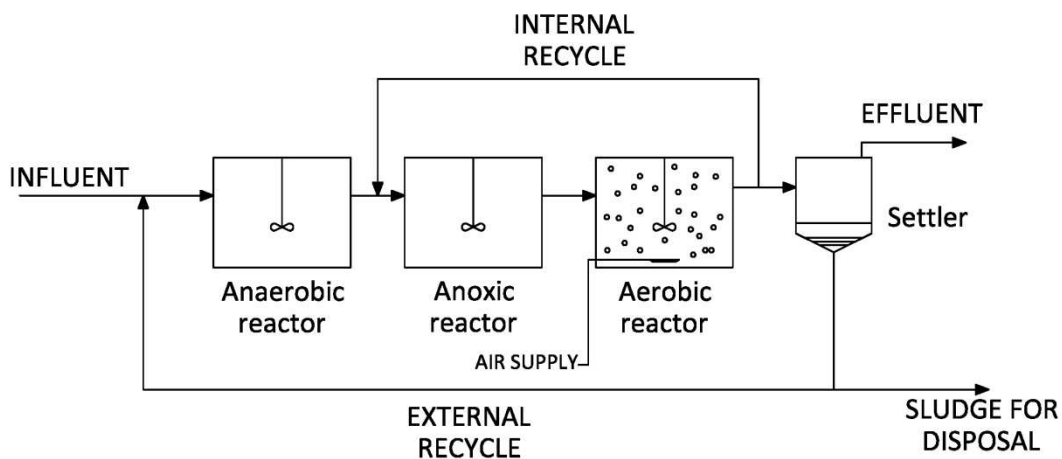


**Figure 1.4** Scheme of A<sup>2</sup>/O process.

Most of the reported WWTP configurations for simultaneous N and P removal have an aerobic zone before the secondary settler which may result in the presence of some nitrate or nitrite (the sum of nitrate and nitrite will be named NO<sub>x</sub> hereafter) in the Q<sub>REXT</sub>. The NO<sub>x</sub> would then enter the anaerobic zone, leading to EBPR failure as reported for many full-scale WWTPs (Henze *et al.*, 2008). Two different hypotheses have been mainly reported so far to describe this failure. On the one hand, the NO<sub>x</sub> presence under anaerobic conditions triggers the activity of OHO that would reduce nitrate using the available COD as electron donor more efficiently than PAO, resulting in less organic substrate for EBPR. In this sense, Cho and Molof (2004) observed that acetic acid was preferentially degraded by denitrifying OHO over PAO, which were outcompeted for the carbon source. Some other studies (Kuba *et al.*, 1994; Patel and Nakhla, 2006) indicated that the presence of nitrate prevented anaerobic P-release

and thus EBPR activity, which only occurred when nitrate concentration was  $<1 \text{ mg NO}_3^- \cdot \text{L}^{-1}$ . On the other hand, Van Niel *et al.* (1998) and Saito *et al.* (2004) linked the detrimental effect of nitrate on EBPR to the presence of some denitrification intermediates (e.g. nitrite or nitric oxide) which would have an inhibitory effect on PAO. More lately, Zhou *et al.*, (2007) and Pijuan *et al.* (2010) observed that nitrite in its protonated form (free nitrous acid, FNA) is more likely the true inhibitor instead of nitrite. In these studies, it was observed a reduction of P-uptake activity around 50% when FNA was up to  $3.6 \cdot 10^{-4} \text{ mg N-HNO}_2 \cdot \text{L}^{-1}$  under aerobic conditions and up to  $2 \cdot 10^{-3} \text{ mg N-HNO}_2 \cdot \text{L}^{-1}$  under anoxic conditions. Nevertheless, the inhibitory effect at such concentrations does not seem to be a strong statement since some acclimation would be possible. In accordance to Guisasola *et al.* (2009), an enriched nitrite-DPAO population can use nitrite as electron acceptor at much higher nitrite levels than those reported as toxic for aerobic P-uptake. Further research on both hypotheses would be very useful to clarify the underlying reasons of EBPR deterioration by anaerobic nitrate presence.

Different solutions have been proposed in the literature, based on the above hypotheses, to reduce the elements that trigger them off. The implementation of alternative plant configurations or the use of an external carbon source are two examples that have been studied in this thesis:

### 1.3.1. ALTERNATIVE PLANT CONFIGURATIONS TO REDUCE ANAEROBIC NITRATE PRESENCE

Among all the possible WWTP configurations, the  $A^2/O$  configuration has been widely applied for municipal WWTP despite the obvious disadvantage that complete denitrification is not possible and some  $\text{NO}_x$  will always enter the anaerobic phase through the  $Q_{\text{REXT}}$  (Henze *et al.*, 2008). Alternative configurations have been designed to reduce the  $\text{NO}_x$  concentration coming to the anaerobic phase and thus, to prevent the EBPR failure (Figure 1.5). The Bardenpho 5-stage (BDP 5-stage) system (Barnard, 1976) improves N removal by adding an extra anoxic–aerobic zone and thus, limits the  $\text{NO}_x$  load in the  $Q_{\text{REXT}}$ . Rabinowitz and Marais (1980) designed the UCT (University of Cape Town) system aiming at preventing the  $Q_{\text{REXT}}$  from entering the anaerobic reactor directly. In this configuration,  $Q_{\text{REXT}}$  is discharged to the anoxic reactor together with the  $Q_{\text{RINT}}$  to denitrify the  $\text{NO}_x$ . A new recycle is then required from the anoxic reactor to the anaerobic reactor to maintain the desired biomass concentration, called here anaerobic recycle ( $Q_{\text{RANAe}}$ ). However, it has been reported for this configuration (Henze *et al.*, 2008) that avoiding  $\text{NO}_x$  presence in  $Q_{\text{RANAe}}$  is critical to achieve a high EBPR activity, but this control is not always possible under full-scale operation. A modification of the UCT (Modified UCT, MUCT) was proposed to avoid this problem and to increase its efficiency. In the MUCT, the  $Q_{\text{REXT}}$  is directed to an anoxic reactor that does not receive the  $Q_{\text{RINT}}$  flow (Figure 1.5), easing the total  $\text{NO}_x$  depletion in the recycling stream to anaerobic phase. On the other hand, most of the denitrification takes place in a second anoxic tank, which receives the  $Q_{\text{RINT}}$  flow. Finally, Osborn and Nicholls (1978) proposed another alternative, the Johannesburg process (JHB). Here, an anoxic reactor is located in the  $Q_{\text{REXT}}$  line so that  $\text{NO}_x$  is predenitrified. The organic electron donor for this process could



be either part of the influent (i.e. influent bypass), an external carbon source addition or stored internal reserves (e.g. PHA).

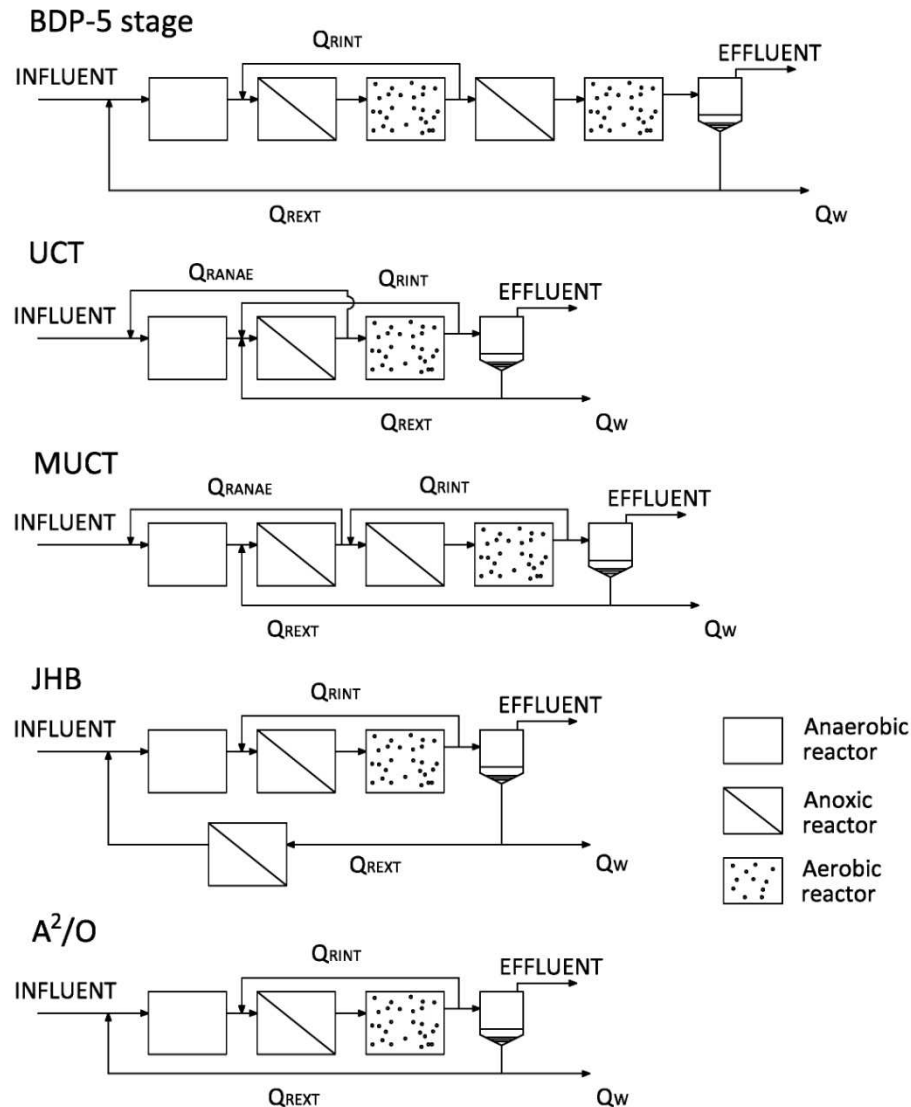


**Figure 1.5** Alternative plant configurations for reducing nitrate inlet in the anaerobic reactor, including A<sup>2</sup>/O configuration.  $Q_w$ : Sludge for disposal (purge).

### 1.3.2. EXTERNAL CARBON ADDITION IN THE ANAEROBIC PHASE

The influent in full-scale WWTP is frequently deficient in readily biodegradable carbon sources (i.e. VFA), which could limit biological P removal process. For these cases, the external addition of a carbon source results as a fast and simple solution to solve COD limitations. Several external carbon sources have been studied (Gerber *et al.*, 1986; Jones *et al.*, 1987; Winter, 1989; Appeldoorn *et al.*, 1992; Isaacs *et al.*, 1994; Hallin *et al.*, 1996). Among those, acetic acid was suggested as the most effective carbon source for improving

both N and P removal. The main problem about the use of VFA is that its purchase is not cost-effective and it also increases the plant carbon footprint (Issacs and Henze, 1995; Yuan *et al.*, 2010). Methanol is another option which is commonly used for N removal due to it is readily biodegradable and provides high denitrification rates (Christensson *et al.*, 1994; Purtschert *et al.*, 1996; Carrera *et al.*, 2003) but it failed when simultaneous N and P removal was intended (Puig *et al.*, 2008). As was commented before, Taya *et al.* (2013) reported that methanol could be used for EBPR but a specific syntrophic consortium should be firstly developed, which could fail when combined with N removal. Further research should be conducted to study the possible interactions when combining the described microbial consortium for methanol together with N removal processes. Puig *et al.* (2008) also demonstrated that ethanol could be used indistinctly for biological N and P removal but an adaptation period was also required.

The on-site production of VFA to increase their content but without an increase on the overall plant costs has been another topic that has gained importance in the recent research studies. One widely used method is based on fermentation of primary sludge or waste from AS systems (Zeng *et al.*, 2006; Zhang *et al.*, 2009; Soares *et al.*, 2010). However, the process is difficult to control for the case of primary sludge fermentation and the reliability of VFA production is sometimes not adequate. For the case of AS waste, its fermentation has some benefits such as a reduction on sludge disposal costs and on the plant overall carbon footprint (Yuan *et al.*, 2010). The only drawback is that high amounts of ammonium and particularly phosphates are released when VFA are generated by fermentation, which could reduce the benefits of VFA production from biomass. In addition to this, the VFA separation from the fermented sludge (i.e. elutriation) is costly and ineffective, since at least 30% of VFA are absorbed in the sludge (Moser-Engeler *et al.*, 1999).

Finally, the utilization of waste materials, that could produce VFA, is a very promising solution to reduce COD competition between OHO and PAO. On this field, crude glycerol from biodiesel production is a good example because it has been reported its use as a proper external carbon source for denitrification (Grabinska-Loniewska *et al.*, 1985; Akunna *et al.*, 1993; Bodík *et al.*, 2009; Torà *et al.*, 2011) and for EBPR with an influent with COD shortage (Guerrero *et al.*, 2012; see Annex II). Unfortunately, as also occurred with methanol, there are currently no studies about crude glycerol dosage for improving EBPR in systems with simultaneous N and P removal.

#### **1.4. Control & Benchmarking for plant performance evaluation**

Stringent legislation for WWTP is a currently top driving force for the development of new treatment technologies as for the optimisation of the existing ones. WWTP can be redesigned to include new treatments or can be upgraded with new control structures. In fact, the utilization of automatic control systems has improved the performance of

numerous WWTP in the past (Ayesa *et al.*, 2006; Benedetti *et al.*, 2010; Cecil and Kozłowska, 2010). For example, single feedback controllers on essential parameters (e.g. DO concentration or recycle flow-rates) have led to better quality effluent in the last decades. However, the efficiency of these is limited by i) the dynamics on the influent or ii) the inherent complexity of the system since control actions applied in one unit can somehow affect posterior subprocesses (Alex *et al.*, 2008). As proposed by Olsson *et al.* (2007), these problems could be overcome by integrating plant-wide control systems with a continuous retuning of the control loops (e.g. via gain scheduling or using adaptive control). Moreover, the high number of variables involved on BNR processes and the multivariable nature of the problem should be also taken into consideration. In the case of model-based design, the development of reliable models has provided tools to facilitate the optimisation of these control systems. For example, the IWA Activated Sludge Model 2d (ASM2d) is a complex kinetic model able to describe biological C/N/P removal processes from wastewater (Henze *et al.*, 1999; 2000). Although this model has a large number of parameters which are difficult to identify due to correlation problems (Machado *et al.*, 2009a), it is able to provide an accurate description of the process with its default parameter values. Finally, another important aspect to consider when designing new control structures should be the best pairing of controlled and manipulated variables (Machado *et al.*, 2009b) to provide better system controllability with fewer operating costs and the most effective wastewater treatment.

Several control strategies have been developed to achieve low effluent concentrations at reasonable operational costs (Baeza *et al.*, 2002; Copp *et al.*, 2002; Nopens *et al.*, 2010) but most of them are only focused on enhancing of C and N removal without paying attention to biological P removal. Such apparent lack of interest can be justified considering the complexity of the EBPR process and the fact that it is not often applied in full-scale WWTP, where P precipitation is the typical process for P removal. On the contrary, the current knowledge gained on EBPR has raised the opportunity of developing new control structures considering simultaneous C/N/P removal (Ingildsen *et al.*, 2005; Machado *et al.*, 2009b; Ostace *et al.*, 2013) that could be employed to solve or reduce some process limitations, for example the detrimental effect of nitrate presence under anaerobic conditions on EBPR. Hence, the improvement of P-removal by designing and implementing novel control strategies deserves more interest.

Once the control strategy is already designed and implemented, another difficulty comes up when evaluating its improvement of the WWTP performance. This point is not a straightforward issue because several indexes must be taken into account. Most of the control strategies reported so far are mainly based on obtaining high effluent quality with the minimal operational cost. For this aim, Vanrolleghem and Gillot (2002) proposed the evaluation of the plant performance with a single cost function based on the operational costs by converting the effluent quality into monetary units. In this case, proper weighing

indexes must be selected to not subordinate the effluent quality to the other operational costs (e.g. electrical costs). Otherwise, an operation with low electrical power consumption could be prioritized instead of a high effluent quality. Multicriteria tools could be very useful avoiding unbalanced weighing indexes since they allow analyse/optimize a system taking into account different criteria, which can be separately evaluated. Different reported studies already applied multi-criteria analysis to evaluate the operational efficiency of different WWTP designs and control strategies (Benedetti *et al.*, 2010; Flores-Alsina *et al.*, 2010).

Along this line of thinking, the evaluation and comparison between different control strategies is also a key issue. This is mainly because there are many variables that affect the overall performance in different WWTP (e.g. the influent conditions, plant configurations or the biological processes occurring in each plant). In addition, the lack of standard evaluation criteria (e.g. regional specific effluent requirements and cost levels) also makes more difficult this task. To avoid comparative problems and to enhance the acceptance of innovating control strategies for the research community, it is important to define a comparative framework in order to analyse all the possible scenarios under unbiased conditions. The Benchmark Simulation Model (BSM) presents a standardised simulation protocol where the simulation and evaluation procedure to study the performance of an urban WWTP is described (Copp *et al.*, 2002; Jeppsson *et al.*, 2007; Nopens *et al.*, 2010; Gernaey *et al.*, 2013). Reactor dimensions, the disturbances to be applied or the evaluation criteria for testing the effectiveness (Table 1.3) of simulated control strategies are presented in BSMs.

**Table 1.3** Benchmarking criteria to evaluate WWTP performance. i: influent and e: effluent.

Criteria	Abbreviation
<i>Influent or Effluent Quality Index</i>	IQI or EQI
TSS concentration	TSS <sub>i or e</sub>
COD concentration	COD <sub>i or e</sub>
BOD <sub>5</sub> concentration	BOD <sub>5, i or e</sub>
TKN concentration	TKN <sub>i or e</sub>
Nitrate concentration	NO <sub>i or e</sub>
Total P concentration	TP <sub>i or e</sub>
<i>Operational Cost Index</i>	OCI
Aeration Energy	AE
Pumping Energy	PE
Mixing Energy	ME
Sludge production	SP
External carbon source dosage	EC

The original benchmark implementation (Copp, 2002), Benchmark Simulation Model No. 1 (BSM1) consists of a 5 reactors AS plant with a non-reactive settler for modelling COD and N removal. Recently, different modifications of the original BSM have been also reported that considered different phenomena of real WWTP operation. For example, Rosen *et al.* (2004) presented a long-term evaluation taking into account yearly temperature variations (BSM1\_LT) and Jeppsson *et al.* (2007) proposed a new plant-wide simulation benchmark (BSM2) by including some other units, such as anaerobic digestion (Figure 1.6). Some limitations were also observed in the initial BSM (Copp *et al.*, 2002) as the evaluation criteria were not very sensitive to the different tested scenarios. The main reason was attributed to the highly loaded system that limits the performance improvement that can be accomplished, for example, by the implementation of active control. Based on these limitations, Nopens *et al.* (2010) proposed some modifications to be adopted for the BSM2: increase of reactor volumes, higher aeration rates for aerobic reactors or changes on influent and recycling streams flow rates. As far as P removal is concerned, Gernaey and Jørgensen (2004) upgraded the BSM1 to include EBPR process for the first time. Currently, other extensions are also being studied to include P chemical precipitation processes (e.g. P recovery as struvite) together with EBPR in the plant-wide operation, the BSM3.

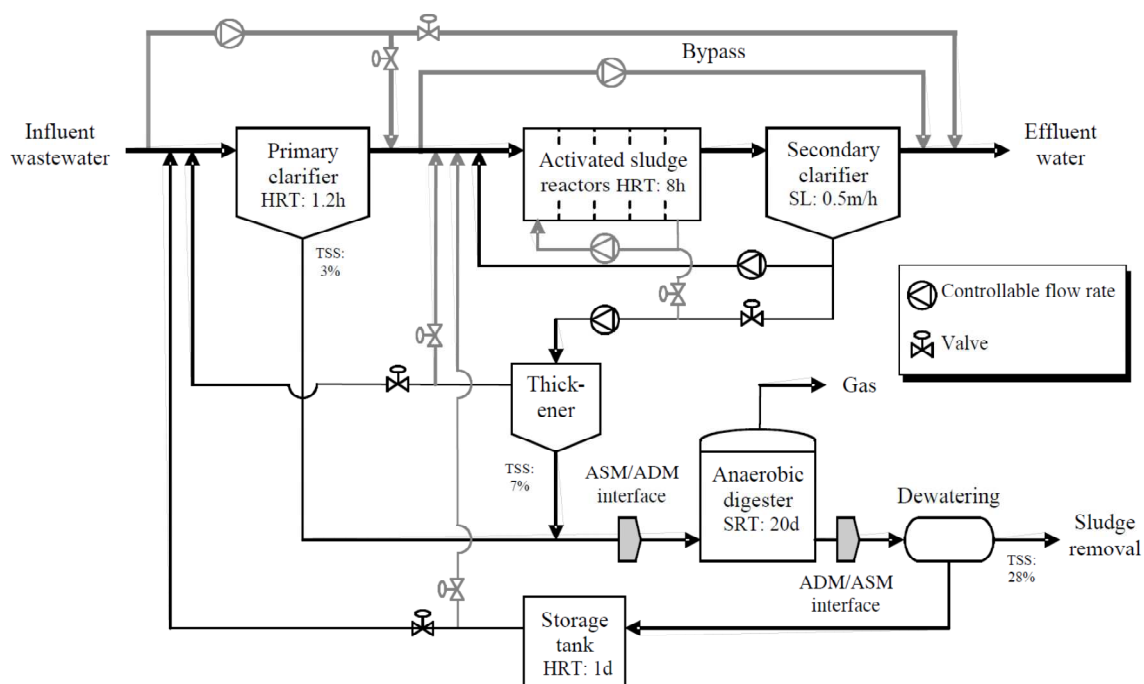


Figure 1.6 Plant layout for BSM2 (Jeppsson *et al.*, 2007).

Regarding BSM criteria for evaluating plant performance, some biological processes not included in the past have recently gained greater importance. For example, the simulated optimal scenario could result in some operating problems of microbiological origin when implemented in real WWTP, mostly related to the final settling step (i.e. development of bulking, foaming or rising sludge) (Jenkins *et al.*, 2003). Comas *et al.* (2008) and Flores-Alsina

*et al.* (2009 a,b) used the textbook knowledge and the operating expertise to expand the existing model to predict the possible occurrence of these microbiology-related problems on COD and N removal WWTP. Although EBPR process was not considered yet, its inclusion in the analysis of possible solid separation problems is necessary since it involves an anaerobic phase that may affect, for example, the presence of filamentous bacteria. On the other hand, the increasing interest in GHG emissions have called for novel approaches to evaluate the performance of new control strategies also quantifying the possible GHG emissions (Corominas *et al.*, 2012; Flores-Alsina *et al.*, 2014). The new knowledge gained on biochemical reactions of GHG production has allowed their inclusion in the traditional models (i.e. Activated Sludge Models, ASM) used to simulate biological WWTP performance: N<sub>2</sub>O and CO<sub>2</sub> emissions quantification (Corominas *et al.*, 2012; Mampaey *et al.*, 2013; Ni *et al.*, 2013) or CH<sub>4</sub> production mainly during anaerobic digestion step (Batstone *et al.*, 2002). As also occurred with microbial risks approach, most of the GHG emissions have been studied in systems for COD and N removal, without including EBPR process. Indeed, there are not studies discussing about N<sub>2</sub>O emissions on continuous EBPR systems. Hence, the integration of both new modelling approaches could be useful to develop a more realistic tool for redesigning plants performing EBPR or for developing new control strategies.

## **1.5. Research Motivations and Thesis Overview**

### **1.5.1. EBPR BACKGROUND ON THE GROUP**

This thesis was framed in one of the research lines of the GENOCOV group (Grup de Tractament Biològic d'Efluent Líquids i Gasosos. Eliminació de Nutrients, Olors i Compostos Orgànics Volàtils) in the Departament d'Enginyeria Química at the Universitat Autònoma de Barcelona. This group was born in the 1990s with the aim to conduct research on improving the existing biological wastewater treatment systems. The thesis here presented is included in the research line of biological wastewater nutrient removal in municipal WWTPs and different PhD theses set the antecedents of the present research. Firstly, Dr. Juan Baeza in his thesis called "Development and implementation of a supervisory system for the management and control of WWTPs" (Baeza, 1999) developed a supervisory control system to improve the operation of a pilot plant with BNR (N and P). Secondly, Dr. David Gabriel was the first one of the group to perform modelling studies about EBPR on a pilot plant in his thesis named "Monitoring and modelling applied to the control of a pilot wastewater treatment plant with nutrient removal" (Gabriel, 2000). Few years later, the research conducted by Dr. Maite Pijuan named "Effect of different carbon sources and continuous aerobic conditions on the EBPR process" (Pijuan, 2004) expanded the knowledge of the group about PAO metabolisms by studying the EBPR response to different organic sources. Additionally, Dr. Guisasaola showed the importance of applying on-line monitoring techniques to supervise EBPR and N removal processes in his thesis named "Modelling biological organic matter and nutrient removal processes from wastewater using

respirometric and titrimetric techniques” (Guisasola, 2005). The theses defended by Dr. Marcos Marcelino and Dr. Mar Vargas named “Biological nutrient removal in advanced SBR systems. Integration of partial nitrification and simultaneous phosphorus and nitrite removal” (Marcelino, 2009) and “Advances in the enhanced biological phosphorus removal process: Use of different electron acceptor and influence of limiting conditions” (Vargas, 2010) also contributed to a better understanding of the PAO activity by linking partial nitrification to EBPR process, the use of nitrite as a sole electron donor (DPAO activity) or long-term permanent aerobic conditions to EBPR on pilot plants. More recently, Dr. Vinicius Cunha Machado defended his thesis titled “Retrofitting analysis for improving benefits of A/O WWTPs considering process control aspects” (Machado, 2012), where a methodology for retrofitting existent Anoxic/Oxic (A/O) WWTP to perform EBPR simultaneously to COD and N removal was developed by also considering process control aspects. That work partly established the starting point for this thesis with respect to simulation studies. Finally, in parallel to the present thesis, Dr. Carlota Tayà, in her PhD studies called “Facing Current Bottlenecks in view of Full-Scale Implementation” (Tayà, 2013), investigated three different approaches related to the occurring issues when EBPR is implemented: i) the negative interactions between P and N removal with PAO-enriched cultures, ii) the use of alternative carbon sources (methanol and glycerol) for EBPR by developing new syntrophic microbial consortiums and iii) the role of nitrite in the competition between PAO and GAO. Some of the results presented by Dr. Tayà were highly helpful for the progress of the present thesis and also complement some studies here presented.

### **1.5.2. RESEARCH MOTIVATIONS**

The integration of EBPR with biological N removal in WWTP for BNR is not a simple issue because it is prone to failure resulting in the deterioration of P removal process. As was commented before, one of the most reported causes of EBPR failure in real WWTP is related to the presence of nitrate under anaerobic conditions and despite its importance, the causes of this failure have not been fully understood yet. A commonly accepted idea is that nitrate presence triggers the competition for the electron donor (i.e. carbon source) between OHO and PAO. However experimental experiences in real systems shows that this hypothesis fails to describe the magnitude of EBPR deterioration when the amount of nitrate entering the anaerobic zone is considered. In addition, although some solutions have been already reported to reduce the entering nitrate, most of them are based on the use of external carbon sources (e.g. acetic acid or glucose) with a consequent increase in operational costs or a redesign of the plant configuration that usually entails a increase of the investment cost due to the requirement of new reactors (e.g. Johannesburg configuration). Taking into account the previous group background, the research motivations of this thesis were:

- i) Studying the underlying mechanisms of EBPR failure due to anaerobic nitrate presence under different operational conditions: effect of plant configuration and effect of the nature of the carbon source. These research objectives motivate the development and

calibration of a nitrification/denitrification model through nitrite to increase the understanding of the studied biological systems.

- ii) Simulation based-design and experimental validation of new approaches to minimise nitrate entering the anaerobic phase: optimised control strategies by using advanced modelling tools and the use of waste materials, such as crude glycerol, as a promising alternative to the conventional external carbon sources.

### 1.5.3. THESIS OVERVIEW

This document is divided into nine chapters. Chapter I, in which this section is included, comprises a general introduction to the topic of the present thesis with a brief literature review of the state of the art. In Chapter II are presented the main objectives of this thesis. The chemical and microbial analyses performed as well as a general description of the pilot plant are showed in Chapter III. The main results of the thesis are presented from Chapters IV to VIII. Chapter IV comprises a simulated-based study about the improvement of the performance of a WWTP with simultaneous C, N and P removal by the setpoint optimisation of the control system. In Chapters V and VI, pilot plant studies are presented: Chapter V demonstrates that the nature of the carbon source rules the competition between OHO and PAO when nitrate was present under anaerobic conditions and Chapter VI shows the applicability of controlled crude glycerol dosage to reduce EBPR failure due to external nitrate recycling. Chapter VII and VIII comprise the benchmark studies results. Chapter VII describes a model-based study of five new benchmark design plant configurations for BNR that were simulated and evaluated under different model assumptions. In addition, several control strategies were proposed in the benchmark framework and were evaluated by using multivariable statistical methods, concretely discriminant analysis. Part of Chapter VII was carried out during a research stay (four months) at the Technical University of Denmark (DTU). In Chapter VIII, the development and the *in silico* evaluation of a novel control strategy aiming at successful biological P removal in an A<sup>2</sup>/O WWTP with carbon shortage are presented. Finally, Chapter IX gives an overview of the main achievements of the thesis. Additionally, Annex I includes the different biochemical models used for simulation based-studies or experimental data description. The study entitled “Glycerol as a sole carbon source for enhanced biological phosphorus removal” (Guerrero *et al.*, 2012) is attached in Annex II.





# **CHAPTER II**

## Objectives



The main objective of this thesis is to understand the underlying mechanisms of EBPR deterioration due to nitrate presence in the anaerobic zone of wastewater treatment plants with simultaneous C/N/P removal. This objective includes the study of the interactions between biological N-removal and EBPR processes and the development of novel alternatives to minimise anaerobic nitrate inlet. Thus, this issue has been approached from different points of view: modelling, microbial analysis, multi-criteria optimisation, multivariate statistical analysis, pilot plant operation and process control.

Following this objective, the specific goals for this thesis are:

- Elucidating the role of the nature of the carbon source and the effect of the operational conditions in the competition between PAO and denitrifiers when nitrate is present under theoretically anaerobic conditions.
- Setpoint optimisation of conventional WWTP control loops to improve biological nutrient removal considering operational costs, effluent quality and risks of developing microbial-related solid separation problems.
- Model-based development and experimental validation of a control strategy based on waste materials (i.e. byproducts) addition as an external carbon source to minimise nitrate effect under anaerobic conditions.
- Development and study of novel control strategies for controlling effluent P concentration without adding an external carbon source or other chemicals for P precipitation.
- Simulating N-removal and EBPR interactions in different WWTP configurations to study the effect of different model assumptions (single or two-step nitrification/denitrification and reactive settler).



# **CHAPTER III**

## Material and Methods



### 3.1. Pilot plant description

The experimental work has been conducted in a pilot wastewater treatment plant (WWTP) located in the Departament d'Enginyeria Química at UAB (Figure 3.1). The pilot plant was operated most of the time with the classical anaerobic/anoxic/aerobic (A<sup>2</sup>/O) configuration for simultaneous C, N and P removal. The first reactor (R1, 28L) was anaerobic to favour PAO growth, the second reactor (R2, 28L) was operated under anoxic conditions for denitrification and the third reactor (R3, 90L) was aerobic to achieve nitrification, complete organic matter and P removal. A settler (50L) was used to separate the treated water from the biomass, which was returned to the system. Additionally, a fourth reactor was also operated (R4, 15L) to denitrify the nitrogen oxides (mainly nitrate) present in the external recycle when Johannesburg configuration (see Chapter VI) was implemented.

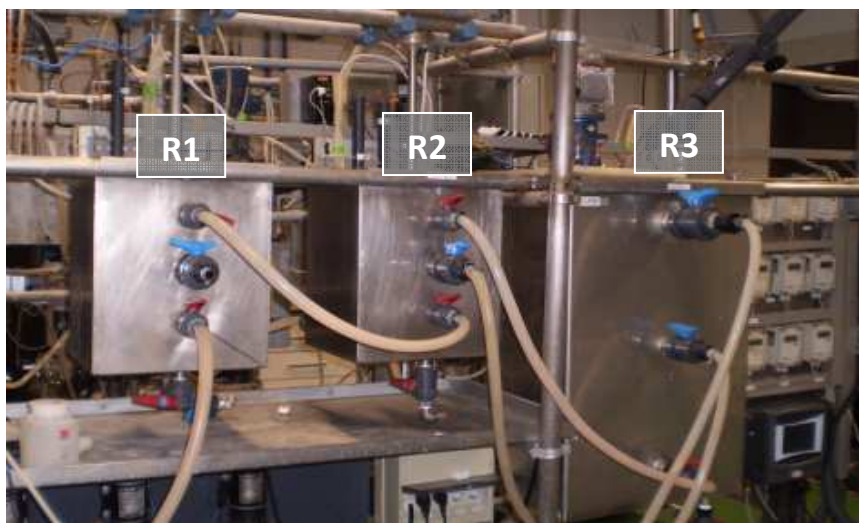


Figure 3.1 Pilot WWTP located in the Departament d'Enginyeria Química labs (UAB).

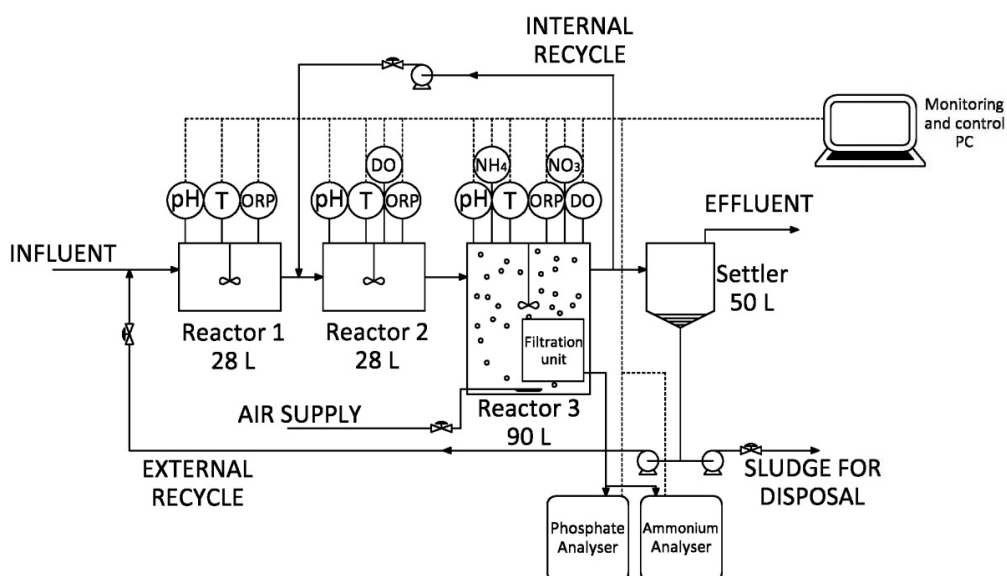


Figure 3.2 Scheme of the pilot plant and the instrumentation used for monitoring.

The reactors R1 to R3 were monitored on-line with dissolved oxygen (Desin DO2-WW), pH (Desin EPH-M11), redox (ORP, Desin EPR-M11) and temperature (Pt-100) probes that were connected to signal converters (Desin TM-3659). R3 was also equipped with ammonium and nitrate probes (Hach Lange scNH4D and scNO3D) and on-line phosphate (Hach Lange PHOSPHAX) and ammonium (Hach Lange AMTAX) analysers with a sample filtration unit (Hach Lange FILTRAX) (Figure 3.2). For the operation of the pilot plant, pH was controlled using an on-off controller with sodium carbonate (1M) or hydrochloric acid (1M) dosage. Dissolved oxygen (DO) in R3 was controlled with a proportional-integral (PI) controller that acted over a mass flow-meter (Bronckhorts HiTec 825) to ensure the desired air-flow rate. On-line data were obtained with a data acquisition card (Advantech PCI-1711) connected to a PC with LabWindows CVI 2010 software (named *AddControl*) for process monitoring and control (Figure 3.3). The data acquisition card had several analogic and digital inputs and outputs for actuation over the pumps, stirrers and valves. R4 was only monitored by off-line chemical analysis (see below), no probes were installed.

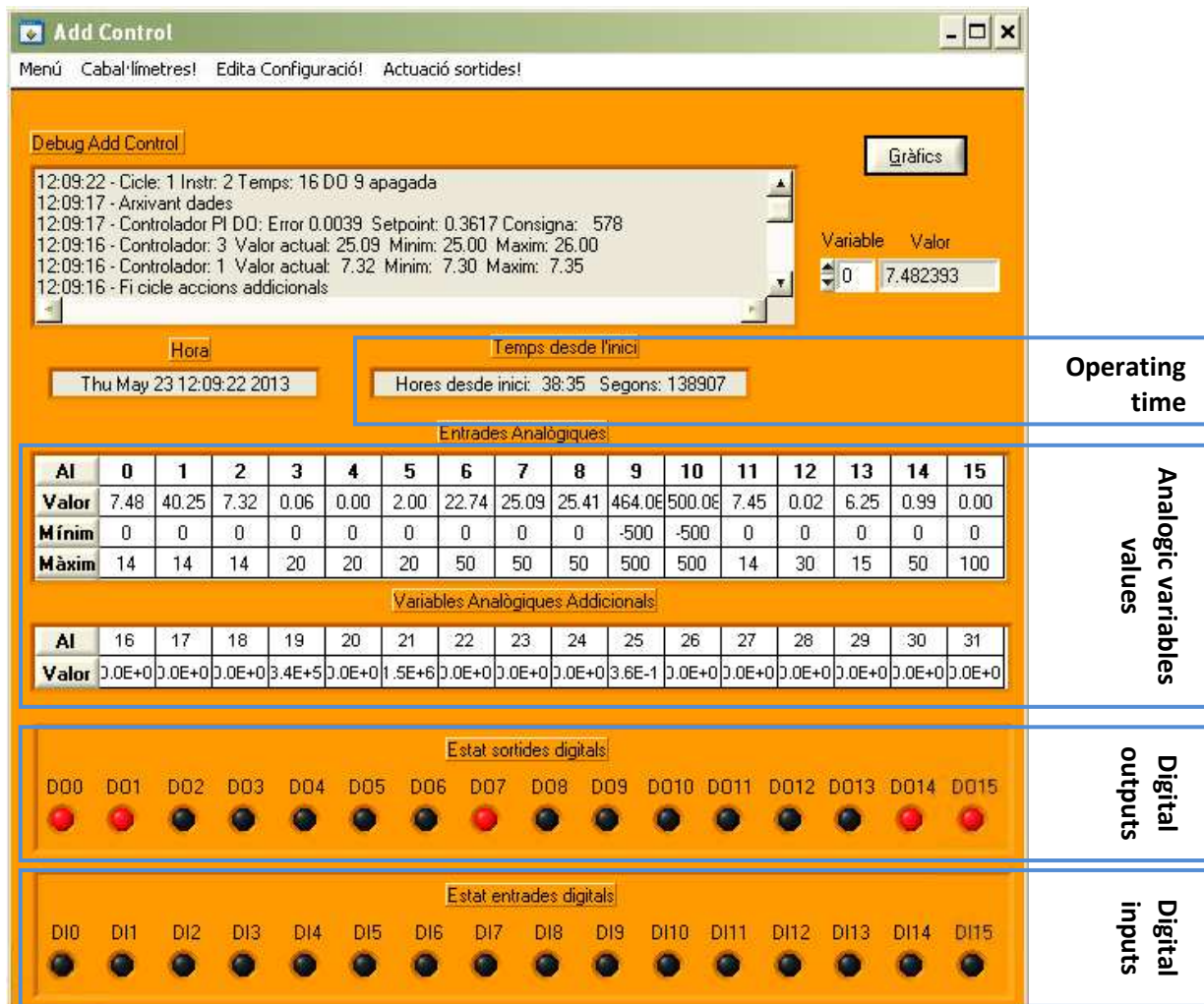


Figure 3.3 Screenshot of the software (*AddControl*) used for pilot plant monitoring and control.



## **3.2. Chemical and biochemical analyses**

---

### **3.2.1. MIXED LIQUOR TOTAL SUSPENDED SOLIDS AND VOLATILE SUSPENDED SOLIDS**

Mixed liquor total suspended solids (TSS) and mixed liquor volatile suspended solids (VSS) were analysed according to standard methods 2540 D and 2540 E, respectively, from APHA (1995).

### **3.2.2. ORTHOPHOSPHATE PHOSPHORUS**

Orthophosphate phosphorus ( $P-PO_4^{-3}$ ) concentration in 0.22  $\mu\text{m}$  filtered samples (Milex GP unites filters, Millipore) was determined by PHOSPHAX sc (Hach Lange) phosphate analyser based on the Vanadomolybdate yellow method, where a two-beam photometer with LEDS measured the phosphate specific yellow colour.

### **3.2.3. AMMONIUM NITROGEN**

Two different equipments were used to measure ammonium nitrogen ( $N-NH_4^+$ ) concentration in 0.22  $\mu\text{m}$  filtered samples: a continuous flow analyser (CFA) based on the potentiometric determination of ammonia (Baeza *et al.*, 1999) and AMTAX sc (Hach Lange) ammonium analyser. For the second case, the analytical method was quite similar to the one used with CFA because AMTAX sc measured the ammonium concentration with an ammonia gas-sensitive electrode. The ammonium in the sample was first converted to gaseous ammonia ( $NH_3$ ) by basifying the medium with NaOH. The  $NH_3$  gas passed through the gas-permeable membrane of the electrode to be then detected.

### **3.2.4. NITRATE AND NITRITE NITROGEN**

Nitrate ( $N-NO_3^-$ ) and nitrite ( $N-NO_2^-$ ) nitrogen concentration in 0.22  $\mu\text{m}$  filtered samples were measured by ionic chromatography (ICS-2000 Dionex) with IonPac AS9-HC column and Anion Self- Regenerating suppressor (ASR ULTRA II 4mm). Eluent solution consisted of KOH 10mM. The conditions of the analyses were 30°C, 25  $\mu\text{L}$  of injection volume, 1  $\text{mL}\cdot\text{min}^{-1}$  of flow injection and 33 min of analytical time.

### **3.2.5. CHEMICAL OXYGEN DEMAND**

Chemical oxygen demand (COD) was measured using colorimetric Dr. Lange kits (LK514) and DR2800 Hach Lange spectrophotometer. The samples were firstly filtered (0.22 $\mu\text{m}$ ) when analysing soluble COD; otherwise total COD (soluble and particulate organic matter) would be measured. The latter analysis was necessary when using complex carbon sources such as milk powder or starch.

### **3.2.6. VOLATILE FATTY ACIDS**

Acetic and propionic acid concentration in 0.22  $\mu\text{m}$  filtered samples were measured by gas chromatography (GC). A volume of 0.2 mL of hexanoic acid solution (internal standard) was added to 0.8 mL of filtered sample. An Agilent Technologies 7820A equipped with a BP21

SGE column (30m x 0.25 mm x 0.25 $\mu$ m) and a flame ionization detector (FID) was used. 1  $\mu$ L sample was injected at 275 $^{\circ}$ C under pulsed split conditions (29 psi). The carrier gas was helium with a split ratio of 10:1 at 2.9 mL/min. The temperature of the column was initially set at 85 $^{\circ}$ C during one minute, followed by a temperature ramp of 3 $^{\circ}$ C $\cdot$ min $^{-1}$  to reach 130 $^{\circ}$ C. Then, a second ramp of 35 $^{\circ}$ C $\cdot$ min $^{-1}$  was maintained until 220 $^{\circ}$ C was reached. Finally, a cleaning step at 230 $^{\circ}$ C during five minutes was performed to remove any residue in the column. The run time was around 24 min per sample and the FID temperature was 275 $^{\circ}$ C.

### 3.3. Microbial analyses

---

#### 3.3.1. FLUORESCENCE IN SITU HYBRIDISATION (FISH)

FISH identification technique consists of the direct analysis of microbial population structures by the *in situ* hybridization of ribosomal rRNA with rRNA-targeted oligonucleotide probes. The oligonucleotides (short strands of nucleic acids) are able to enter into bacterial cells and form stable associations with specific regions of the 16S rRNA ribosomal of a specific microbial population. The oligonucleotides also contain a substance called fluorochrome that can be directly visualized by epifluorescent microscope or a confocal laser scanning microscope (CLSM), if the hybridization successfully occurs. Contrary, if there is not a complementary 16S rRNA in the ribosome, stable hybridization does not occur and the oligonucleotides are washed from the bacterial cell.

FISH protocol was performed according to the principles described in Amann (1995) and it is next summarized:

##### 3.3.1.1. Sample fixation:

Paraformaldehyde (PFA) solution was used to fixate the samples. For its preparation, 4 g of PFA were mixed in 65 mL of Milli-Q-water and heated to 60 $^{\circ}$ C. Then, 2M of NaOH were added drop by drop and stirred rapidly until the solution was nearly clarified (1-2min). The solution was removed from the heat source and 33 mL of 0.03M phosphate buffered saline (PBS) (prepared with 7.74 g of Na<sub>2</sub>HPO<sub>4</sub>·12H<sub>2</sub>O, 1.31 g NaH<sub>2</sub>PO<sub>4</sub>·2H<sub>2</sub>O and 22.62 g NaCl in 1000 mL of Milli-Q-water) were added. Then, pH was adjusted to 7.2 with HCl and remaining crystals were removed by sterile filtration (0.2  $\mu$ m). The solution was quickly cooled to 4 $^{\circ}$ C and stored at this temperature for no longer than 2 days or stored in 1.5 mL aliquots (in 2 mL centrifuge tubs) at -20 $^{\circ}$ C.

Once PFA solution was prepared, 3 volumes of this solution were added to 1 volume of sample and held at 4 $^{\circ}$ C for 1 to 3 hours. After that time, the samples were centrifuged (5000g) and the supernatant (mainly PFA solution) was removed. Subsequently, the cells were washed twice with 0.01M PBS and resuspended in one volume of 0.01M PBS per one volume of ice cold ethanol. Fixed cells can be spotted onto glass slides or stored at -20 $^{\circ}$ C for several months.

### **3.3.1.2. Application of samples to slides:**

5-20  $\mu\text{L}$  of fixed sample (depending on the sample concentration and biomass structure, e.g. granular or suspended biomass) were added to each well in the glass slide, which was dried with air or heating (max. 60°C). Then, the cells were dehydrated in ethanol series (3 min each): 50%, 80% and 98% ethanol and dried again with air.

### **3.3.1.3. Probe hybridization:**

The hybridization buffer was prepared in 2 mL microcentrifuge tubes at the time of use. The hybridization buffer was composed by: 360  $\mu\text{L}$  of 5M NaCl (autoclaved), 40  $\mu\text{L}$  of 1 M Tris/HCl (autoclaved), 2  $\mu\text{L}$  of 10% SDS and 898  $\mu\text{L}$  of Milli-Q-water. Formamide was also added in the hybridization buffer but its concentration depended on the probe used (Table 3.1). When the buffer was prepared, 8  $\mu\text{L}$  were added to each well on the slide and the rest was used to moisten a tissue paper in a 50 mL tube. Then, 1  $\mu\text{L}$  of the selected probe at 25  $\text{ng}\cdot\mu\text{L}^{-1}$  was added to each well and mixed carefully. The slide was placed in the 50 mL tube containing the moistened tissue that was closed and put in the hybridization oven at 46°C for 1 to 2 hours.

### **3.3.1.4. Washing:**

The washing buffer (50mL) was prepared with: 80  $\mu\text{L}$  of NaCl 5M (autoclaved), 500  $\mu\text{L}$  EDTA 0.5M, 1 mL Tris/HCl 1M (autoclaved), 43.8 mL Milli-Q-water (autoclaved) and 50  $\mu\text{L}$  10% SDS (added last); and it was warmed in a bath at 48°C during the hybridization step. After the hybridization step, slides were carefully removed from their tube and placed in the warm washing tube with the buffer solution at 48°C during 10-15 min. Rapid transfer of slides prevented cooling and avoided non-specific probe binding. After that time, the slide was rinsed with cold Milli-Q-water. Water was directed above wells and allowed to flood over them. Both sides of the slide were washed to remove possible salt presence which is highly autofluorescent. After the washing step, compressed air was applied to remove all droplets of water from the wells.

### **3.3.1.5. Embedding:**

A drop of reagent Citifluor AF1 was applied on each well to increase probe fluorescence. Slide was then covered with large coverslip that had to be pressed down to remove reagent excess. Slides, at that point, can be kept at -20°C for some weeks without fluorescent losing.

### **3.3.1.6. Visualisation and quantification:**

FISH preparations were visualised with a CLSM (Olympus Fluoview 1000 CLSM). The quantification of the different cells hybridized as a proportion of all bacteria was done using the analysis technique pointed out in Jubany *et al.* (2009): 40 randomly chosen fields from different x, y and z coordinates were treated using the Matlab® Image Processing Toolbox. The area containing the specific probe (e.g. PAOmix) cells was quantified as a percentage of the area of the general probe (EUBmix) considering simultaneously 40 images. Ten images

obtained with the same sludge and procedures, but with no probe addition, were used to evaluate the autofluorescence of the sample.

### 3.3.1.7. Probes for FISH analysis:

The probes used in this thesis are summarized in Table 3.1.

**Table 3.1** Oligonucleotide probes used in this thesis.

Probe Name	Specificity	Fluorochrome	Mixed probe name	Formamide (%)	Reference
EUB338	Many but not all bacteria	Cy5	EUBmix	0-50	Amann <i>et al.</i> (1995)
EUB338-II	Planctomycetales	Cy5	EUBmix	0-50	Daims <i>et al.</i> (1999)
EUB338-III	Verrucomicrobiales	Cy5	EUBmix	0-50	Daims <i>et al.</i> (1999)
PAO462	"Candidatus Accumulibacter phosphatis"	Cy3	PAOmix	35	Crocetti <i>et al.</i> (2000)
PAO651	"Candidatus Accumulibacter phosphatis"	Cy3	PAOmix	35	Crocetti <i>et al.</i> (2000)
PAO846	"Candidatus Accumulibacter phosphatis"	Cy3	PAOmix	35	Crocetti <i>et al.</i> (2000)
Acc-I-444	"Candidatus Accumulibacter phosphatis" clade I	Cy3	PAOmix C1	35	Flowers <i>et al.</i> (2009)
Acc-II-444	"Candidatus Accumulibacter phosphatis" clade II	Cy5	PAOMIX C2	35	Flowers <i>et al.</i> (2009)
GAOQ431	"Candidatus Competibacter phosphatis"	Cy3	GAOmix	35	Crocetti <i>et al.</i> (2002)
GAOQ989	"Candidatus Competibacter phosphatis"	Cy3	GAOmix	35	Crocetti <i>et al.</i> (2002)
TFO_DF218	"Defluviicoccus-related TFO"	Cy3	DF1mix	35	Wong <i>et al.</i> (2004)
TFO_DF618	"Defluviicoccus-related TFO"	Cy3	DF1mix	35	Wong <i>et al.</i> (2004)
DF988*	"Defluviicoccus-vanus" cluster II	Cy3	DF2mix	35	Meyer <i>et al.</i> (2006)
DF1020**	"Defluviicoccus-vanus" cluster II	Cy3	DF2mix	35	Meyer <i>et al.</i> (2006)
H966	Helper probe	-	-	-	Meyer <i>et al.</i> (2006)
H1038	Helper probe	-	-	-	Meyer <i>et al.</i> (2006)
Nso190	Betaproteobacterial ammonia oxidizing bacteria	Cy3	-	35	Mobarry <i>et al.</i> (1996)
NIT3	Nitrobacter spp.	Cy3	-	40	Wagner <i>et al.</i> (1996)

\* DF988 in conjunction with helper probes H966 and H4038

\*\*DF1020 in conjunction with helper probe H1038

## **CHAPTER IV**

# Improving the performance of a biological nutrient removal WWTP by model-based setpoint optimisation

Part of this chapter has been published as:

Guerrero, J., Guisasola, A., Vilanova, R., Baeza, J.A., 2011. Improving the performance of a WWTP control system by model-based setpoint optimisation. *Environmental Modelling and Software* 26, 492-497.

Guerrero, J., Guisasola, A., Comas, J., Rodríguez-Roda, I., Baeza, J.A., 2012. Multi-criteria selection of optimum WWTP control setpoints based on microbiology-related failures, effluent quality and operating costs. *Chemical Engineering Journal* 188, 23-29.



## **Abstract**

*This work aims at improving the performance of WWTP with simultaneous biological C, N and P removal by a model-based setpoint optimisation of the control system. These setpoints were optimised to achieve the best effluent quality with the lower operating costs and, at the same time, ensuring an operation with low probability to develop biomass settling problems. Two different objective functions were used to optimise the setpoints of the tested control strategies: i) OCF: a cost function based on the operational costs by converting the effluent quality into monetary units and ii) MCF: a multi-criteria function based on the effluent quality, the operational costs and the appearance of settling problems of microbiological origin (bulking, foaming or rising sludge). For this purpose, an anaerobic/anoxic/aerobic (A<sup>2</sup>/O) pilot WWTP was simulated using the IWA ASM2d model under different influent conditions. Several control strategies for an efficient biological C/N/P removal were implemented and evaluated: i) open-loop with controlled TSS concentration (reference operation); ii) dissolved oxygen control in the aerated reactors; iii) maximum performance of nutrient removal; iv) optimised fixed setpoints for the controlled variables; v) daily optimised setpoints; vi) two different sets of optimised setpoints for weekdays and weekends and vii) hourly optimised setpoints. The optimised control system resulted in around a 45% decrease of operational costs, a significant improvement of the effluent quality and a decrease on the probability of settling problems occurrence. The multi-criteria optimisation resulted in a set of optimal setpoints with a Pareto distribution. Moreover, it was concluded that the optimisation process could be enhanced by using both objective functions in a complementary way. While the MFC enabled a more extensive evaluation of the different alternatives, once the weights are selected the OCF optimisation could be used to define an optimum set of setpoints to adapt the system to influent variations.*

## **4.1. Motivations**

Meeting stringent concentration requirements for C, N and P discharge limits has raised the need of a more efficient operation. The implementation of automatic control systems has improved the performance of numerous WWTP (Benedetti *et al.*, 2010; Cecil and Kozłowska, 2010) and thus further research on designing new and more efficient control strategies is a promising solution to meet discharge limits with the minimal operational costs. Although many control strategies have been already reported, most of them were only based on improving C and N removal. According to the European Water Framework Directive (2000/60/CE), P removal has been fixed as a new objective for urban WWTP and thus, its improvement by control implementation is a short term aim. With respect to the existing control strategies, little attention has been paid to the tuning of controllers (Ruano *et al.*, 2010) or to the setpoint optimisation for WWTP performance purposes (Stare *et al.*, 2007). Additionally, the development of reliable models has provided tools to allow the model-based optimisation of these control systems. For example, IWA ASM2d (Henze *et al.*, 2000) is a complex kinetic model able to describe biological C/N/P removal processes from wastewater. Although this model has a large number of parameters which are difficult to

identify due to correlation problems (Machado *et al.*, 2009a), it is able to provide an accurate description of the process with its default parameter values.

The evaluation of the improvement of WWTP when a control system is implemented is not a straightforward issue because several performance indexes must be taken into account, for example operational costs (OC) or effluent quality (EQ). However, although most of the control strategies reported so far are only based on these two indexes, even with a proper operation in terms of OC and EQ, the optimal scenario could result in operating problems. For example, problems with a microbiological origin mostly related to the final settling step (bulking, foaming or rising sludge) could appear (Jenkins *et al.*, 2003). A modelling effort to include these microbiology-related problems using knowledge-based flow diagrams has been recently reported (Comas *et al.*, 2008; Flores-Alsina *et al.*, 2009a, b). Thus, the risk of developing settling problems of microbial origin (microbial risks, MR) can be considered as new criteria when evaluating the WWTP operation.

The study presented in this chapter aims at designing optimum control strategies for a WWTP with simultaneous biological C, N and P removal by means of model-based setpoint optimisation. For this purpose, two activated sludge pilot plants with several control loops were simulated using ASM2d. The success of optimisation step fully relies on a proper construction of the objective function that will be used for the setpoint optimisation of some of the implemented control loops. Then, two different objective functions were compared: (i) an operating costs function (OCF) calculated by adding EQ converted into monetary units to OC (Vanrolleghem *et al.*, 1996; Gillot *et al.*, 1999) and (ii) a new multi-criteria function (MCF) based on three performance indexes: EQI, OC and MR related to solid separation problems. This study was the first work which links possible microbiology-related failures to the inclusion of EBPR when developing optimum control strategies for a WWTP (i.e. previously, MR criterion has only been applied to systems with C and N removal).

## **4.2. Material and Methods**

---

### **4.2.1. PLANTS DESCRIPTION**

Two different A<sup>2</sup>/O pilot plant designs were simulated in this chapter (Figure 4.1), the most significant parameters of which are summarized in Table 4.1. These hydraulic models were chosen because they mimicked the configuration of two real pilot plants, where the results here presented could be further evaluated. The main difference between both plants was the volume of the aerobic zone, which was increased in pilot plant II to increase nitrate production and so to favour its deleterious effect on EBPR under anaerobic conditions and the development of MR related to high nitrate effluent (i.e. rising sludge).



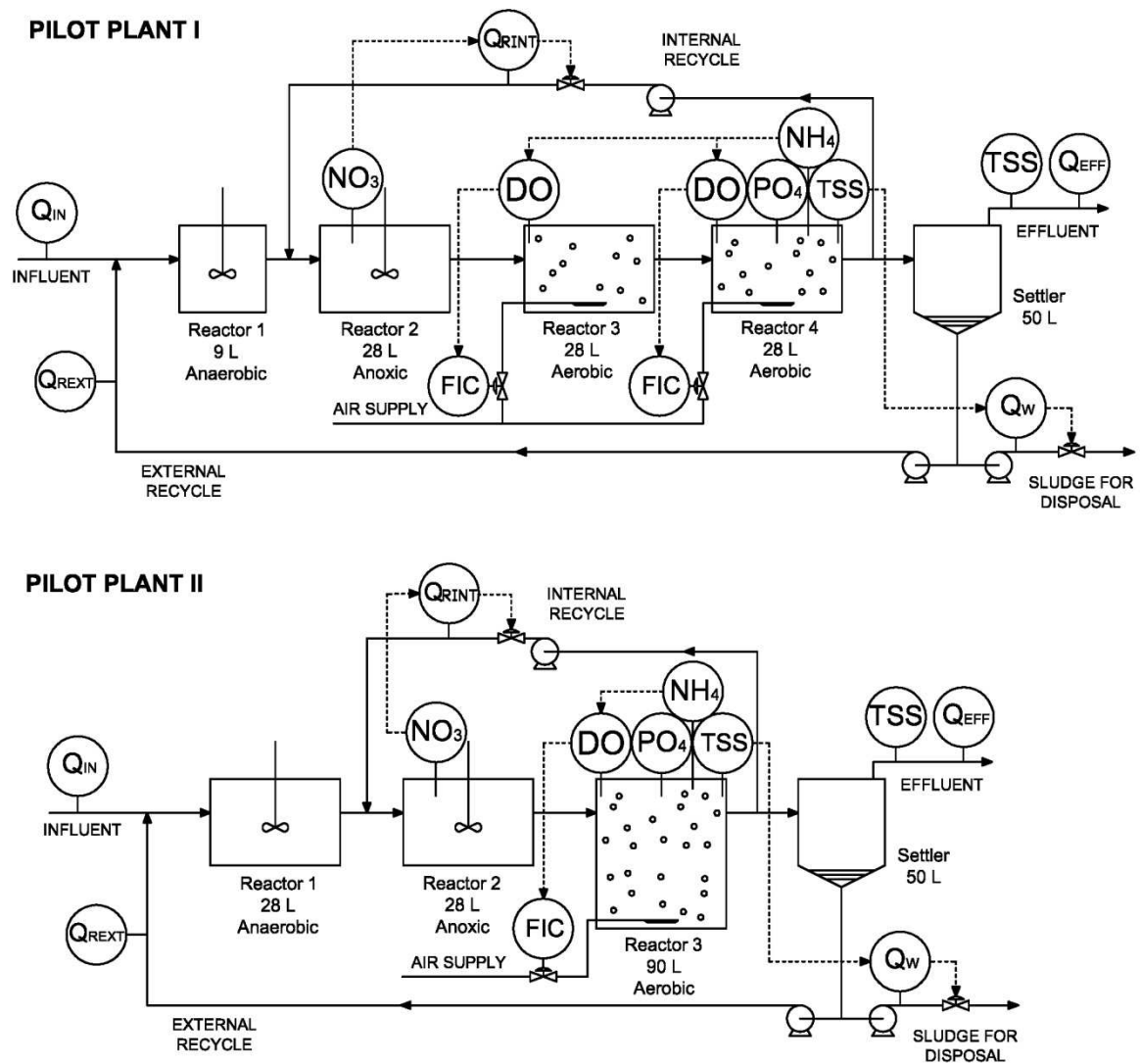


**Figure 4.1** Scheme of the A<sup>2</sup>/O pilot plants I and II simulated for simultaneous C/N/P removal. Dotted lines represent the control actions over the manipulated variables.

**Table 4.1** Operational parameters for both pilot plants under reference operation.

	Pilot Plant I	Pilot Plant II
<b>Configuration</b>	A <sup>2</sup> /O	
<b>Reactor volumes</b>	Anaerobic reactor (R1 – 8L) Anoxic reactor (R2 -28 L) Aerobic reactor (R3 and R4 -28L)	Anaerobic reactor (R1 – 28L) Anoxic reactor (R2 – 28 L) Aerobic reactor (R3 – 90L)
<b>Total volume</b>	93 L	146 L
<b>Settler volume</b>	50 L	
<b>k<sub>L</sub>a</b>	R3 – 600 d <sup>-1</sup> and R4 – 400 d <sup>-1</sup>	R3 – 240 d <sup>-1</sup>
<b>Influent flow-rate, Q<sub>IN</sub></b>	0.25 m <sup>3</sup> ·d <sup>-1</sup>	0.40 m <sup>3</sup> ·d <sup>-1</sup>
<b>Internal recycle, Q<sub>REXT</sub></b>	300% Q <sub>IN</sub>	
<b>External recycle, Q<sub>REXT</sub></b>	100% Q <sub>IN</sub>	
<b>HRT</b>	9 h	
<b>SRT</b>	12.5 d	7.0 d

The flow rate and the composition of the influent ( $Q_{IN}$ ) varied in time according to the influents proposed by the IWA Task Group on Benchmarking (Gernaey and Jørgensen, 2004), the average values were  $0.25 \text{ m}^3 \cdot \text{d}^{-1}$  for pilot plant I and  $0.40 \text{ m}^3 \cdot \text{d}^{-1}$  for pilot plant II. Three different dynamic plant influents were simulated: Dry-2, Rain-2 and Storm-2 (Figure 4.2). Each influent contained 14 days of data at 15-min intervals.

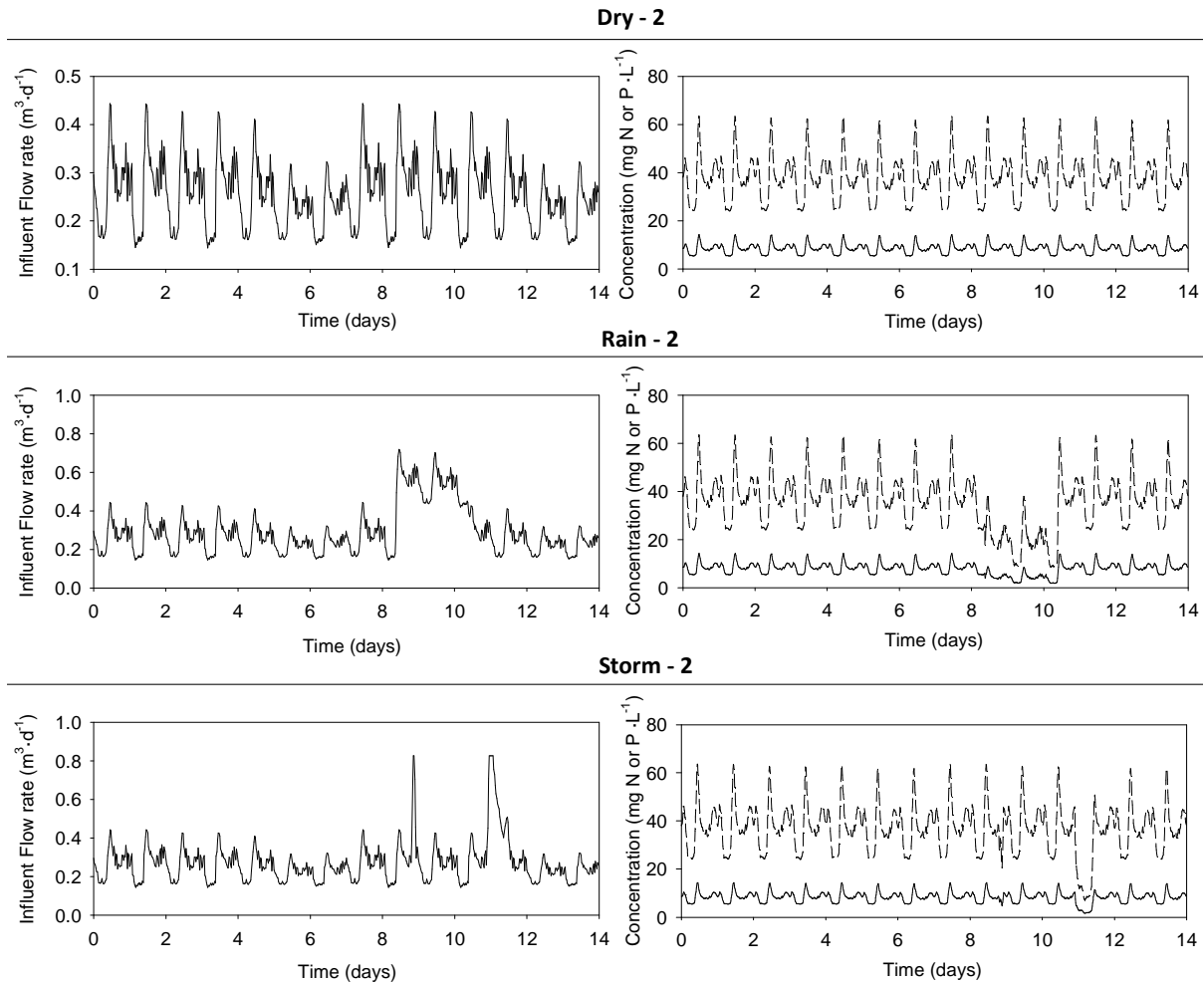


**Figure 4.2** Example of the influent data for Dry-2, Rain-2 and Storm-2 scenarios for pilot plant I. Left: Influent flow rate. Right: Dashed lines belong to influent ammonium nitrogen concentration and solid lines belong to influent phosphate phosphorus concentration.

The simulated plants included four local PI-control loops:

- **Dissolved Oxygen (DO)** feedback control in the aerobic reactors using the oxygen transfer coefficient ( $k_L a$ ) as the manipulated variable. In pilot plant I, both reactors had the same DO setpoint.
- **Effluent ammonium** was controlled in the last aerobic reactor by the setpoint of DO control loop using a cascade control structure. The thresholds of DO and ammonium setpoints were  $0 - 4 \text{ mg DO} \cdot \text{L}^{-1}$  and  $0 - 10 \text{ mg N-NH}_4^+ \cdot \text{L}^{-1}$ , respectively.

- **Nitrate** feedback control in R2 with setpoints' limits between 0 – 3 mg N-NO<sub>3</sub><sup>-</sup> ·L<sup>-1</sup> and using Q<sub>RINT</sub> as manipulated variable.
- **Total suspended solids (TSS)** feedback control in R4 (pilot plant I) or in R3 (pilot plant II) by acting in the purge flow (Q<sub>W</sub>). To avoid the effect of a possible change in TSS concentration on the treatment capacity or on the sludge age and in order to compare the removal efficiency related only with the tested control strategies, TSS were considered as inventory variable (i.e. variables that must be controlled for a proper plant management) (Steffens and Lant, 1999; Machado *et al.*, 2009b). Thus, TSS were always controlled at a fixed setpoint of 4500 mgTSS·L<sup>-1</sup> for pilot plant I and 2500 mg TSS ·L<sup>-1</sup> for plant II. Q<sub>W</sub> was limited from 0.002 to 0.02 times the influent flow rate, providing an SRT around 12.5 days for pilot plant I and 7 days for pilot plant II.

#### 4.2.2. DESCRIPTION OF THE SIMULATED CONTROL STRATEGIES

The different control strategies tested are next summarised:

##### Non-optimised control strategies:

- **Reference operation (RO):** The system was simulated according to the operational characteristics presented in table 4.1 (i.e. all the control strategies were disabled, except for TSS control loop).
- **DO control (DOC):** DO control was activated with a setpoint of 4 mg DO·L<sup>-1</sup> in the aerobic reactors.

##### Optimised control strategies:

- **Maximum performance for nutrient removal (MPR):** Control setpoints were fixed to obtain the maximum removal performance. Ammonia setpoint was 0 mg·L<sup>-1</sup> and nitrate setpoint was optimised to minimise nitrate in the effluent.
- **Ammonium and nitrate fixed setpoints (A&N-FS):** This strategy consisted of using fixed ammonium and nitrate setpoints during the simulated period.
- **Ammonium and nitrate daily variable setpoints (A&N-DVS):** The setpoints of ammonium and nitrate were daily redefined in order to adapt the plant operation to the daily influent flow pattern.
- **Ammonium and nitrate weekly variable setpoints (A&N-WVS):** The major inlet variations take place between weekdays and the weekend. Thus, two different sets of setpoints were fixed, one for weekend and one for the weekdays. For rain-2 and storm-2 scenario, one more set of setpoints was proposed to adapt the plant operation to such rain or storm episodes.
- **Ammonium and nitrate hourly variable setpoints (A&N-HVS):** The control setpoints were hourly modified to adapt the plant operation to the hourly influent flow pattern.

Ammonium and nitrate control setpoints were optimised using the methodology described in section 4.2.4.

### 4.2.3. PLANT PERFORMANCE FUNCTION DEVELOPMENT

Two different plant performance functions were used for optimising the setpoints of the control strategies.

#### 4.2.3.1. Operating costs function (OCF)

The OCF (equations 4.1-4.6) was calculated following the methodology of Vanrolleghem and Gillot (2002), which described the cost of the secondary treatment of a WWTP by including the EQ converted into monetary units. We propose to also include the influent ( $Q_{IN}$ ) in the cost calculations (equations 4.2-4, 4.6) in order to obtain the costs per  $m^3$  of wastewater treated. Thus, specific plant characteristics are avoided and the comparison between different plants becomes easier.

$$OCF \left[ \text{€} \cdot m^{-3} \right] = \gamma_E (AE+PE) + \gamma_{SP} SP + EF \quad (4.1)$$

AE corresponds to energy invested in aeration, PE is the necessary pumping energy, SP the sludge production and EF the effluent fines,  $\gamma_E$  ( $0.1 \text{ €} \cdot kWh^{-1}$ ) represents the cost per kWh and  $\gamma_{SP}$  ( $0.5 \text{ €} \cdot kg^{-1}$ ) stands for the cost of the treatment per g of produced sludge (Stare *et al.*, 2007). AE between  $t_{start}$  and  $t_{end}$  period was calculated as proposed in Jeppsson (2005) by using equation 4.2, where  $k_L a_i$  is the global oxygen transfer coefficient [ $d^{-1}$ ] of each aerobic reactor.  $V_i$  is the volume of each aerobic reactor in both pilot plants and  $V_{ref}$  is the reference aerobic reactor volume from Benchmark Simulation Model n<sup>o</sup>1 (BSM1) with a value of  $1333 m^3$  (Alex *et al.*, 2008).

$$AE \left[ kWh \cdot m^{-3} \right] = \frac{24}{t_{end} - t_{start}} \cdot \int_{t_{start}}^{t_{end}} \left[ \frac{1}{Q_{IN}(t)} \cdot \sum_{i=3}^4 \left( 0.0007 \cdot (k_L a_i(t))^2 \cdot \left( \frac{V_i}{V_{ref}} \right) + 0.3267 \cdot k_L a_i(t) \cdot \left( \frac{V_i}{V_{ref}} \right) \right) \right] \cdot dt \quad (4.2)$$

PE was calculated with equation 4.3, where  $P_F$  ( $0.04 kWh \cdot m^{-3}$ ) converts the pump flow into required energy (Copp *et al.*, 2002).

$$PE \left[ kWh \cdot m^{-3} \right] = \frac{P_F}{t_{end} - t_{start}} \cdot \int_{t_{start}}^{t_{end}} \left[ \frac{1}{Q_{IN}(t)} \cdot (Q_{RINT}(t) + Q_{REXT}(t) + Q_W(t)) \right] \cdot dt \quad (4.3)$$

SP was calculated as equation 4.4:

$$SP \left[ g \text{ TSS} \cdot m^{-3} \right] = \frac{1}{t_{end} - t_{start}} \cdot \int_{t_{start}}^{t_{end}} \left[ \frac{1}{Q_{IN}(t)} \cdot TSS_W(t) \cdot Q_W(t) \right] \cdot dt \quad (4.4)$$

The solids content in the purge ( $TSS_W$ ) were estimated via mass balance of the settler (equation 4.5), using the total suspended solids concentration in the last aerobic reactor ( $TSS_{AER}$ ), assuming negligible suspended solids concentration in the effluent and constant biomass hold up in the settler.

$$TSS_W(t) \left[ g \text{ TSS} \cdot m^{-3} \right] = \left( \frac{Q_{IN}(t) + Q_{REXT}(t)}{Q_W(t) + Q_{REXT}(t)} \right) \cdot TSS_{AER}(t) \quad (4.5)$$

EF (equation 4.6) were calculated comparing the effluent ammonium nitrogen, total nitrogen (TN) and phosphate phosphorus with the value of their respective discharge limits, being TN the sum of nitrogen as ammonium, nitrate and nitrite in the effluent (Vanrolleghem *et al.*, 1996).

$$EF [\text{€} \cdot \text{m}^{-3}] = \frac{1}{t_{\text{end}} - t_{\text{start}}} \cdot \int_{t_{\text{start}}}^{t_{\text{end}}} \left[ \frac{1}{Q_{\text{IN}}(t)} \cdot \left( \sum_{j=\text{N-NH}_4, \text{TN}, \text{P-PO}_4} \left( Q_{\text{EFF}}(t) \cdot \Delta\alpha_j \cdot C_{\text{EFF},j}(t) + \left( Q_{\text{EFF}}(t) \cdot [\beta_{0,j} + (C_{\text{EFF},j}(t) - C_{L,j}) \cdot (\Delta\beta_j - \Delta\alpha_j)] \right) \cdot \text{Heaviside}(C_{\text{EFF},j}(t) - C_{L,j}) \right) \right) \right] \cdot dt \quad (4.6)$$

Where  $C_{\text{EFF},j}$  and  $C_{L,j}$  are the effluent concentration and discharge limit of the pollutant “j”, respectively;  $\Delta\alpha_j$  is the slope of the curve cost per volume versus  $C_{\text{EFF},j}$  when  $C_{\text{EFF},j}$  is lower than or equal to  $C_{L,j}$ ;  $\Delta\beta_j$  is the slope of the same curve when  $C_{\text{EFF},j}$  is higher than  $C_{L,j}$ ; and  $\beta_{0,j}$  is the increment of fines when  $C_{\text{EFF},j}$  was higher than  $C_{L,j}$  (Figure 4.3). The Heaviside function is equal to 1 when  $C_{\text{EFF},j}$  is greater than  $C_{L,j}$ . Otherwise, its value is 0. The values of all the parameters involved in the EF calculation are given in table 4.2. The parameters for ammonium nitrogen and TN were obtained from Stare *et al.* (2007). Phosphate-related parameters were assumed equal to ammonium parameters, except for the effluent discharge limit that was the same as was reported by Gernaey and Jørgensen (2004).

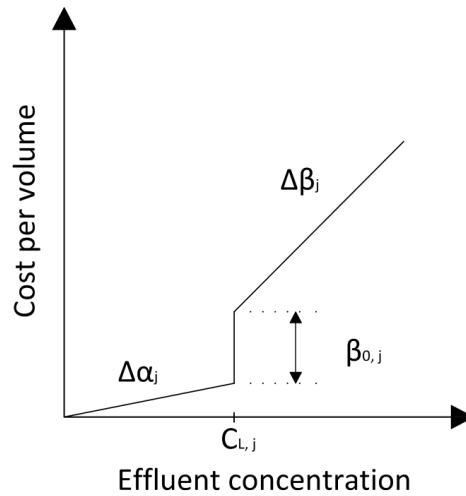


**Figure 4.3** Cost function for effluent fines. Adapted from Stare *et al.*, (2007).

**Table 4.2** Parameters used to evaluate the effluent fines.

Effluent Variable	$\Delta\alpha_j (\text{€} \cdot \text{kg}^{-1})$	$\Delta\beta_j (\text{€} \cdot \text{kg}^{-1})$	$\beta_{0,j} (\text{€} \cdot \text{m}^{-3})$	$C_{L,j} (\text{mg} \cdot \text{L}^{-1})$
Ammonium	4.00	12.00	$2.70 \cdot 10^{-3}$	4.00
Total Nitrogen	2.70	8.10	$1.40 \cdot 10^{-3}$	18.00
Phosphate	4.00	12.00	$2.70 \cdot 10^{-3}$	1.50

#### 4.2.3.2. Multi-criteria function (MCF)

Figure 4.4 shows the MCF used, which analyses the performance of the process by means of a three-dimensional function.

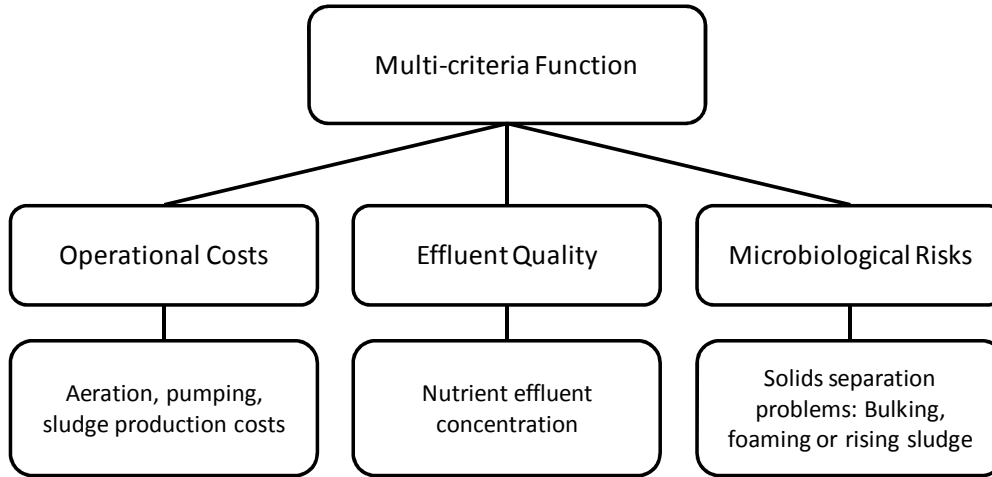


**Figure 4.4** Three dimensional multi-criteria function.

In this case, operating costs (OC) were calculated similarly to Copp (2002) but considering cost per cubic meter of wastewater treated (equation 4.7), as was above indicated for OCF calculation. AE, PE and SP were calculated as for OCF.

$$OC \left[ \text{€} \cdot \text{m}^{-3} \right] = v_E (AE+PE) + v_{SP} SP \quad (4.7)$$

EQI (effluent quality index) was evaluated in terms of pollutant units (PU) concentration in the effluent according to equation 4.8 (Copp, 2002; Gernaey and Jørgensen, 2004). It is important to note that EQ was not converted into monetary units when using MCF. Hence, EQ did not have any weight on the OC calculation, contrary to OCF.  $PU_x$  represents the product between the weights  $\beta_x$  and the concentration of the considered pollutant at time  $t$  (equation 4.9). The weights  $\beta_x$  were extracted from Gernaey and Jørgensen (2004):  $\beta_{TSS} = 2 \text{ kg PU} \cdot \text{kg TSS}^{-1}$ ,  $\beta_{COD} = 1 \text{ kg PU} \cdot \text{kg COD}^{-1}$ ,  $\beta_{TKN} = 20 \text{ kg PU} \cdot \text{kg TKN}^{-1}$ ,  $\beta_{NOx} = 20 \text{ kg PU} \cdot \text{kg NOx}^{-1}$ ,  $\beta_{TP} = 20 \text{ kg PU} \cdot \text{kg TP}^{-1}$ .  $NO_x$  represents the sum of nitrate and nitrite effluent concentrations.

$$EQI \left[ \text{kg PU} \cdot \text{m}^{-3} \right] = \frac{1}{1000 \cdot (t_{\text{start}} - t_{\text{end}})} \int_{t_{\text{start}}}^{t_{\text{end}}} [PU_{TSS}(t) + PU_{COD}(t) + PU_{BOD}(t) + PU_{TKN}(t) + PU_{NOx}(t) + PU_{TP}(t)] \cdot dt \quad (4.8)$$

$$PU_x = \beta_x \cdot C_x \quad (4.9)$$

A third criterion, MR, which considers risk of microbiology-related solids separation problems, was also applied for the first time in a simulated plant that included biological P removal. The possible occurrence of such solids separation problems was assessed according to a risk assessment model that determines the possible occurrence of settling problems of microbiological origin (filamentous bulking, foaming and rising sludge) as a function of the operating conditions and the influent composition (Dalmau, 2009). The relationship between operation conditions or influent composition and the fact of developing settling problems are determined based on the different knowledge-based decision trees proposed by Comas *et al.* (2008). The evaluation of these risks is tackled using the principles of fuzzy decision theory (Bellmann and Zadeh, 1970; Pedrycz, 1995). This theory has been widely used in environmental modelling applications due to its simplicity and efficiency (Olsson and Newell, 1999; Fleming *et al.*, 2007;). Hence, the risks estimation is based on four main steps (Figure 4.5):

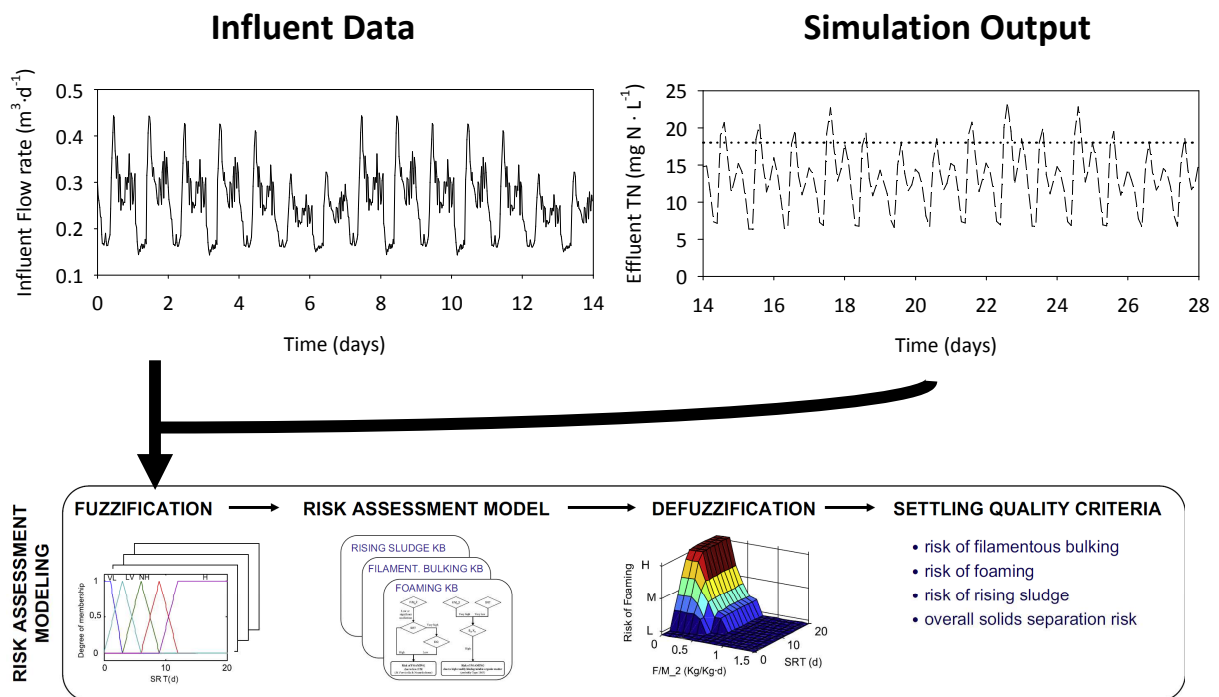


**Figure 4.5** Scheme of the risks assessment model for microbiology-related solids separation problems. Adapted from Comas *et al.* (2008).

- i) **Fuzzification:** The numerical data obtained from the simulation step are converted into qualitative values or fuzzy sets (i.e. low, high, etc) by means of the corresponding membership function. This membership functions are defined for each variable as risks assessment indicators based on the decision trees of each microbiology-related problem (e.g. a pilot plant with a high SRT and low concentration of influent readily biodegradable organic substrate would have a high

risk on developing bulking) listed in Martinez (2006). Triangular or pseudo-trapezoidal functions are used to define these membership functions (Figure 4.6).

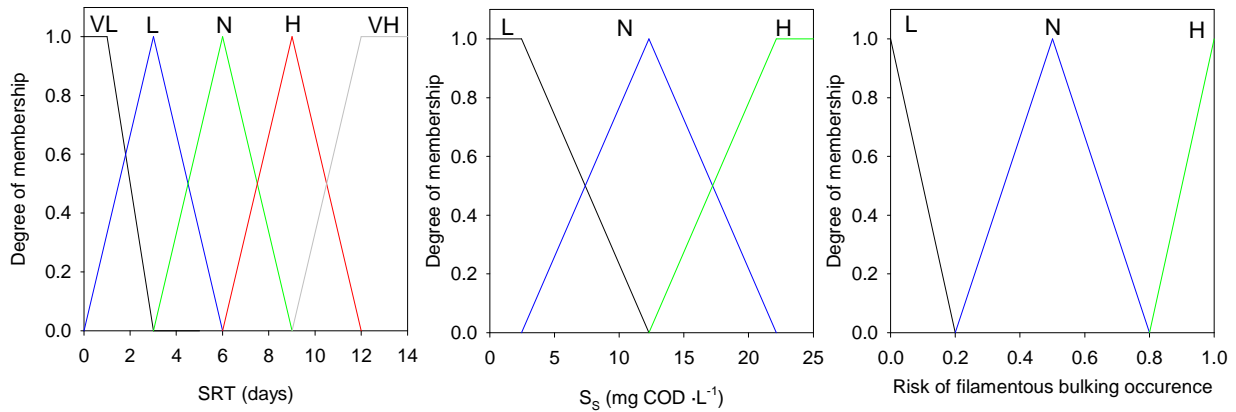


**Figure 4.6** Example of membership functions for input and output variables for the risk of bulking due to SRT and readily biodegradable organic substrate ( $S_s$ ) influent concentration in the anoxic reactor.

- ii) Fuzzy inference of the risks through a Mamdani approach: Mamdani approach allows generating a fuzzy output from the corresponding input fuzzy sets depending on different rules. All the fuzzy rules in the model are extracted from the empirical expertise about cause-effect relationships of microbiology-related solids separation problems in WWTP. Table 4.3 shows the IF-THEN rules of the risks assessment model used in this study. Figure 4.7 shows an example of response surface to develop bulking problems depending on SRT and readily organic substrate ( $S_s$ ) concentration in the first biological reactor.
- iii) Defuzzification of the output data: The fuzzy output is translated into numerical data as the outcome of the risk assessment (i.e. new membership functions are defined for the three outputs variables: risk of bulking, foaming or rising sludge). Hence, the final outcome of this model is a risk to develop such problems between 0 and 1, considering a threshold of 0.8 as a high risk. Figure 4.6 (right) presents an example of the membership function used for defuzzification, where the risks of filamentous bulking ratio can be determined depending on the degree of membership obtained from the previous steps.



**Table 4.3** Knowledge bases of the risks assessment model. The extension to include P in the risks assessment model is presented in grey. Adapted from Comas *et al.* (2008).

<b>Foaming due to low F/M ratio</b>						
		F/M fed				
		L	N	H	VH	
SRT (days)	VL	Low	Low	Low	Low	
	L	Low	Low	Low	Low	
	N	Normal	Low	Low	Low	
	H	High	Normal	Low	Low	
	VH	High	normal	Low	Low	
<b>Foaming due to high readily biodegradable organic matter fraction</b>						
		$S_s/X_s$				
		L	N	H		
SRT (days)	VL	Low	Normal	High		
	L	Low	Low	Medium		
	N	Low	Low	Low		
	H	Low	Low	Low		
	VH	Low	Low	Low		
F/M fed	L	Low	Low	Low		
	N	Low	Low	Low		
	H	Low	Normal	Normal		
	VH	Low	Normal	High		
	<b>Bulking due to low DO</b>					
		DO (mg·L <sup>-1</sup> )				
		VL	L	N	H	VH
F/M removed	L	Low	Low	Low	Low	Low
	N	High	Normal	Low	Low	Low
	H	High	High	Normal	Low	Low
	VH	High	High	High	Normal	Low
<b>Bulking due to low organic loading</b>						
		SRT (days)				
		VL	L	N	H	VH
$S_s$	L	Low	Low	Normal	High	High
	N	Low	Low	Low	Low	Low
	H	Low	Low	Low	Low	Low
F/M fed	L	Low	Low	High	High	High
	N	Low	Low	Low	Normal	Normal
	H	Low	Low	Low	Low	Low
	VH	Low	Low	Low	Low	Low
<b>Bulking due to nutrient deficiency</b>						
BOD <sub>5</sub> /N	L	Low				
	N	Low				
	H	High				
BOD <sub>5</sub> /P	L	Low				
	N	Low				
	H	High				
<b>Rising sludge</b>						
		Nitrogen gas production time				
		L	N	H		
NO <sub>3</sub>	L	Low	Low	Low		
	N	Normal	Low	Low		
	H	High	Normal	Low		

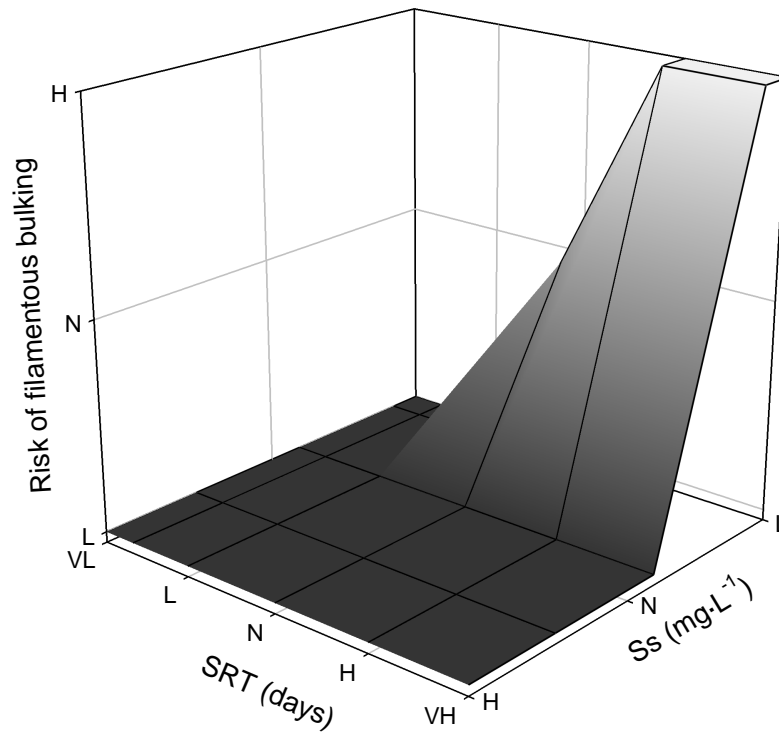


**Figure 4.7** Response surface filamentous bulking risk depending on SRT and readily biodegradable organic substrate.

The risks assessment model was developed by Dalmau (2009) where the equations for membership function calculation, fuzzification and defuzzification procedure can be found. However, when the study presented in this chapter started, this model had been mainly tested for BSM1 and BSM1\_LT where biological P removal and nitrite as state variable were not considered. Hence, it was necessary to expand the risks assessment by including P-removal and nitrite presence effect on developing solid separation problems before including MR in MCF. The risks of developing filamentous bulking is the main separation problem that can appear when considering P removal processes (i.e. high BOD<sub>5</sub>/P influent ratio has a high risk on developing bulking problems). In the case of nitrite inclusion, rising sludge problem was the main process affected by nitrite presence. Table 4.4 presents detailed data about the membership functions structure. The parameters to include P and nitrite in the risks assessment model are presented in grey.

**Table 4.4** Membership functions for each variable considered in the risk assessment model. The extension to include P in the risks assessment model is presented in grey. Adapted from Comas *et al.* (2008).

Variable/modality	Type	Very Low	Low	Normal	High	Very High
F/M removed	Input	shape	-	Trapezoidal	Triangular	Trapezoidal
	Rank	-	[-0.14 -0.14 0.25 0.50]	[0.25 0.50 0.75]	[0.50 0.75 1.00]	[0.75 1.00 4.027 4.19]
F/M fed	Input	Shape	-	Trapezoidal	Triangular	Trapezoidal
	Rank	-	[-0.05 -0.05 0.25 0.50]	[0.25 0.50 0.75]	[0.50 0.75 1.00]	[0.75 1.00 1.51 1.57]
DO in reactor 3	Input	Shape	Trapezoidal	Triangular	Triangular	Trapezoidal
	Rank	[-0.45 -0.12 0.00 1.00]	[0.00 1.00 2.00]	[1.00 2.00 3.00]	[2.00 3.50 5.00]	[3.50 5.00 8.02 8.26]
SRT	Input	Shape	Trapezoidal	Triangular	Triangular	Trapezoidal
	Rank	[-7.20 -0.80 1.00 3.00]	[0.00 3.00 6.00]	[3.00 6.00 9.00]	[6.00 9.00 12.00]	[9.00 12.00 20.29 23.40]
BOD <sub>5</sub> /N influent	Input	Shape	Trapezoidal	Triangular	Trapezoidal	-
	Rank	[-7.14 -7.14 10.00 20.00]	[10.00 20.00 33.33]	[20.00 33.33 201.30 209.30]	-	-
BOD <sub>5</sub> /P influent	Input	Shape	Trapezoidal	Triangular	Trapezoidal	-
	Rank	[-10.00 -1.00 10.00 50.00]	[10.00 50.00 100.00]	[50.00 100.00 200.00 210.00]	-	-
S <sub>5</sub> first biological reactor	Input	Shape	Trapezoidal	Triangular	Trapezoidal	-
	Rank	[-4.64 -4.64 4.00 14.00]	[9.00 20.00 34.00]	[29.00 40.00 131.60 143.00]	-	-
S <sub>5</sub> /X <sub>5</sub> influent	Input	Shape	Trapezoidal	Triangular	Trapezoidal	-
	Rank	[-0.08 -0.02 0.10 0.20]	[0.15 0.25 0.35]	[0.30 0.45 1.55 1.56]	-	-
S <sub>NOx</sub> last aerobic reactor	Input	Shape	Trapezoidal	Triangular	Trapezoidal	-
	Rank	[-1.43 -1.43 2.00 5.00]	[2.00 5.00 8.00]	[5.00 8.00 40.27 41.87]	-	-
Time for nitrogen gas production	Input	Shape	Trapezoidal	Triangular	Trapezoidal	-
	Rank	[-0.13 -0.04 0.05 0.06]	[0.05 0.06 0.07]	[0.06 0.07 2.21 2.27]	-	-
<b>Risk of filamentous bulking</b>	Output	Shape	Triangular	Triangular	-	-
	Rank	[-0.20 0.00 0.20]	[0.20 0.50 0.80]	[0.80 1.00 1.20]	-	-
<b>Risk of foaming</b>	Output	Shape	Triangular	Triangular	-	-
	Rank	[-0.20 0.00 0.20]	[0.20 0.50 0.80]	[0.80 1.00 1.20]	-	-
<b>Risk of rising sludge</b>	Output	Shape	Triangular	Triangular	-	-
	Rank	[-0.20 0.00 0.20]	[0.20 0.50 0.80]	[0.80 1.00 1.20]	-	-

Figure 4.8 presents the rules for the determination of a hypothetical problem (red line). As can be observed, only rules 2 and 3 are taken into account. According to the fuzzy rule 2: if variable I is “low” and variable II is “high”, then the membership function  $A_I$  has a “normal” membership function (represented in blue). According to fuzzy rule 3: if variable I is “normal” and variable II is “high”, then the membership function  $A_{II}$  is “low”. The sum up of the different rules contribution is presented in the last figure (function B). In this case, it can be concluded that the membership function for the risk of occurrence is mainly “normal” (i.e.  $A_I$  represents around 0.8 of the degree of membership, while  $A_{II}$  has only a value of 0.2).

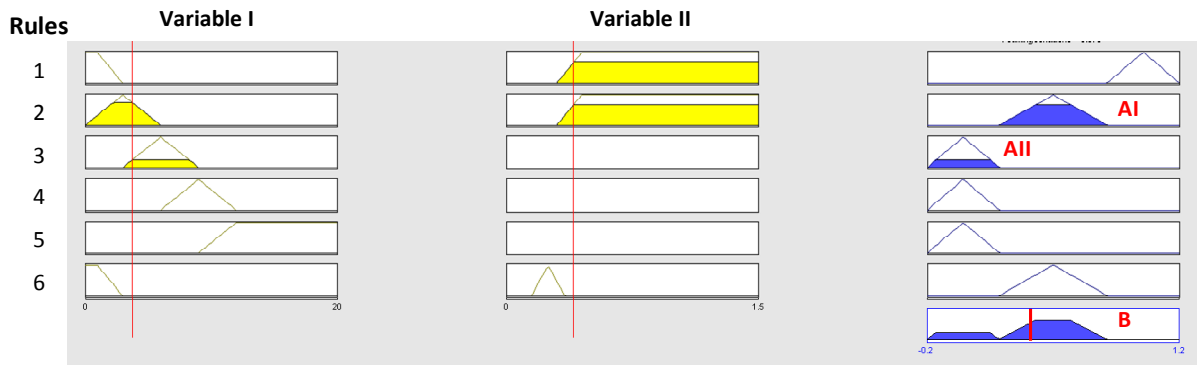


**Figure 4.8** Example of the rules for the determination of a hypothetical problem development risk. Adapted from Dalmau (2009).

Considering MR criterion in the optimisation process allowed more realistic optimal scenarios, in contrast to OCF, because the operational point optimised should guarantee a good effluent quality (low EQI), reduced operating costs (low OC) and low risk to develop settling problems (low MR).

#### 4.2.4. SIMULATION AND OPTIMISATION

As was stated before, this study was divided into two different parts. The first part of the study was based on the setpoint optimisation of the control system implemented in pilot plant I by means of OCF. The biological kinetic model used to describe C/N/P removal was IWA ASM2d (Henze *et al.*, 2000) and it was implemented in MATLAB® and integrated using *ode15s*, a variable order method recommended for stiff systems. In the second part, a new plant design was simulated, pilot plant II. In this case, the model used was an extension of ASM2d that included nitrite as additional state variable (see Annex I). Hence, nitrification and denitrification were modelled as two-step processes with nitrite as intermediate to describe accurately the anoxic COD consumption. The settling process was simulated using the model of Takács *et al.* (1991) and non-reactive settler was considered in this chapter.

Each control strategy was simulated during 28 days under different influent conditions (Dry-2, Rain-2 or Storm-2 influents proposed by the IWA Task Group on Benchmarking) and the setpoint optimisation was conducted using the results of the last 14 days of simulation. The

starting point for each simulation was the steady-state reached after a simulation of 100 days with Dry-2 influent under RO conditions. The setpoint optimisation aimed to find the maximum performance that a specific control structure could achieve. A perfect knowledge of the influent characteristics was considered for performing the optimisation (i.e. using the influent pattern presented before). Ammonium setpoint in R3 or R4 (for pilot plants I or II, respectively) and nitrate setpoint in R2 were optimised using two different methods:

- i) **OCF:** The optimal setpoints aimed at obtaining the minimum OCF under constrained conditions. Optimisation of a complex system as the operation of a WWTP is a challenging task, as the minimisation of functions depending on highly nonlinear dynamic systems may easily result in local minima. A previous test of different search methods was required in order to determine which method avoided local minima. Thus, the Genetic Algorithm, the Nelder-Mead method and Pattern Search were tested in Matlab® in order to optimise the setpoints of A&N-FS control strategy under Dry-2 influent conditions. All the optimisation methods were simulated with the same constrained conditions as shown in table 4.5.
- ii) **MCF:** Monte Carlo simulation principles were followed and thus, 1500 sets of setpoints in the proposed search space were randomly generated and evaluated. As was commented above, this optimisation method was only studied in the pilot plant II.

**Table 4.5** Initial setpoints and constrains for the evaluation of the different optimisation methods.

Initial setpoints (mg·L <sup>-1</sup> )		Lower bounds (mg·L <sup>-1</sup> )		Upper bounds (mg·L <sup>-1</sup> )	
N-NH <sub>4</sub> <sup>+</sup>	N-NO <sub>3</sub> <sup>-</sup>	N-NH <sub>4</sub> <sup>+</sup>	N-NO <sub>3</sub> <sup>-</sup>	N-NH <sub>4</sub> <sup>+</sup>	N-NO <sub>3</sub> <sup>-</sup>
1.0	0.5	0.0	0.0	10.0	5.0

## 4.3. Results and Discussion

### 4.3.1. EVALUATION OF DIFFERENT OPTIMISATION METHODS – PILOT PLANT I

In the first step of the study, different search methods were tested in order to determine which avoided local minima. A&N-FS control strategy with Dry-2 influent in pilot-plant I was used as case study because its optimisation could present local minima problems. The Genetic Algorithm (GA), the Nelder-Mead (NM) and Pattern Search (PS) methods were tested. According to table 4.6, the main differences among the search methods tested appeared when optimising ammonium setpoint value. Contrary, nitrate setpoint optimisation may not present multiplicity of local solutions and thus, no differences on the value for nitrate setpoint were observed. The optimised setpoints obtained using the GA method resulted in the highest operational costs. GA tends to converge asymptotically to a

particular value, which may or not be the absolute minimum (Nye, 2004). An asymptotic convergence implies that the results of the initial tested points will have an effect on the optimisation line, the following points to iterate; therefore, if the initial points are too different to the optimum, problems with local minima could appear. The application of Nelder-Mead (NM) search method, based on a modified simplex method, gave better results than GA. NM algorithm is prone to find local minima solutions; consequently, problems in the optimisation process could appear if the tested initial point had not been close to the absolute minimum or if the system had presented multiplicity of local solutions (Mathews and Fink, 2004), as could be expected in our case. For that reason NM method was discarded in this study. The minimal operational costs were obtained using the optimal values found with the Pattern Search (PS) method. PS algorithm operates by searching a set of points called pattern, which expands or shrinks depending on whether any point within the pattern has a lower objective function value than the current point. The search stops after a minimum pattern size is reached. This behaviour enables PS to explore more points in each iteration and thereby potentially avoids a local minimum that is not the global minimum (Doherty *et al.*, 2004). Therefore, PS was used as search method to optimise the different control strategies when using OCF.

**Table 4.6** Results of the optimisation of A&N-FS strategy with different search methods using Dry-2 influent in pilot plant I.

Search method	Optimised setpoints (mg·L <sup>-1</sup> )		Total Costs (€·m <sup>-3</sup> )
	N-NH <sub>4</sub> <sup>+</sup>	N-NO <sub>3</sub> <sup>-</sup>	
Pattern Search	2.90	0.10	0.195
Nelder-Mead	3.40	0.10	0.196
Genetic Algorithm	1.10	0.10	0.220

#### 4.3.2. OPERATIONAL COSTS FUNCTION – PILOT PLANT I

Table 4.7 summarises the main results for the different control strategies implemented in pilot plant I. For the three influents tested, the optimum N-NO<sub>3</sub><sup>-</sup> and N-NH<sub>4</sub><sup>+</sup> setpoints to minimise OCF were calculated. All the proposed control strategies were more efficient (in terms of lower effluent discharges and lower OC) than the RO. Each of the control strategies was simulated for 28 days. In parallel, some of these simulations were also run during 100 days in order to confirm that 28 days was a good approximation with a balanced computation time, with results differing less than 1%.

**Table 4.7** Summary of the different control strategies for the Dry-2, Rain-2 and Storm-2 influents and the main results of pilot plant I. CI is the cost improvement with respect to the reference operation.

	Operational Costs (€·m <sup>-3</sup> )						Setpoints (mg·L <sup>-1</sup> )		Time above limits (d)	Mean concentration (mg·L <sup>-1</sup> )			
	AE	PE	SP	EF	OCF	CI (%)	N-NH <sub>4</sub> <sup>+</sup>	N-NO <sub>3</sub> <sup>-</sup>		N-NH <sub>4</sub> <sup>+</sup>	TN	P-PO <sub>4</sub> <sup>3-</sup>	
Dry-2	RO	0.14	0.016	0.053	0.132	<b>0.341</b>	-	-	<b>14.00</b>	0.59	9.11	9.35	
	DOC	0.099	0.016	0.054	0.122	<b>0.291</b>	<b>14.83</b>	-	<b>14.00</b>	0.62	8.96	8.50	
	MPR	0.096	0.025	0.048	0.138	<b>0.308</b>	<b>9.70</b>	0.00	1.40	<b>14.00</b>	0.66	7.52	10.11
	A&N-FS	0.050	0.010	0.067	0.063	<b>0.190</b>	<b>44.31</b>	2.90	0.10	<b>8.32</b>	2.90	11.66	2.03
	A&N-WVS	0.051	0.009	0.069	0.059	<b>0.188</b>	<b>44.90</b>	3.00 <sup>wd</sup> 1.90 <sup>we</sup>	0.10 <sup>wd</sup> 0.06 <sup>we</sup>	<b>5.60</b>	2.43	12.27	1.34
	A&N-DVS	0.050	0.008	0.069	0.061	<b>0.188</b>	<b>44.90</b>	Variable	Variable	<b>5.10</b>	3.25	14.27	0.89
	A&N-HVS	0.036	0.006	0.070	0.101	<b>0.214</b>	<b>37.28</b>	Variable	Variable	<b>12.44</b>	7.02	15.49	0.33
	RO	0.14	0.019	0.024	0.138	<b>0.321</b>	-	-	-	<b>14.00</b>	0.75	8.18	8.96
DOC	0.096	0.019	0.025	0.129	<b>0.27</b>	<b>15.93</b>	-	-	<b>14.00</b>	0.83	8.02	8.29	
MPR	0.098	0.027	0.010	0.14	<b>0.275</b>	<b>14.28</b>	0.00	1.25	<b>14.00</b>	0.71	6.95	9.37	
A&N-FS	0.053	0.013	0.029	0.069	<b>0.164</b>	<b>48.86</b>	2.70	0.10	<b>9.04</b>	2.70	10.20	2.37	
A&N-WVS	0.055	0.009	0.035	0.064	<b>0.163</b>	<b>49.30</b>	3.30 <sup>wd</sup> 2.10 <sup>we</sup> 2.90 <sup>ra</sup>	0.10 <sup>wd</sup> 0.06 <sup>we</sup> 0.10 <sup>ra</sup>	<b>3.90</b>	2.88	12.01	0.94	
A&N-DVS	0.056	0.008	0.036	0.063	<b>0.163</b>	<b>49.24</b>	Variable	Variable	<b>3.53</b>	3.00	12.28	0.71	
A&N-HVS	0.038	0.007	0.037	0.09	<b>0.172</b>	<b>46.34</b>	Variable	Variable	<b>9.05</b>	5.74	14.01	0.50	
Storm-2	RO	0.14	0.017	0.034	0.136	<b>0.326</b>	-	-	<b>14.00</b>	0.68	8.67	9.18	
	DOC	0.098	0.018	0.035	0.126	<b>0.277</b>	<b>15.10</b>	-	<b>14.00</b>	0.74	8.55	8.37	
	MPR	0.098	0.027	0.031	0.141	<b>0.296</b>	<b>9.25</b>	0.00	1.40	<b>14.00</b>	0.74	7.29	9.78
	A&N-FS	0.055	0.012	0.052	0.066	<b>0.185</b>	<b>43.47</b>	2.80	0.10	<b>8.15</b>	2.80	11.28	2.01
	A&N-WVS	0.058	0.009	0.056	0.062	<b>0.184</b>	<b>43.65</b>	3.10 <sup>wd</sup> 2.30 <sup>we</sup> 1.60 <sup>st</sup>	0.10 <sup>wd</sup> 0.06 <sup>we</sup> 1.30 <sup>st</sup>	<b>4.60</b>	2.53	12.03	1.34
	A&N-DVS	0.057	0.009	0.056	0.063	<b>0.184</b>	<b>43.50</b>	Variable	Variable	<b>4.43</b>	3.09	14.98	0.60
	A&N-HVS	0.037	0.007	0.057	0.106	<b>0.206</b>	<b>36.76</b>	Variable	Variable	<b>11.37</b>	5.95	13.73	0.70

<sup>wd</sup> Weekdays, <sup>we</sup> Weekend, <sup>ra</sup> Rain and <sup>st</sup> Storm.

In the RO, ammonium and nitrate concentrations were always below the discharge limits (Tables 4.2 and 4.7). However, the excessive aeration together with the high nitrate recycled to the anaerobic reactor outcompeted PAO for the carbon source in favour of OHO. As a result, effluent average phosphate concentration (9.35 mg P-PO<sub>4</sub><sup>3-</sup>·L<sup>-1</sup> for Dry-2 influent) was well above the discharge limit resulting in the highest OCF among all the control strategies proposed for the three studied influents.

DOC strategy avoided unnecessary aeration, leading to a decrease of aeration costs (Table 4.7 and Figure 4.9). Besides, less DO in the reactors involved lower nitrifying activity and thus, lower nitrate recycle to the anaerobic reactor. This lower presence of nitrate and DO under anaerobic conditions reduce the competition between OHO and PAO for the carbon source, resulting in more COD available for EBPR. Thus, some reduction in the effluent fines for the three influents tested was observed due the slight improvement of P removal.

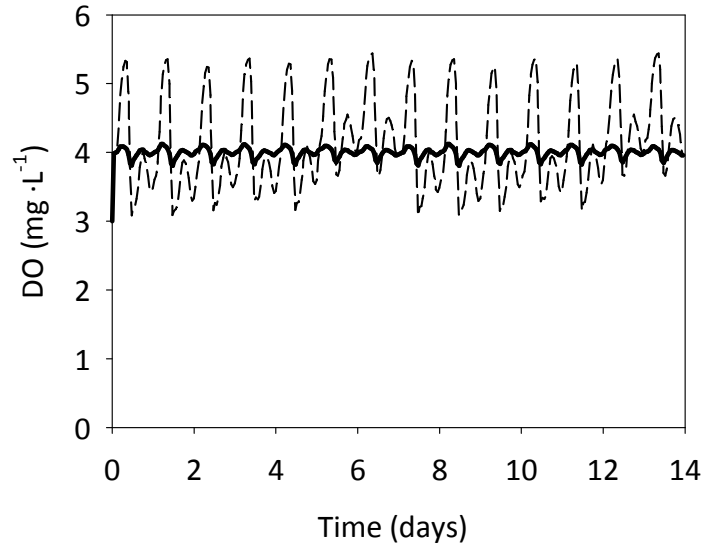


**Figure 4.9** DO concentration in R4 of pilot plant I under RO conditions (dashed lines) and after the implementation of DOC strategy with a setpoint of  $4 \text{ mg DO}\cdot\text{L}^{-1}$  (solid line).

In the MPR strategy, ammonium setpoint was fixed to  $0 \text{ mg N-NH}_4^+\cdot\text{L}^{-1}$  and the nitrate setpoint in R2 was optimised to minimise the effluent nitrate concentration (Table 4.7). This strategy did not result in the minimal OCF because EBPR was not favoured and thus, effluent phosphate was always above the discharge limit, as also occurred in the RO. Moreover, the ammonium concentration could not be reduced to  $0 \text{ mg}\cdot\text{L}^{-1}$  even though the maximum aeration was reached ( $4 \text{ mg DO}\cdot\text{L}^{-1}$ ) almost all the simulated period.

When A&N-FS was tested (Figure 4.10), the major cost reduction appeared in the aeration term. As figure 4.10 F shows, only the strictly necessary oxygen for nitrification was supplied to achieve the optimised ammonium setpoint ( $2.90 \text{ mg N-NH}_4^+\cdot\text{L}^{-1}$ ), which was increased with respect to the MPR strategy ( $0 \text{ mg N-NH}_4^+\cdot\text{L}^{-1}$ ). An increase in the total nitrogen effluent was also observed in comparison with MPR strategy. In order to ensure the optimum nitrate setpoint ( $0.10 \text{ mg N}\cdot\text{L}^{-1}$ ) less nitrate was recycled to R2 and thus, less nitrogen was denitrified. Under these conditions, despite more nitrate was recycled to R1 by the  $Q_{\text{REXT}}$ , R2 behaved as anaerobic reactor enabling some P release and favouring PAO growth (e.g. steady state values of PAO population of 18 and  $760 \text{ mg COD}\cdot\text{L}^{-1}$  were obtained for MPR and A&N-FS, respectively). In addition, the reduction of DO concentration in the aerobic reactors to ensure ammonium setpoint also favoured EBPR process because less oxygen was recycled to the anaerobic reactor by  $Q_{\text{REXT}}$ . As a result, the time that phosphate was above the discharge limits and the total effluent fines value decreased (Table 4.7). This fact reveals the importance of a setpoint optimisation with a cost function which weighs up all the nutrient concentrations in the effluent (including P). In other words, the optimal setpoints chosen favoured P removal, although there was not any specific control-loop implemented for phosphorus concentration.



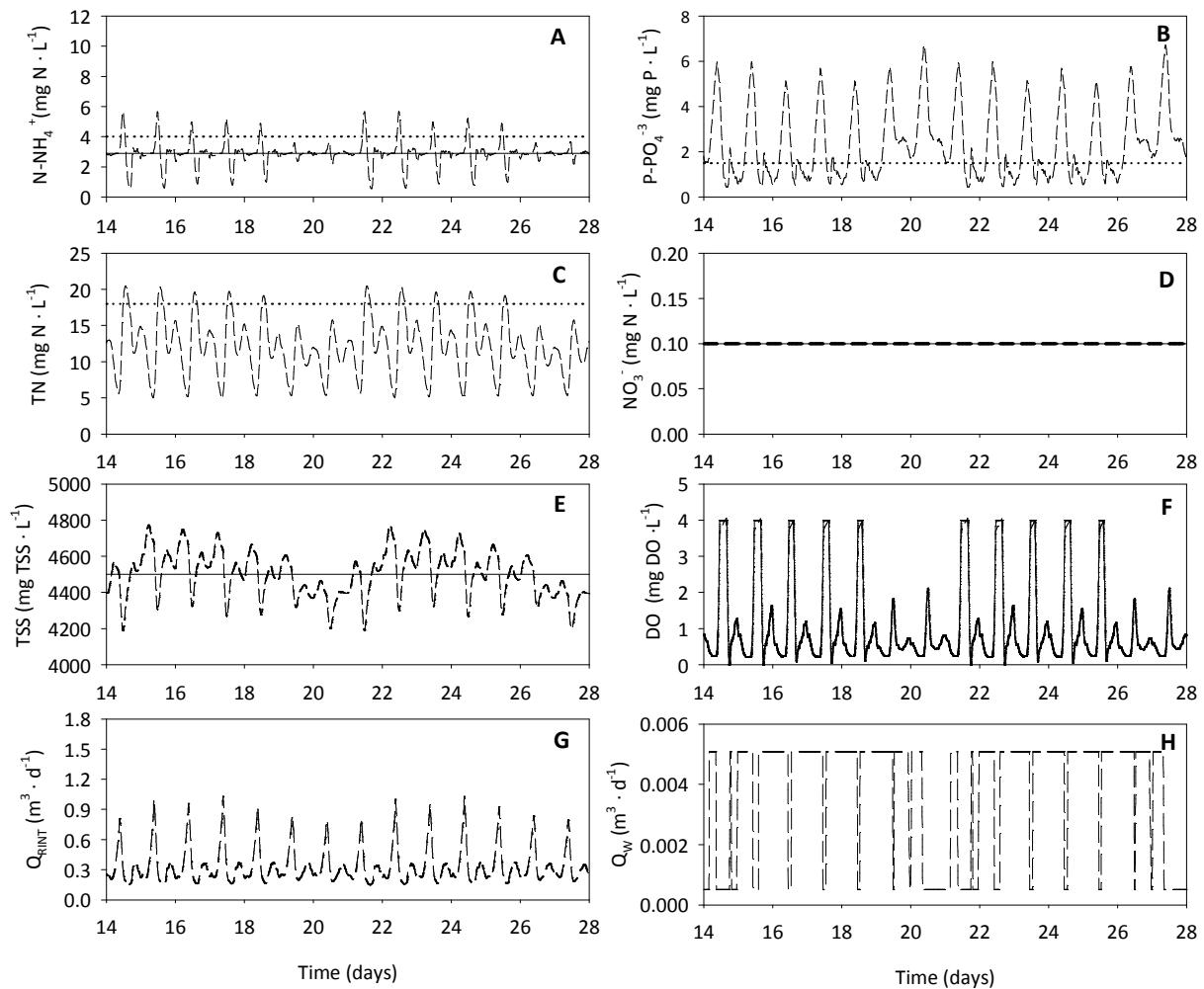


**Figure 4.10** A&N-FS control strategy behaviour for Dry-2 influent in pilot plant I. (A) Ammonium R4; (B) Phosphate R4; (C) Total Nitrogen R4; (D) Nitrate R2; (E) TSS R4; (F) DO setpoint R4; (G)  $Q_{RINT}$ ; (H)  $Q_W$ . Dashed lines belong to system measurements, dotted lines belong to the limit of pollutant ( $4 \text{ mg N-NH}_4^+ \cdot \text{L}^{-1}$ ,  $18 \text{ mg TN} \cdot \text{L}^{-1}$  and  $1.5 \text{ mg P-PO}_4^{3-} \cdot \text{L}^{-1}$ ) and solid lines to optimised setpoints.

The simulated influent flow pattern presented significant time variations mimicking real WWTP influents. Hence, the A&N-DVS strategy was believed to be a sensible alternative to reduce the OCF (Figure 4.11). The new daily control setpoints would adapt the plant operation to the daily influent variations intensifying the C/N/P removal when necessary. Unexpectedly, the implementation of this control strategy did not result in an important OCF reduction when compared to the A&N-FS strategy (Table 4.7), despite a 40% decrease of time above discharge limits, in the three studied scenarios, was observed. This could be explained because of phosphate effluent concentration was below the discharge limits when A&N-DVS was applied, contrary to A&N-FS. Once again, the increase of effluent nitrate evidenced a decrease of the nitrate recycled to R2 to achieve the desired setpoint and thus, obtaining anaerobic conditions that favoured EBPR process.

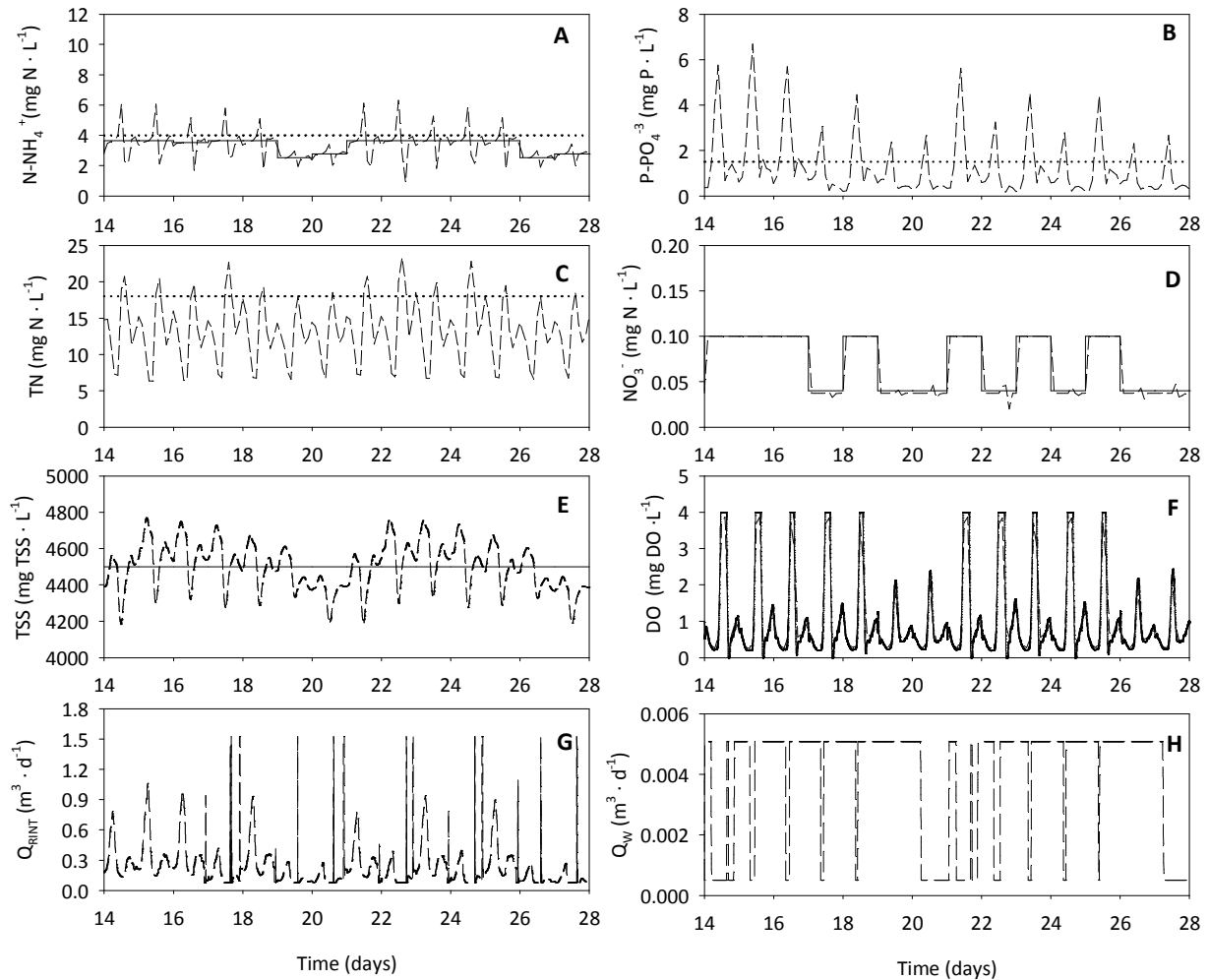


**Figure 4.11** A&N-DVS control strategy behaviour for Dry-2 influent in pilot plant I. (A) Ammonium R4; (B) Phosphate R4; (C) Total Nitrogen R4; (D) Nitrate R2; (E) TSS R4; (F) DO setpoint R4; (G)  $Q_{RINT}$ ; (H)  $Q_W$ . Dashed lines belong to system measurements, dotted lines belong to the limit of pollutant ( $4 \text{ mg N-NH}_4^+ \cdot \text{L}^{-1}$ ,  $18 \text{ mg TN} \cdot \text{L}^{-1}$  and  $1.5 \text{ mg P-PO}_4^{3-} \cdot \text{L}^{-1}$ ) and solid lines to optimised setpoints.

The optimised setpoints obtained for A&N-DVS presented substantial differences between weekend and weekdays for ammonium setpoints. For this reason, the utilization of two different sets of setpoints (one for weekend and one for the weekdays) was tested in the strategy A&N-WVS (Figure 4.12). For Rain-2 and Storm-2 influents, a third set of setpoints was proposed (Table 4.7) since differences in rain and storm periods were also observed in daily setpoint optimisation. Nevertheless, the results of A&N-WVS were very similar to the ones obtained with A&N-DVS; however this strategy allowed a reduction in the number of parameters to be optimised (i.e. the required time in the optimisation step decreased). The observed changes in the setpoint for nitrate were marginal: a maximum difference of  $0.05 \text{ mg N-NO}_3^- \cdot \text{L}^{-1}$  was detected. This small range is below the usual margin of accuracy of an on-line sensor for nitrate and, hence, a fixed setpoint around  $0.1 \text{ mg N-NO}_3^- \cdot \text{L}^{-1}$ , the value obtained in A&N-FS strategy, can be recommended for this WWTP configuration. Therefore, the implementation of A&N-WVS strategy could be more feasible in a real WWTP than the

daily optimisation, although a low increase in time above discharges limits could be observed when compared to A&N-DVS.

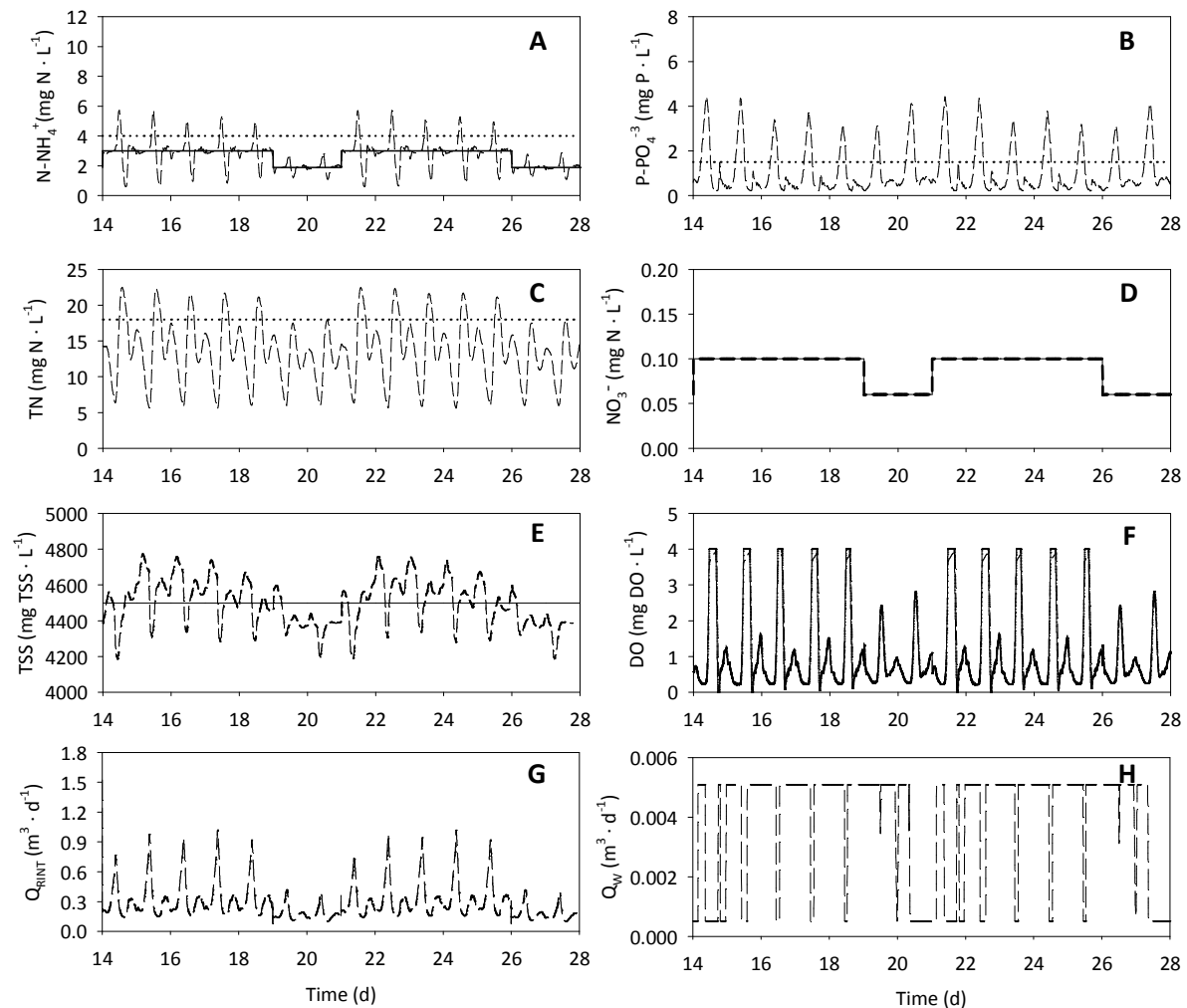


**Figure 4.12** A&N-WVS control strategy behaviour for Dry-2 influent in pilot plant I. (A) Ammonium R4; (B) Phosphate R4; (C) Total Nitrogen R4; (D) Nitrate R2; (E) TSS R4; (F) DO setpoint R4; (G)  $Q_{RINTE}$ ; (H)  $Q_W$ . Dashed lines belong to system measurements, dotted lines belong to the limit of pollutant ( $4 \text{ mg N-NH}_4^+ \cdot \text{L}^{-1}$ ,  $18 \text{ mg TN} \cdot \text{L}^{-1}$  and  $1.5 \text{ mg P-PO}_4^{-3} \cdot \text{L}^{-1}$ ) and solid lines to optimised setpoints.

Influent pattern also presented hourly variations, and then a new control strategy was proposed to adapt the plant operation to these changes. When hourly optimised setpoints strategy was tested (A&N-HVS), the OCF increased with respect to A&N-FS or A&N-WVS. Although the system achieved the highest phosphate removal (Table 4.7), ammonium and nitrate removal was worsened and the time above the discharged limits and the effluent fine costs increased. As can be observed in figure 4.13, the ammonium setpoint was above the discharge limit ( $4 \text{ mg} \cdot \text{L}^{-1} \text{ N-NH}_4^+$ ) almost all the simulated period and the denitrification capacity was highly reduced due to the low nitrate setpoint value ( $<0.05 \text{ mg} \cdot \text{L}^{-1}$ ), what improved P-removal.

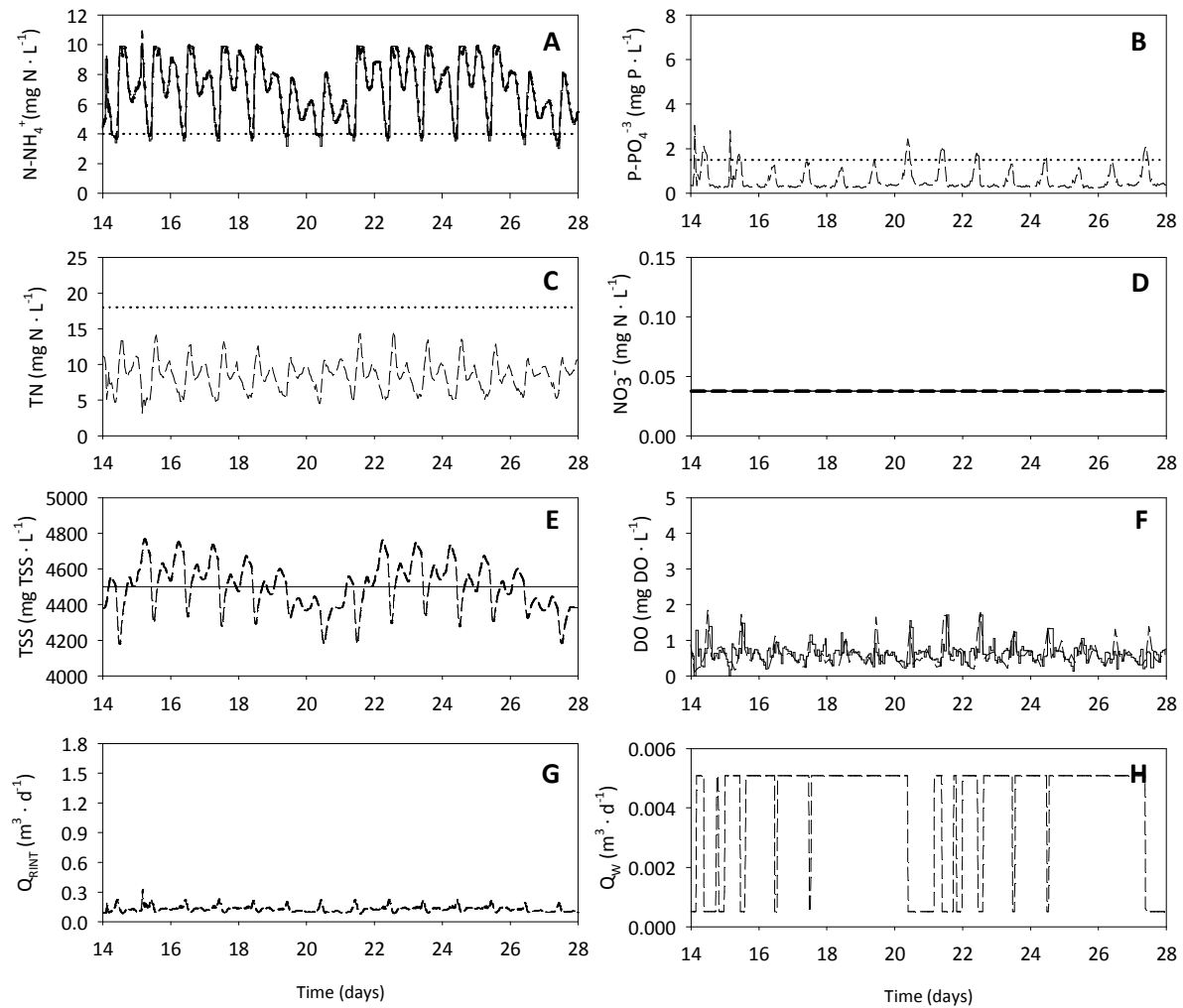


**Figure 4.13** A&N-HVS control strategy behaviour for Dry-2 influent in pilot plant I. (A) Ammonium R4; (B) Phosphate R4; (C) Total Nitrogen R4; (D) Nitrate R2; (E) TSS R4; (F) DO setpoint R4; (G)  $Q_{RINT}$ ; (H)  $Q_W$ . Dashed lines belong to system measurements, dotted lines belong to the limit of pollutant ( $4 \text{ mg N-NH}_4^+ \cdot \text{L}^{-1}$ ,  $18 \text{ mg TN} \cdot \text{L}^{-1}$  and  $1.5 \text{ mg P-PO}_4^{3-} \cdot \text{L}^{-1}$ ) and solid lines to optimised setpoints.

The A&N-HVS strategy aimed at finding the optimum set of setpoints for a specific hour without taking into account the state of the system at the end of that hour, i.e. the initial conditions for the next optimisation. The influent pattern had load variations along the time, so the optimum setpoints applied in low load periods reduced the system treatment capacity. When a peak load then appeared, the plant was not capable to remove efficiently the pollutants in a short term. This fact led the system to a new situation where the new optimised set of setpoints guaranteed the minimum OCF in that hour, but did not reach a decrease in the total costs after the whole period of 14 days. These results suggested that when a peak load appeared, the optimum points obtained from A&N-HVS described a scenario where the minimal OCF value was obtained reducing the operating costs, such low aeration energy for example (Figure 4.13 F), at expenses of high pollutant content in the effluent. Hence, the weight selection to translate the different components of OCF into monetary units needs special attention. When A&N-DVS was applied, the aforementioned

behaviour for A&N-HVS was not observed due to the influent pattern described daily cycles (i.e. the initial conditions for the next optimisation were almost the same for all the days) and only weekend days were different to the rest.

Based on the simulated results, from an operational point of view, the utilisation of different set of setpoints that have to be optimised hinders the real implementation of some of the control strategies proposed. Hence, new simulations were proposed to study whether the optimum A&N-WVS set of setpoints found for Dry-2 provided good results under Storm-2 and Rain-2 influent conditions. As can be observed in table 4.8, OCF and the time above the limits obtained using the Dry-2 optimised setpoints with the Rain-2 and Storm-2 influents were very similar to those obtained with the specific optimum setpoints for these influents. This observation casts doubts on the need of specific sets of setpoints for storm or rain periods. Rain influent was the only case that presented a little increase in the time above limits (10%) when optimum A&N-WVS setpoints for Dry-2 were used due to the higher duration of the rain scenario compared to storm scenario. The similarity in the results obtained is an advantage, as an accurate optimisation of only week and weekend days can provide a set of setpoints that improves the WWTP operation for different scenarios where some influent perturbations could appear.

**Table 4.8** Performance comparison of A&N-WVS with setpoints optimised for each influent or with a general set of optimised setpoints (Dry-2 influent) in pilot plant I.

	Specific influent optimised setpoints		Dry-2 influent optimised setpoints	
	OCF (€·m <sup>-3</sup> )	Time above discharges limits (d)	OCF (€·m <sup>-3</sup> )	Time above discharges limits (d)
<b>Dry-2</b>	0.192	5.60	0.192	5.60
<b>Rain-2</b>	0.163	3.90	0.164	4.30
<b>Storm-2</b>	0.184	4.60	0.184	4.70

Finally, in order to gain more insight about the importance of the weight selection in OCF, a sensitivity analysis for the A&N-WVS was performed (Table 4.9). For this purpose, the values of the effluent fines parameters (i.e.  $\Delta\alpha_j$ ,  $\Delta\beta_j$  and  $\beta_{0,j}$  from table 4.2) were increased and decreased  $\pm 50\%$ . When EF parameters were increased, the obtained optimum setpoints resulted in a decrease of 15.5 % in the effluent time above limits, although an increase less than 1.9 % in terms of aeration, pumping or sludge production costs (APSC) was observed. Contrary, reducing the effluent fines had a low effect in the time above discharge limits (1.3% higher) and in the APSC value (2.4% lower). As can be observed APSC values were not highly affected when effluent fines parameters were modified. These results suggest that the APSC may have an excessive weight in contrast to the monetary effluent quality penalties. Along this line of thinking, it could be extracted that optimising the setpoints when all the criteria are converted into monetary units as in OCF could unfortunately lead to

high EQI compensated with minimal APSC (e.g. low aeration allow high energy savings but limiting nitrification process). Hence, the weight selected for the effluent fines is a key factor to avoid not subordinating the costs of plant operation (aeration, pumping and the sludge production) to the quality of the effluent. To overcome these problems, multi-criteria tools were studied in the next step of the study since they allow optimizing a system with different criteria which are not conditioned by other.

**Table 4.9** Summary of sensitivity analysis results for different values of effluent fines for pilot plant I. VI is the variation interval of the values when compared to A&N-WVS. APSC is the sum of the Aeration costs, Pumping costs and Sludge production costs. *wd* Week days and *we* Weekend days.

	APSC (€·m <sup>-3</sup> )	VI (%)	N-NH <sub>4</sub> <sup>+</sup> Setpoint (mg·L <sup>-1</sup> )	VI (%)	N-NO <sub>3</sub> <sup>-</sup> Setpoint (mg·L <sup>-1</sup> )	VI (%)	Time above limits (d)	VI (%)
<b>A&amp;N-WVS</b>	0.129	-	3.00 <sup>wd</sup>	-	0.10 <sup>wd</sup>	-	5.60	-
			1.90 <sup>we</sup>	-	0.06 <sup>we</sup>	-		
<b>A&amp;N-WVS + 50% EF</b>	0.131	1.9	2.80 <sup>wd</sup>	- 6.67	0.08 <sup>wd</sup>	- 20.0	4.73	- 15.5
			1.90 <sup>we</sup>	0.00	0.04 <sup>we</sup>	- 33.3		
<b>A&amp;N-WVS - 50% EF</b>	0.126	-2.4	3.70 <sup>wd</sup>	23.33	0.10 <sup>wd</sup>	0.0	5.67	1.3
			2.40 <sup>we</sup>	26.32	0.06 <sup>we</sup>	0.0		

#### 4.3.3. OPERATIONAL COSTS FUNCTION *versus* MULTI-CRITERIA FUNCTION – PILOT PLANT II

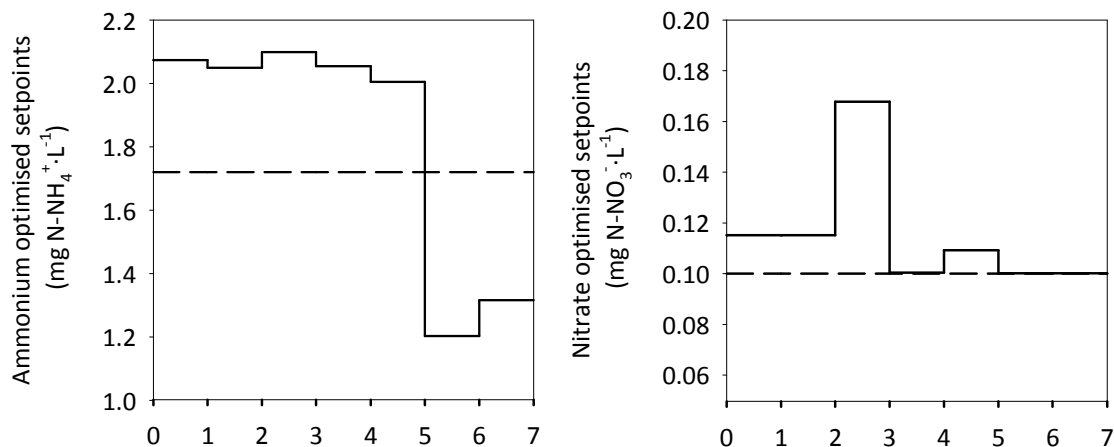
Based on the above results, it was studied how the setpoint optimisation could be affected by the construction of the objective function, for example by the weight selection when calculating the operational costs or by the evaluation of the effluent quality. For this aim, the OCF was compared with a multi-criteria function (MCF). The main difference between both functions is the fact that none of the criterion studied was conditional to the other in MCF (i.e. EQI and OC were analyzed separately in MFC), contrary to OCF where the effluent quality was translated into monetary units. The setpoints of A&N-FS and A&N-DVS were then optimised using both objective functions under Dry-2 conditions in pilot plant II. As was commented before, pilot plant II mimicked the hydraulic model of a real pilot plant, where the results here presented would be further evaluated.

Table 4.10 summarises the main results obtained when OCF was minimised. EQI and MR indexes were also quantified for comparison purposes, although they were not used directly for the minimization. The optimised control strategies resulted in a more efficient operation than the RO, as was above observed in pilot plant I. A decrease of 40% in the OCF was obtained mainly due to the decrease of the EF (the pollutant effluent content, EQI, was reduced by up to 28% when comparing to RO). P-removal efficiency was again improved

from 8.5% obtained in RO to 84% for the optimised control strategies, despite there was not any specific control-loop implemented for P-removal. As was commented for pilot plant I, the optimised setpoints for nitrate in R2 and ammonium in R3 resulted in proper operational conditions to favour EBPR process. The utilization of fixed and daily variable optimised setpoints provided similar results (Table 4.10) and A&N-DVS optimised setpoints could be again grouped in two different set of setpoints, one for weekdays and the other for weekends (Figure 4.14). The setpoints were directly related to wastewater load and so, lower optimum setpoints especially for ammonium were obtained for weekend days.

**Table 4.10** Summary of the different control strategies for the Dry-2 influent in pilot plant II. CI is the cost improvement with respect to the reference operation expressed in percentage.

	Operational Costs (€·m <sup>-3</sup> )					CI (%)	Time above limits (d)	EQI (kg Pu·m <sup>-3</sup> )
	AE	PE	SP	EF	OCF			
RO	0.053	0.018	0.047	0.136	<b>0.253</b>	-	13.90	0.292
A&N-FS	0.032	0.011	0.068	0.045	<b>0.156</b>	<b>38.37</b>	3.50	0.212
A&N-DVS	0.030	0.013	0.067	0.044	<b>0.154</b>	<b>39.17</b>	4.00	0.208



**Figure 4.14** Best setpoints obtained by OCF optimisation in pilot plant II. Dashed lines belong to ammonium (Left) and nitrate (Right) for A&N-FS control strategy and solid lines the setpoints for A&N-DVS control strategy.

The percentage of time with high MR occurrence (i.e. percentage of simulated time above a risk of 0.8) was also reduced by up to 25% when comparing the optimised control strategies to the RO, even though this criterion was not included in the optimisation process. As figure 4.15 shows, the possibility to develop bulking or foaming formed the main contribution in the MR value. The setpoint optimisation resulted in better removal efficiency and in higher biomass growth, so the purge flow rate had to be increased to maintain the TSS setpoint (2500 mg TSS·L<sup>-1</sup>) of the system. This behaviour resulted in a decrease in the SRT, which reduced the probability to develop bulking or foaming problems (Comas *et al.*, 2008), the main microbial risks in the RO.

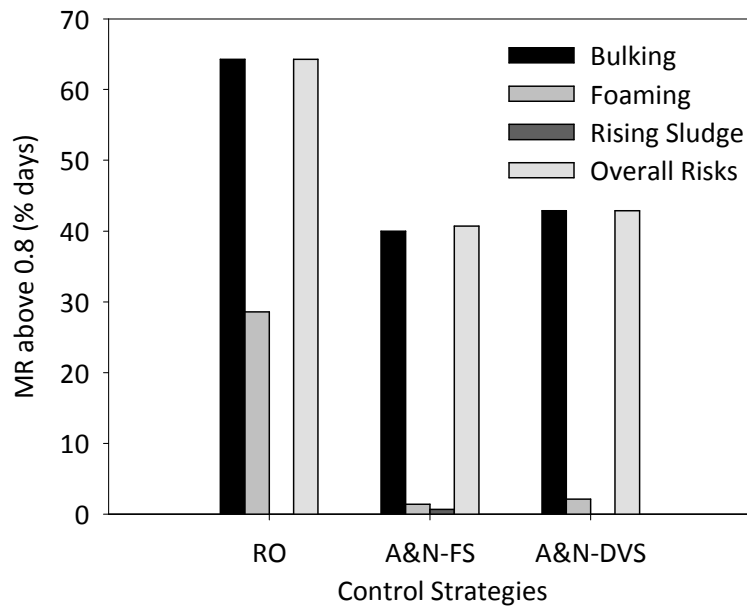


**Figure 4.15** Percentage of simulated time (14 days) that microbiological risks probability to develop solid separations problems was above 0.8 in pilot plant II.

Optimising the setpoints when all the criteria are converted into monetary units as in OCF could unfortunately lead to high EQI value compensated with minimal OC. In MFC, the OC and the EQI were analyzed separately and an additional performance criterion was considered, MR. Hence, theoretical optimal scenarios (i.e. low EQI and OC) but with an unrealistic application in full-scale WWTP due to high risk of MR occurrence could be rejected. MCF was evaluated for 1500 randomly generated sets of setpoints for A&N-FS control strategy. The results obtained for the three criteria were represented in pairs (Figure 4.16), resulting in the formation of Pareto fronts except for the MR-OC pair. In the Pareto front, any point is better than other on both criteria at the same time or, in other words, any point could be improved in one criterion without worsening the other. Hence, improving the EQ (i.e. low EQI) by reducing the amount of pollutants in the effluent resulted in an OC increase. This was caused by the increase of the aeration required for nitrification and the increase of the internal recycle flow rate required to denitrify the produced nitrate. These facts resulted in an increase of energy consumption and thus, in the OC. For MR-EQI pair, setpoints leading to high concentration of pollutants in the effluent resulted in lower MR. In these scenarios, more readily biodegradable organic substrates ( $S_5$ ) would enter to the aerated reactor (less organic matter was used for denitrification process) increasing biomass growth. Consequently, the purge flow rate would be increased to maintain the TSS setpoint resulting in a decrease of SRT, which lowers the risk for occurrence of bulking or foaming (Comas *et al.*, 2008). For MR-OC pair (Figure 4.16, right), although the points tested could not be approximated by a Pareto front, a point with the lowest OC ( $0.10 \text{ €}\cdot\text{m}^{-3}$ ) was found. Moreover, a limit of minimal occurrence of MR (around 40%) for any OC and a maximum of



67% was obtained. Figure 4.16 also shows that the operating point found by OCF optimisation (i.e. calculated by using different weights to convert EQ and OC into monetary units) was well located in the Pareto front of OC and EQ. This result demonstrates that the OCF optimisation was a specific case of the Pareto front for OC and EQ. Moreover, as MR was not included in the OCF, this optimised operating point does not appear in the Pareto front of EQ-MR or in MR-OC as expected.

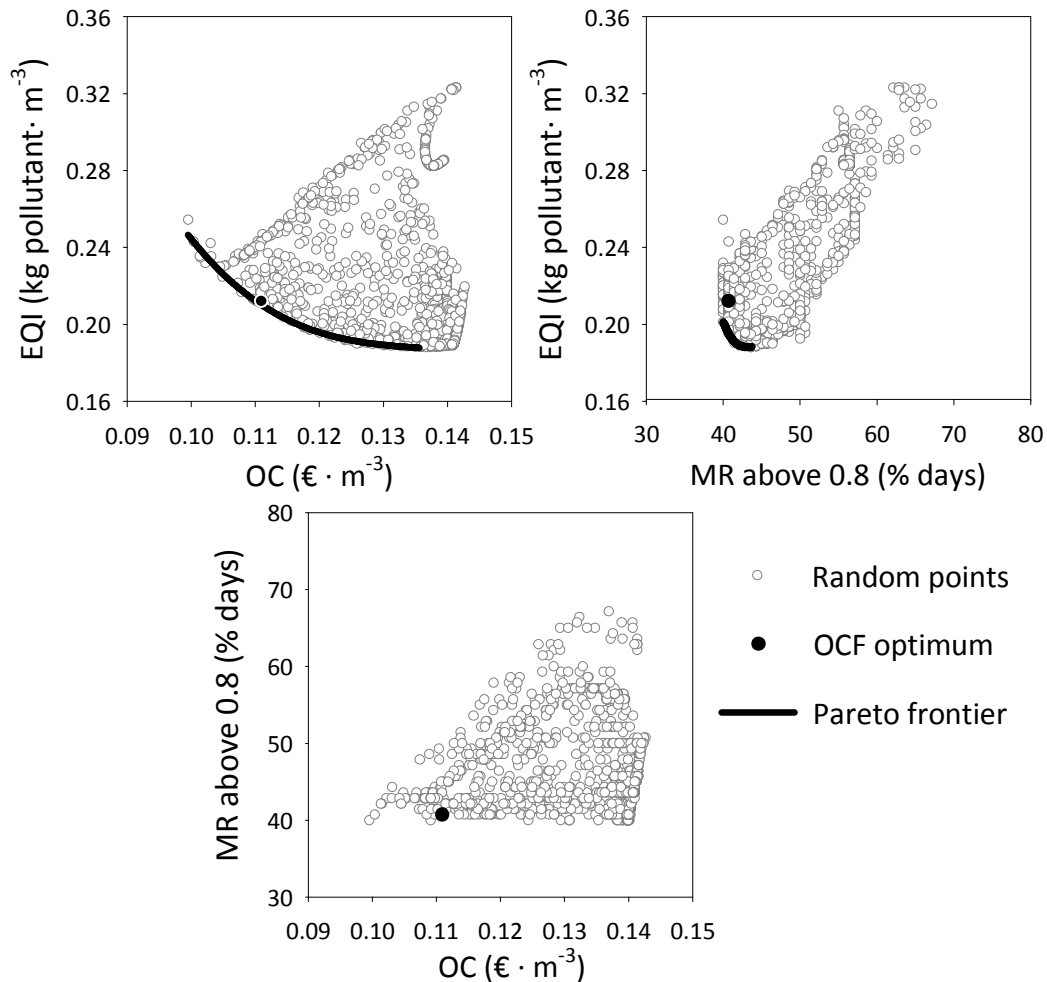


**Figure 4.16** Results of the Monte Carlo simulations (1500 random set of setpoints) for A&N-FS control strategy using the MCF for pilot plant II.

Figure 4.17 represents the three criteria evaluated with the MCF in a single graph for the A&N-FS control strategy. As can be observed, the optimal points could be approximated by a Pareto surface. The optimum point obtained with the OCF was practically part of the Pareto surface, being a nice example of such optimal operational scenarios that are defined by the weight selection. Hence, the regional effluent quality requirements or electricity cost would play the major role in the selection of a setpoint from the Pareto surface to obtain a particular operational scenario.

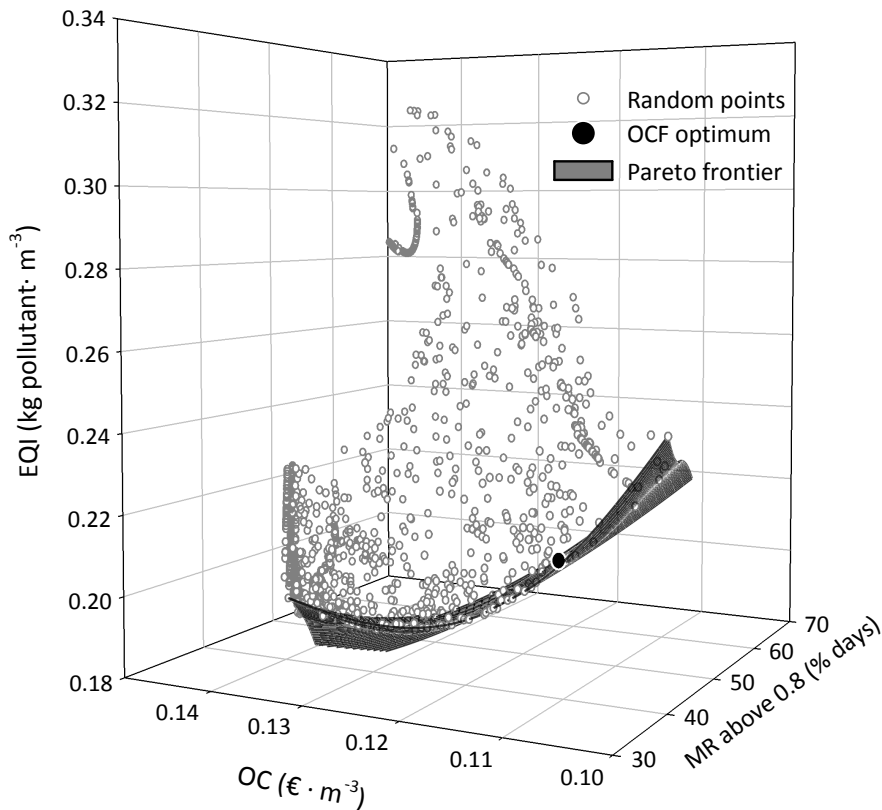


**Figure 4.17** Three-dimensional representation of the A&N-FS control strategy for pilot plant II in terms of OC, EQI and MR for 1500 random set of daily setpoints.

Table 4.11 shows the results obtained for two different points situated at the edges of the Pareto surface where the value of one of the criteria was minimal. The operating point that resulted in the lowest OC value conducted the system to aeration energy savings (i.e. reduction of aeration costs) but limiting the nitrification process (i.e. the ammonium nitrogen setpoint was  $9.71 \text{ mg}\cdot\text{L}^{-1}$ ). Moreover, the internal recycle, which was involved in the nitrate control loop, was extremely reduced in order to decrease the pumping costs (i.e. nitrate setpoint was  $< 0.01 \text{ mg}\cdot\text{L}^{-1}$ ). Consequently, the biological nutrient capacity of the system was reduced and the effluent pollutant concentration obviously increased. Hence, these actions resulted in high EQI values. When the scenario with the minimal value of EQI was selected ( $2.35$  and  $0.44 \text{ mg}\cdot\text{L}^{-1}$  were the setpoints for ammonium and nitrate nitrogen, respectively), the removal capacity of the plant was highly enhanced resulting in an effluent with low pollutant content. However, the aeration invested to improve the nitrification process and the energy applied in the internal recycle increased the OC. With respect to the MR, both scenarios resulted in a similar plant performance. In both cases, the low SRT obtained resulted in a lower risk for occurrence of bulking problems, the major microbiology-related problem observed in this study. In fact, the rest of the parameters to determine MR were related to the influent conditions, which were the same for all the operational scenarios and thus, no important variations in MR determination were observed.

**Table 4.11** Results obtained for two operating points at the edges of the Pareto surface.

Criteria minimised	Operational Costs (€ · m <sup>-3</sup> )	Effluent Quality (kg pollutant · m <sup>-3</sup> )	Microbiological Risks above 80% (%)
Operational Costs	0.099	0.254	40.00
Effluent Quality	0.137	0.188	42.14

For A&N-DVS strategy, a daily profile of setpoints was generated from the 1500 random set of setpoints tested in the A&N-FS (i.e. the average value of the daily profile was the setpoint tested in the A&N-FS). The optimal daily setpoints found with the OCF evidenced substantial differences between weekend and weekdays (Figure 4.14), for this reason, the setpoints for the weekend period were randomly reduced in order to adapt the system to the above-mentioned flow pattern behaviour.

Figure 4.18 shows the results of MCF when the A&N-DVS control strategy was implemented. As also was observed in section 4.3.2 for OCF, this strategy did not result in a significant improvement of any criterion compared to A&N-FS and it was required a much more complex optimisation process since 28 setpoints were evaluated (2 setpoints for each of the 14 days). In a preliminary optimisation test, an unconstrained random generation of the setpoints for A&N-DVS control strategy was performed resulting in a non-practical plant operation since a highly variable and inconsistent profile of setpoints was obtained. This fact showed the importance of using optimisation methods without random point generation as for example the minimisation method (PS) used in the OCF optimisation. Hence, the complementarity of MCF and OCF methods should be considered. Once a consistent set of weights is chosen (i.e. according to the legislation), the OCF-strategy could be used to obtain an optimum setpoint profile that could adapt the plant operation to the influent variations with lower calculation efforts. On the other hand, the utilization of MCF led to a more thorough evaluation where none of the criteria was conditional to the other. Moreover, a Pareto surface could be drawn using MCF approach including microbiological problems related to the solids separation encountered in the daily operation of the plant. The inclusion of MR index ensures that the optimum control strategy obtained has low risk of developing settling problems of microbiological origin. If the OCF approach had to be used, the translation of MR into monetary units would be required. In this sense, some authors (Flores-Alsina *et al.*, 2009b) have already reported model-based studies where the settling process was modified according to the occurrence of such solid separation problems. The change in settleability would have an impact on the effluent TSS concentration, which is used to calculate EQ, and would finally provide a measurable effect of MR on EQ and in the effluent fines calculation.

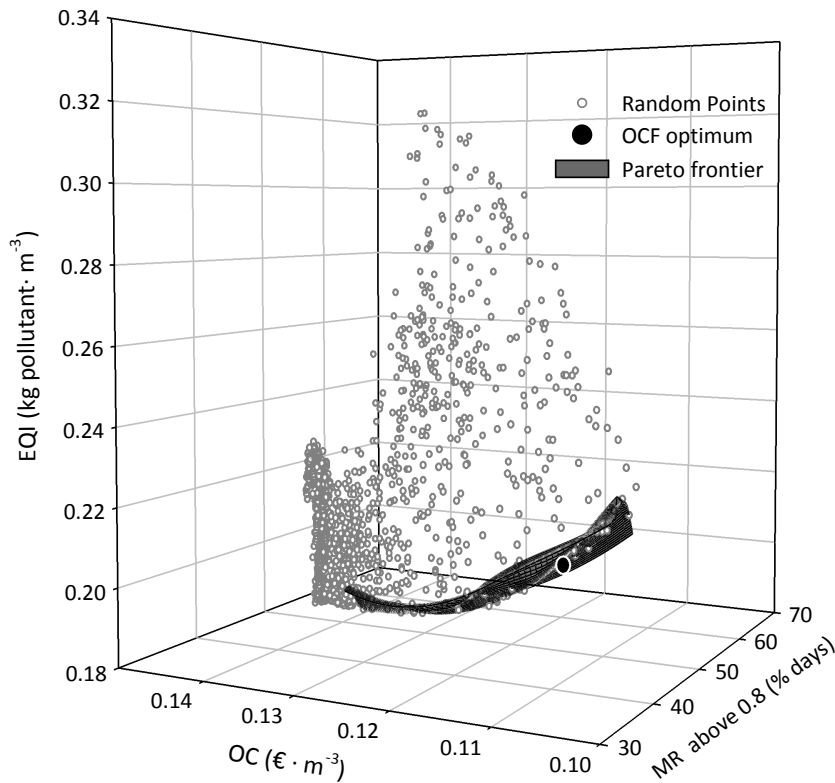


**Figure 4.18** Three-dimensional representation of the A&N-DVS control strategy for pilot plant II in terms of OC, EQI and MR for 1500 random set of daily setpoints.

#### 4.4. Practical Implications

Some limitations could appear for the implementation of the proposed approach in a full-scale WWTP with a highly variable influent (mainly for A&N-DVS implementation), since perfect knowledge of the influent is required for finding the optimum setpoints. In this case, the utilization of feed-forward control is recommended in order to adapt the plant operation to the highly variable influent, although additional sensors gathering information of the influent would be required (Shen *et al.*, 2009). For example, in A&N-HVS strategy the utilization of feed-forward control would be helpful to anticipate the plant operation to sudden peak loads and thus, avoiding the hourly constrained optimisation problem with simple PI-controls. However, here it is proved that if a usual influent profile is available, an optimum set of setpoints for the control structure proposed could be found and an important improvement in the operation could be obtained without the need of using feed-forward control. Hence, more simple controllers could be used (i.e. PI-controller) in comparison to other controllers that present more complex structures and may lead to technical difficulties.

For a full-scale WWTP, it is also important to consider the reliability and accuracy of the measurements used in the control loops. Measurements of nutrients as ammonium and

nitrate in activated sludge systems can be noisy or low accurate and, for example, the daily tuning of setpoints may be not feasible because the different theoretical setpoints are all around the same value considering the measurement error. In any case, the results presented demonstrate that an optimised fixed setpoint (as the points on the Pareto surface) would provide a better performance than using control loops without optimised setpoints (other points of figure 4.17 out of the Pareto surface). In addition, this improvement was much better when the performance is compared to the operation with no control implementation (Reference operation), because these non-controlled approaches are not able to react properly to important changes of the influent characteristics.

The adaptation of the MCF modelling approach presented in this work to a full-scale WWTP would be useful to study different optimal scenarios considering the three criteria presented. Once this step is finished, the optimal scenario could be selected according to the regional discharge limits or operational requirements for that WWTP in order to prioritize some criteria against the rest (e.g. the effluent quality against the operational costs or settling problems) by selecting their weights. The OCF approach is more useful when the weights of EQ and OC are already selected, since it simplifies the optimisation process for finding the best setpoints for the local controllers.

## **4.5. Conclusions**

---

The present study concludes that a model-based optimisation of the setpoints of WWTP control loops can improve the WWTP management, providing low effluent discharges with minimal OC and with a low risk to develop settling problems such as bulking, foaming or rising sludge.

Compared to the reference operation, the optimised control strategies resulted in a decrease of the OCF (up to 45% and 40% for pilot plants I and II, respectively) and in a reduction of the time that pollutants were above the discharge limits. In addition, the implementation of control strategies with optimal ammonium and nitrate setpoints improved not only the removal of these compounds, but also enhanced EBPR.

The implementation of different sets of setpoints for weekdays, weekends and storm or rain episodes (A&N-WVS) was the most efficient control strategy considering the OCF and the time that the effluent quality was above the discharge limits. Nevertheless, the utilization of a fixed set of setpoints during all the week (A&N-FS) also provided reasonable performance.

The hourly retuning of the control setpoints was not an efficient strategy because it increased the total costs. These results demonstrate that a more complex control strategy

does not result always in a plant performance improvement compared to more simple strategies.

One of the major achievements of this work was the inclusion for the first time of the risk for occurrence of microbiology-related failures as part of the multi-criteria optimisation in a WWTP that included biological P removal. The multi-criteria optimisation resulted in a set of optimal operation setpoints that could be approximated by a Pareto surface. The optimised setpoint within this surface could be selected by the requirements that are established for each WWTP in terms of the three criteria. These requirements could be translated into monetary weights as was done with OCF. Hence, the OCF optimisation resulted in an optimised scenario that was located on this surface.

Finally, it was observed that the optimisation process could be enhanced by using both objective functions in a complementary way. The multi-criteria function enabled a more extensive evaluation of different alternatives where none of the criterion is conditional to the other, as could occur with OCF. Once the weights are selected according to the WWTP requirements, the OCF optimisation could be used to adapt the plant operation to the influent variations.

## **CHAPTER V**

# Elucidating the role of the carbon source nature and the plant configuration on the EBPR failure due to anaerobic nitrate presence

Part of this chapter has been published as:

Guerrero, J., Guisasola, A., Baeza, J.A., 2011. The nature of the carbon source rules the competition between PAO and denitrifiers in systems for simultaneous biological nitrogen and phosphorus removal. *Water Research* 45 (16), 4793-4802.

Guerrero, J., Tayà, C., Guisasola, A., Baeza, J.A., 2012. Understanding the detrimental effect of nitrate presence on EBPR systems: effect of the plant configuration. *Journal of Chemical Technology and Biotechnology* 87 (10), 1508-1511.

Guerrero, J., Tayà, C., Guisasola, A., Baeza, J.A., 2014. Eliminación biológica de fósforo: avances en el estudio de su deterioro por recirculación de nitrato. *TecnoAqua* 6, 58-65.





## Abstract

*The presence of nitrate in the anaerobic reactor of municipal wastewater treatment plants (WWTPs) aiming at simultaneous biological C, N and P removal usually leads to Enhanced Biological Phosphorus Removal (EBPR) failure due to the competition between PAO and denitrifiers for organic substrate. This problem was studied in a continuous pilot plant (146 L) operating with good nutrient removal performance and a PAO-enriched sludge (72%). Nitrate presence in the anaerobic reactor was studied by switching the operation of the plant from an anaerobic/anoxic/aerobic (A<sup>2</sup>/O) to an anoxic-aerobic configuration (Modified Ludzack-Ettinger). When the influent COD composition was a mixture of different carbon sources (acetic acid, propionic acid and sucrose) the system was surprisingly able to maintain EBPR, even with internal recycle ratios up to ten times the influent flow-rate and COD limiting conditions. However, the utilisation of sucrose as sole carbon source resulted in a fast EBPR failure. A model based on Activated Sludge Model 2d (ASM2d) but considering two step nitrification and denitrification was developed and experimentally validated. Simulation studies showed that anaerobic volatile fatty acids (VFA) availability was critical to maintain EBPR activity. In addition, for studying the effect of the plant configuration on EBPR failure due to anaerobic nitrate presence, several batch experiments were performed with different carbon sources (acetic acid, propionic acid and sucrose) at different nitrate concentrations using PAO-enriched sludge from two different pilot plants: an anaerobic/aerobic sequential batch reactor (SBR) to favour PAO growth and the A<sup>2</sup>/O pilot plant. The results imply that the operational conditions of the A<sup>2</sup>/O pilot plant selected a PAO population capable of i) coexisting with nitrate without an inhibitory effect when VFA were selected as sole carbon source and ii) outcompeting denitrifying bacteria for the carbon source, in contrast to the SBR pilot plant where nitrate had an inhibitory effect on EBPR.*

## 5.1. Motivations

Nowadays, several WWTPs have already adapted their operation to meet the increasingly stricter nutrient discharge requirements in wastewater treatment. However, many WWTP do not satisfy these requirements due to failures in the biological nutrient removal (BNR) processes. For example, unpredictable EBPR failures still occur in practice when P removal process is coupled to N removal due to nitrate recirculation to the anaerobic reactor through the external recycle. Two main different explanations have been reported in the literature so far: a possible inhibitory effect of some denitrification intermediates, such nitrite or nitric oxide (Van Niel *et al.*, 1998; Saito *et al.*, 2004; Pijuan *et al.*, 2010; Zhou *et al.*, 2011) and nitrate or nitrite triggering off the activity of ordinary heterotrophic organisms (OHO), would reduce nitrate or nitrite using COD as electron donor and result in less COD available for PAO growth. Therefore, the delicate balance between organic carbon, N and P levels has a major impact to enhance the P removal in BNR systems. In this sense, EBPR failures from numerous urban wastewaters with low or medium organic content have been reported (Tasli *et al.*, 1999). More information about the detrimental effect of nitrate of P removal can be found in the introduction section (Chapter I).

The nature of the carbon source, acting as electron donor, also plays a major role. On this context, Randall *et al.* (1997) reported that the presence of VFA is critical to obtain high EBPR activity and, Pijuan *et al.* (2004) and Oehmen *et al.* (2006) showed that propionic acid favoured PAO enrichment. On the contrary, Cho and Molof (2004) reported that, when nitrate was present under anaerobic conditions, acetic acid was preferentially degraded by denitrifying bacteria over PAO, which were outcompeted for the carbon source. Thus, although EBPR fundamentals are currently understood, more research is required on this topic for a full understanding of the different experimental results obtained in the literature.

The overall objective of this chapter was to study the role played by the operational conditions and the nature of the carbon source in the intricate competition between PAO and OHO for the organic substrate. In the first step of the study, an anoxic/aerobic modified Ludzack-Ettinger (MLE) continuous pilot plant for simultaneous biological organic matter, N and P removal was operated with different internal recycle ratios to study the detrimental effect of nitrate presence in the anaerobic reactor. Different organic matter concentrations and compositions were also used at different steps to induce EBPR failure. Based on the experimental data from this step, a mathematical model to describe the behaviour of the system was developed and validated. Different scenarios were simulated to obtain a better understanding on the role of the carbon source on EBPR feasibility under anoxic and aerobic conditions. In a second step, several batch experiments with different carbon sources (acetic acid, propionic acid and sucrose) were run at different nitrate concentrations (0, 40 and 60 mgNL<sup>-1</sup>) with the sludge from two different pilot plants: an anaerobic/aerobic SBR to favour PAO growth and a continuous pilot plant with A<sup>2</sup>/O configuration.

## 5.2. Material and Methods

---

### 5.2.1. PILOT PLANT DESCRIPTION

The pilot plant (146 L) consisted of three continuous stirred tank reactors and one settler (Figure 5.1). The plant was initially operated with the classical A<sup>2</sup>/O configuration for simultaneous C, N and P removal. The first reactor (R1, 28L) was anaerobic so that PAO were selected against OHO. The second reactor (R2, 28L) was operated under anoxic conditions and the nitrate entering with the internal recycle ( $Q_{RINT}$ ) was denitrified by either OHO or denitrifying PAO (DPAO). The third reactor (R3, 90 L) worked under aerated conditions and complete organic matter and P removal took place together with nitrification. The settler (50 L) produced an effluent stream and a biomass enriched stream which was returned to R1 through the external recycle ( $Q_{REXT}$ ). Mixed liquor was withdrawn daily from the aerobic reactor in order to keep the desired sludge retention time (SRT) around  $15 \pm 2$  d. The influent ( $Q_{IN}$ ) flow-rate was  $140 \text{ L}\cdot\text{d}^{-1}$  and  $Q_{RINT}$  was initially fixed around  $420 \text{ L}\cdot\text{d}^{-1}$ .  $Q_{REXT}$  was maintained around  $125 \text{ L}\cdot\text{d}^{-1}$  during all the experiments. The pH was controlled at  $7.25 \pm 0.05$  using an on-off controller with sodium carbonate (1M) dosage. Dissolved oxygen (DO) in R3

was controlled at  $1.75 \pm 0.25 \text{ mg DO}\cdot\text{L}^{-1}$  with an on/off controller. Synthetic influent was prepared from a concentrated feed (Table 5.1) that was diluted (20:1) with tap water resulting in a wastewater with  $400 \text{ mg}\cdot\text{L}^{-1}$  COD,  $40 \text{ mg}\cdot\text{L}^{-1}$   $\text{N-NH}_4^+$  and  $10 \text{ mg}\cdot\text{L}^{-1}$   $\text{P-PO}_4^{3-}$ . This configuration was maintained during 4 months under steady state conditions with a high P and N removal capacity.

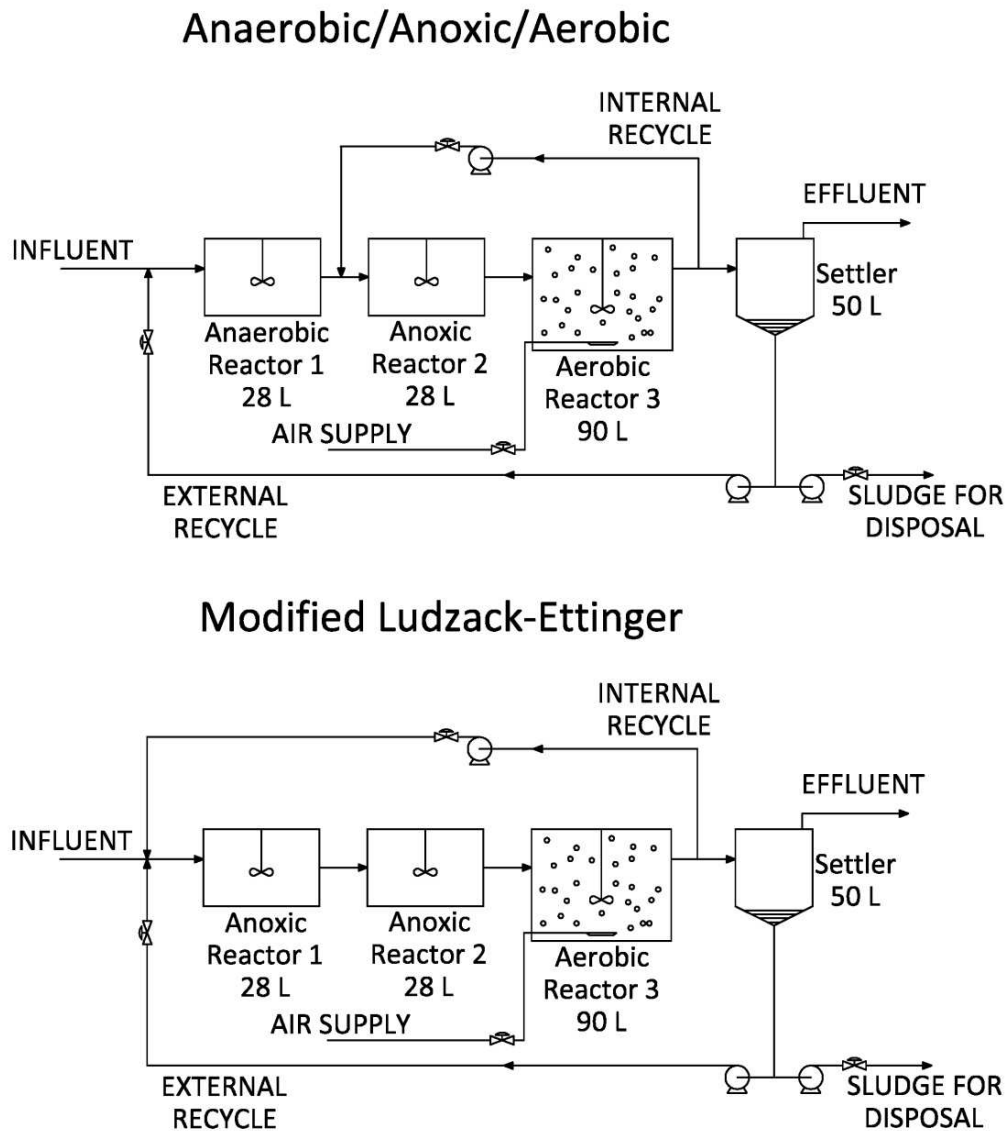


Figure 5.1 Scheme of A<sup>2</sup>/O and MLE pilot plant configurations

**Table 5.1** Synthetic wastewater composition.

Composition	$\text{g} \cdot \text{L}^{-1}$
<b>Macronutrients</b>	
Sodium acetate ( $\text{C}_2\text{H}_3\text{O}_2\text{Na}$ ) *	2.20 / 4.39
Sodium propionate ( $\text{C}_3\text{H}_5\text{NaO}_2$ ) *	1.38 / 2.77
Sucrose ( $\text{C}_{12}\text{H}_{22}\text{O}_{11}$ ) *	0.94 / 1.87
Ammonium chloride ( $\text{NH}_4\text{Cl}$ ) *	3.06
Dipotassium phosphate ( $\text{K}_2\text{HPO}_4$ ) *	0.74
Potassium phosphate ( $\text{KH}_2\text{PO}_4$ ) *	0.29
Magnesium sulphate ( $\text{MgSO}_4 \cdot 7\text{H}_2\text{O}$ )	0.88
Calcium chloride ( $\text{CaCl}_2 \cdot 2\text{H}_2\text{O}$ )	1.40
Potassium chloride (KCl)	0.38
<b>Micronutrients**</b>	
Ferric chloride ( $\text{FeCl}_3 \cdot 6\text{H}_2\text{O}$ )	1.50
Potassium iodide (KI)	0.18
Boric acid ( $\text{H}_3\text{BO}_3$ )	0.15
Cobalt chloride ( $\text{CoCl}_2 \cdot 6\text{H}_2\text{O}$ )	0.15
Manganese chloride ( $\text{MnCl}_2 \cdot 4\text{H}_2\text{O}$ )	0.12
Zinc sulphate ( $\text{ZnSO}_4 \cdot 7\text{H}_2\text{O}$ )	0.12
Sodium molybdate ( $\text{Na}_2\text{MoO}_4 \cdot 2\text{H}_2\text{O}$ )	0.06
Copper sulphate ( $\text{CuSO}_4 \cdot 5\text{H}_2\text{O}$ )	0.03
EDTA ( $\text{C}_{10}\text{H}_{16}\text{N}_2\text{O}_8$ )	10.00

\*Main components: 4 / 8  $\text{g COD} \cdot \text{L}^{-1}$  (37.5% sodium acetate, 37.5% sodium propionate and 25% sucrose), 0.8  $\text{g N} \cdot \text{L}^{-1}$  and 0.2  $\text{g P} \cdot \text{L}^{-1}$

\*\*Trace solution: 1 mL introduced per L of concentrated influent

Although the plant was initially operated with the A<sup>2</sup>/O configuration, during most of this work the plant was working with MLE configuration (anoxic/aerobic), moving  $Q_{\text{RINT}}$  to R1 (Figure 5.1), which was not anaerobic anymore. This configuration, typical of systems designed for only biological C and N removal, was chosen for gaining insight into the effect of nitrate entering to the anaerobic phase on the P removal (i.e. MLE configuration could be considered the most unfavourable situation for PAO due to the high amount of nitrate recycled by  $Q_{\text{REXT}}$ ). In practice, in most cases, nitrate was completely depleted in R1 resulting in an anoxic/anaerobic/aerobic configuration.

The concentration of organic matter in the influent was different throughout the study (Table 5.2) and the micronutrients composition was adapted from Smolders *et al.* (1994). Sludge from the municipal WWTP of Granollers (Barcelona) was used to inoculate the pilot plant. PAO content from the inoculum was analysed by fluorescence in situ hybridisation (FISH) quantification resulting in less than 2% of the total biomass.

**Table 5.2** Pilot plant conditions for each experimental step.

Experiment	Influent composition, mg·L <sup>-1</sup> (COD:N:P)	Q <sub>RINT</sub> flow rate, L·d <sup>-1</sup>	Q <sub>RINT</sub> /Q <sub>IN</sub>	Plant configuration
Step 0	400:40:10	420	3	A <sup>2</sup> O
Step I	400:40:10	420	3	MLE
Step II	400:40:10	840	6	MLE
Step III	400:40:10	1400	10	MLE
Step IV	200:40:10	420	3	MLE
Step V*	400:40:10	420	3	MLE

\* Sucrose was used as sole carbon source

### 5.2.2. BATCH EXPERIMENTS

Several off-line batch experiments were performed aiming at studying the effect of the plant configuration in the competition between OHO and PAO for influent COD in presence of nitrate. These experiments were performed in a magnetically stirred vessel (2 L) that could be operated either under anaerobic/anoxic or aerated conditions by sparging nitrogen or oxygen gas, respectively. These gases were supplied through a microdiffuser which ensured good transfer from gas to liquid phase. The gas flow was controlled with a mass flow-meter (Bronckhorst HiTec 825) to ensure a constant flow. The pH (WTW Sentix 81) and DO (WTW Cellox 325) probes were connected to a multiparametric reception equipment (WTW INOLAB 3) which was in turn connected via RS232 to a PC allowing for data monitoring and storage. This software also manipulated a high precision microdispenser (Crison Multiburette 2S) for pH control with acid (HCl 1M) or base (NaOH 1M) addition. More detailed information about this equipment can be found at Guisasola *et al.* (2007)

For the first set of experiments the procedure followed was: i) the vessel was filled with biomass extracted from the A<sup>2</sup>/O pilot plant (2000 mg·L<sup>-1</sup> TSS) and was aerated for, at least, 12 h to ensure most PHA reserves depletion; ii) a pulse of the electron donor (200 ± 25 mg COD L<sup>-1</sup> of acetic acid, propionic acid or sucrose) at different nitrate concentrations (0, 40 and 60 mg N·L<sup>-1</sup>) was added and; iii) the major components (COD, P-PO<sub>4</sub><sup>-3</sup>, N-NO<sub>3</sub><sup>-</sup>) were monitored under nitrogen-sparging conditions. The same batch tests were performed with the biomass extracted from a SBR of 10 L operated under anaerobic/aerobic conditions to favour PAO growth. In this case, the influent was synthetic wastewater with 200 mg COD L<sup>-1</sup> as propionic acid, 25 mg N-NH<sub>4</sub><sup>+</sup> L<sup>-1</sup> and 20mgP-PO<sub>4</sub><sup>-3</sup> L<sup>-1</sup>. The micronutrient solution also contained Allylthiourea (ATU) to avoid the interference of nitrification with PAO. Thus, the effect of nitrate presence under anaerobic conditions could be studied for two different biomass populations: i) A<sup>2</sup>/O biomass that was acclimated to nitrate presence under anaerobic conditions due to nitrate Q<sub>REXT</sub> inlet and ii) SBR biomass that was never in presence of nitrate due to the nitrification inhibition by ATU.

In order to calibrate the mathematical model used in this study, one more batch test was performed. The procedure in this case was: i) the 2L vessel was filled with biomass (around  $2000 \text{ mg TSS}\cdot\text{L}^{-1}$ ) from the A<sup>2</sup>/O pilot plant and it was again left under aerobic conditions for 12 hours to ensure PHA depletion; ii) a pulse of acetic acid ( $350 \text{ mg COD}\cdot\text{L}^{-1}$ ) and nitrate ( $40 \text{ mg N-NO}_3^-\cdot\text{L}^{-1}$ ) were added under nitrogen-sparging conditions and the major components (COD, P- $\text{PO}_4^{3-}$ , N- $\text{NO}_2^-$ , N- $\text{NO}_3^-$ ) were again monitored; iii) after total COD depletion, a second pulse of nitrate was added ( $20 \text{ mg}\cdot\text{L}^{-1}$ ) to monitor the anoxic P-removal activity of DPAO biomass and finally iv) the system was switched to aerobic conditions to monitor aerobic P-removal.

### 5.2.3. MODEL DESCRIPTION

The model used (see Annex I) is an extension of the well-known ASM2d proposed by IWA that describes the different processes occurring in a system for simultaneous biological organic matter and nutrient removal (Henze *et al.*, 2000). The major extension was the inclusion of nitrite as a state variable. Nitrite is a key intermediate to understand the behaviour of the different PAO fractions: PAO clade I and II (Oehmen *et al.*, 2010). According to the classification proposed by Flowers *et al.* (2009), both PAO population (clade IA and clade IIA) could denitrify from nitrite, but only clade IA could do this process from nitrate. No inhibitory kinetics related to nitrite were considered in this model, although it may have an inhibitory effect on EBPR (Van Niel *et al.*, 1998; Saito *et al.*, 2004; Pijuan *et al.*, 2010; Zhou *et al.*, 2011), due to the lack of evidences of inhibition during batch experiments. Nitrification was modelled as a two-step process, including AOB and NOB. Denitrification was also described in two steps (nitrate to nitrite and nitrite to nitrogen gas) to understand the COD fate under anoxic conditions and the possible substrate competition between PAO and OHO. The extended model included 21 compounds, which were divided into soluble or particulate, and 28 processes. The process kinetics, the stoichiometry and the parameter values matrix can be found in the Annex I.

The set of differential equations (odes) of the model were integrated with Matlab<sup>®</sup> using the *ode15s* function, a variable order method recommended for stiff systems. The parameter estimation of the new processes considered and the calibration of the model were carried out by using Pattern Search method (*patternsearch* Matlab function). In order to calibrate the initial conditions of the plant (Step 0), the starting point for each simulation was the steady state obtained after 100 days operating under A<sup>2</sup>/O conditions. The settler was modelled using the non-reactive settling model of Takács *et al.* (1991).

## 5.3. Results and Discussion

### 5.3.1. FEASIBILITY OF P-REMOVAL IN A MLE SYSTEM

An A<sup>2</sup>/O plant was changed to an anoxic/aerobic MLE configuration (Figure 5.1) to study in depth the role played by the nature of the carbon source in the intricate competition between PAO and OHO under anoxic conditions. Moving R1 from anaerobic to anoxic would maximize the theoretical detrimental effect of NO<sub>x</sub> (nitrate, nitrite or denitrification intermediates) in the EBPR performance. Table 5.3 presents the steady state effluent composition of the different plant configurations tested and figure 5.2 shows the experimental profiles of the main compounds of the influent and the effluent during the steps 0 to III. Step 0 corresponds to the starting point of this study, the A<sup>2</sup>/O configuration, and the following steps (Step I-III) when plant configuration was moved to a MLE configuration. The value of Q<sub>RINT</sub> was gradually increased among these periods (Table 5.2).

**Table 5.3** Steady-state effluent composition obtained at the end of each experimental step.

Experiment	COD (mg COD·L <sup>-1</sup> )	N-NH <sub>4</sub> <sup>+</sup> (mg N·L <sup>-1</sup> )	N-NO <sub>x</sub> <sup>-</sup> (mg N·L <sup>-1</sup> )	P-PO <sub>4</sub> <sup>-3</sup> (mg P·L <sup>-1</sup> )	PAO biomass (%)*
Step 0	22.4±0.1	0.21±0.07	7.89±0.25	0.21±0.01	72±9
Step I	23.2±0.8	0.08±0.01	9.48±0.85	0.26±0.04	77±5
Step II	22.8±1.4	<0.05	5.46±0.46	0.23±0.05	68±5
Step III	18.4±0.7	0.32±0.15	4.68±0.80	1.09±0.67	71±5

\* Biomass quantified by FISH technique coupled with confocal microscopy

High N and P removal (around 80% and 98% respectively) was achieved with the conventional A<sup>2</sup>/O configuration (Step 0) despite a little amount of NO<sub>x</sub> entering the anaerobic phase with the Q<sub>REXT</sub> (8 mg N-NO<sub>x</sub><sup>-</sup>·L<sup>-1</sup>, being nitrate the main compound). Assuming default growth yields (Henze *et al.*, 2000), the recycle of 1 mg N-NO<sub>3</sub><sup>-</sup> to the anaerobic phase would consume 7.6 mg COD, whereas 1mg P-PO<sub>4</sub><sup>-3</sup> released would consume 2.5 mg COD as VFA. Hence, under anaerobic conditions (R1), 13.6% of the total COD inlet was consumed in order to denitrify the amount of nitrate recycled (8mg·L<sup>-1</sup>), while 53% was taken up by PAO resulting in P-release. FISH quantification performed during A<sup>2</sup>/O step (Figure 5.3) clearly indicated the development of an enriched PAO sludge (72% of PAO) comparing with PAO content in the start-up of the plant (2% of PAO was detected in the biomass from the WWTP of Granollers, Spain). Therefore, the existing PAO were able to coexist with denitrifying OHO in the A<sup>2</sup>/O configuration despite the anaerobic NO<sub>x</sub> inlet. This observation contrasted to the common textbook knowledge that a strict anaerobic phase is mandatory to achieve high EBPR activity and that NO<sub>x</sub> presence in the anaerobic reactor can be detrimental to EBPR success (Simpkins and McLaren, 1978; Van Niel *et al.*, 1998; Henze *et al.*, 2008). Most of these studies were referred to full-scale WWTPs, where real wastewater with complex carbon sources was treated and not mainly VFA as in step 0. In those cases, the presence of NO<sub>x</sub> under anaerobic conditions caused a disproportionately decrease of the EBPR process.

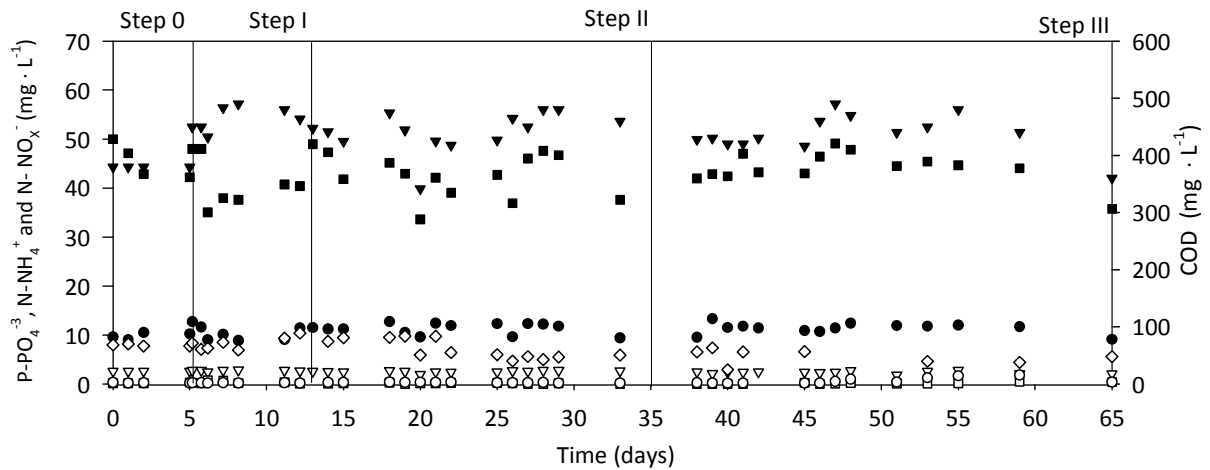


**Figure 5.2** Influent and effluent concentrations during the experimental steps 0-III. ▼ COD inlet, ▽ COD outlet, ■ ammonium inlet, □ ammonium outlet, ● phosphorus inlet, ○ phosphorus outlet and ◇ NO<sub>x</sub> outlet.

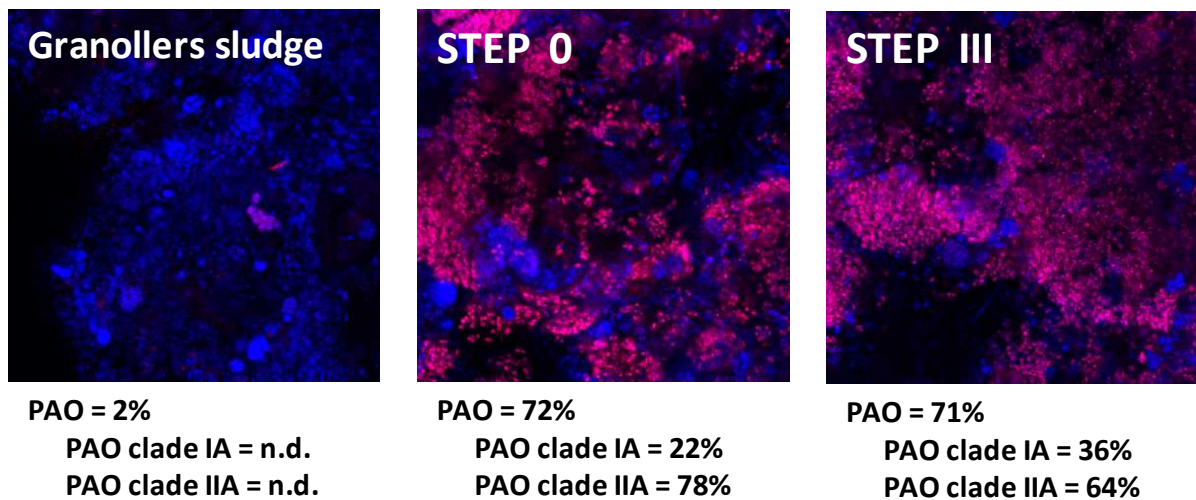


**Figure 5.3** FISH representative images in confocal laser scanning microscope of the sludge from A<sup>2</sup>/O pilot plant during steps 0 and III and the biomass inoculated in the start-up step, sludge from WWTP of Granollers. Specific probe PAOmix is shown in pink and EUBmix probes in blue.

When the plant configuration was changed from A<sup>2</sup>/O to MLE (Step I, Table 5.2), N and P removal efficiencies slightly decreased to 74% and 97%, respectively (Table 5.3). The increase of Q<sub>RINT</sub> during step II resulted in a decrease of the effluent NO<sub>x</sub> (more than 40%) as more NO<sub>x</sub> was brought to R1 to be denitrified. However, the subsequent increase of the internal recycle (Step III) did not result in an important decrease in the NO<sub>x</sub> (less than 15%) effluent content mainly because the COD concentration became limiting under anoxic



conditions. The measured effluent COD (Table 5.3) could be related to inert organic components. Surprisingly, the net-P removal efficiency was never affected during the abovementioned MLE operation (i.e. P-removal was never lower than 85%) suggesting that COD was preferentially consumed for EBPR than OHO for denitrification. This fact was corroborated with the FISH quantification obtained for steps I-III (table 5.3 and figure 5.3), where PAO population did not show an important shift during more than 60 days. Once again, these results seem to challenge the widely accepted idea that an anaerobic phase at the beginning of the WWTP is critical to favour PAO growth and diminish PAO-OHO competition for the carbon source (Henze *et al.*, 2008). In our case, the high content of VFA in the synthetic wastewater (75%) would be the reason because a PAO population capable to outcompete OHO for the carbon source was developed. These results were also clearly in disagreement with the reported observation that acetic acid is preferentially used for denitrification rather than for EBPR (Cho and Molof, 2004; Elefsiniotis *et al.*, 2004). However, it was also reported that propionate may be relatively easily sequestered and metabolized by PAOs compared to other microorganisms (Pijuan *et al.*, 2004; Oehmen *et al.*, 2006), which could explain the observation that PAO outcompeted OHO when the carbon source was mainly formed by VFA.

In step IV, a COD-limited influent ( $200 \text{ mg COD}\cdot\text{L}^{-1}$  with the composition shown in table 5.1) was proposed to gain more insight into the substrate competition between PAO and OHO (Figure 5.4). Again, EBPR was not significantly affected by the COD decrease and thus, P effluent concentration was always lower than  $1.5 \text{ mg P}\cdot\text{L}^{-1}$ . On the contrary, the denitrification process was limited by the reduction of the carbon source and  $\text{NO}_x$  effluent concentration increased from 7 to  $15 \text{ mg N-NO}_x\cdot\text{L}^{-1}$  (nitrate was around 97% of the total  $\text{NO}_x$ ). The complete denitrification of the  $\text{N-NO}_x$  brought by the  $Q_{\text{RINT}}$  and  $Q_{\text{REXT}}$  to R1 would have required a higher COD influent concentration. As a result,  $\text{NO}_x$  accumulation was observed in R1 (Figure 5.4). It was again proved that, even under COD-limited conditions, PAO was able to consume preferentially VFA than OHO under anoxic conditions. This capacity of PAO to outcompete OHO for the carbon source is not only intrinsically linked to the high amount of PAO present in the system but also to the nature of the organic matter. For the study of this latter point, a new experiment was performed in step V (Figure 5.4, right). Sucrose was used as sole carbon source (i.e. VFA were removed from the synthetic wastewater). The utilization of a complex a carbon source than VFA, such as sucrose, favoured the OHO denitrification process against EBPR. Hence, P-removal capacity was progressively lost after only 4 days resulting in an increase of the P effluent concentration from  $0.57 \text{ mg}\cdot\text{L}^{-1}$  to  $6.63 \text{ mg}\cdot\text{L}^{-1}$ . On the contrary,  $\text{NO}_x$  outlet presented a decreasing trend showing that most of the sucrose was oxidised by denitrifying OHO in both anoxic reactors ( $\text{NO}_x$  decreased in R1). Under strictly anaerobic conditions, OHO can act as fermentative bacteria (FB) consuming sucrose and producing VFA, which could be used for EBPR. However, in presence of nitrate, the consumption of sucrose to denitrify is more energetically favoured avoiding then fermentation process. This idea is in agreement with

the observations reported by Kuba *et al.* (1994) and Patel and Nakhla (2006) that P-release only occurred when nitrate concentration was below than  $1.0 \text{ mg}\cdot\text{L}^{-1}$ . Therefore, when sucrose and  $\text{NO}_x$  coexisted in step V, most of the sucrose was mainly oxidised by OHO to denitrify (around 70% of the COD influent content) instead of producing the VFA for EBPR. This fact explained the EBPR failure when sucrose was the sole carbon source in contrast to the situation when VFA were added.

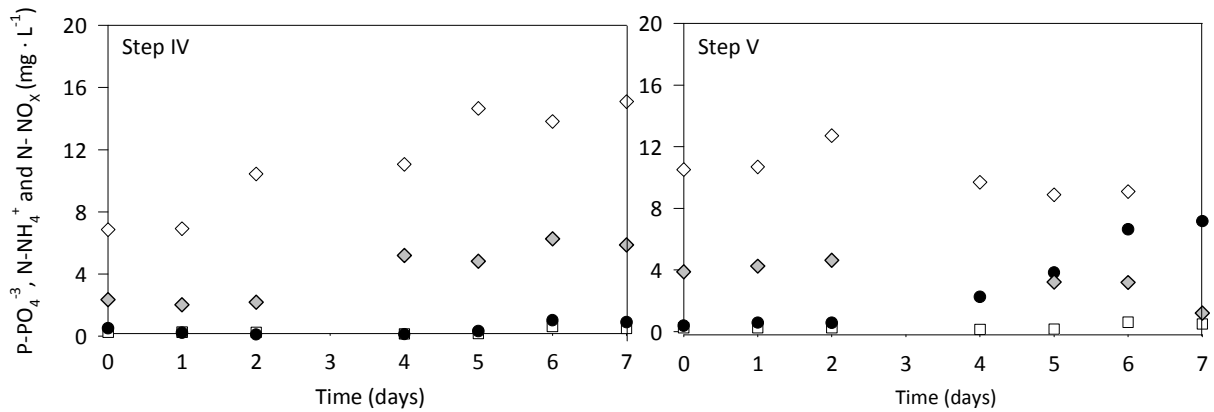


**Figure 5.4** Pilot plant behaviour under carbon shortage conditions. Step IV: VFA were the main components of the total carbon source inlet. Step IV: sucrose was used as a sole carbon source inlet (Step V).  $\square$  represents effluent ammonium,  $\blacklozenge$   $\text{NO}_x$  in R1,  $\diamond$  effluent  $\text{NO}_x$  and  $\bullet$  effluent phosphorus.

### 5.3.2. MODEL CALIBRATION AND VALIDATION

An extended version of ASM2d was used for a better understanding of the causes of the experimentally observed EBPR non-deterioration. Unfortunately, the experimental results obtained could not be reliably described using the extended AMS2d model with default parameters reported in Henze *et al.*, (2000). For that reason, a calibration process was required. The model was calibrated with the experimental data of a batch experiment where a pulse of acetic acid and nitrate were simultaneously added to  $\text{A}^2/\text{O}$  sludge (Figure 5.5). The biomass diversity was fixed according to FISH quantification results: 72% of PAO, 4 % of AOB, 7% of NOB and 1% of GAO, which was not included in the model. The rest (16 %) was considered OHO.

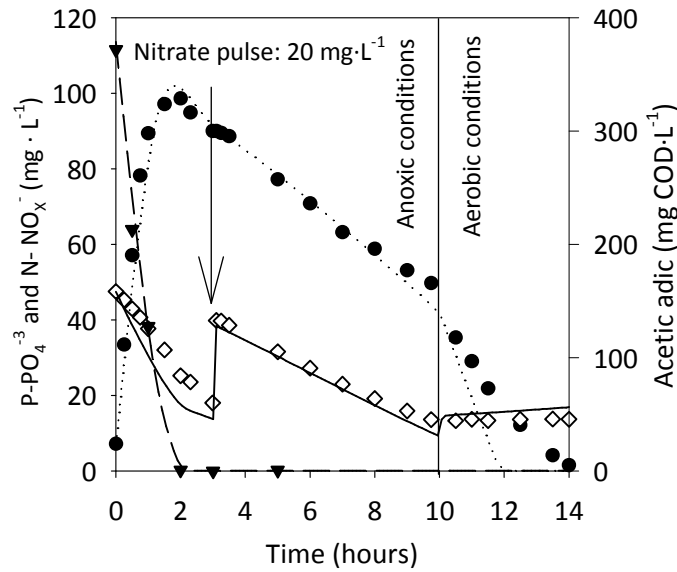


**Figure 5.5** Experimental batch test for model calibration purposes. ▼ COD, ◇ NO<sub>x</sub> and ● phosphorus. Dotted line belongs to the phosphorus behaviour described by the model, solid line to NO<sub>x</sub> and dashed line to COD.

The parameters obtained after the model calibration process are presented in table 5.4. The higher maximum rate of PHA storage ( $q_{PHA}$ ) obtained after the calibration process could suggest that the PAO population could be more effectively consuming VFA than with the standard ASM2d values (Henze *et al.*, 2000). This increase was necessary to describe that PAO would be more favoured than OHO in terms of VFA competition. Consequently, P-release capacity was almost not affected by NO<sub>x</sub> presence (Figure 5.5), as also occurred during MLE operation. The obtained nitrate reduction factor for denitrification PAO ( $\eta_{NO_3, PAO}$ ) indicated a low capacity to denitrify from nitrate to nitrite. However, it was enough to obtain the denitrification rates registered in the experimental data. This fact was in agreement with FISH quantification results, PAO clade IA was only the 22.3% of the total PAO bacteria contrary to clade IIA that was quantified as the 77.6%. Finally, the results of the model calibration also indicated a lower P-uptake capacity ( $q_{PP}$ ) and lower PAO growth rate ( $\mu_{PAO}$ ) than the standard values of ASM2d, which did not affect the EBPR process.

**Table 5.4** Calibrated parameters obtained for the batch experiment with acetate and nitrate.

Parameters	ASM2d value (20°C)	Calibrated value	Units
$q_{PHA}$	3.00	5.00	$\text{mg } X_{PHA} \cdot \text{mg } X_{PAO}^{-1} \cdot \text{d}^{-1}$
$q_{PP}$	1.50	0.60	$\text{mg } X_{PP} \cdot \text{mg } X_{PAO}^{-1} \cdot \text{d}^{-1}$
$\mu_{PAO}$	1.00	0.56	$\text{d}^{-1}$
$\eta_{NO_3, PAO}$	0.60	0.07	-
$\eta_{NO_2, PAO}^*$	-	0.90	-
$\eta_{NO_3, OHO}$	0.80	0.90	-
$\eta_{NO_2, OHO}^*$	-	0.90	-

\* These parameters do not appear in ASM2d model (Henze *et al.*, 2000)

The utilisation of the model with the calibrated parameters allowed a proper description of the experimental results during MLE operation in steps I-III (Figure 5.6). No EBPR failure was predicted in coincidence with the experimental results, even when a low COD content influent was used (step IV, Figure 5.7).

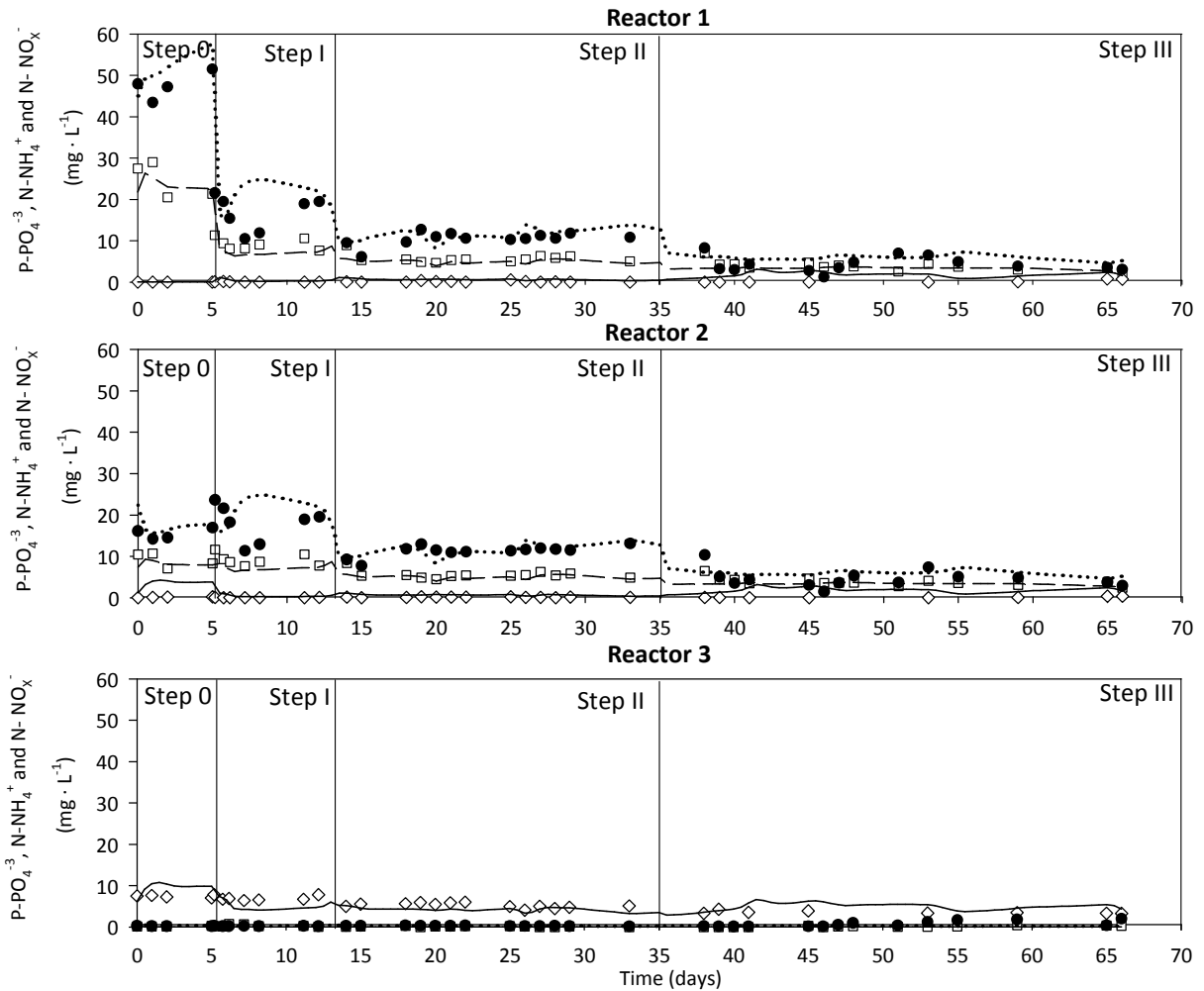


**Figure 5.6** Model validation. Pilot plant behaviour and model predictions for steps 0 to III.  $\square$  ammonium,  $\diamond$   $\text{NO}_x$  and  $\bullet$  phosphorus. Dotted line belongs to the phosphorus model prediction, dashed line to ammonium and solid line to  $\text{NO}_x$ .

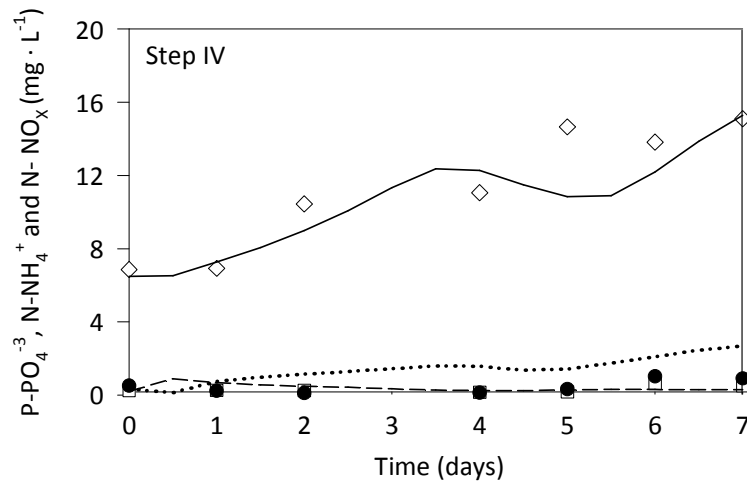


**Figure 5.7** Effluent composition and model predictions with a low COD inlet (Step IV).  $\square$  ammonium,  $\diamond$  NO<sub>x</sub> and  $\bullet$  phosphorus. Dotted line belongs to the model prediction for phosphorus, dashed line to ammonium and solid line to NO<sub>x</sub>.

### 5.3.3. SIMULATED CASE STUDIES: PAO AND OHO COMPETITION

Two different simulated case studies were performed in order to investigate the competition between PAO and OHO for the carbon source in different scenarios: i) the effect of COD influent concentration (with the same composition shown in Table 5.1) and ii) how EBPR process could be affected by the nature of the carbon source (i.e. different VFA and sucrose ratios were simulated) under COD limiting conditions (200 mg·L<sup>-1</sup>). Each scenario was simulated with the default ASM2d model and with the extended model proposed in this chapter during 7 days to mimic the experimental conditions of steps IV and V (Figure 5.8).

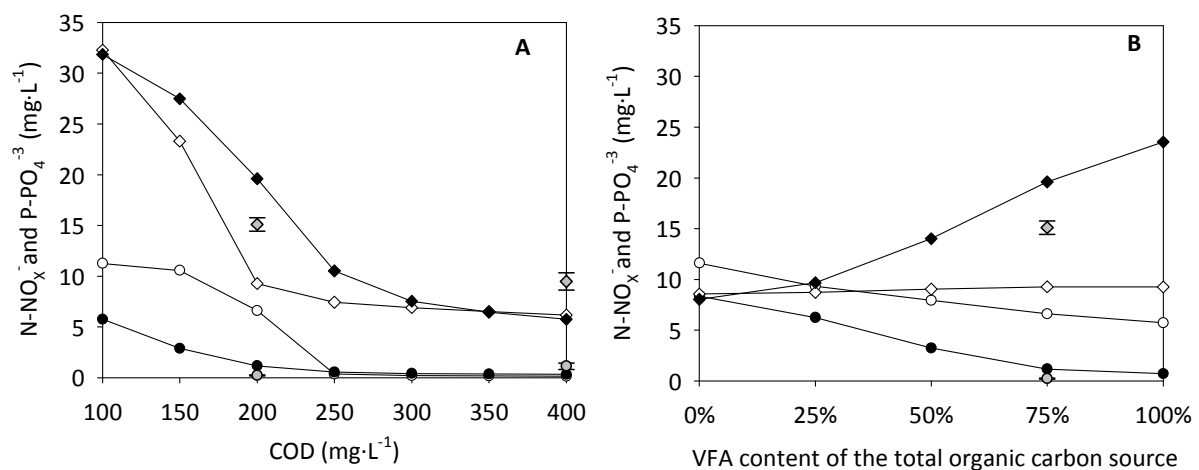


**Figure 5.8** Simulation results to study the effect of influent COD content (A) and the nature of the carbon source (B) in the EBPR process.  $\diamond$  NO<sub>x</sub> and  $\circ$  phosphorus. White symbols represent the simulated results of default ASM2d and black symbols the calibrated model results. Grey symbols correspond to experimental values obtained during pilot plant operation.

For the first issue (Figure 5.8 A), the non-calibrated model predicted the total EBPR failure when COD content was below  $200 \text{ mg}\cdot\text{L}^{-1}$  (i.e. P effluent concentration was almost the same as in the influent). In contrast, only a partial EBPR failure was observed with the calibrated model, even under strong COD limiting conditions ( $100 \text{ mg}\cdot\text{L}^{-1}$ ). It should be noted that when COD content was reduced from 300 to  $150 \text{ mg}\cdot\text{L}^{-1}$ , the denitrification process was more limited with the calibrated model than with the default model resulting in effluents with higher nitrate content (from  $7.54$  to  $27.48 \text{ mg N}\cdot\text{L}^{-1}$  for calibrated model and from  $6.91$  to  $23.3 \text{ mg N}\cdot\text{L}^{-1}$  for default ASM2d). The PAO capacity to outcompete OHO for the carbon source would explain this fact. Steady-state experimental data (grey points) were also included in figure 5.8. As can be observed, model predictions properly described the experimental phosphorus values. However, less  $\text{NO}_x$  effluent content was experimentally obtained in contrast to model predictions, suggesting that denitrification process was more efficient at practice. These divergences could be explained if one takes into account that the model was calibrated when the pilot plant was operated under  $\text{A}^2/\text{O}$  conditions. FISH quantification results showed an increase on PAO clade IA population after step III (from 22.3% to 35.6%) and thus, an increase in the denitrification capacity by DPAO activity would explain these divergences between model predictions and the experimental results. Another explanation could be related to the biological denitrification occurring during the settling process, which was not considered in the model and could increase the overall nitrogen removal capacity. According to the experimental data from  $\text{A}^2/\text{O}$  operation (Step 0), in our case the denitrification capacity of the settler was around 13% of the total nitrogen denitrified in the system (effluent  $\text{NO}_x$  concentration was  $7.89\pm 0.25 \text{ mg N}\cdot\text{L}^{-1}$  while in  $Q_{\text{REXT}}$  after settling step was  $2.75\pm 0.56 \text{ mg N}\cdot\text{L}^{-1}$ ). This value was quite similar to 15% reported by Siegrist *et al.* (1995) in observations in full-scale WWTP settlers.

When the nature of the carbon source was analysed (Figure 5.8 B), the predictions of both models were quite different. With the default parameters, P-removal was almost negligible and denitrification was never deteriorated when changing VFA carbon source content. In this case, it is assumed that the carbon source is preferentially used for denitrification rather than for EBPR for all the cases. Contrary, the simulations results with the calibrated model showed that P and N removal described an inverse behaviour. EBPR capacity was highly affected by the VFA influent content and thus, P-removal decreased as the VFA influent content also decreased. On the contrary, denitrification was favoured when the influent was enriched in a complex carbon source (e.g. sucrose).

These results may be very helpful in view the design of new systems for simultaneous biological C, N and P removal when the influent wastewater composition is known. Also, it could be used to explain the reasons why some EBPR failures are observed with nitrate presence and how to solve them.

### 5.3.4. BATCH EXPERIMENTS RESULTS

Different batch experiments were performed aiming at studying the role of the plant operation/configuration, together with the nature of the carbon source, in PAO and OHO competition. Hence, batch experiments were conducted with PAO-enriched sludge coming from two different set-ups (SBR and A<sup>2</sup>/O pilot plant) under different scenarios (three carbon sources at different amount of initial nitrate concentration). Figure 5.9 shows the experimental results for the SBR and the A<sup>2</sup>/O sludge, respectively, and table 5.5 summarises the major experimental conversions obtained. Lower P/C ratios (i.e. P released over carbon taken up in molar basis) were always obtained when nitrate was present. Three different hypotheses could explain this observation: i) nitrate or denitrification intermediates (nitrite or nitric oxide) caused inhibition on EBPR activity (Patel and Nakhla, 2006; Zhou *et al.*, 2011), ii) the occurrence of simultaneous P-release/anoxic-P-uptake due to the coexistence of an electron donor (carbon source) and an electron acceptor (nitrate) and iii) the consumption of part of the initial COD preferentially by denitrifying OHO (Cho and Molof, 2004), decreasing thus the amount of initial carbon source available for PAO.

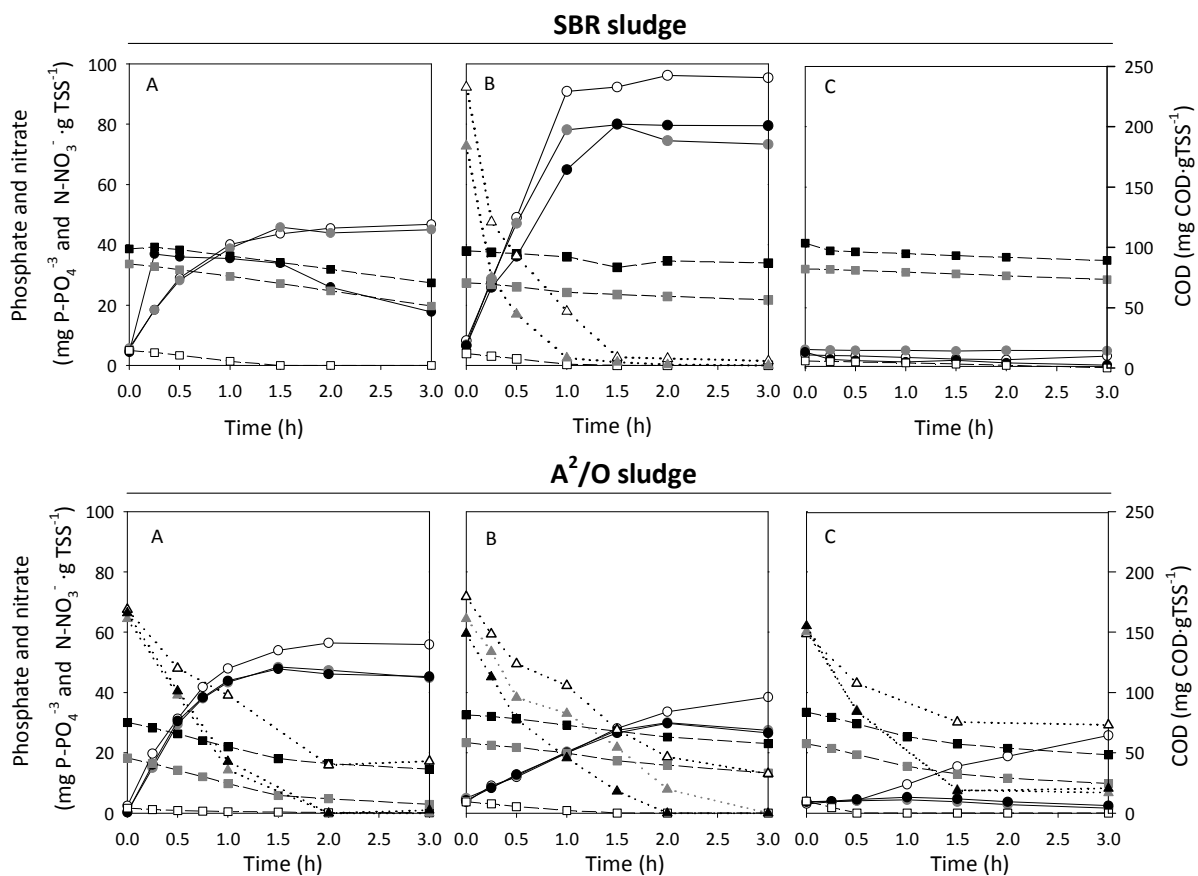


**Figure 5.9** Batch tests results obtained with sludge from A<sup>2</sup>/O (up) and SBR (down) by adding different carbon sources (A acetic acid, B propionic acid and C sucrose). Dotted line and  $\triangle$  represent COD, solid line and  $\circ$  P- $\text{PO}_4^{3-}$  and dash line and  $\square$  N- $\text{NO}_3^-$ . The symbol filling corresponds to the initial nitrate concentration: 0  $\text{mg}\cdot\text{L}^{-1}$  (white), 40  $\text{mg}\cdot\text{L}^{-1}$  (grey) and 60  $\text{mg}\cdot\text{L}^{-1}$  (black).

**Table 5.5** Major transformations obtained in the batch studies with different carbon sources. *Hac* Acetic Acid and *Hprop* Propionic Acid.

	Initial N-NO <sub>3</sub> <sup>-</sup> (mg·L <sup>-1</sup> )	SBR			A <sup>2</sup> /O		
		Hac	Hprop	Sucrose	Hac	Hprop	Sucrose
<b>P-release Rate</b> (g P-PO <sub>4</sub> <sup>-3</sup> ·g TSS <sup>-1</sup> ·d <sup>-1</sup> )	0	0.82	1.99	0.00	1.27	0.44	0.23
	40	0.78	1.69	0.00	1.22	0.42	0.00
	60	0.59*	1.36	0.00	1.23	0.42	0.00
<b>Nitrate Uptake Rate</b> (g N-NO <sub>3</sub> <sup>-</sup> ·g TSS <sup>-1</sup> ·d <sup>-1</sup> )	0	-	-	-	-	-	-
	40	0.10	0.08	0.07	0.20	0.11	0.20
	60	0.06	0.05	0.03	0.19	0.11	0.22
<b>COD Uptake Rate</b> (g COD·g TSS <sup>-1</sup> ·d <sup>-1</sup> )	0	2.19	5.45	0.00	1.55	3.00	1.31
	40	4.01	4.36	0.00	3.01	3.52	2.36
	60	4.20	4.23	0.00	2.96	3.63	2.45
<b>P-release/C- uptake</b> (P mmol/ Cmmol)	0	0.47	0.45	0.00	0.43	0.28	0.20
	40	0.26	0.38	0.00	0.35	0.21	0.00
	60	0.16*	0.38	0.00	0.35	0.20	0.00

\*These values were calculated considering the initial concentrations and at 1.5 hours.

For the experiments performed with the biomass withdrawn from the SBR, it was observed that nitrate uptake rate (NUR) and P-release rate decreased in parallel to a nitrate concentration increase. These results are in agreement with the hypothesis that nitrate and some denitrification intermediates (nitrite or nitric oxide) had a detrimental effect on the EBPR process. As an example, for the case of propionic acid, P-release rate and NUR were reduced 24% and 41%, respectively, when the nitrate concentration was increased from 40 to 60 mg·L<sup>-1</sup>. In the daily operation of the SBR, the synthetic wastewater fed contained ATU to avoid nitrification and, therefore, the SBR sludge was never in contact with nitrate. Hence, it is logical that a sudden nitrate addition results in some inhibition. In any case, this inhibitory effect was considerably lower than other studies (Akin and Ugurlu, 2004; Patel and Nakhla, 2006), where EBPR activity was only observed when nitrate concentration was below 1 mg·L<sup>-1</sup>. Even though ATU prevented nitrate production in the SBR and therefore denitrification processes, some denitrification activity was observed in the batch tests proving DPAO activity. The biomass from SBR contained a certain amount of PAO-clade IA (Table 5.6) that could explain the lower inhibitory effect of nitrate on EBPR and the observed denitrifying capacity. In conventional anaerobic/aerobic (AO) systems without nitrate/nitrite presence, the denitrification capabilities do not seem a key feature for survival or competition and as such, the abundance of IA or IIA cannot be predicted *a priori*. We hypothesize that AO systems with abundance of PAO-clade IIA could not reduce nitrate and would be much more affected by nitrate presence.

P-release rate results with SBR biomass not only support the hypothesis of the inhibitory effect of nitrate but also were in agreement with the hypothesis of simultaneous P-release and P-uptake phenomenon. A decrease in the P-release rate was detected when increasing nitrate concentration and thus, it could mean that part of P was uptaken by DPAO activity at the same time that was released.



**Table 5.6** Biomass quantification using FISH technique. Results expressed in % of total biomass quantified.

		Population distribution (%)				
		SBR		A <sup>2</sup> /O		
PAO	68	Clade IA	49	72	Clade IA	22
		Clade IIA	51		Clade IIA	78
GAO	20			<1		

Finally, a low presence of OHO was detected in SBR biomass quantification according to FISH results (as shown in table 5.6, around 12% could be considered as). ATU presence in synthetic wastewater prevented nitrate presence under anaerobic conditions and thus, the hypothesis of COD loss due to OHO denitrification could be considered not predominant in this case. However, in acetic acid experiment it was observed that the P/C ratio decreased and COD uptake increased when nitrate concentration increased. These results suggest that some other organisms, a part from PAO and OHO, were consuming the carbon source. FISH quantification (table 5.6) showed that some GAO or DGAO (GAO with denitrifying capacity) were present in the system (20%), which could compete with PAO for the carbon source. According to Oehmen *et al.* (2010) some GAO groups are able to growth using nitrate as electron acceptor and acetic or propionic as carbon source.

For the case of sucrose, no COD uptake was detected (Table 5.5) which corroborated the low OHO presence in the SBR biomass (Table 5.6). Hence, sucrose fermentation by FB for VFA production could be considered as negligible resulting in no EBPR activity (P-release activity was neither observed). This result was not surprising since sucrose was not the common carbon source in the daily operation of the SBR.

Different results were obtained with the sludge withdrawn from A<sup>2</sup>/O pilot plant (figure 5.9). P-release rate only decreased around 4% and the NUR levels were constant despite the nitrate increase, whereas the P/C ratio decreased when nitrate was present. These observations indicate that both nitrate inhibition and simultaneous P-release/anoxic-P-uptake hypothesis could be rejected with the A<sup>2</sup>/O sludge. As was proved in pilot plant experiments, the operational A<sup>2</sup>/O set-up (i.e. constant nitrate inlet to the anaerobic reactor through Q<sub>REXT</sub>) allowed the development of an acclimated PAO population capable to coexist with nitrate without resulting in EBPR failure. Hence, the only reason for observing a decrease in the P/C ratio as nitrate increased was the simultaneous consumption of the electron donor by PAO and denitrifying OHO. Moreover, the results were in agreement with the abovementioned idea that PAO could outcompete OHO when VFA were the predominant carbon source. An increase of nitrate concentration in A<sup>2</sup>/O experiments did not increase COD uptake rate or NUR showing that denitrification process was constrained to degrade only the COD that was not consumed in the P-release process. Otherwise, an increase of nitrate concentration would result in an increase of the NUR or COD uptake rate

and a reduction of P-release rate. These results with the A<sup>2</sup>/O sludge were in agreement with the observations from A<sup>2</sup>/O and MLE operation (see Section 5.3.1), where the high amount of PAO in the sludge (72% of total biomass quantified by FISH, table 5.6) suggested that PAO growth was more favoured than OHO growth when VFA were predominant in the COD fed. The higher P/C ratio was observed when acetic acid was used as the carbon source. This behaviour is in agreement with Pijuan *et al.* (2004) who observed that acetic acid produced a higher P/C ratio than propionic acid. Contrary, propionic acid resulted in the higher P/C ratio and P-release rate with the SBR sludge; it was expected since propionic acid was the sole carbon source used in the daily operation of the pilot plant.

Denitrification activity, i.e. nitrate reduction, was also observed with the sludge extracted from A<sup>2</sup>/O after total COD depletion (Figure 5.9). According to FISH quantification, this denitrifying capacity can be attributed to DPAO presence since 22% of the total PAO population belonged to DPAO clade IA, which can denitrify from nitrate.

When sucrose was added to the A<sup>2</sup>/O sludge, P-release was only observed when nitrate concentration was below <1 mg·L<sup>-1</sup>. As was commented before, sucrose was mainly used by denitrifying OHO when nitrate was present avoiding sucrose fermentation to VFA. For that reason, EBPR activity was only possible after total nitrate depletion as in agreement with Kuba *et al.* (1994) and Patel and Nakhla (2006).

## 5.4. Conclusions

---

The nature of the carbon source rules the competition between PAO and denitrifying OHO in systems with simultaneous biological N and P removal. After switching the operation of an A<sup>2</sup>/O pilot plant to MLE configuration, no inhibitory effect on EBPR due to anaerobic NO<sub>x</sub> presence was observed. When the carbon source presented a high VFA content, PAO could outcompete OHO even under anoxic/aerobic configuration. As a result, heterotrophic denitrification activity was more affected than EBPR when working with low influent COD.

EBPR only failed when a more complex compound (sucrose) was used as a sole carbon source. In that case, NO<sub>x</sub> presence had an inhibitory effect in EBPR, not to inhibit the P-release process itself but to prevent the fermentation process for the VFA production by the fermentative bacteria.

A model was developed and experimentally validated which explained the EBPR feasibility with nitrate presence under anoxic-aerobic conditions. The model calibration allowed a better understanding of the experimental results in terms of kinetic parameters of PAO and OHO. The simulation of different scenarios evidenced again that the PAO population could be more effective than OHO consuming VFA even under anoxic conditions. Although no total

EBPR failure was observed even under COD limiting conditions ( $100 \text{ mg}\cdot\text{L}^{-1}$ ), VFA presence was demonstrated as the key point to trigger EBPR activity. The calibrated model was validated as a helpful tool to set the limits to avoid EBPR failures linked to nitrate presence.

The results obtained from the batch tests with biomass withdrawn from two different pilot plants conclude that the PAO response to nitrate, apart from the nature of the carbon source, also depends on the operational conditions. The common presence of nitrate under anaerobic conditions from A<sup>2</sup>/O operation selected a PAO population capable of coexisting with nitrate without an inhibitory effect. Contrary, the PAO population developed in the SBR, which had never worked with nitrate before, showed a decrease of the EBPR activity when nitrate concentration increased.



## **CHAPTER VI**

# Reducing EBPR failure due to external nitrate recycling by controlled crude glycerol addition

Part of this chapter is in preparation for publication as:

Guerrero, J., Guisasola, A., Baeza, J.A., 2014. Controlled crude glycerol dosage to prevent EBPR failures due to nitrate external recycle. *In preparation*.



## Abstract

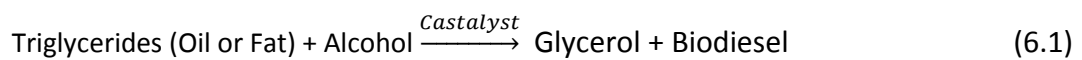
The addition of an external carbon source is a widely used solution to prevent Enhanced Biological Phosphorus Removal (EBPR) failure due to nitrate presence in the theoretically anaerobic phase. Unfortunately, most of carbon sources that could be used (volatile fatty acids, glucose, synthetic glycerol...) are not cost-effective and thus, new and low-cost alternatives should be proposed. In this chapter, the use of a biodiesel by-product such as crude glycerol has been studied as a promising carbon source to improve N and P removal processes in a wastewater treatment plant (WWTP). For this aim, two pilot plant configurations were operated (anaerobic/anoxic/aerobic, A<sup>2</sup>/O, and Johannesburg, JHB) under two different disturbance steps for increasing nitrate and nitrite load to the anaerobic reactor: i) increase of ammonium nitrogen in the influent and ii) additional nitrite inlet in the external recycle. In the first part of the study, the role of plant configuration on EBPR failure and recovery capacity was studied under open-loop conditions. JHB operation resulted in a shorter recovery period after EBPR failure in comparison to A<sup>2</sup>/O, even under more unfavourable conditions (EBPR failed when ammonium nitrogen was increased from 40 to 120 mg N·L<sup>-1</sup> in JHB and from 40 to 80 mg N·L<sup>-1</sup> in A<sup>2</sup>/O). In the second part, the effectiveness of a PI feedback control loop based on crude glycerol addition in the anaerobic reactor for controlling P effluent concentration was tested for the first time. A model for describing the experimental pilot plant data was defined, calibrated and used for controller design and tuning. The best results were again obtained for the JHB pilot plant: P effluent concentration was controlled around the setpoint value (1mg P·L<sup>-1</sup>) by adding less crude glycerol (18% less than the A<sup>2</sup>/O pilot plant). Some limitations on the control setup were observed due to the slow effect of glycerol addition on P effluent concentration variations. Two corrective alternatives were tested in two different simulated case studies: i) control of P concentration in the anaerobic reactor instead of in the effluent and ii) feedforward actuation (glycerol addition based on N influent concentration) in combination with simple feedback control of effluent P. The stability of control actuation was highly improved in both cases. As an example, feedforward inclusion resulted in 1.03±0.29 mg P-PO<sub>4</sub><sup>-3</sup>·L<sup>-1</sup> in the effluent for A<sup>2</sup>/O and 0.88 ±0.41 mg P-PO<sub>4</sub><sup>-3</sup>·L<sup>-1</sup> for the JHB configuration during the disturbance of high influent ammonium.

## 6.1. Motivations

One of the most extended explanations for EBPR failure in A<sup>2</sup>/O WWTP with biological N and P removal assumes that when an excess of nitrate is recycled to the anaerobic reactor, denitrifying ordinary heterotrophic organisms (OHO) can preferentially use the carbon source over polyphosphate accumulating organisms (PAO), resulting in less COD for EBPR (Cho and Molof, 2004). The addition of an external carbon source is presented as a fast and successful solution to solve COD deficiencies. However, as is showed in Chapter V, not only the COD availability is important in this interaction between N and P removal but also the nature of the carbon source plays an important role. Several studies (Randall *et al.*, 1997; Merzouki *et al.*, 2005) reported that the presence of volatile fatty acids (VFA) in the wastewater is mandatory to obtain a high P removal capacity. Unfortunately, an external

VFA addition is not usually cost-effective and it increases the overall plant carbon footprint (Issacs and Henze, 1995; Yuan *et al.*, 2010). A promising and very attractive alternative would be focused on the utilization of waste materials that could be fermented to VFA.

Crude glycerol is a good example of such wastes materials since it is a by-product of biodiesel fuel production (Equation 6.1): about 1 L of glycerol is generated for every 10 L of produced biodiesel fuel (Johnson and Taconi, 2007). Moreover, the impurities of crude glycerol derived from biodiesel production (e.g. long chain fatty acids or high salts concentration) together with the increase of its production have resulted in a drop of crude glycerol prices. Regarding its utilization on wastewater treatment, many studies reported successful glycerol utilization as an external carbon source for denitrification process (Grabinska-Loniewska *et al.*, 1985; Aunna *et al.*, 1993; Bodík *et al.*, 2009; Torà *et al.*, 2011) and for improving EBPR activity when treating influents with carbon shortage (Guerrero *et al.*, 2012; see Annex II). In this latter study, it was developed a syntrophic consortium of fermentative bacteria and PAO: the first fermented glycerol to VFA, which in turn were used by PAO for biological phosphorus removal. Taking into account all these considerations, crude glycerol could be a very practical and cost-effective external carbon source to reduce the detrimental effect of nitrate under anaerobic conditions since it could be used in both N and P removal processes. However, there are not previous studies about crude glycerol utilization as carbon source for improving EBPR in a system with simultaneous N and P removal.



The distribution of the required anaerobic, anoxic or aerobic phases of the plant also plays an important role when minimizing the detrimental effect of nitrate presence on EBPR. Alternative configurations to A<sup>2</sup>/O have been proposed to reduce somehow the nitrate content in the external recycle and thus, in the anaerobic phase. For example, JHB configuration is based on the inclusion of an additional reactor in the external recycle for nitrate denitrification, while UCT configuration adds an extra recycling flow to avoid nitrate presence in the anaerobic reactor (Metcalf and Eddy, 2003; Henze *et al.*, 2008).

Along this line of thinking, the main objective of this chapter is to study the feasibility of using crude glycerol as an external carbon source to avoid EBPR failure due to anaerobic nitrate and nitrite presence. In the first part of the study, the nutrient removal efficiency of two pilot plant configurations (A<sup>2</sup>/O and JHB) was compared when introducing two different disturbances for increasing nitrate or nitrite load to the anaerobic reactor under open-loop operation. Then, an effluent phosphorus feedback control loop based on crude glycerol addition in the anaerobic reactor was developed to reduce the negative effects of disturbances on the EBPR process. For this aim, a calibrated mathematical model was used for optimum phosphorus control-loop tuning. The efficiency of this control loop was



experimentally validated in both pilot plants. Finally, two new control strategies were also simulated: P control in R1 and anticipative control (feedforward).

## 6.2. Material and Methods

### 6.2.1. PILOT PLANTS DESCRIPTION

Two different pilot plants with simultaneous C, N and P removal were used in this chapter. The first one was operated under A<sup>2</sup>/O similarly as was described in Chapter V and it consisted of three continuous stirred tank reactors with a total volume of 146 L and one 50 L settler (Figure 6.1 up). Mixed liquor was withdrawn daily from the aerobic reactor in order to keep the sludge retention time (SRT) around 11 days. The influent ( $Q_{IN}$ ) flow-rate was 240 L·d<sup>-1</sup> resulting in a hydraulic retention time (HRT) of 14.6 hours. During all the experiments, the internal recycle ( $Q_{RINT}$ ) was fixed around 624 L·d<sup>-1</sup> and the external recycle ( $Q_{REXT}$ ) was maintained around 190 L·d<sup>-1</sup>. The pH was controlled at  $7.25 \pm 0.05$  using an on-off controller with sodium carbonate (1M) dosage and dissolved oxygen (DO) in R3 was controlled at  $2.50 \pm 0.25$  mg DO·L<sup>-1</sup> with a PI controller. The pilot plant was inoculated with sludge from the municipal WWTP from Granollers (Barcelona). This configuration was maintained during more than 30 days under steady state conditions with a high nutrient removal capacity.

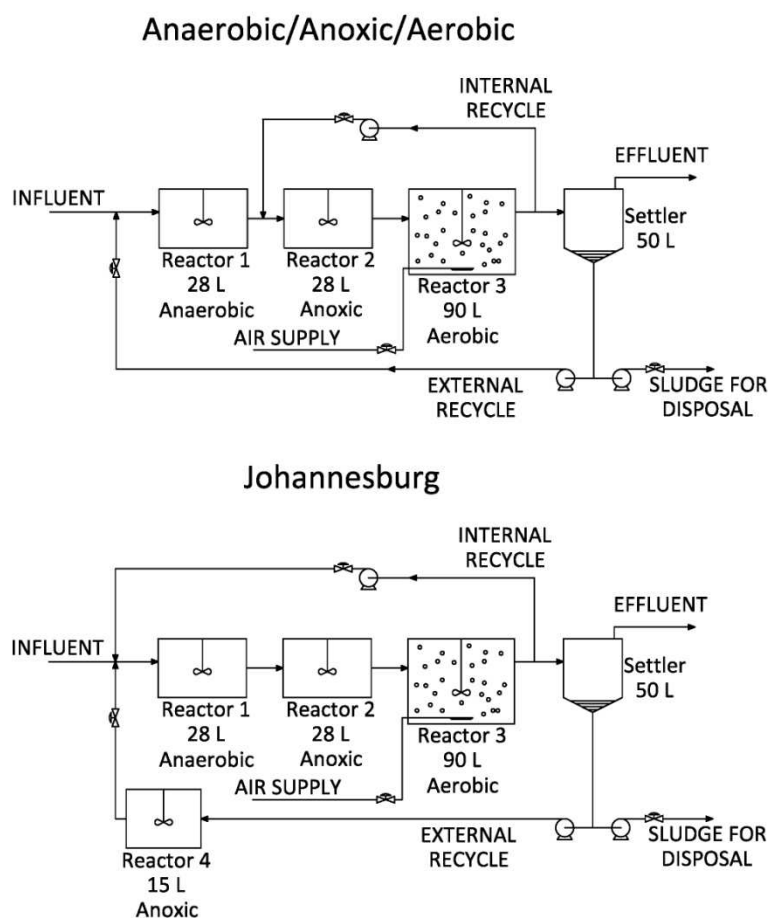


Figure 6.1 Scheme of the A<sup>2</sup>/O and JHB pilot plant configurations.

In the second part of the study, the results of the A<sup>2</sup>/O configuration were compared to the JHB configuration (Figure 6.1 down). In this case, a fourth anoxic reactor (R4, 15 L) was used in order to denitrify the nitrate and nitrite recycled by Q<sub>REXT</sub> and thus, preventing these species to enter to the anaerobic reactor R1. The system was operated with the same experimental conditions used for the A<sup>2</sup>/O pilot plant.

### 6.2.2. SYNTHETIC WASTEWATER AND DISTURBANCES

Synthetic influent was prepared from a concentrated feed (Table 6.1) that was diluted (15:1) with tap water resulting in a wastewater with 400 mg·L<sup>-1</sup> COD, 40 mg·L<sup>-1</sup> N-NH<sub>4</sub><sup>+</sup> and 10 mg·L<sup>-1</sup> P-PO<sub>4</sub><sup>-3</sup>. Contrary to Chapter V, in this case different carbon sources (i.e. readily and slowly biodegradable substrates) were used to mimic a real urban wastewater and to facilitate EBPR failure due to nitrate and nitrite presence under anaerobic conditions. If VFA had been used as the main carbon source component, PAO would have outcompeted OHO for the carbon source avoiding EBPR failure as in Chapter V, which is contrary to the focus of the study here presented. The micronutrient solution was adopted from Smolders *et al.*, (1994).

**Table 6.1** Synthetic wastewater composition.

Composition	g · L <sup>-1</sup>
<b>Macronutrients</b>	
Milk powder*	2.25
Starch*	1.86
Sucrose*	0.71
Sodium acetate (C <sub>2</sub> H <sub>3</sub> O <sub>2</sub> Na)*	0.54
Sodium propionate (C <sub>3</sub> H <sub>5</sub> NaO <sub>2</sub> )*	0.35
Ammonium chloride (NH <sub>4</sub> Cl)*	2.28
Dipotassium phosphate (K <sub>2</sub> HPO <sub>4</sub> )*	0.58
Potassium phosphate (KH <sub>2</sub> PO <sub>4</sub> )*	0.22
Magnesium sulphate (MgSO <sub>4</sub> ·7H <sub>2</sub> O)	0.88
Calcium chloride (CaCl <sub>2</sub> ·2H <sub>2</sub> O)	1.40
Potassium chloride (KCl)	0.38
<b>Micronutrients**</b>	
Ferric chloride (FeCl <sub>3</sub> ·6H <sub>2</sub> O)	1.50
Potassium iodide (KI)	0.18
Boric acid (H <sub>3</sub> BO <sub>3</sub> )	0.15
Cobalt chloride(CoCl <sub>2</sub> ·6H <sub>2</sub> O)	0.15
Manganese chloride (MnCl <sub>2</sub> ·4H <sub>2</sub> O)	0.12
Zinc sulphate (ZnSO <sub>4</sub> ·7H <sub>2</sub> O)	0.12
Sodium molybdate (Na <sub>2</sub> MoO <sub>4</sub> ·2H <sub>2</sub> O)	0.06
Copper sulphate (CuSO <sub>4</sub> ·5H <sub>2</sub> O)	0.03
EDTA (C <sub>10</sub> H <sub>16</sub> N <sub>2</sub> O <sub>8</sub> )	10.00

\* Main components: 6 g COD·L<sup>-1</sup> (37.5% milk powder, 37.5% starch, 12.5% sucrose, 6.25% sodium acetate and 6.25% sodium propionate), 0.6 g N·L<sup>-1</sup> and 0.15 g P·L<sup>-1</sup>.

\*\* Trace solution: 1 mL introduced per L of concentrated influent.

Two different disturbances were performed in both configurations to study the detrimental effect of nitrate and nitrite presence on EBPR in the anaerobic phase: i) increase of ammonium influent concentration and ii) increase of nitrite concentration in  $Q_{REXT}$  by adding an additional nitrite inlet. During the disturbance experiments, ammonium and nitrite concentrations were increased until P-removal capacity was reduced to 50%; after this partial failure, the disturbance was stopped and the pilot plant was operated under default conditions to study EBPR recovery capacity.

### 6.2.3. MODEL DESCRIPTION

The model used was an extension of ASM2d (Henze *et al.*, 2000), where nitrite was included as another state variable. The process kinetics, stoichiometry and parameter values can be found in the Annex I. In contrast to Chapter V, in this case the settler was simulated using the model of Takács *et al.* (1991) but considering the reactive capacity of the settler (Siegrist *et al.*, 1995; Koch *et al.*, 1999). A virtual tank inserted after the secondary settler (i.e. in the  $Q_{REXT}$ ) was considered in order to simulate the reactions that take place in the sludge blanket (Ráduly *et al.*, 2004). The main assumption of this modelling approach is that the settler reactions only occur in the sludge blanket and that the reactivity capacity depends on the sludge mass concentration on it. For that reason, the volume of the virtual reactor was constantly adjusted according to variations on sludge blanket concentration. The reactor volume was, thus, calculated using TSS concentration in the bottom layer of the settler and reactions were modelled using the extended ASM2d equations. The sludge blanket cannot be considered as a perfectly stirred tank (e.g. some mass transfer limitations could appear), therefore a global efficiency factor was also considered to decrease the reaction rates in the tank. The value of this factor was calibrated according to the experimental data (see Section 6.3.2 and 6.3.5).

All the simulations were performed with Matlab® and the differential equations (ode) of the model were solved with *ode15s* function, a variable order method recommended for stiff systems. The parameter estimation to fit the model with the experimental data was carried out by using Pattern Search method (*patternsearch* function in Matlab®).

### 6.2.4. CONFIDENCE INTERVAL DETERMINATION OF CALIBRATED PARAMETERS

The confidence interval calculation of the calibrated parameters is based on the Fisher Information Matrix (FIM) approach (Dochain and Vanrolleghem, 2001). This matrix evaluates the importance of each calibrated parameter over the outputs because it measures the variation of the output variables (e.g. P concentration in R3) with respect to the calibrated parameters. The algebraic expression for FIM is:

$$FIM = \sum_{k=1}^N Y_{\theta}(k) \cdot Q_k^{-1} \cdot Y_{\theta}^T(k) \quad (6.2)$$

For  $r$  outputs variables and  $p$  parameters, the FIM is a  $p \times p$  matrix, where  $k$  represents each sampling data point,  $Q_k$  is the  $r \times r$  covariance matrix of the measurement noise,  $\theta$  is the vector of  $p$  parameters,  $N$  is the total number of samples and  $Y_\theta$  is the  $p \times r$  output sensitivity function matrix, expressed by:

$$Y_\theta^T = \left[ \frac{\partial y(t, \theta_0)}{\partial \theta^T} \right]_{\theta_0} \quad (6.3)$$

Where  $\theta_0$  is the complete calibrated model parameter vector used for calculating derivatives and  $\theta^T$  is the transposed parameters vector with the elements under study. In this study, the derivative part of equation 6.3 was numerically obtained by finite differences (i.e. central approximation) using a perturbation factor of  $10^{-4}$ . The measurement noise was calculated as the standard deviation of different measurements of sample triplicates.

The inverse of the FIM provides the lower bound of the parameter estimation error covariance matrix (Dochain and Vanrolleghem, 2001) as is shown in equation 6.4. Thus, this procedure could be used for assessing the uncertainty estimation of the calibrated parameters ( $\theta_0$ ). Examples of FIM analysis for uncertainty estimation applied to wastewater research can be found in Guisasola *et al.* (2006) or Machado *et al.* (2009).

$$COV(\theta_0) \geq FIM^{-1} \quad (6.4)$$

Finally, the FIM property was used to determine the confidence interval ( $\Delta\theta_j$ ) for a given parameter  $\theta_j$  (Seber and Wild, 1989):

$$\Delta\theta_j = t_{\alpha, N-p} \cdot \sqrt{COV(\theta_j)} \quad (6.5)$$

Where  $t$  is the *t-Student* with a 95% of confidence ( $\alpha$ ) and  $N-p$  degrees of freedom (number of experimental data values minus number of calibrated model parameters).

### 6.2.5. CONTROL LOOP DESIGN

A control loop based on the addition of crude glycerol as external carbon source was proposed to diminish the  $NO_x$  (nitrate, nitrite and denitrification intermediates) presence under anaerobic conditions and thus, its detrimental effect on EBPR. The aim of this control loop was to provide enough carbon source to avoid the competition between OHO and PAO under anaerobic conditions. When glycerol is added, enough COD is available to denitrify  $NO_x$  entering R1 without limiting EBPR processes. The control strategy was based on the classical digital proportional-integral (PI) controller, where the controlled variable was the P concentration in R3, with a setpoint of  $1 \text{ mg P} \cdot \text{L}^{-1}$ , and the flow of glycerol added in R1 was the manipulated variable. The glycerol solution ( $48000 \text{ mg COD} \cdot \text{L}^{-1}$ ) was prepared with crude

glycerol obtained as a byproduct during biodiesel production from waste frying oils (*Biodiesel Peninsular*, Barcelona). The actuation of the control loop was set every 2 hour and the maximum glycerol addition was fixed at  $1.0 \text{ L}\cdot\text{d}^{-1}$  (0.4% the influent flow rate), which represented a maximum extra inlet of  $48 \text{ g COD}\cdot\text{d}^{-1}$  ( $200 \text{ mg COD}\cdot\text{L}^{-1}$  in the influent). The algorithm of the digital PI control, in the velocity form (see Section 6.3.3), was programmed in the PC by using LabWindows CVI 2010 software. The control loop implementation in the  $A^2/O$  pilot plant is schematically shown in figure 6.2.

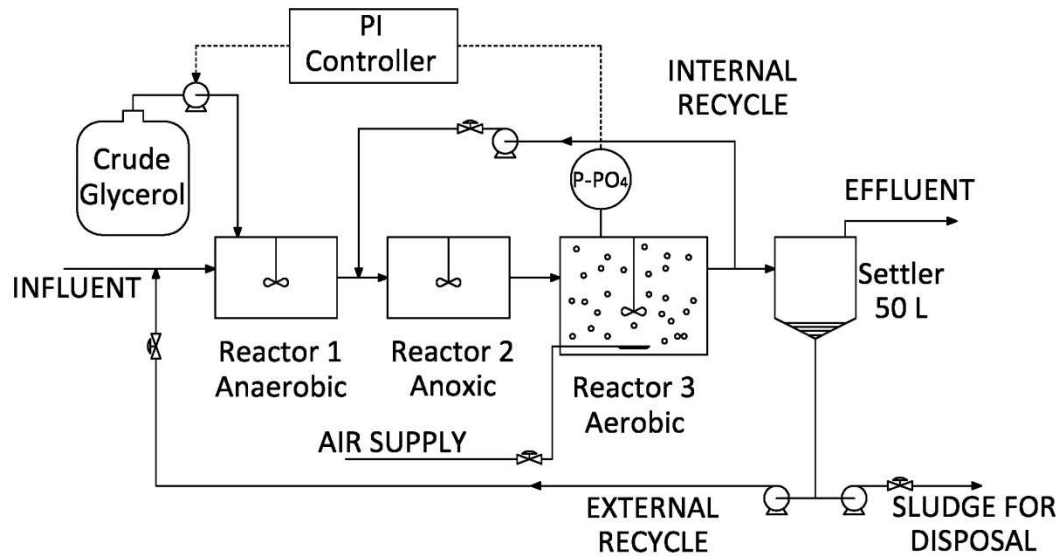


**Figure 6.2** Diagram of the feedback PI phosphorus control-loop for crude glycerol dosage in the  $A^2/O$  pilot plant.

## 6.3. Results and Discussion

### 6.3.1. PILOT PLANT CONFIGURATION *versus* NITROGEN DISTURBANCES

#### 6.3.1.1 $A^2/O$ pilot plant

In the first step of this study, a pilot plant with conventional  $A^2/O$  configuration was operated achieving successful nutrient removal. P-removal efficiency was higher than 90% for a period of 27 days (Figure 6.3). The reactive capacity of the settler allowed denitrifying part of the  $\text{NO}_x$  coming from  $Q_{\text{REXT}}$  (around 48.5% of reduction) reducing its detrimental effect under anaerobic conditions (R1). Under default operation conditions, the influent carbon source concentration was enough to guarantee fast  $\text{NO}_x$  denitrification in R1, achieving strict anaerobic conditions. Then, the amount of carbon source (i.e. milk or starch) that was not consumed for denitrification could be fermented to more readily biodegradable substrates (mainly VFA) by OHO, which in turn could be consumed by PAO favouring EBPR activity. As a result, an effluent with a P concentration lower than  $1 \text{ mg}\cdot\text{L}^{-1}$  was obtained.

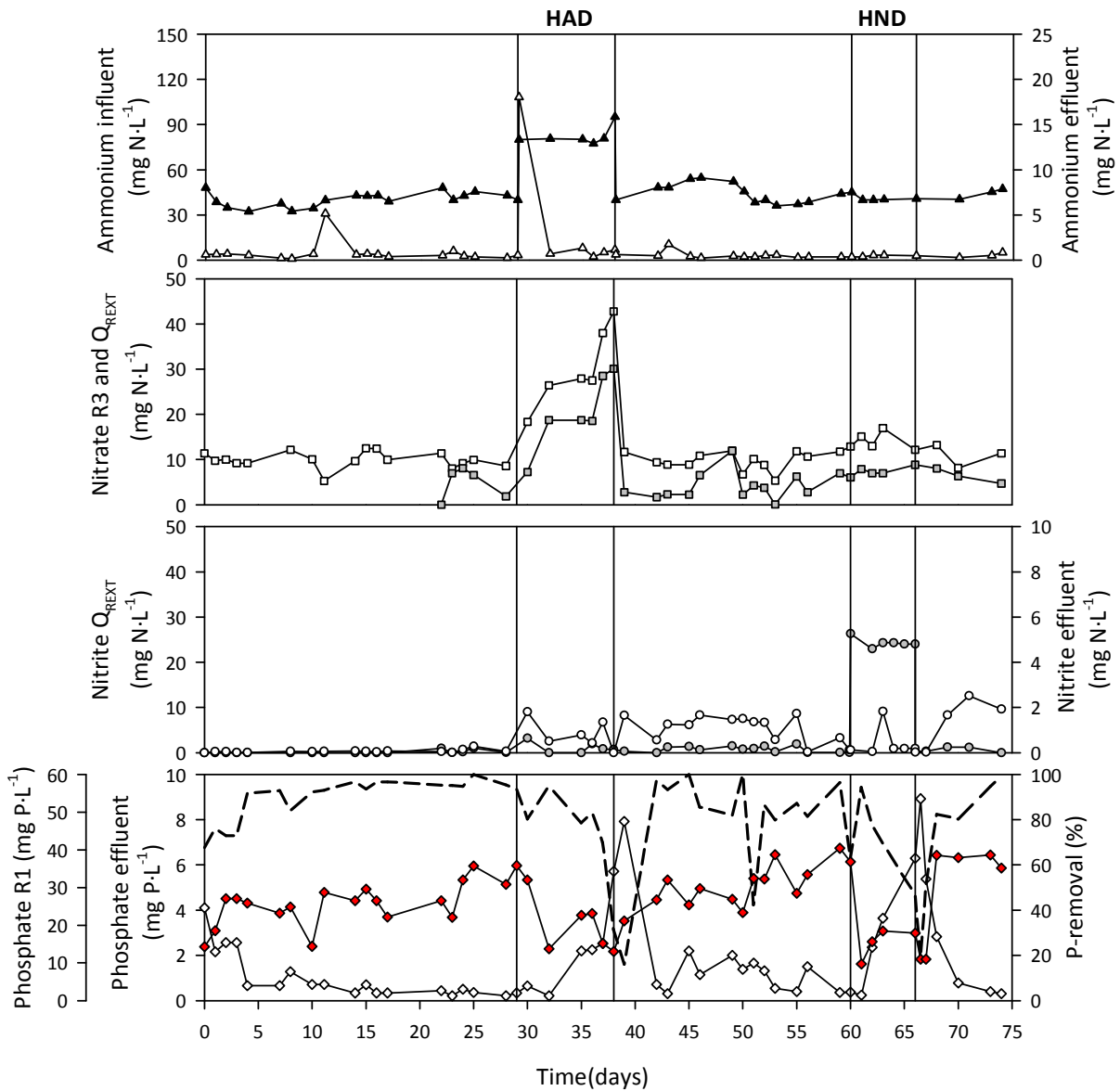


**Figure 6.3** Effect of nitrogen disturbances on P-removal efficiency in A<sup>2</sup>/O pilot plant. HAD = High ammonium influent disturbance. HND = High nitrite Q<sub>REXT</sub> disturbance.  $\triangle$  stands for ammonium,  $\square$  nitrate,  $\circ$  nitrite and  $\diamond$  phosphorus. Black colour belongs to influent compounds concentrations, red colour to R1 (anaerobic reactor), white colour to R3 (effluent) and grey colour to Q<sub>REXT</sub> concentrations. Dashed black line represents percentage of P-removal efficiency.

An increase in the influent ammonium nitrogen from 40 mg·L<sup>-1</sup> to 80 mg·L<sup>-1</sup> (high ammonium disturbance, HAD) was introduced at day 27. Total ammonium nitrification was observed from the beginning of the disturbance resulting in a fast increase of NO<sub>x</sub> in the aerobic reactor (R3). As a result, complete denitrification was not obtained in the settler and thus, high amount of NO<sub>x</sub> entered in the anaerobic reactor (23.6±5.9 mgN-NO<sub>x</sub>·L<sup>-1</sup>). This presence of anaerobic NO<sub>x</sub> favoured the denitrifying activity of OHO instead of its fermentative capacity to transform the carbon source into VFA, as was also observed with sucrose in Chapter V. Therefore, COD was mainly used to denitrify NO<sub>x</sub> reducing COD available for PAO and worsening EBPR process. As can be observed in figure 6.3, after HAD started, less P was

released under anaerobic conditions which could be related to lower VFA uptake and hence to lower PHA formation. This storage polymer is essential for the later P uptake in both anoxic and aerobic reactors and its low production resulted in a drop of P-removal capacity to 50% after 10 days under HAD conditions (day 37). Then, the perturbation was stopped to study the recovery capacity of the EBPR process in the A<sup>2</sup>/O pilot plant. Although ammonium nitrogen influent was reduced to 40 mg N·L<sup>-1</sup> on day 38, NO<sub>x</sub> entering to R1 did not instantly decrease and thus, P-removal capacity decreased even more reaching a value below 20% (day 39). Only when NO<sub>x</sub> levels in Q<sub>REXT</sub> were again similar to the values observed before HAD (from day 39), EBPR process was again favoured resulting in an increase of the P-removal efficiency (80% at day 42). As figure 6.3 shows, an increase of the P released to the bulk liquid in R1 was also observed after HAD ended due to more COD was again available in the anaerobic phase for PAO. These results are in agreement with the widely accepted idea that almost total NO<sub>x</sub> depletion in Q<sub>REXT</sub> is mandatory to achieve stable EBPR in WWTP with A<sup>2</sup>/O configuration (Simpkins and McLaren, 1978; Van Niel *et al.*, 1998; Henze *et al.*, 2008). However, it is also important to note that the nature of the carbon source played an important role in this EBPR failure. As was explained in Chapter V, very different results would have been obtained if the carbon source had been mainly constituted by VFA instead of a more complex carbon source like powder milk or starch.

During the HAD, NO<sub>x</sub> entering R1 was mainly formed by nitrate nitrogen whereas nitrite nitrogen concentration was never above 2 mg N·L<sup>-1</sup>. For that reason, an external high nitrite disturbance (HND) of 25 mg N·L<sup>-1</sup> was added to Q<sub>REXT</sub> in order to study how the presence of this compound in the anaerobic phase could affect to the EBPR process (HND period on figure 6.3). Once HND started, P-release in R1 rapidly decreased (from 36.8 to 9.7 mg P-PO<sub>4</sub><sup>-3</sup>·L<sup>-1</sup> in only one day) indicating that the EBPR process was negatively affected by the nitrite inlet in the anaerobic phase. As a result, the P-removal efficiency dropped after six days under HND conditions to 47% (day 66 in figure 6.3). In this case, the NO<sub>x</sub> present in Q<sub>REXT</sub> was around 31.8±0.7 mg N·L<sup>-1</sup>, higher than in the HAD. However, similar COD requirements for total NO<sub>x</sub> denitrification in R1 were obtained: 178 ± 45 and 168 ± 5 mg COD·L<sup>-1</sup> for HAD and HND, respectively. The main component of recycled NO<sub>x</sub> was nitrite in this case and less COD was necessary for its denitrification: 22.8±5.3 mg N-NO<sub>3</sub><sup>-</sup>·L<sup>-1</sup> and 0.7±0.5 mg N-NO<sub>2</sub><sup>-</sup>·L<sup>-1</sup> during HAD, and 7.5±1.0 mg N-NO<sub>3</sub><sup>-</sup>·L<sup>-1</sup> and 24.3±1.1 mg N-NO<sub>2</sub><sup>-</sup>·L<sup>-1</sup> during HND. These values were calculated assuming default growth yields: 7.6 mg COD would be required to denitrify 1 mg N-NO<sub>3</sub><sup>-</sup> whereas around 4.6 mg COD would be consumed for 1 mg N-NO<sub>2</sub><sup>-</sup> denitrification (Henze *et al.*, 2000). According to this, EBPR failure in HND experiment was again explained due to the fact that denitrification processes were favoured (i.e. almost total NO<sub>x</sub> denitrification was observed in R1) instead of complex carbon source fermentation to VFA. At day 66, HND was stopped and EBPR activity was rapidly recovered increasing the P removal efficiency of the system above 80% (Figure 6.3).

Free nitrous acid (FNA) concentration in anoxic and aerobic reactors was calculated for HAD and HND periods according to acid-base equilibriums (Jubany *et al.*, 2008) to discard the EBPR failure due to a inhibitory effect of FNA on P-uptake process. The highest FNA values obtained for both HAD and HND periods were  $2.2 \cdot 10^{-4}$  mg N-HNO<sub>2</sub>·L<sup>-1</sup> under anoxic conditions and  $8.8 \cdot 10^{-5}$  mg N-HNO<sub>2</sub>·L<sup>-1</sup> under aerobic conditions. In both cases, FNA concentrations were never above the reported values that could induce P-uptake inhibition: FNA >  $2 \cdot 10^{-3}$  mg N-HNO<sub>2</sub>·L<sup>-1</sup> under anoxic conditions according to Zhou *et al.* (2007) and FNA >  $4 \cdot 10^{-4}$  mg N-HNO<sub>2</sub>·L<sup>-1</sup> under aerobic conditions according to Pijuan *et al.* (2010). Hence, this hypothesis could be rejected being COD limitations the most likely reason to explain EBPR failure.

### 6.3.1.2 Johannesburg pilot plant

In the second step of the study, the configuration was moved to a JHB setup (Figure 6.1 down) aiming to evaluate the effect of the plant configuration on P removal efficiency against ammonium and nitrite disturbances. JHB configuration enhances EBPR activity by decreasing NO<sub>x</sub> load to the anaerobic reactor (Henze *et al.*, 2008). For this aim, an extra anoxic reactor (R4, 15L) was added to denitrify the NO<sub>x</sub> coming through Q<sub>REXT</sub> using the organic matter from the lysis of biomass and the internal storage products (PHA) as electron acceptor. Total NO<sub>x</sub> denitrification was obtained in R4 before entering in R1 (Figure 6.4) favouring almost total influent COD fermentation to VFA under anaerobic conditions (i.e. more COD was available for EBPR) and thus, PAO growth. In fact, some P-release was observed in R4 (data not shown) showing that this reactor could already operate as a pre-anaerobic phase. As a result, higher P-release was obtained in comparison to the A<sup>2</sup>/O configuration ( $41.2 \pm 4.3$  and  $26.4 \pm 4.8$  mg P-PO<sub>4</sub><sup>-3</sup> in R1 for JHB and A<sup>2</sup>/O configurations, respectively). High EBPR activity was then reached with P-removal efficiency above 95% before introducing any disturbance.

In HAD1, the same ammonium increase as in the A<sup>2</sup>/O pilot plant was performed (40 to 80 mg N·L<sup>-1</sup>). Ammonium was again totally nitrified increasing NO<sub>x</sub> concentration in Q<sub>REXT</sub> ( $21.5 \pm 3.4$  mgN-NO<sub>x</sub>·L<sup>-1</sup>). The extra anoxic reactor (R4) highly reduced NO<sub>x</sub> in Q<sub>REXT</sub> before entering the anaerobic phase of R1, resulting in a concentration of  $8.3 \pm 5.8$  mgN-NO<sub>x</sub>·L<sup>-1</sup>. Less COD was then needed for total NO<sub>x</sub> depletion in R1 avoiding EBPR failure unlike to A<sup>2</sup>/O operation. P-removal efficiency only decreased from 95% to approximately 86% after 16 days under HAD1 conditions. A second increase of the ammonium influent concentration (HAD2), from 80 to 120 mg·L<sup>-1</sup>, was performed aiming to study the denitrifying capacity limits of R4. Once HAD2 started, P release under anaerobic conditions rapidly decreased together with EBPR activity of the system (Figure 6.4). After only 4 days (day 28), HAD2 was stopped due to P-removal efficiency decreased to 50%. In this case, the denitrifying capacity of R4 was not enough to reduce NO<sub>x</sub> amount from Q<sub>REXT</sub> and  $19.7 \pm 3.1$  mgN-NO<sub>x</sub>·L<sup>-1</sup> entered the anaerobic phase causing the EBPR failure. This value was similar to the one that also provoked EBPR failure in the A<sup>2</sup>/O configuration under HAD conditions (see above). The total



depletion of  $\text{NO}_x$  observed in R1 proved again that denitrification processes were favoured and predominant under anaerobic conditions reducing the COD available for PAO activity. Once HAD2 ended, P removal efficiency did not further decrease as was observed for the  $\text{A}^2/\text{O}$  configuration because R4 allowed a faster reduction of the  $\text{NO}_x$  content in  $Q_{\text{REXT}}$  to the values observed before HAD1 and 2. After 2 days from HAD2 finalization, high EBPR activity was recovered (higher P release and uptake capacity) resulting in P effluent concentration under  $1 \text{ mg}\cdot\text{L}^{-1}$  at day 34 (Figure 6.4). FNA was also calculated for HAD1 and HAD2, which was also below inhibitory values ( $<2\cdot 10^{-4} \text{ mg N}\cdot\text{HNO}_2\cdot\text{L}^{-1}$  under anoxic and aerobic conditions).

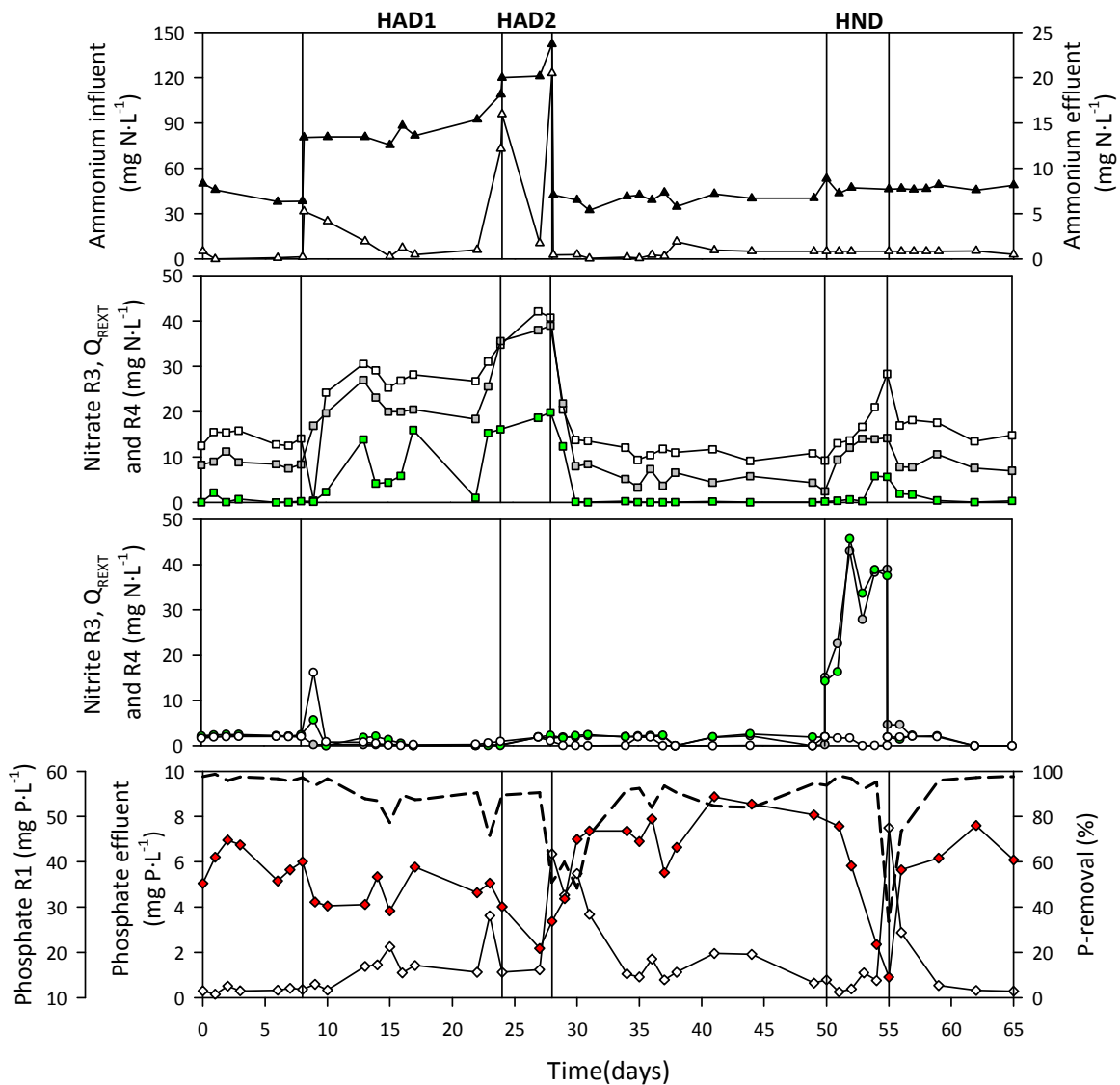


**Figure 6.4** Effect of nitrogen disturbances on P-removal efficiency in the JHB pilot-plant. HAD 1 and 2 = High ammonium influent disturbances 1 and 2. HND = High nitrite  $Q_{\text{REXT}}$  disturbance.  $\triangle$  represents ammonium,  $\square$  nitrate,  $\circ$  nitrite and  $\diamond$  phosphorus. Black colour belongs to influent compounds concentrations, red colour to R1 (anaerobic reactor), white colour to R3 (effluent), grey colour to  $Q_{\text{REXT}}$  concentrations and green colour to R4 (Johannesburg reactor). Dashed black line represents percentage of P-removal efficiency.

HND experiment was also performed in the JHB configuration. Nitrite concentration was increased to  $37.0 \pm 6.4 \text{ mg N-NO}_2^- \cdot \text{L}^{-1}$  in  $Q_{\text{REXT}}$  to obtain a high  $\text{NO}_x$  inlet in R4 ( $50.5 \pm 5.9 \text{ mg N-NO}_x \cdot \text{L}^{-1}$ ) with similar COD denitrifying requirements as HAD2 ( $273 \pm 26$  and  $292 \pm 15 \text{ mg COD} \cdot \text{L}^{-1}$  for HND and HAD2, respectively). Under these conditions, the amount of P released to the bulk liquid drastically decreased from 47.8 to 15.8  $\text{mg P-PO}_4^{3-} \cdot \text{L}^{-1}$  in four days (from day 50 to 55). From that point on, fast EBPR failure was observed and P effluent concentration rose from 0.75 to 7.5  $\text{mg P-PO}_4^{3-} \cdot \text{L}^{-1}$  in only one day. Regarding R4, nitrite concentration remained almost constant during all the HND ( $31.1 \pm 2.4 \text{ mg N-NO}_2^- \cdot \text{L}^{-1}$ ), contrary to nitrate that was almost totally denitrified (from  $13.5 \pm 1.0 \text{ mg N-NO}_3^- \cdot \text{L}^{-1}$  in  $Q_{\text{REXT}}$  to  $2.1 \pm 2.0 \text{ mg N-NO}_3^- \cdot \text{L}^{-1}$  after R4). Although part of the nitrite was obviously denitrified, partial denitrification of nitrate to nitrite and not to nitrogen gas could explain this stable value of nitrite. It was also observed that the denitrifying levels in R4 surprisingly decreased in comparison with HAD2 period. Only the 17% of the total  $\text{NO}_x$  that entered in R4 was denitrified in comparison to the 49% observed in HAD2 period (Figure 6.4). The high amount of nitrite in R4 resulted in a FNA concentration around  $4.9 \cdot 10^{-3} \text{ mg N-HNO}_2 \cdot \text{L}^{-1}$  which could partially inhibit the denitrification capacity of DPAO and denitrifying OHO. This value was quite lower than the observation reported by Zhou *et al.* (2007) and Ma *et al.* (2010), where an important decrease of the nitrite reduction capacity was observed when FNA concentration was around  $2 \cdot 10^{-2} \text{ mg N-HNO}_2 \cdot \text{L}^{-1}$ . However, the fact that biomass was not acclimated before to coexist with these FNA levels could explain this inhibitory effect at lower concentrations. As a consequence, more  $\text{NO}_x$  entered in the anaerobic reactor ( $42.0 \pm 5.6 \text{ mg NO}_x \cdot \text{L}^{-1}$ ) resulting in higher COD requirements for total  $\text{NO}_x$  denitrification. After EBPR failure, HND was stopped at day 55. P effluent concentration did not continue increasing but also a fast recovery of EBPR activity was observed unlike to the  $\text{A}^2/\text{O}$ . P-removal efficiency increased above 70% in only one day after HND ended. As also occurred in HAD2, R4 allowed faster denitrification of the  $\text{NO}_x$  present in  $Q_{\text{REXT}}$ . Here it was clearly confirmed that JHB configuration reduced the recovery time of EBPR activity in comparison with the  $\text{A}^2/\text{O}$  configuration even under more unfavourable conditions (HAD2 in JHB in comparison with HAD in  $\text{A}^2/\text{O}$ ).

### 6.3.2. MODEL CALIBRATION AND VALIDATION I

An extended version of ASM2d (see section 6.2.3 and Annex I) was used to design a phosphorus controller based on crude glycerol addition. For this purpose, it was firstly necessary to calibrate the model in order to accurately describe the experimental results. The experimental data corresponding to  $\text{A}^2/\text{O}$  operation from day 0 to day 45 (Figure 6.3) was used for these purposes. The selection of the parameters to be calibrated was performed by prioritizing those that had a strong effect on PAO and OHO competition. Table 6.2 presents the values of the calibrated parameters and their confidence intervals, which were calculated with the FIM criteria.

**Table 6.2** Parameters obtained from model calibration by using the experimental data of normal operation and HAD in A<sup>2</sup>/O configuration. GEF: Global efficiency factor applied to the reactive settler capacity. Confidence interval was calculated by applying FIM approach.

Parameters	ASM2d value (20°C)	Calibrated value	Units
$q_{PHA}$	3.00	2.76±0.04	mg $X_{PHA}$ · mg $X_{PAO}^{-1}$ · d <sup>-1</sup>
$q_{PP}$	1.50	1.70±0.02	mg $X_{PP}$ · mg $X_{PAO}^{-1}$ · d <sup>-1</sup>
$\mu_{HET}$	6.00	4.10±0.04	d <sup>-1</sup>
$\eta_{NO_3, OHO}$	0.80	0.32±0.06	-
$\eta_{NO_2, OHO}^*$	-	0.48±0.02	-
GEF*	-	0.59±0.03	-

\* These parameters do not appear in the default ASM2d model (Henze *et al.*, 2000)

Some other parameters were also initially used during calibration step that are not shown in this table because no differences with the default ASM2d values were obtained. Despite considering only measurement errors in matrix  $Q_K$  (and not modelling errors) on confidence intervals calculation (Dochain and Vanrolleghem, 2001), the low values obtained corroborated that the calibrated parameters were properly selected without correlations between them.

Regarding the values of the estimated parameters, the lower PHA storage rate ( $q_{PHA}$ ) suggested that PAO from A<sup>2</sup>/O were less efficient at consuming VFA than with the standard ASM2d values. On the contrary, higher value of P uptake rate ( $q_{PP}$ ) was obtained, which means that PAO was more effectively taking up P under anoxic and aerobic conditions. Regarding OHO parameters, the experimental data was correctly described by assuming a lower capacity to denitrify from nitrate to nitrite and from nitrite to nitrogen gas, so lower reduction factors from denitrification ( $\eta_{NO_3, OHO}$  and  $\eta_{NO_2, OHO}$ ) were obtained. In addition, OHO biomass presence in the system was also limited by decreasing heterotrophic growth rate ( $\mu_{HET}$ ). Finally, a global efficiency factor of 0.59 was applied to the reactions occurring in the settler.

Figure 6.5 shows the experimental data and the model predictions for the A<sup>2</sup>/O pilot plant. A proper description of the experimental behaviour was obtained with the new parameters for the calibration data, but also even after HAD and for HND experiment, whose experimental data were not used for the calibration process. Only some deviations in P-release prediction in R1 were observed under the HND period (from day 60 to 66), where the model predicted higher P concentrations in R1. As was commented above, the system was never exposed to high nitrite concentration before HND and a possible inhibitory effect not considered in the model (i.e. inhibitory kinetics related to FNA presence were not included in the model) could cause this divergences. In any case, proper description of P concentration in R3 was obtained even under HND conditions, and the predictive capacity of the model was therefore validated.

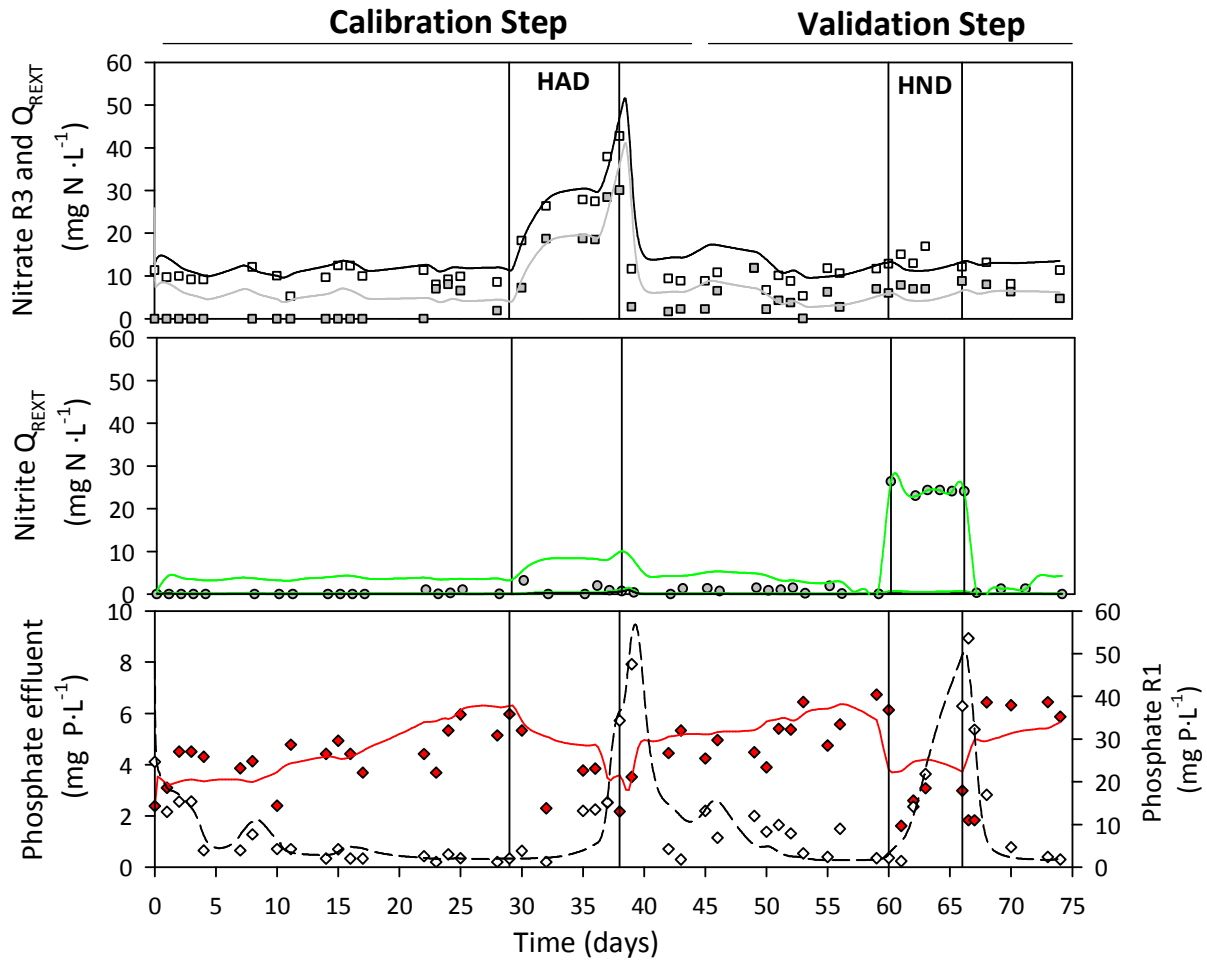


**Figure 6.5** Model calibration and validation. A<sup>2</sup>/O pilot plant experimental behaviour and model predictions. Experimental data:  $\square$  stands for nitrate,  $\circ$  nitrite and  $\diamond$  phosphorus. Red colour belongs to R1 (anaerobic reactor) concentrations, white colour to R3 (effluent), grey colour to  $Q_{REXT}$ . Model predictions: black line belongs to nitrate in R3, grey line to nitrate in  $Q_{REXT}$ , green line to nitrite in  $Q_{REXT}$ , red line to phosphate in R1 and black dashed line to phosphate in R3.

### 6.3.3. CRUDE GLYCEROL CONTROL LOOP (CGCL)

The controller algorithm consisted of a feedback proportional-integral (PI) controller that was implemented in the simulator in the velocity form of the corresponding digital algorithm (equation 6.6), where  $C$  was the controller output variable at moment  $n$  and  $n-1$  (crude glycerol flow added in R1),  $K_C$  was the proportional gain,  $\tau_i$  was the integral time constant, the increment  $t_n - t_{n-1}$  was the control interval time (set to two hours) and  $\varepsilon$  was the error of the measured variable ( $P-PO_4^{-3}$  in R3) respect to the desired setpoint ( $1 \text{ mg} \cdot \text{L}^{-1}$ ). The velocity form presents some advantages as i) it does not need initialization, ii) it is protected against integral “windup” and iii) it preserves the process against computer failure (Stephanopoulos, 1984).

$$C_n = C_{n-1} + K_C \cdot \left[ (\varepsilon_n - \varepsilon_{n-1}) + \frac{t_n - t_{n-1}}{\tau_i} \cdot \varepsilon_n \right] \quad (6.6)$$

The parameters of the digital PI controller ( $K_C$  and  $\tau_i$ ) were tuned according to ITAE criterion (equation 6.7), which is based on the minimization of the integral of time weighted absolute error of the entire process response (Stephanopoulos, 1984). ITAE was selected aiming at obtaining a short settle time.

$$\text{ITAE} = \int_0^{t_{\text{end}}} |\varepsilon(t)| \cdot t \cdot dt \quad \text{or} \quad \text{ITAE} = \sum_{i=0}^{t_{\text{end}}} \varepsilon_i \cdot t_i \cdot (t_i - t_{i-1}) \quad (6.7)$$

The calibrated model (Table 6.2) was used to simulate the experimental data of A<sup>2</sup>/O pilot plant for controller tuning. Hence, the values that resulted in the minimum ITAE value were:  $K_C = -0.1 \text{ L} \cdot \text{d}^{-1} (\text{mg P} \cdot \text{L}^{-1})^{-1}$  and  $\tau_i = 9 \text{ d}$ . The negative value of  $K_C$  indicates an inverse controller actuation. When more glycerol is added to R1, more carbon source is available for OHO to denitrify anaerobic NO<sub>x</sub> or to be fermented to VFA. Both processes increase EBPR activity reducing P effluent concentration. Controller parameter values also showed a slow and soft control actuation. This is mainly because glycerol addition in R1 (manipulated variable) does not have an instantaneous effect on the phosphate concentration in R3 (controlled variable) and some time is necessary to observe this effect (Olsson *et al.*, 2007).

Figure 6.6 presents the simulation results when the feedback CGCL was implemented in A<sup>2</sup>/O pilot plant with the optimum ITAE controller parameters. CGCL was not activated until day 29 (i.e. open-loop operation). It is important to remark that the control algorithm was programmed so that there was not glycerol addition until the P setpoint was overcome for the first time (at day 36); from that point the controller was always activated. According to the simulation results, controlled addition of crude glycerol in R1 could potentially reduce the negative effect of nitrate and nitrite presence under anaerobic conditions, if compared with open-loop operation when crude glycerol was not added (Figure 6.6 up). In this sense, effluent P was never above  $2.5 \text{ mg P-PO}_4^{-3} \cdot \text{L}^{-1}$  during HAD and HND.

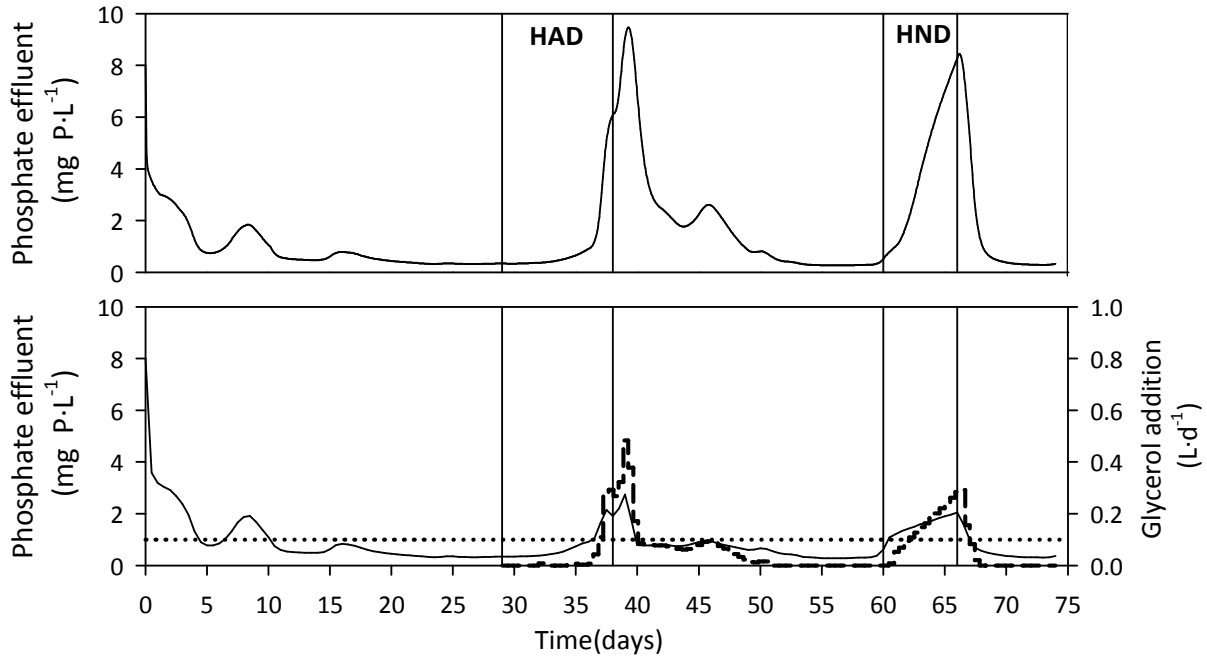


**Figure 6.6** Comparison of P-removal capacity for open-loop operation (up) and for optimum ITAE CGCL implementation (down). In black solid lines is presented phosphate concentration in R3, dashed line represents the glycerol addition due to CGCL actuation and the black dotted line the setpoint of  $\text{P-PO}_4^{3-}$  in R3 ( $1 \text{ mg}\cdot\text{L}^{-1}$ ).

#### 6.3.4. CGCL *versus* NITROGEN DISTURBANCES: EXPERIMENTAL VALIDATION

In the next step of the study the experimental validation of CGCL was performed. For this aim, the optimised CGCL was implemented in  $\text{A}^2/\text{O}$  and JHB pilot plants to analyse its real feasibility at preventing EBPR failure under HAD and HND scenarios.

Figure 6.7 shows the main results when CGCL was implemented in the  $\text{A}^2/\text{O}$  pilot plant for HAD and HND experiments. Online P and inline  $\text{N-NO}_3^-$  measurements in R3 by PHOSPHAX analyser and  $\text{NO}_3\text{sc}$  probe (see Chapter III for further information) are represented instead of offline measurements.

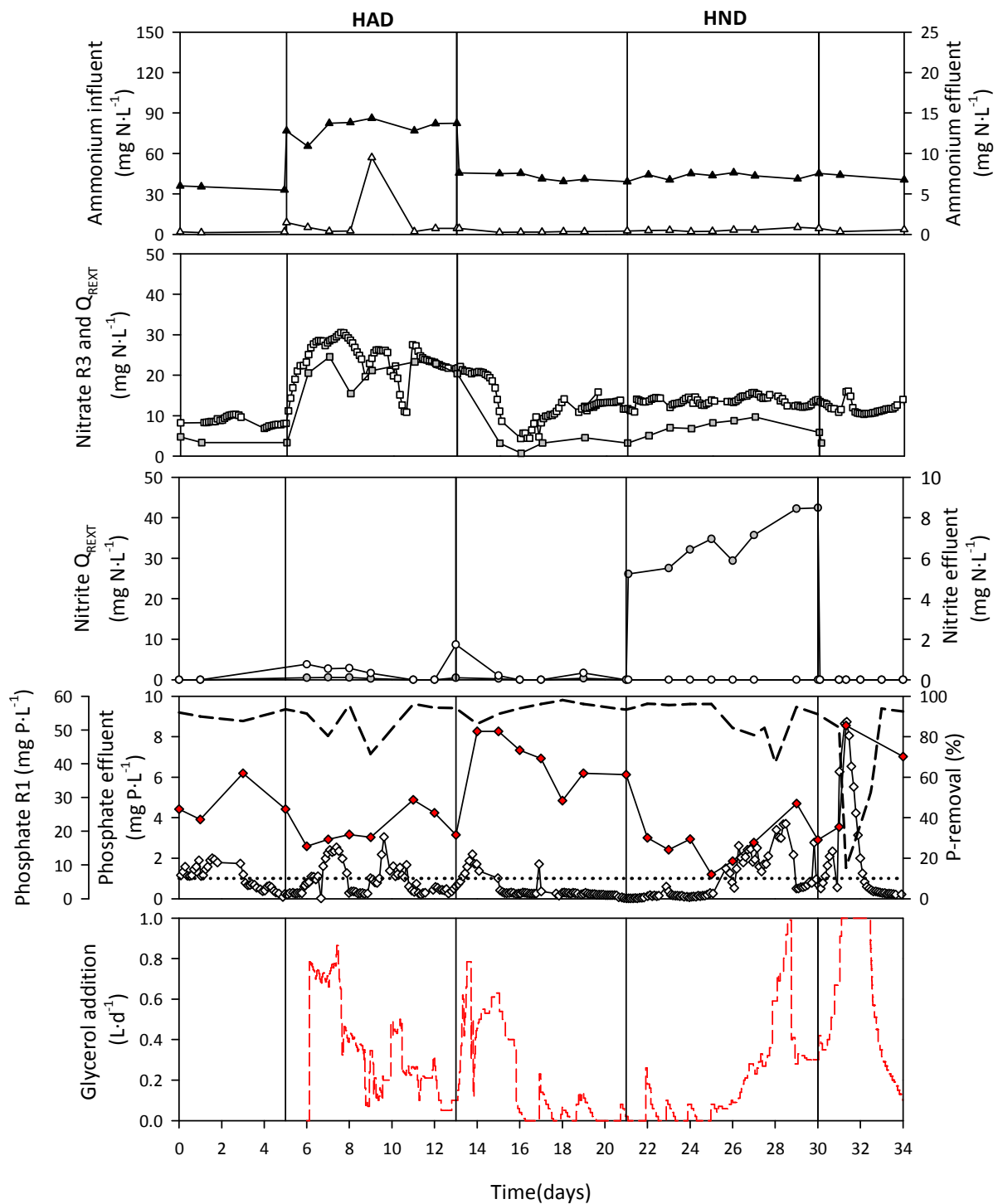


**Figure 6.7** Effects of nitrogen disturbances on P-removal efficiency in A<sup>2</sup>/O pilot plant with implemented CGCL.  $\triangle$  represents ammonium,  $\square$  nitrate,  $\circ$  nitrite and  $\diamond$  phosphorus. Black colour belongs to influent compounds concentrations, red colour to R1 (anaerobic reactor), white colour to R3 (effluent) and grey colour to Q<sub>REXT</sub> concentrations. Dashed black line represents P-removal efficiency, dotted line the P setpoint of CGCL (1 mg P-PO<sub>4</sub><sup>-3</sup>·L<sup>-1</sup>) in R3 and red line the glycerol addition.

As observed before, P release dropped when HAD started (day five) mainly due to COD was more effectively consumed for denitrification than for VFA production. Consequently, P concentration in R3 started to increase over the P setpoint value ( $1 \text{ mg P-PO}_4^{-3}\cdot\text{L}^{-1}$ ) at day six, which activated crude glycerol dosage by CGCL. The EBPR failure was successfully stopped and PAO activity in the system was again recovered at day 8. The amount of crude glycerol added by CGCL favoured EBPR due to three main interrelated reasons: i) there was enough COD for total denitrification of  $\text{NO}_x$  coming from  $Q_{\text{REXT}}$  ( $21.2\pm 2.7 \text{ mgN-NO}_x\cdot\text{L}^{-1}$ ); ii) strict anaerobic conditions were ensured in R1; and iii) there was also enough COD to be fermented to VFA favouring EBPR activity. The later point was in agreement with Guerrero *et al.* (2012) (see Annex II), who demonstrated that glycerol could be fermented to VFA by a syntrophic consortium of microorganisms improving EBPR activity when treating wastewater with carbon shortage. During the rest of HAD, P concentration value in R3 did not present a constant trend around the setpoint value. In some cases this value increased above  $3 \text{ mg P-PO}_4^{-3}\cdot\text{L}^{-1}$  and in some others, the value was below  $0.5 \text{ mg P-PO}_4^{-3}\cdot\text{L}^{-1}$ . This fluctuating behaviour could be explained because the P removal process is based on the combination of anaerobic, anoxic and aerobic processes and thus, it presented a slow response to the control loop actuation. Hence, when EBPR partially failed and effluent P increased, some time was required to observe the corrective effect of crude glycerol addition. It has to be also considered the disturbing effect in the control actuation of some possible noise in the controlled variable (P concentration in R3) or experimental errors. In any case, total EBPR failure was never observed in contrast to the open-loop operation without CGCL implementation (Figure 6.3) and P-removal efficiency was always above 70% during the HAD.

At day 13, although HAD was stopped and  $\text{NO}_x$   $Q_{\text{REXT}}$  content rapidly decreased, the extra COD entering the anaerobic reactor favoured VFA production, which was taken up by PAO resulting in a fast increase of P release. This increase occurred so fast that total P uptake was not achieved then under aerobic conditions and P concentration in R3 increased up to  $2.0 \text{ mg}\cdot\text{L}^{-1}$  at day 14. However it was only a temporary episode since after only one day, total P uptake was again observed and crude glycerol addition by CGCL was then gradually reduced.

To reduce this oscillatory control of P, a correction of the PI controller by adding a feedforward controller measuring the ammonium inlet could be recommended. Hence, the new control structure would have the capacity to start adding glycerol when HAD started and to reduce this addition when HAD finished. A fast decrease or increase of P released under anaerobic conditions would be avoided. In other words, an observed EBPR failure would not be necessary to activate glycerol addition and thus, more constant P-removal efficiency would be observed under HAD conditions. This alternative has been tested in a simulation-based study and the main results are presented in section 6.3.7.



HND was initiated at day 21 by introducing  $34.5 \pm 5.8 \text{ mgN-NO}_2^- \cdot \text{L}^{-1}$  in  $Q_{\text{REXT}}$  (Figure 6.7) to obtain similar COD requirements for  $\text{NO}_x$  denitrification as in HAD ( $173 \pm 27 \text{ mg COD} \cdot \text{L}^{-1}$  for HND and  $161 \pm 21 \text{ mg COD} \cdot \text{L}^{-1}$  for HAD). P-release started to decrease from  $36.8$  to  $7.2 \text{ mgP-PO}_4^{-3} \cdot \text{L}^{-1}$  at day 25 resulting in a deterioration of EBPR. As a result, P concentration in R3 increased to  $1.52 \text{ mg} \cdot \text{L}^{-1}$ , leading to more glycerol addition due to a higher CGCL actuation (i.e. CGCL remained active until activation during HAD). The crude glycerol dosage ensured total denitrification of  $\text{NO}_x$  in  $Q_{\text{REXT}}$  and EBPR activity was again favoured (i.e. P release capacity was again recovered). However, slow response of the P removal process to the CGCL actuation was again observed and P effluent concentration continued increasing until a maximum value of  $3.7 \text{ mg} \cdot \text{L}^{-1} \text{ P-PO}_4^{-3}$  at day 28. As a consequence, the CGCL kept adding more glycerol until an upper constraint was reached ( $1 \text{ L glycerol} \cdot \text{d}^{-1}$ ). As commented before, a maximum dosage rate was necessary in the controller algorithm to avoid excessive glycerol addition. One day after, the effect of CGCL was visible in EBPR (i.e. higher P uptake capacity) and P concentration in R3 decreased to the setpoint value. Glycerol addition also decreased accordingly.

When HND finished (day 30), P release in R1 drastically increased from  $21.3$  to  $51.3 \text{ mgP-PO}_4^{-3} \cdot \text{L}^{-1}$  exceeding temporarily the P-uptake capacity of the system and thus, P concentration in R3 rose to  $8.5 \text{ mgP-PO}_4^{-3} \cdot \text{L}^{-1}$  (day 31). This behaviour can be explained because when HND was stopped, the extra nitrite inlet to  $Q_{\text{REXT}}$  was stopped and the remaining nitrite was instantly denitrified (Figure 6.7). As a result, the carbon source present in R1 (COD from influent plus crude glycerol addition) was mainly fermented and consumed by PAO. Once again, such sudden P increase in R3 resulted in an increase of glycerol addition due to CGCL reaching again the maximum addition value. After one day under these conditions (from day 31 to day 32), high P uptake capacity was recovered with P removal efficiency above 85%.

CGCL was also tested in the JHB configuration (Figure 6.8). As expected, the controller actuation reduced the detrimental effect of  $\text{NO}_x$  on EBPR process in both HAD and HND experiments. Different to open-loop experiments, the same disturbances as in  $\text{A}^2/\text{O}$  were performed in JHB to compare the control response in different plant configurations (HAD2 was not performed in this case). During the disturbance periods, P concentration in R3 was well controlled around the P setpoint value:  $0.95 \pm 0.58 \text{ mg P-PO}_4^{-3} \cdot \text{L}^{-1}$  and  $1.31 \pm 0.67 \text{ mg P-PO}_4^{-3} \cdot \text{L}^{-1}$  for HAD and HND, respectively. The highest P effluent concentrations observed were  $2.37 \text{ mg P-PO}_4^{-3} \cdot \text{L}^{-1}$  at day 9 for HAD and  $2.5 \text{ mg P-PO}_4^{-3} \cdot \text{L}^{-1}$  at day 23 for HND. The main difference with respect to  $\text{A}^2/\text{O}$  configuration was not observing the P effluent increase at the end of HND (day 31). The inclusion of R4 in JHB configuration explained this fact. During HND, part of the  $\text{NO}_x$  from  $Q_{\text{REXT}}$  was denitrified in R4 (55.2%), reducing the required COD amount for denitrification in R1 ( $85 \pm 19 \text{ mg COD} \cdot \text{L}^{-1}$  for JHB in comparison to  $173 \pm 27 \text{ mg COD} \cdot \text{L}^{-1}$  for  $\text{A}^2/\text{O}$ ). It resulted in more COD available for PAO and EBPR process was not significantly affected during HND, so that no sudden changes on the amount of P released in

R1 were observed when HND was stopped (Figure 6.8). By the same token, P concentration in R3 did not present a fluctuating trend as for  $A^2/O$ .

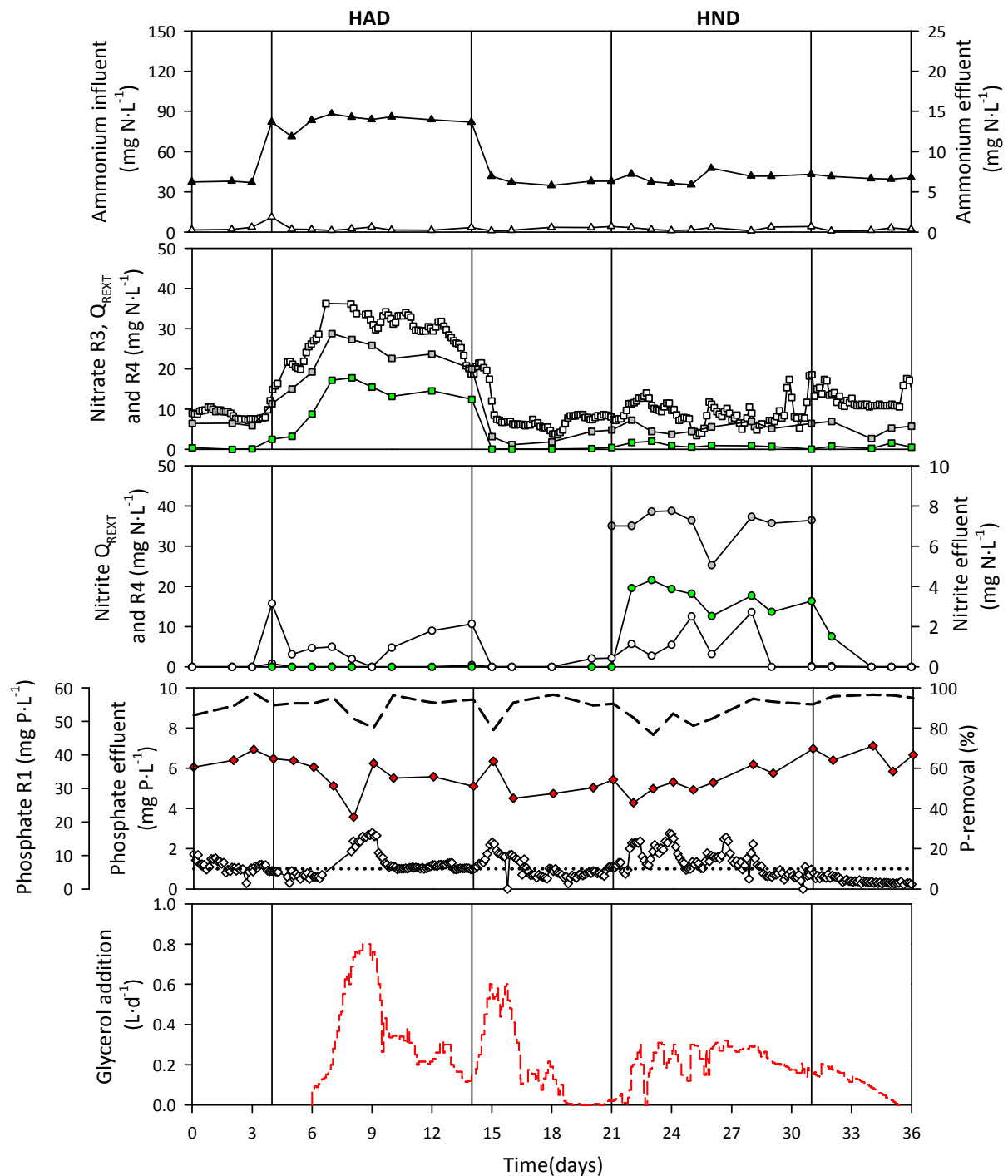


**Figure 6.8** Effect of nitrogen disturbances on P-removal efficiency in the JHB pilot-plant.  $\triangle$  represents ammonium,  $\square$  nitrate,  $\circ$  nitrite and  $\diamond$  phosphorus. Black colour belongs to influent compounds concentrations, red colour to R1 (anaerobic reactor), white colour to R3 (effluent), grey colour to  $Q_{REXT}$  concentrations and green colour to R4 concentrations. Black dashed line represents percentage of P-removal efficiency, red dashed line the glycerol addition and black dotted line the P setpoint of CGCL ( $1 \text{ mg P-PO}_4^{3-} \cdot \text{L}^{-1}$ ) in R3.

The amount of glycerol used by CGCL during HAD and HND was also different for both pilot plants. When CGCL was implemented in the A<sup>2</sup>/O configuration, the total amount of crude glycerol added was 8.29 L while 6.77L (18% lower) were only needed in the JHB pilot plant. This difference can be explained by the extra anoxic volume for denitrification of R4 in JHB. R4 prevented part of the NO<sub>x</sub> to enter in the anaerobic phase reducing crude glycerol requirements to maintain enough COD for OHO and PAO. In other words, JHB configuration smoothed the negative effect of HAD and HND on EBPR process and so the CGCL actuation and crude glycerol was reduced.

Regarding these results, crude glycerol was proved for the first time to be useful to prevent the EBPR failure due to NO<sub>x</sub> presence under anaerobic conditions. As shown, crude glycerol was a suitable carbon source to denitrify the NO<sub>x</sub> coming from Q<sub>REXT</sub> and to favour EBPR activity. In the latter case, it was assumed that crude glycerol was likely fermented to VFA, which were uptake by PAO for biological phosphorus removal (Guerrero *et al.*, 2012; see Annex II). Thereby, its controlled addition was also demonstrated as a good alternative to reduce the negative effect of HAD and HND on EBPR when compared to open-loop operation.

### 6.3.5. MODEL CALIBRATION AND VALIDATION II

The model predictions when simulating the CGCL experiments with the calibrated parameters from table 6.2 were not satisfactory. For that reason, a second calibration step was performed by using the experimental data of A<sup>2</sup>/O when CGCL was implemented. The parameters to be calibrated were again selected by prioritizing those that have a strong effect on PAO and OHO competition.

**Table 6.3** Parameters obtained after model calibration by using the experimental data of A<sup>2</sup>/O configuration with implemented CGCL. GEF: Global efficiency factor applied to the reactive settler capacity. Confidence interval was calculated by applying FIM approach.

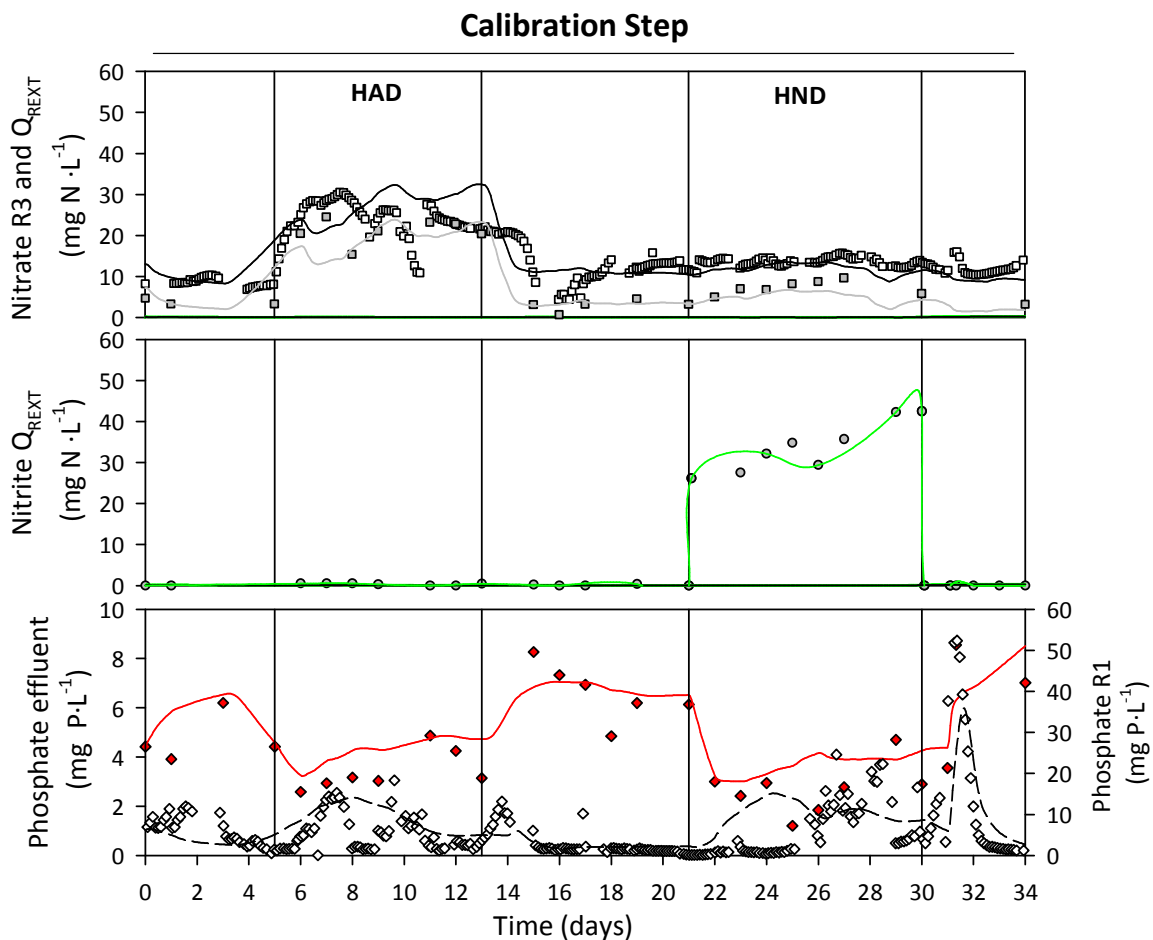
Parameters	ASM2d value (20°C)	Calibrated value	Units
q <sub>PHA</sub>	3.00	5.03±0.04	mg X <sub>PHA</sub> · mg X <sub>PAO</sub> <sup>-1</sup> · d <sup>-1</sup>
q <sub>PP</sub>	1.50	1.35±0.01	mg X <sub>PP</sub> · mg X <sub>PAO</sub> <sup>-1</sup> · d <sup>-1</sup>
η <sub>NO<sub>2</sub>, PAO</sub> *	-	0.60±0.02	-
μ <sub>HET</sub>	6.00	5.13±0.06	d <sup>-1</sup>
η <sub>NO<sub>3</sub>, OHO</sub>	0.80	0.61±0.01	-
μ <sub>AOB</sub> *	-	1.42±0.01	d <sup>-1</sup>
GEF*	-	0.61±0.01	-

\*These parameters do not appear in ASM2d model (Henze *et al.*, 2000)

As shows table 6.3, the calibrated parameter values were rather different to those presented for the A<sup>2</sup>/O in open-loop operation (Table 6.2). The evolution of the microbial community could explain this fact. The second set of experiments was carried out around six months later after the first one, where different operational conditions were applied and some biomass reinoculations were needed after occurring biomass washout episodes.

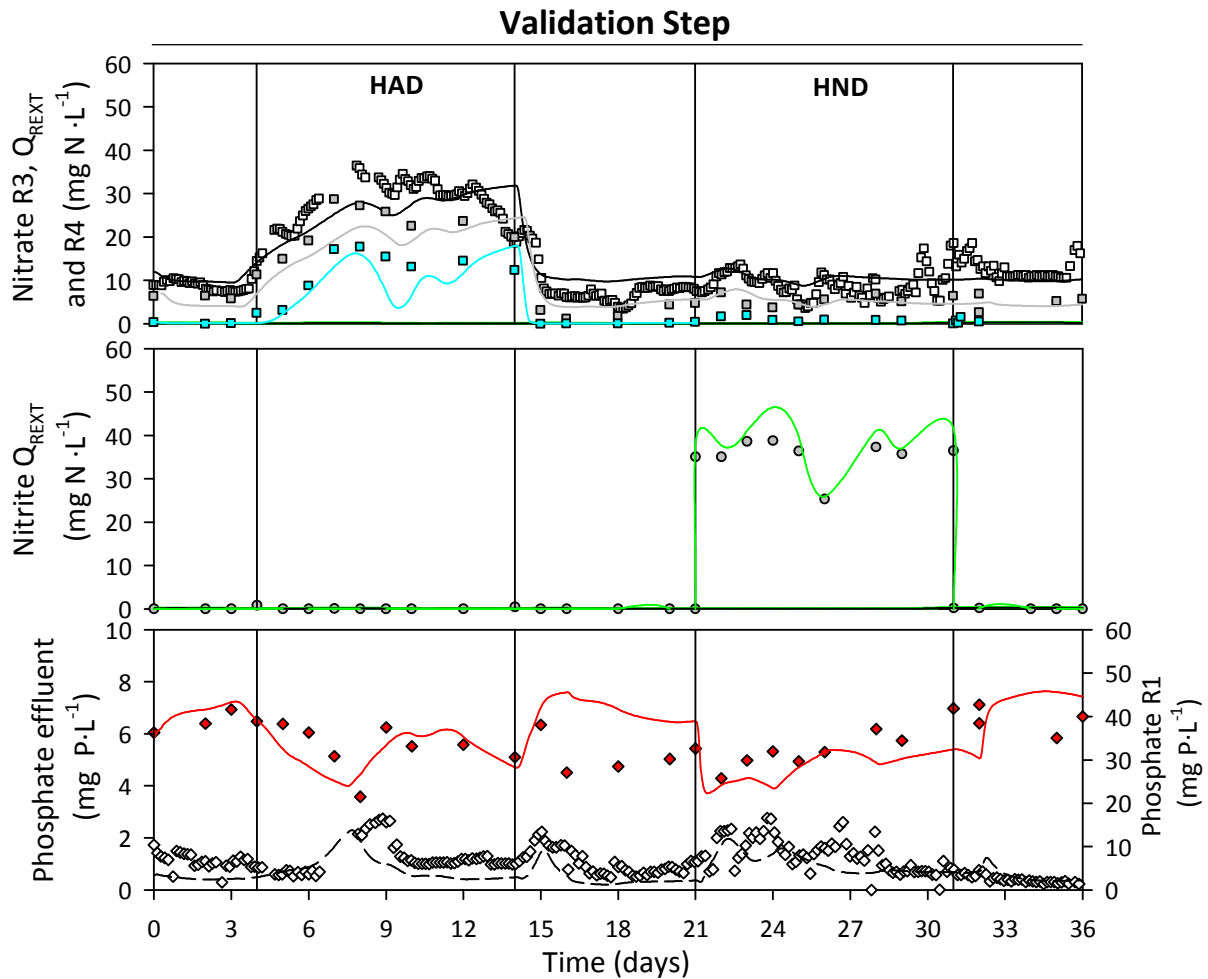
Regarding the new calibrated parameters, PHA storage rate ( $q_{\text{PHA}}$ ) obtained for experimental data description was higher than the standard ASM2d values. On the other hand, P uptake rate ( $q_{\text{PP}}$ ) was a little bit lower than the standard ASM2d value, which means that PAO was slightly slower taking up P under anoxic and aerobic conditions. As also was observed in the other calibration step (Table 6.2), the decrease of nitrate reduction factor for heterotrophic denitrification ( $\eta_{\text{NO}_3, \text{OHO}}$ ) indicates that denitrification was limited and thus, the heterotrophic biomass presence too. This fact was also reflected in a lower growth rate of OHO ( $\mu_{\text{HET}}$ ). Finally, a similar reactive settler global efficiency factor ( $\text{GEF}=0.61$ ) was obtained.

Figure 6.9 shows the A<sup>2</sup>/O pilot plant experimental data used for the calibration step and the model predictions. Proper description of the experimental behaviour was obtained with the calibrated parameters.



**Figure 6.9** Model calibration. A<sup>2</sup>/O pilot plant behaviour and model predictions when CGCL was implemented. Experimental data:  $\square$  represents nitrate,  $\circ$  nitrite and  $\diamond$  phosphorus. Red filled colour belongs to R1 (anaerobic reactor), white colour to R3 (effluent) and grey colour to  $Q_{\text{REXT}}$  concentrations. Model predictions: black line belongs to nitrate in R3, grey line to nitrate in  $Q_{\text{REXT}}$ , green line to nitrite in  $Q_{\text{REXT}}$ , red line to phosphate in R1 and black dashed line to phosphate in R3.

In figure 6.10, the model predictions for the JHB pilot plant when CGCL was implemented are presented. A proper description of the experimental results was also obtained with the model although the experimental data of JHB operation were not used in the calibration process. Hence, the predictive capacity of the model was validated.



**Figure 6.10** Model validation. JHB pilot plant behaviour and model predictions when CGCL was implemented.  $\square$  represents nitrate,  $\circ$  nitrite and  $\diamond$  phosphorus. Experimental data: Red filled colour belongs to R1 (anaerobic reactor), white colour to R3 (effluent), grey colour to  $Q_{REXT}$  and cyan colour to R4 concentrations. Model predictions: black line belongs to nitrate in R3, grey line to nitrate in  $Q_{REXT}$ , grey dashed line to nitrite in  $Q_{REXT}$ , red line to phosphate in R1, black dashed line to phosphate in R3, green solid line to nitrite in  $Q_{REXT}$  and cyan line to nitrate concentration in R4 (JHB reactor).

### 6.3.6. SIMULATION CASE STUDY I: P-RELEASE AS CONTROLLED VARIABLE – CGCL<sub>P-R1</sub>

A simulated case study was performed to study the feasibility of a new control structure (CGCL<sub>P-R1</sub>): control of  $P-PO_4^{-3}$  concentration in R1 by glycerol addition (Figure 6.11). The control algorithm was again defined by using discrete PI expression in the velocity form (equation 6.6), but in this case the error ( $\epsilon$ ) was referred to phosphorus concentration in R1 compared to a setpoint of  $30 \text{ mg } P-PO_4^{-3} \cdot L^{-1}$ . This setpoint value was optimised to obtain an

average concentration of  $1 \text{ mg}\cdot\text{L}^{-1}$  of P in R3 during HAD and HND. In addition, the controller parameters were tuned again by using ITAE criterion (equation 6.7), which resulted in:  $K_C = 0.6 \text{ L}\cdot\text{d}^{-1} (\text{mg P}\cdot\text{L}^{-1})^{-1}$  and  $\tau_I = 10.3 \text{ d}$ . Compared to CGCL, glycerol addition resulted in fermentation to VFA that directly resulted in P-release under anaerobic conditions (controlled variable) and hence the gain obtained was positive. The higher  $K_C$  obtained for  $\text{CGCL}_{\text{P-R1}}$  denotes a faster response of the controlled variable to the control actuation. Similar to CGCL, glycerol addition was programmed to be activated when P concentration decreased for the first time below the setpoint value ( $30 \text{ mg P}\cdot\text{L}^{-1}$ ). All the simulations were conducted with the calibrated model presented in table 6.3.

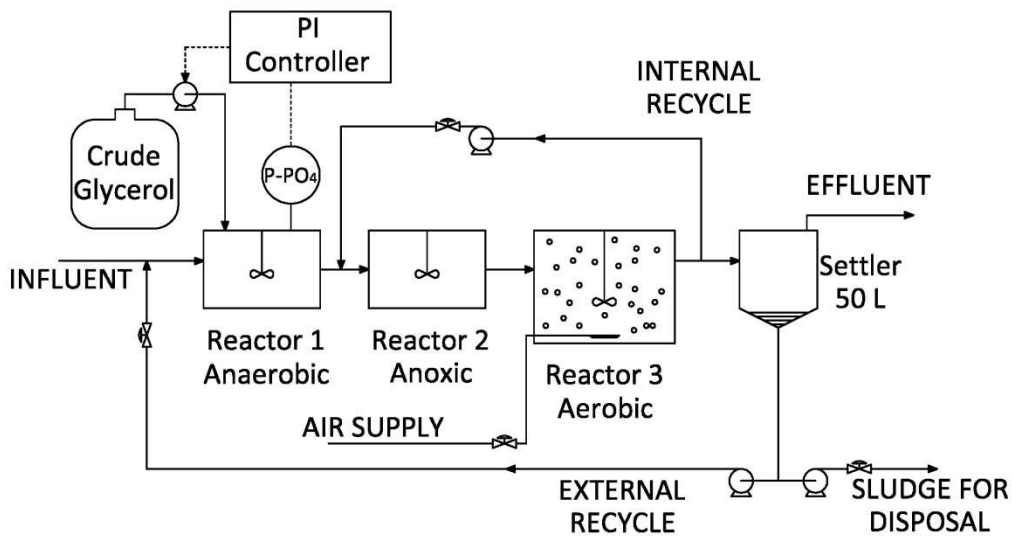


**Figure 6.11** Diagram of the feedback PI control-loop for controlling phosphorus concentration in R1 by adding crude glycerol in the A<sup>2</sup>/O pilot plant.

To study the benefits of  $\text{CGCL}_{\text{P-R1}}$ , HAD and HND scenarios were again simulated by implementing this new control structure and compared to CGCL results. As shown in figure 6.12, P concentration in R1 was well controlled around the setpoint value when  $\text{CGCL}_{\text{P-R1}}$  was implemented during the disturbances episodes for the two pilot plants. The new controller allowed a fast correction of the controlled variable and P concentration did not present fluctuations around the setpoint value as observed for CGCL.

The major differences between both control strategies were observed for the A<sup>2</sup>/O pilot plant. The implementation of  $\text{CGCL}_{\text{P-R1}}$  resulted in a more stable P effluent concentration around the setpoint value ( $1 \text{ mg P}\cdot\text{L}^{-1}$ ) when disturbance periods were simulated. This new control strategy allowed a better control over P effluent because a partial EBPR failure as in CGCL was not necessary to activate controller actuation. In other words, a possible EBPR failure was rapidly corrected when P-release started to decrease due to nitrate presence under anaerobic conditions without jeopardizing P-uptake capacity. Moreover, the sudden

increase of P after HND for CGCL (dashed lines) was totally avoided in this case when CGCL<sub>P-R1</sub> was implemented. The fact that high P-release and P-uptake was always maintained during HND step enabled PAO to maintain low P effluent concentration even when a sudden increase of P under anaerobic conditions occurred at the end of such disturbance.

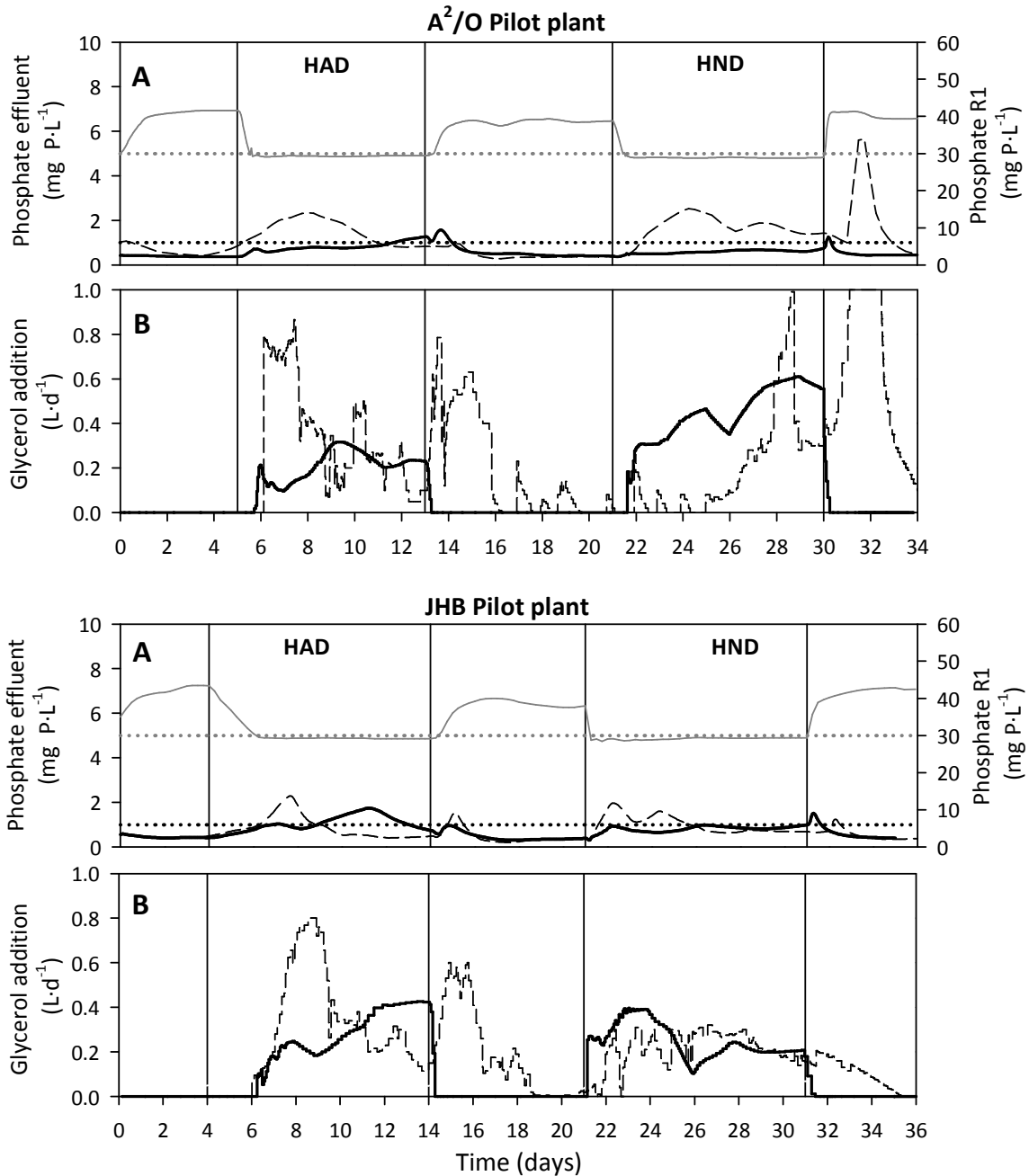


**Figure 6.12** Comparison of CGCL<sub>P-R1</sub> and CGCL performance for A<sup>2</sup>/O and JHB pilot plants when simulating HAD and HND periods. A graphs: Grey solid and dotted lines belong to P-PO<sub>4</sub><sup>-3</sup> concentration in R1 for CGCL<sub>P-R1</sub> and to P-PO<sub>4</sub><sup>-3</sup> setpoint in R1 (30 mg·L<sup>-1</sup>), black dashed and solid lines to P concentration in R3 for CGCL and for CGCL<sub>P-R1</sub>, respectively. Black dotted line represents P-PO<sub>4</sub><sup>-3</sup> setpoint in R3 (1 mg·L<sup>-1</sup>) for CGCL. B graphs: Glycerol addition. Black dashed line represents CGCL actuation and black solid line CGCL<sub>P-R1</sub>.

In the case of JHB, more stable operation was also observed when CGCL<sub>P-R1</sub> was implemented. However, the benefits of this new control strategy were lower since the inclusion of an extra anoxic reactor already reduced the negative effect of both HAD and HND on EBPR.

When comparing crude glycerol consumption, lower addition was necessary for both pilot plants for CGCL<sub>P-R1</sub>: 5.9 L and 4.9 L of total crude glycerol during HAD and HND for A<sup>2</sup>/O and JHB, respectively. These lower glycerol requirements can be explained by taking into account the actuation capacity of the control setup over the controlled variable. In the case of CGCL operation, it could be extracted that the slow response of the manipulated variable (P concentration in the aerobic reactor) to the controlled variable changes (glycerol addition in the anaerobic reactor) could possibly result in some extra glycerol addition not directly used under anaerobic conditions. On the contrary, the fast effect of crude glycerol addition in P-release evolution for CGCL<sub>P-R1</sub> suggested that such glycerol was mainly used for NO<sub>x</sub> denitrification or VFA production reducing then unnecessary addition. The observed less amount of glycerol required in JHB pilot plant was expected in accordance to the results presented above.

Considering all these points, CGCL<sub>P-R1</sub> implementation would be recommended instead of CGCL in order to reduce more efficiently HAD and HND negative effects of EBPR for both pilot plant configurations. Further research will be necessary for the experimental validation of this statement.

### **6.3.7. SIMULATION CASE STUDY II: FEEDFORWARD IMPROVEMENT**

In this section, the benefits of including a feedforward action to the feedback control structure were studied in a new simulated case study. The feedforward structure was implemented in the CGCL (FF-CGCL) (Figure 6.13) following the principles pointed out in Samuelsson and Carlsson (2001). In that study, the authors proposed the addition of acetic acid based on the ammonium influent concentration in an activated sludge system with N and COD removal, EBPR was not considered. The novelty proposed in the present study was based on the controlled addition of a new carbon source such as crude glycerol in R1 depending on the P concentration on R3 (feedback component) and the ammonium concentration in the influent (feedforward component).



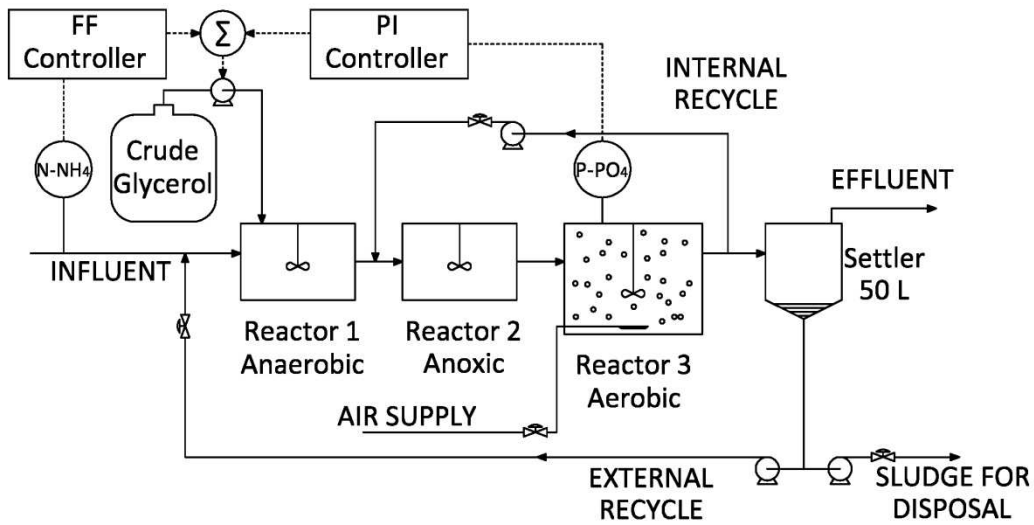


**Figure 6.13** Diagram of the new feedback + feedforward control structure for P control in R3 by crude glycerol addition in the A<sup>2</sup>/O pilot plant.

The algorithm consisted on the feedback PI controller expressed by equation 6.6 but including a new parameter that modifies the controller actuation depending on the ammonium concentration in the influent (equation 6.8), feedforward (FF) control. The feedforward part was defined as a proportional gain ( $K_{FF}$ ) related to ammonium influent variations. In order to avoid excessive and unnecessary glycerol additions due to instantaneous ammonium influent increases, a dynamic average of the ammonium concentration was used. The dynamic average was performed taking into account the discrete ammonium influent values of the last 24 hours and it was compared with the same average obtained 2 hours before (i.e.  $C_{NH_4, in_{av, n}}$  was compared to  $C_{NH_4, in_{av, n-1}}$  being 2 hours the difference between  $n$  and  $n-1$  moments). The rest of parameters were maintained as used for the CGCL.

$$C_n = C_{n-1} + K_C \cdot \left[ (\epsilon_n - \epsilon_{n-1}) + \frac{t_n - t_{n-1}}{\tau_i} \cdot \epsilon_n \right] + K_{FF} \cdot (C_{NH_4, in_{av, n}} - C_{NH_4, in_{av, n-1}}) \quad (6.8)$$

$K_{FF}$  parameter was tuned according to ITAE (equation 6.7) resulting in an optimised value of  $0.0065 \text{ L} \cdot \text{d}^{-1} (\text{mg N-NH}_4^+ \cdot \text{L}^{-1})^{-1}$ . The low optimised value also avoided sudden disproportionate glycerol addition when ammonium influent increased from 40 to  $80 \text{ mg N} \cdot \text{L}^{-1}$ , otherwise unstable P effluent concentration would be obtained. The feedback controller parameters ( $K_C$  and  $\tau_i$ ) were not tuned again because the aim of this section was to study how the feedforward actuation could improve the feedback controller. The calibrated model presented in table 6.3 was used to study the effect of including the feedforward actuation. Only HAD was evaluated since no influent variations on ammonium or N pollutants content were performed during HND. Figure 6.14 presents the main results obtained with FF-CGCL in comparison with CGCL.

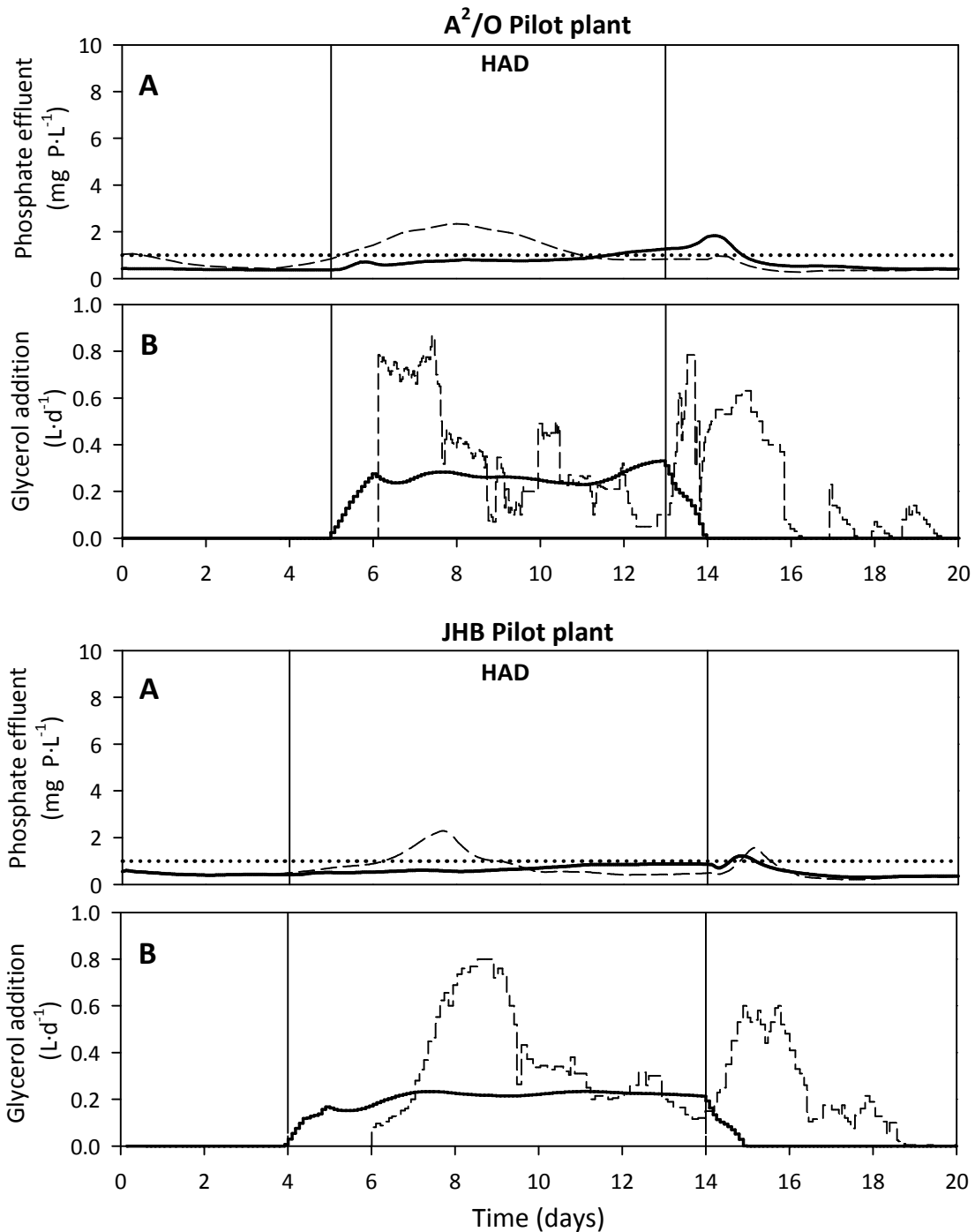


**Figure 6.14** Comparison of CGCL and FF-CGCL performance for A<sup>2</sup>/O and JHB pilot plants during HAD. A graphs: Black dashed line belongs to P concentration in R3 as resulted for CGCL actuation and black solid line to FF-CGCL. Black dotted line represents P-PO<sub>4</sub><sup>-3</sup> setpoint in R3 (1 mg·L<sup>-1</sup>). B graphs: Black dashed line represents glycerol addition for CGCL and black solid line belongs to glycerol addition for FF-CGCL.

For both pilot plants, the implementation of the FF-CGCL highly improved the stability of effluent  $\text{P-PO}_4^{-3}$  around the setpoint value during HAD ( $1.03 \pm 0.29 \text{ mg P-PO}_4^{-3} \cdot \text{L}^{-1}$  and  $0.88 \pm 0.41 \text{ mg P-PO}_4^{-3} \cdot \text{L}^{-1}$  for A<sup>2</sup>/O and JHB, respectively). As can be observed, the anticipative effect of FF-CGCL activated the glycerol addition when HAD started (e.g. day five for A<sup>2</sup>/O pilot plant) despite  $\text{P-PO}_4^{-3}$  concentration was below the setpoint value. As a result, no oscillatory behaviour was observed in contrast to operation with the simple feedback controller. For CGCL, the competition between PAO and OHO for the carbon source resulted in the partial failure of EBPR and in an increase of  $\text{P-PO}_4^{-3}$  in R3, which activated the control actuation (e.g. day six for A<sup>2</sup>/O pilot plant). This failure was not instantly corrected with the glycerol addition and an oscillatory trend of  $\text{P-PO}_4^{-3}$  in R3 was observed. However, when FF-CGCL was implemented, enough carbon source was available from the beginning of HAD, which reduced carbon source competition when more nitrate was recycled to the anaerobic phase. At the end of HAD, the decreasing trend of glycerol addition due to ammonium influent reduction suggested that feedforward contribution mainly governed controller actuation. In fact, during all HAD, feedback component did not seem to have a role on control actuation. This was mainly caused by feedforward actuation at the beginning of HAD that already ensured a  $\text{P-PO}_4^{-3}$  concentration in R3 around setpoint value. It is important to note that when FF-CGCL was implemented, no EBPR failure was necessary to activate glycerol addition.

In the case of the JHB pilot plant, similar results were observed. However, the benefits of FF-CGCL implementation were again less evident than for A<sup>2</sup>/O pilot plant mainly because to the presence of the extra-anoxic reactor (Figure 6.1).

As was commented before, FF-CGCL implementation resulted in a more relaxed control actuation without sudden increases in the glycerol addition. Hence, around 50% decrease on the glycerol needs was obtained in comparison to CGCL during HAD (e.g. for A<sup>2</sup>/O configuration 4.1 L of glycerol were needed for CGCL and only 2.1 L for FF-CGCL).

## **6.4. Practical Implications**

---

This is the first work detailing how the controlled addition of a biodiesel byproduct (crude glycerol) can reduce the detrimental effect of nitrate on EBPR. The potential utilisation of crude glycerol in both denitrification and P-removal processes indicates its feasibility to be an alternative carbon source for nutrient removal in WWTP facing carbon shortages.

The utilization of a waste material would reduce the running costs of the process in comparison with more expensive carbon sources, such as VFA, commonly used in real WWTP. In addition, crude glycerol also would simplify WWTP management avoiding the utilization of more dangerous carbon sources as methanol, which must be diluted to reduce its fire hazard.

The results here showed open a new range of possibilities. With a similar approach, other wastes products could also be used as carbon source to reduce the detrimental effect of nitrate on EBPR. This study completes previous works where synthetic glycerol was shown as a good carbon source for improving EBPR in a system without N-removal processes (Guerrero *et al.*, 2012; see Annex II) and for denitrification processes (Torà *et al.*, 2011).

Based on the evidences showed in this chapter, simple PI feedback control for crude glycerol dosage could be effective to maintain an adequate P-removal efficiency in full-scale WWTP. However, some limitations on control performance could appear when treating influents with sudden changes in N influent concentration, because the controlled variable (P effluent concentration) has a slow response in front of manipulated variable changes (crude glycerol addition). Two different approaches were proposed and studied to solve this behaviour with high positives results: i) a simple modification of the control strategy by controlling the P concentration in R1 and ii) feedforward control in combination with feedback control. In both cases, a faster adaptation of crude glycerol flow to N influent variations was obtained and the detrimental effect of external NO<sub>x</sub> recycling was reduced. Nevertheless, some drawbacks have to be considered when considering their real implementation. For the first approach, P should be at least monitored in two points: under anaerobic conditions for control actuation (i.e. comparison with setpoint value) and in the aerobic phase to guarantee that P concentration is not above discharge limits. Thereby, this approach would result in an increase of the investment costs in comparison with simple P control in aerobic reactor where only one P-analyser would be necessary. For the second approach, if the influent was not well-know or if it presented a high variability, the feed-forward part should not be only governed by ammonia influent but also COD/N ratio would have to be also considered. High ammonia influent values together with high COD content would not necessarily limit P-removal process as long as enough carbon source would be available for denitrifying OHO and PAO under anaerobic conditions. Because of this, COD influent should be also monitored involving an increase on the investment cost (more sensors) and complicating the control algorithm. In any case, it is important to remark that the sudden changes on pollutants concentrations here tested are not pretty common in WWTP treating urban mainstream (i.e. daily variation are more expected instead of instant variations) and thus, simple PI feedback control in R3 could result in an important improvement of P-removal efficiency without a big impact on overall running costs.

## 6.5. Conclusions

---

The major achievement of this work is the demonstration that an automated crude glycerol dosage was a successful alternative to prevent EBPR failure due to anaerobic NO<sub>x</sub> presence in two different pilot plants (A<sup>2</sup>/O and JHB) even under different NO<sub>x</sub> disturbances. A model was developed and experimentally validated to tune a PI feedback control loop based on crude glycerol addition in the anaerobic reactor for controlling phosphorus effluent

concentration. The best results were obtained when the control loop was implemented in the Johannesburg pilot plant. In this configuration, the inclusion of an extra-anoxic reactor for  $\text{NO}_x$  denitrification before entering the anaerobic phase reduced the competition between OHO and PAO for the carbon source and consequently, EBPR failure. Contrary, for  $\text{A}^2/\text{O}$  configuration, denitrification was favoured against P-removal process due to the high  $\text{NO}_x$  levels entering the anaerobic phase. As a result, more glycerol (18% more than in Johannesburg configuration) was needed to be added to ensure enough carbon source for both denitrification and EBPR processes.

In the  $\text{A}^2/\text{O}$  configuration, P effluent concentration was not well controlled around the setpoint value during the disturbance steps. The alternating anaerobic and aerobic conditions needed for P-removal process and the fact that those phases were physically separated in both pilot plants was translated in a delay on control actuation when HAD and HND were performed. As a result, a fluctuation trend on glycerol addition was observed. For Johannesburg setup, this behaviour was not so important mainly because  $Q_{\text{REXT}}$  denitrification smoothed  $\text{NO}_x$  variations entering to the anaerobic phase.

The calibrated model was used to propose two different approaches to correct this delay on the controller actuation: i) the modification of P control setup by changing P control from R3 to R1 and ii) the inclusion of a feedforward control action that considered N influent variations. In both cases, a better and more stable control actuation was observed during disturbance periods maintaining a P effluent concentration always around  $1 \text{ mg}\cdot\text{L}^{-1}$ .



## **CHAPTER VII**

Effect of different model assumptions, plant configurations and control strategies on the C/N/P removal WWTP performance: Benchmarking studies I

Part of this chapter has been published as:

Guerrero, J., Flores-Alsina, X., Guisasola, A., Baeza, J.A., Gernaey, K.V., 2013. Effect of nitrite, limited reactive settler and plant design configuration on the predicted performance of a simultaneous C/N/P removal WWTP. *Bioresource Technology* 136, 680-688.





## **Abstract**

*The first part of this chapter describes a modelling study where five new benchmark plant design configurations for biological nutrient removal (anaerobic/anoxic/aerobic, Bardenpho 5-stage, UCT Modified UCT, and Johannesburg) were simulated and evaluated under different model assumptions. The ASM2d including electron dependent decay rates was used as the reference model. A second case added nitrite as a new state variable, describing nitrification and denitrification as two-step processes. The third set of models considered different reactive settlers types (diffusion-limited/non limited). This study analyses the importance of these model extensions to correctly describe the nitrification behaviour and the carbon source competition between ordinary heterotrophic organisms (OHO) and polyphosphate accumulating organisms (PAO) under certain operating conditions. The economic and environmental aspects when meeting the P discharge limits by adding an external carbon source were also studied.*

*In the second part, the efficiency of eight different control strategies using a multivariate statistical method, the discriminant analysis, was evaluated. The environmental impact, the economic cost and the degree of accomplishment of effluent regulations of 32 different alternatives (eight control strategies in four plant configurations) for a period of one year were studied. Two parallel discriminant analyses were performed in order to find the most important differences between plant configurations and control strategies. The sequence of anaerobic/anoxic/aerobic phases and the number/type of internal/external recycles highly affected nitrogen removal efficiency. In fact, denitrification related criteria were the most discriminant factors amongst the studied configurations, independently of the control strategy. In contrast, phosphorus removal processes were mostly influenced by the type of control strategy. Thus, the way the plant was operated had a larger impact on favouring PAO growth than the plant design itself.*

## **7.1. Motivations**

The most widespread mathematical models to describe enhanced biological phosphorus removal (EBPR) in a wastewater treatment plant (WWTP) are the Activated Sludge Model No. 2d (ASM2d) (Henze *et al.*, 2000) and the extended Activated Sludge Model No. 3 (ASM3) incorporating EBPR process (ASM3-BioP) (Rieger *et al.*, 2001). The formulation of these models includes some simplifications to reduce the model complexity and thus, they may not be valid for all scenarios (Sin and Vanrolleghem, 2006). For example the ASM2d default model structure does not differentiate amongst the anaerobic, anoxic and aerobic decay rates while experimental results show the contrary (Nowak *et al.*, 1995; Siegrist *et al.*, 1999). Gernaey and Jørgensen (2004) and Flores-Alsina *et al.* (2012) therefore formulated an updated ASM2d model with electron acceptor dependent decay rates. Furthermore, nitrite is not considered as a state variable in ASM2d despite the fact that it is a key intermediate to describe accurately the anoxic organic matter consumption and nitrification process (particularly at low dissolved oxygen, DO, concentrations). Regarding EBPR, the recent

advances on anoxic P removal have increasingly set the focus on the denitrifying PAO (DPAO) fraction (Ahn *et al.*, 2001; Guisasola *et al.*, 2009; Tayà *et al.*, 2011; 2013). He *et al.* (2007) reported that different types of DPAO have different denitrification capabilities, and that nitrite may be an important electron acceptor under some operational conditions. In addition, nitrite could also play an important role on the competition between OHO and PAO if high amounts of nitrite are present in the external recycle. Although most of the research reports the EBPR failure as a consequence of nitrate presence, nitrite could also play a similar role triggering off denitrification process instead of P release. Hence, including nitrite in the activated sludge models (ASM) is also essential for achieving a proper description of EBPR in a WWTP. In this sense, most of the studies that included nitrite as state variable considered two-step nitrification and denitrification processes. Two-step nitrification assumption is commonly accepted but two-step denitrification modelling is not well established and different approaches have been proposed (Wett and Rauch, 2003; Sin and Vanrolleghem, 2006; Xavier *et al.*, 2007). Sin *et al.* (2008) analysed some of these models and proposed some guidelines for a consistent description of activated sludge systems including nitrite and considering two-step nitrification and denitrification.

The biological reactions occurring in the secondary settler are another factor to take into consideration when modelling biological nutrient removal (BNR). Although the settling process is usually considered non-reactive (e.g. Takács *et al.*, 1991), some studies (Siegrist *et al.*, 1995; Koch *et al.*, 1999) reported that biological reactions also occur, in particular denitrification processes, despite of the mass transfer limitations present in the settler (concentration gradients and preferential pathways). Gernaey *et al.* (2005) and Flores-Alsina *et al.* (2012) presented a reactive settler model that considered each layer of the settler as a continuously stirred tank reactor (CSTR). Unfortunately this approach seems to overestimate the reactive capacity of the settler, since mass transport limitations were not considered. More research should be conducted on this topic to correctly simulate a reactive settler.

The A<sup>2</sup>/O (anaerobic/anoxic/aerobic) configuration has been the most widely used WWTP in benchmark studies to perform simultaneous biological carbon (C), nitrogen (N) and phosphorus (P) removal (Gernaey and Jørgensen, 2004; Machado *et al.*, 2009b; Flores-Alsina *et al.*, 2012; Ostace *et al.*, 2013). Nevertheless, complete denitrification is not possible in this configuration and some NO<sub>x</sub> (nitrate and nitrite, hereafter) will always enter the anaerobic phase through the external recycle (Henze *et al.*, 2008). In fact, there are no previous benchmark studies with alternative configurations such as Johannesburg (JHB), UCT, Modified UCT (MUCT) or Bardenpho 5-stage (BDP-5 stage), which have been designed to prevent the deleterious effect on EBPR by reducing the NO<sub>x</sub> inlet in the anaerobic phase. A detailed description of these plant configurations as well as the benchmarking concept can be found in Chapter I. Hence, the application of the benchmarking protocol could be very useful to compare what is the best plant configuration at reducing the detrimental effect of NO<sub>x</sub> on EBPR together with the lowest running costs and with the highest effluent quality.

The utilization of these alternative plant configurations is not always enough to avoid EBPR failure and the implementation of control strategies is sometimes required. Unfortunately, as explained in detail in Chapter I, the selection of the proper control strategy is not a straightforward issue since the different biological processes are highly correlated (i.e. actuations applied to control a specific biological process could affect some others). In these sense, benchmark simulations models (BSM) can be also used to analyse the efficiency of the control strategies. However, the high number of evaluation criteria involved hinders the selection of the best alternatives. To overcome this problem, multivariable statistical techniques, such as discriminant analysis (DA) or principal component analysis (PCA), have been widely used in order to impartially analyse complex data where many criteria and operation conditions are considered (Johnson and Wichern, 1992; Hair *et al.*, 1998). These techniques can be used to find some correlations between different treatment alternatives, operating variables or evaluation criteria and to highlight information that is not easy to extract at first glance. Flores-Alsina *et al.* (2010) applied these techniques to find similar patterns between different control strategies and the minimum set of criteria to differentiate them when modelling a WWTP with BNR.

Based on all above considerations, the objectives of this study were i) to evaluate the effect of different model assumptions in five benchmark WWTP configurations, ii) to analyse the impact of different WWTP configurations on the performance of EBPR coupled to biological N removal and iii) to ease the selection of the best plant configuration or control strategy by using DA. For the first point, the inclusion of nitrite as state variable and biochemical reactions in the settler (with and without considering mass transfer limitations) were analysed and compared under long-term operation (364 days). On top of that, all the model assumptions were also applied to the five most common EBPR plant configurations found in full-scale WWTPs. For the third point, seven reported control strategies in benchmarking studies were simulated and compared by using DA, in order to select the best operational scenario and to find possible correlations or similarities among them. Effluent quality, operational costs and discharge levels were proposed as discriminant criteria to evaluate the performance of the different plant configurations and the control strategies tested.

## **7.2. Material and Methods**

---

### **7.2.1. WASTEWATER TREATMENT PLANTS CONFIGURATIONS UNDER STUDY**

Five different benchmark WWTP configurations for simultaneous C/N/P removal were considered in this study: A<sup>2</sup>/O, BDP-5 stage, UCT, MUCT and JHB (Figure 7.1). The most significant parameters of each configuration are summarised in table 7.1. The volumes of the anaerobic/anoxic/aerobic zones were considered constant for all the plant configurations and the different configurations were implemented by changing the location of specific reactors and by adding the required recycle streams (e.g. Q<sub>RANA</sub>E and IB). As these new

recycle streams had not been reported in any previous benchmark study, their flow rates were set according to common textbook knowledge (Metcalf and Eddy, 2003; Henze *et al.*, 2008). The volumes of the anoxic and aerobic reactors were determined according to the current plant-wide benchmark for C and N removal outlined in Nopens *et al.* (2010). The two additional anaerobic reactors included for EBPR were assumed to have a volume of 1250 m<sup>3</sup> each.

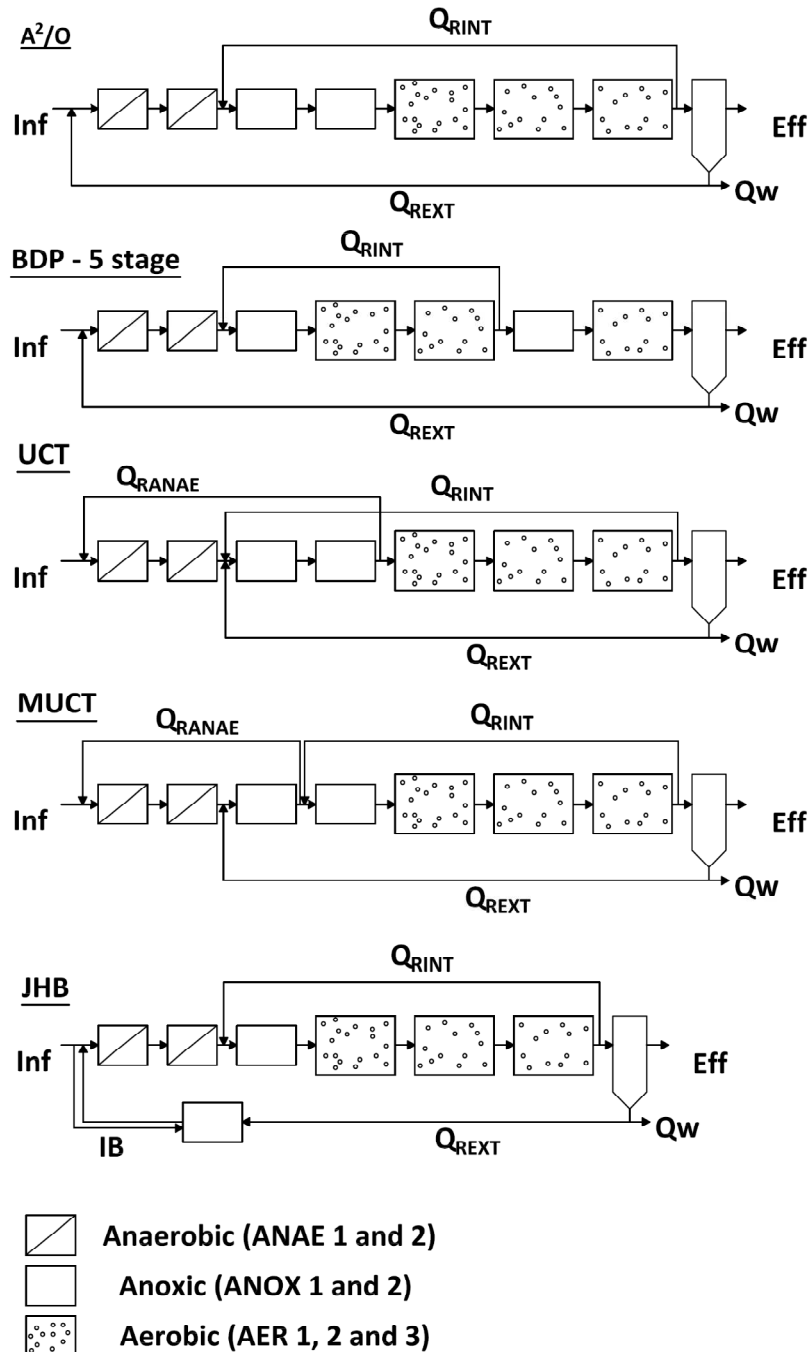


**Figure 7.1** Plant configurations for simultaneous C/N/P removal: A<sup>2</sup>/O, BDP-5 stage, UCT, MUCT and JHB. Inf: Influent, Eff: Effluent, Q<sub>RINT</sub>: Internal recycle, Q<sub>REXT</sub>: External recycle, Q<sub>RANAE</sub>: Anaerobic recycle, Q<sub>W</sub>: Waste sludge or purge and IB: Influent bypass.

**Table 7.1** Operational parameters for the plant configurations.

Parameters	Values
Reactor volumes	
Anaerobic, ANAE 1 and 2	1250 m <sup>3</sup>
Anoxic, ANOX 1 and 2	1500 m <sup>3</sup>
Aerobic, AER 1, 2 and 3	3000 m <sup>3</sup>
$k_{La}$ AER 1,2 and 3	120 d <sup>-1</sup> , 120 d <sup>-1</sup> and 60 d <sup>-1</sup>
Influent average flow-rate	20648 m <sup>3</sup> ·d <sup>-1</sup>
Internal recycle, $Q_{RINT}$	61944 m <sup>3</sup> ·d <sup>-1</sup> (300% Influent)
External recycle, $Q_{REXT}$	20648 m <sup>3</sup> ·d <sup>-1</sup> (100% Influent)
Anaerobic recycle, $Q_{RANAe}$ *	41296 m <sup>3</sup> ·d <sup>-1</sup> (200% Influent)
Influent bypass, IB **	6814 m <sup>3</sup> ·d <sup>-1</sup> (33% Influent)
Waste sludge, $Q_w$	385 m <sup>3</sup> ·d <sup>-1</sup>

\* UCT and MUCT    \*\*JHB

### 7.2.2. MATHEMATICAL MODELS

In the first part of the study, four different approaches to describe BNR and the settling process were evaluated (Table 7.2). The biological kinetic model used to describe BNR was the ASM2d (Henze *et al.*, 2000), similarly to other benchmark studies on new model extensions (Gernaey and Jørgensen, 2004; Flores-Alsina *et al.*, 2012). For the first approach (A1), ASM2d was extended with electron acceptor dependent decay rates as described by Gernaey and Jørgensen (2004). The secondary settler behaviour was modelled using the 10-layer (non-reactive) settler model of Takács *et al.* (1991). In the second approach (A2), A1 was modified including nitrite as a new state variable, considering nitrification and denitrification as two-step processes (see Annex I for the complete stoichiometric and kinetic description of the model). Once nitrite is considered, two alternative electron acceptors (nitrate and nitrite) are present for denitrification. Hence, a mixed substrate approach was used similar to the ASM2d mixed substrate implementation for acetate (SA) versus fermentable COD (SF) in biological carbon removal processes (i.e. including a  $SNO_2/(SNO_2 + SNO_3)$  reduction term in the nitrite degradation rate and a  $SNO_3/(SNO_2 + SNO_3)$  term in the nitrate degradation rate) (Sin and Vanrolleghem, 2006). The third approach (A3) introduced the reactive settler concept to consider biotransformations of both soluble and particulate compounds during the settling process. The full set of equations used in A2 was therefore considered in the settler, where each layer was simulated as a CSTR (Gernaey *et al.*, 2005). However, it is known that this approach results in an overestimation of the reactive capacity of the settler since mass transfer problems or limitations (i.e. concentration gradients or preferential pathways) are not considered. For that reason, a fourth approach (A4) was proposed to describe such settler limitations by adding a global efficiency factor (i.e. limiting reactive settler) to the kinetics in the settler.

**Table 7.2** Summary of the modelling approaches studied in this work.

Approach	ASM2d	ASM2d + Nitrite Inclusion	Reactive Settler	Limited reactive settler
A1	X			
A2		X		
A3		X	X	
A4		X		X

All the simulations were conducted in accordance to the benchmarking principles (Jeppsson *et al.*, 2007): 300 days simulation to reach steady state using predefined constant influent data, then 609 days of long term (LT) dynamic influent. Only the last 364 days were used for evaluation and comparison purposes. The influent profile was generated following the principles outlined in Gernaey *et al.* (2011). All the plant configurations/mathematical models were simulated with identical influent flow rate (with an average value of 20648 m<sup>3</sup>·d<sup>-1</sup>) and pollutant loads in terms of COD (12250 kg·d<sup>-1</sup>), N (932 kg·d<sup>-1</sup>) and P (255 kg·d<sup>-1</sup>), which are the default loads created by the influent generator. The LT influent included daily, weekly and seasonal changes both in flow rate and pollutant loads. A daily/yearly temperature variation profile was also considered. Finally, occasional events such as the dilution effect after a rainy period or the first flush of the particulates after a storm were also simulated. The constant influent represents the average values of the 364-days dynamic input data.

### 7.2.3. DESCRIPTION OF PLANT PERFORMANCE

#### 7.2.3.1. Operational cost index (OCI)

The OCI (Equation 7.1) was calculated according to the BSM1 guidelines (Alex *et al.*, 2008). Aeration energy (AE), mixing energy (ME), pumping energy (PE), sludge production (SP) and the external carbon source addition (EC) were considered.

$$OCI = AE + ME + PE + 5 \cdot SP + 3 \cdot EC \quad (7.1)$$

Aeration was recently found to play a major role in the OCI and thus, AE has a significant impact on the evaluation process (Nopens *et al.*, 2010). To address this dominating impact, the expression used to calculate AE in Chapter IV (Equation 4.2) was changed to a more widely accepted expression that describes the Oxygen Transfer Rate (OTR) that in turn is related to power consumption. The OTR calculation for a reactor (i) was defined in equation 7.2, where V was the volume of reactor (i), k<sub>L</sub>a was the oxygen transfer coefficient in such reactor and S<sub>O<sub>2</sub>sat</sub> was the oxygen saturation concentration in the liquid at 15°C (8.0 mg·L<sup>-1</sup>).

$$OTR_i(t) \left[ \text{kg O}_2 \cdot \text{d}^{-1} \right] = V_i \cdot k_L a_i(t) \cdot (S_{O_2 \text{sat}}) / 1000 \quad (7.2)$$

Assuming that the transfer efficiency is 1.8 kg oxygen per kWh used, the AE was calculated with equation 7.3 (Nopens *et al.*, 2010).

$$AE \left[ \text{kWh} \cdot \text{d}^{-1} \right] = \frac{1}{1.8 \cdot (t_{\text{end}} - t_{\text{start}})} \cdot \int_{t_{\text{start}}}^{t_{\text{end}}} \sum_{i=1}^7 \text{OTR}_i(t) \cdot dt \quad (7.3)$$

Mixing was necessary when there is no aeration (i.e. anaerobic and anoxic reactors) or to avoid settling when aeration is very low. Thus, ME was calculated as:

$$ME \left[ \text{kWh} \cdot \text{d}^{-1} \right] = \frac{24}{t_{\text{end}} - t_{\text{start}}} \cdot \int_{t_{\text{start}}}^{t_{\text{end}}} \sum_{i=1}^7 \left( \begin{array}{l} 0.005 \cdot V_i \text{ if } k_L a_i(t) < 20 \text{d}^{-1} \\ \text{otherwise} = 0 \end{array} \right) \cdot dt \quad (7.4)$$

The SP was calculated from the total solids flow from wastage and the solids accumulated in the system over the simulated time (364 days) with the equation 7.5, where  $TSS_W$  was the total suspended solids concentration in the purge. The rest of parameters are described below.

$$SP \left[ \text{kg} \cdot \text{d}^{-1} \right] = \frac{1}{t_{\text{end}} - t_{\text{start}}} \cdot \left( TSS_{s, t_{\text{end}}} - TSS_{s, t_{\text{start}}} + \int_{t_{\text{start}}}^{t_{\text{end}}} TSS_W \cdot Q_W(t) \cdot dt \right) \quad (7.5)$$

The amount of solids in the system ( $TSS_S$ ) at time  $t$  was calculated as:

$$TSS_S(t) = TSS_{\text{react}}(t) + TSS_{\text{settler}}(t) \quad (7.6)$$

Where  $TSS_{\text{react}}$  was the amount of solids in the reactors ( $TSS_r$ ):

$$TSS_{\text{react}}(t) = \sum_{i=1}^7 TSS_{r, i} \cdot V_i \quad (7.7)$$

$TSS_{\text{settler}}$  is the amount of solids in the settler. Settling process was simulated with the 10-layers model of Takács *et al.* (1991):

$$TSS_{\text{settler}}(t) = (V_{\text{settler}} / 10) \cdot \sum_{j=1}^{10} X_{TSS, j} \quad (7.8)$$

$V_{\text{settler}} = 6000 \text{ m}^3$  represented the total volume of the settler.

PE was also differently calculated as in Chapter IV (Equation 4.3). In this case different pumping factors (PF) were used (Equation 7.9) to consider that pumping energy depends on how the various tanks are arranged on the available space (Alex *et al.*, 2008).

$$PE[\text{kWh}\cdot\text{d}^{-1}] = \frac{1}{t_{\text{end}} - t_{\text{start}}} \cdot \int_{t_{\text{start}}}^{t_{\text{end}}} (PF_{Q_{\text{RANA E}}} \cdot Q_{\text{RANA E}}(t) + PF_{Q_{\text{RINT}}} \cdot Q_{\text{RINT}}(t) + PF_{Q_{\text{REXT}}} \cdot Q_{\text{REXT}}(t) + PF_{Q_{\text{W}}} \cdot Q_{\text{W}}(t) \cdot dt) \quad (7.9)$$

Where  $PF_{Q_{\text{RANA E}}} = 0.004 \text{ kWh}\cdot\text{m}^{-3}$  represented the pumping factor for the  $Q_{\text{RANA E}}$ ,  $PF_{Q_{\text{RINT}}} = 0.004 \text{ kWh}\cdot\text{m}^{-3}$  for the  $Q_{\text{RINT}}$ ,  $PF_{Q_{\text{REXT}}} = 0.008 \text{ kWh}\cdot\text{m}^{-3}$  for the  $Q_{\text{REXT}}$  and  $PF_{Q_{\text{W}}} = 0.05 \text{ kWh}\cdot\text{m}^{-3}$  for the  $Q_{\text{W}}$ . These values were adopted from BSM1 guidelines (Alex *et al.*, 2008).

The consumption of external carbon addition (EC) was also calculated according to the following BSM1 expression (Alex *et al.*, 2008):

$$EC [\text{kg COD}\cdot\text{d}^{-1}] = \frac{\text{COD}_{\text{EC}}}{t_{\text{end}} - t_{\text{start}}} \cdot \int_{t_{\text{start}}}^{t_{\text{end}}} \sum_{i=1}^7 (Q_{\text{EC},i}(t)) \cdot dt \quad (7.10)$$

$Q_{\text{EC},i}$  is the external carbon flow rate added to reactor (i) and  $\text{COD}_{\text{EC}} = 4 \cdot 10^5 \text{ mg}\cdot\text{L}^{-1}$  was the concentration of readily biodegradable substrate (i.e. simulated as SA in the model).

### 7.2.3.2. Influent and effluent quality indexes (IQI and EQI)

IQI and EQI (Equation 7.11) were evaluated similarly to Copp (2002).  $Q_j$  is the influent or effluent flow rate.  $\text{PU}_X$  (pollutant units of component X) represents the product between weights  $\beta_X$  and the concentration of the considered pollutant at time t. The weights  $\beta_X$  suggested by Gernaey and Jørgensen (2004) were used for IQI and EQI evaluation. However, the fact that ammonium is more harmful for the environment than nitrate or nitrite (Carmango and Alonso, 2006) was also considered and thus, the weights for total Kjeldahl nitrogen (TKN) and for  $\text{NO}_x$  were changed from 20 to 30  $\text{kg PU}_X \cdot \text{kg X}^{-1}$  and from 20 to 10  $\text{kg PU}_X \cdot \text{kg X}^{-1}$ , respectively, to take this effect into account (Nopens *et al.*, 2010). Finally, the weight for total phosphorus (TP) was also increased from 20 to 50  $\text{kg PU}_X \cdot \text{kg X}^{-1}$  in order to favour those plant configurations or control strategies that resulted in higher bio-P removal.

$$\text{IQI or EQI (kgPU}\cdot\text{d}^{-1}) = \frac{1}{1000 \cdot (t_{\text{end}} - t_{\text{start}})} \int_{t_{\text{start}}}^{t_{\text{end}}} 1 [\text{PU}_{\text{TSS}}(t) + \text{PU}_{\text{COD}}(t) + \text{PU}_{\text{BOD}}(t) + \text{PU}_{\text{TKN}}(t) + \text{PU}_{\text{NOx}}(t) + \text{PU}_{\text{TP}}(t)] \cdot Q_j(t) \cdot dt \quad (7.11)$$

### 7.2.4. CONTROL STRATEGIES DESCRIPTION

Table 7.3 summarizes the control loops activated for each control strategy (C1-C7). All the control loop structures as well as their tuning parameters (data not shown) were extracted from previous simulation studies where their effectiveness was proved in a BSM framework. C0 corresponds to open-loop simulation.



**Table 7.3** Summary of the control loops studied.  
DO: Dissolved oxygen; TSS: Total suspended solids;  $Q_{CARB}$ : Carbon addition.

Characteristics	DO – I	DO – II	NO <sub>x</sub>	NH <sub>4</sub>	Q <sub>CARB</sub>
Controlled Variable	DO AER2	DO AER3	NO <sub>2</sub> +NO <sub>3</sub> ANOX2	NH <sub>4</sub> AER3	NO <sub>2</sub> +NO <sub>3</sub> ANOX2
Setpoint	2 mg O <sub>2</sub> ·L <sup>-1</sup>	1 mg O <sub>2</sub> ·L <sup>-1</sup>	1 mg N·L <sup>-1</sup>	A4 & A5: 1.5 mg N·L <sup>-1</sup> A6 & A7: 3 mg N·L <sup>-1</sup>	1 mg N·L <sup>-1</sup>
Manipulated variable	k <sub>1a</sub> AER1 k <sub>1a</sub> AER2	k <sub>1a</sub> AER3	Q <sub>RINT</sub>	DO SP AER 1,2 & 3	Q <sub>CARB</sub> ANOX 1
Control algorithm	PI	PI	PI	Cascade PI	PI
Control strategies	C1-C7	C1-C7	C2, C4, C6	C4-C7	C3, C5, C7
Reference	Nopens <i>et al.</i> , (2010)	Nopens <i>et al.</i> , (2010)	Gernaey <i>et al.</i> , (2004)	Gernaey <i>et al.</i> , (2004)	Vrecko <i>et al.</i> , (2006)

The dynamics of the sensors have to be also considered since they are used when monitoring some variables involved in the control actuation at full scale operation. The response delay or the signal noise were therefore simulated according to principles reported by Rieger *et al.* (2003). Different types of sensors were considered in this study depending on the measured variable. The DO sensors were assumed to be ideal (type A), with no delay or noise and a measurement frequency of 0 minutes. On the contrary, the N-NH<sub>4</sub><sup>+</sup> and N-NO<sub>x</sub> sensors (type B1) had a time delay of 10 minutes and white, normally distributed, zero mean noise (standard deviation of 0.1 mg·L<sup>-1</sup>). Further information about the sensor types and the typical characteristics thereof can be found in BSM1 description (Alex *et al.*, 2008).

### 7.2.5. DISCRIMINANT ANALYSIS (DA)

DA is a multivariate statistical technique used to determine the criteria (e.g. OCI or EQI) which allow characterization/separation between two or more naturally occurring groups (Johnson and Wichern, 2002). The method operates on scaled data and the technique constructs a discriminant function (DF) identifying the most relevant criteria:

$$DFz = C_{i,k} + \sum_{k=1}^n w_{i,k} \cdot X_{i,k} \quad (7.12)$$

Where z is the number of function, C<sub>k</sub> is the constant inherent to each function, n is the number of parameters used to classify a set of data into a given group and w<sub>i</sub> is the weight coefficient assigned by DA to a given performance evaluation parameter (X<sub>i</sub>). In this study, DA was applied following the principles pointed out in Flores *et al.* (2007) and Flores-Alsina *et al.*, (2010). Two different DA were performed to identify the best criteria for discrimination when comparing the plant configurations (MUCT was not considered in this part) and the control strategies. Hence, the plant configurations (DA1) and the control strategies (DA2) were the grouping variables, while all the evaluation criteria were the parameters X<sub>i</sub> (independent variables). The IBM-SPSS® 17.0 software was used for weights

determination as well as to perform DA itself. As a brief summary of expected outcome, DA determined a new set of axes that separate the data into categories. As much discriminant capacity of DFz more separation between data would be obtained (Figure 7.2).

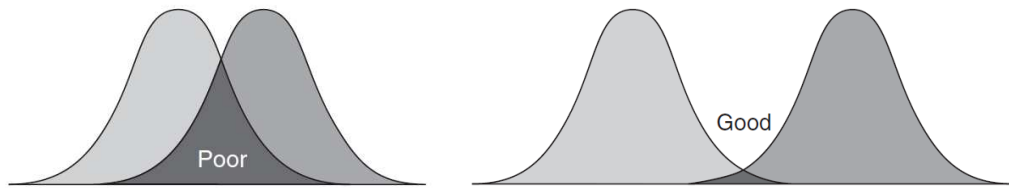


Figure 7.2 Examples of discriminant distributions.

## 7.3. Results and Discussion

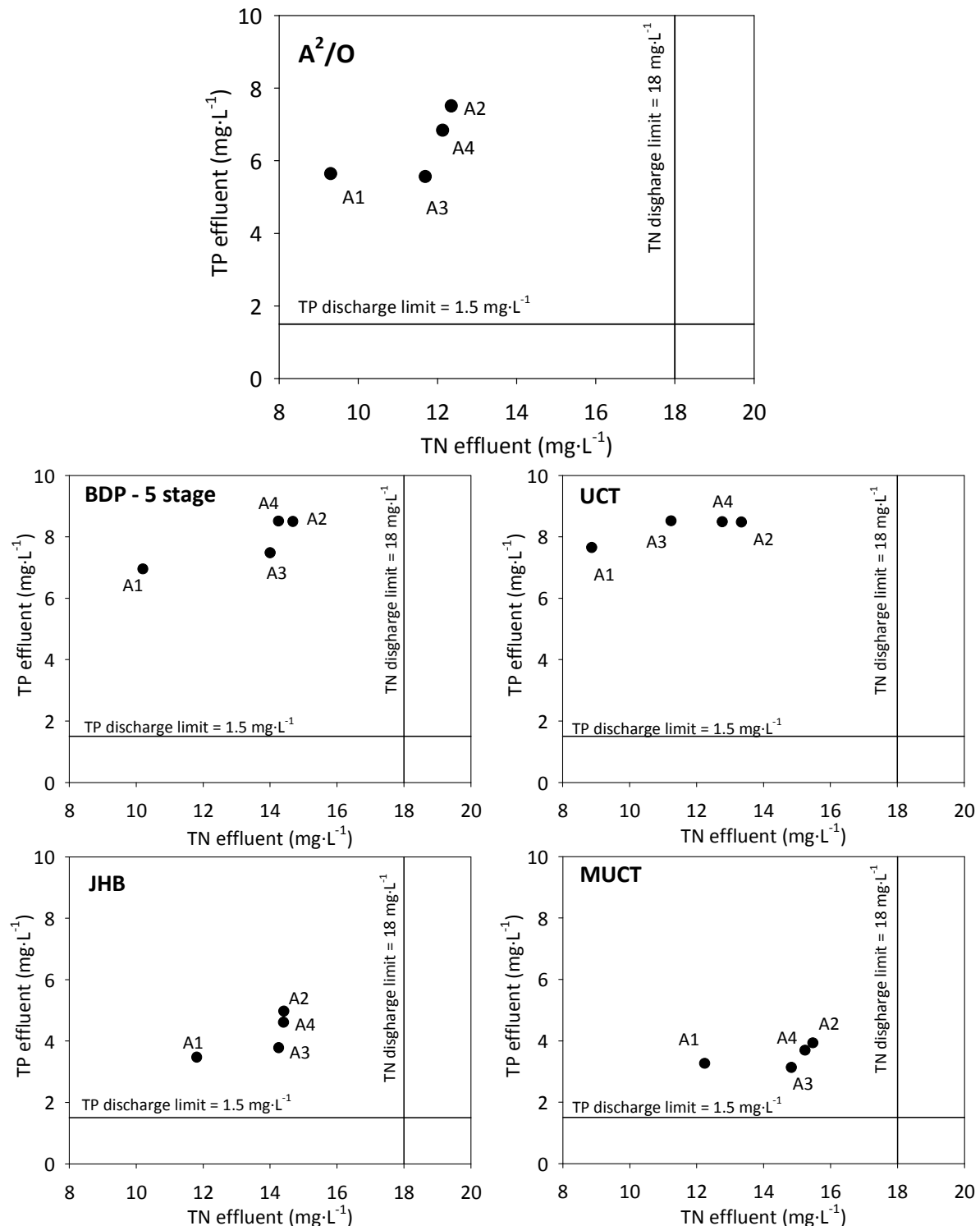
### 7.3.1. N REMOVAL AND EBPR PERFORMANCE UNDER DIFFERENT MODEL ASSUMPTIONS

Figure 7.3 shows the summary of the average effluent concentrations of TP and TN obtained in the LT simulations (Figure 7.4) for the five configurations studied. Similar results were obtained for the different plant configurations allowing to highlight the differences in the process performance when the plants are simulated for these four different sets of model assumptions. The discussion of the results is mainly referred to the A<sup>2</sup>/O configuration.

#### 7.3.1.1 Nitrite as state variable

According to figure 7.3, the predicted effluent total nitrogen (TN) and TP increased after the inclusion of nitrite as new state variable (i.e. comparing A2 simulations with A1). This increase was essentially due to the denitrification kinetics used when the model was extended with nitrite as an intermediary by using the mixed substrate approach (see Section 7.2.2). This assumption indeed results in a lower denitrification capacity when nitrite and nitrate coexist in similar concentrations and thus, in higher effluent TN with respect to A1 (Figure 7.4). For example, when simulating the A<sup>2</sup>/O configuration using the A2 approach, nitrite and nitrate concentrations in the ANOX2 were 1.87 mg N-NO<sub>2</sub><sup>-</sup>·L<sup>-1</sup> and 2.59 mg N-NO<sub>3</sub><sup>-</sup>·L<sup>-1</sup>. Thus, the denitrification rate from nitrate to nitrite was reduced by around 42% and the denitrification from nitrite to nitrogen by around 58%, in comparison with the default ASM2d with single step denitrification (i.e. mixed substrate terms are not considered). Despite this behaviour, the mixed substrate approach was chosen for the inclusion of nitrite in ASM2d because is more conservative than considering only substrate limitations (i.e. nitrate limitations in denitrification and nitrite limitations in denitrification). The latter approach may lead to simultaneous nitrite and nitrate reduction and, consequently, to a denitrification rate which would be higher than the aerobic respiration, which is incorrect from a bioenergetics point of view (Sin *et al.*, 2008). Hence, two-step denitrification rates will be dependent on both the concentration of nitrite and nitrate under anoxic conditions. Not surprisingly, some studies that considered this mixed substrate approach when modelling experimental data observed that, depending on nitrate or nitrite concentrations,

sometimes denitritation was faster than denitratation and *vice versa* (Sin and Vanrolleghem, 2006; Wett and Rauch, 2003). Similar results were also observed when the other plant configurations were simulated (Figure 7.3).



**Figure 7.3** Average effluent concentrations compared to discharge limits (TN = 18 mg·L<sup>-1</sup> and TP = 1.5 mg·L<sup>-1</sup> according to BSM guidelines; Gerney and Jørgensen, 2004) for the four model assumptions and with the five plant configurations.

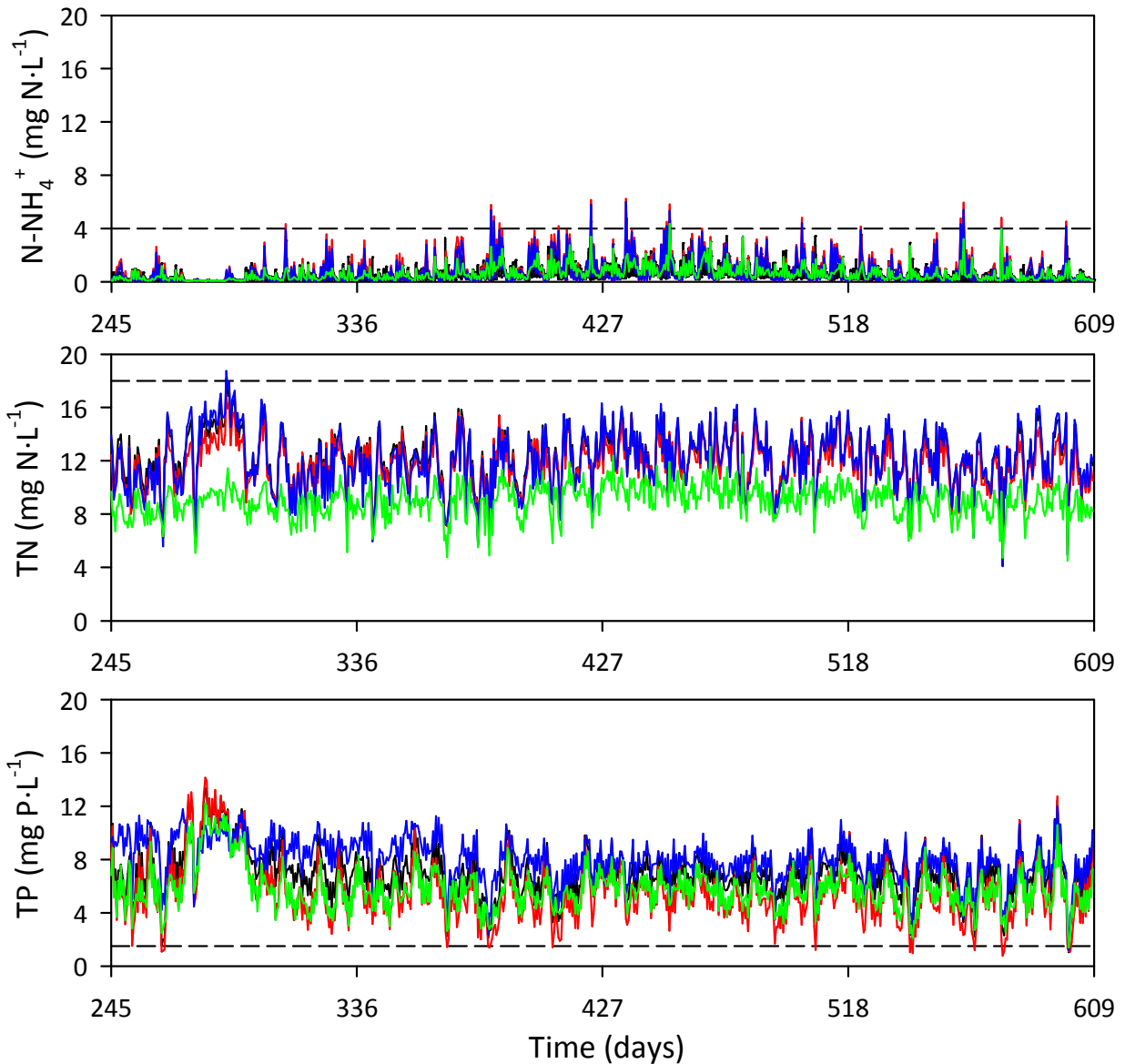


**Figure 7.4** Ammonium nitrogen, TN and TP dynamic evolution when the four model approaches studied were tested in the A<sup>2</sup>/O configuration. Green lines corresponds to A1, blue lines to A2, red lines to A3 and black lines to A4. Dashed lines correspond to the discharge limits of the pollutants.

### 7.3.1.2 Importance of including nitrite to describe certain scenarios

A scenario case analysis (SCA1) was conducted to emphasise the importance of nitrite inclusion in the ASM2d so the plant configurations were simulated under different dissolved oxygen concentrations. In the first case scenario (SCA1-A), the default operation mode (Table 7.1) was maintained while in the second case (SCA1-B), the air supply in AER1 and AER2 was decreased (from  $k_L a = 120 \text{ d}^{-1}$  to  $k_L a = 80 \text{ d}^{-1}$ ). Figure 7.5 presents the main results of SCA1 for the five configurations using a constant influent wastewater.

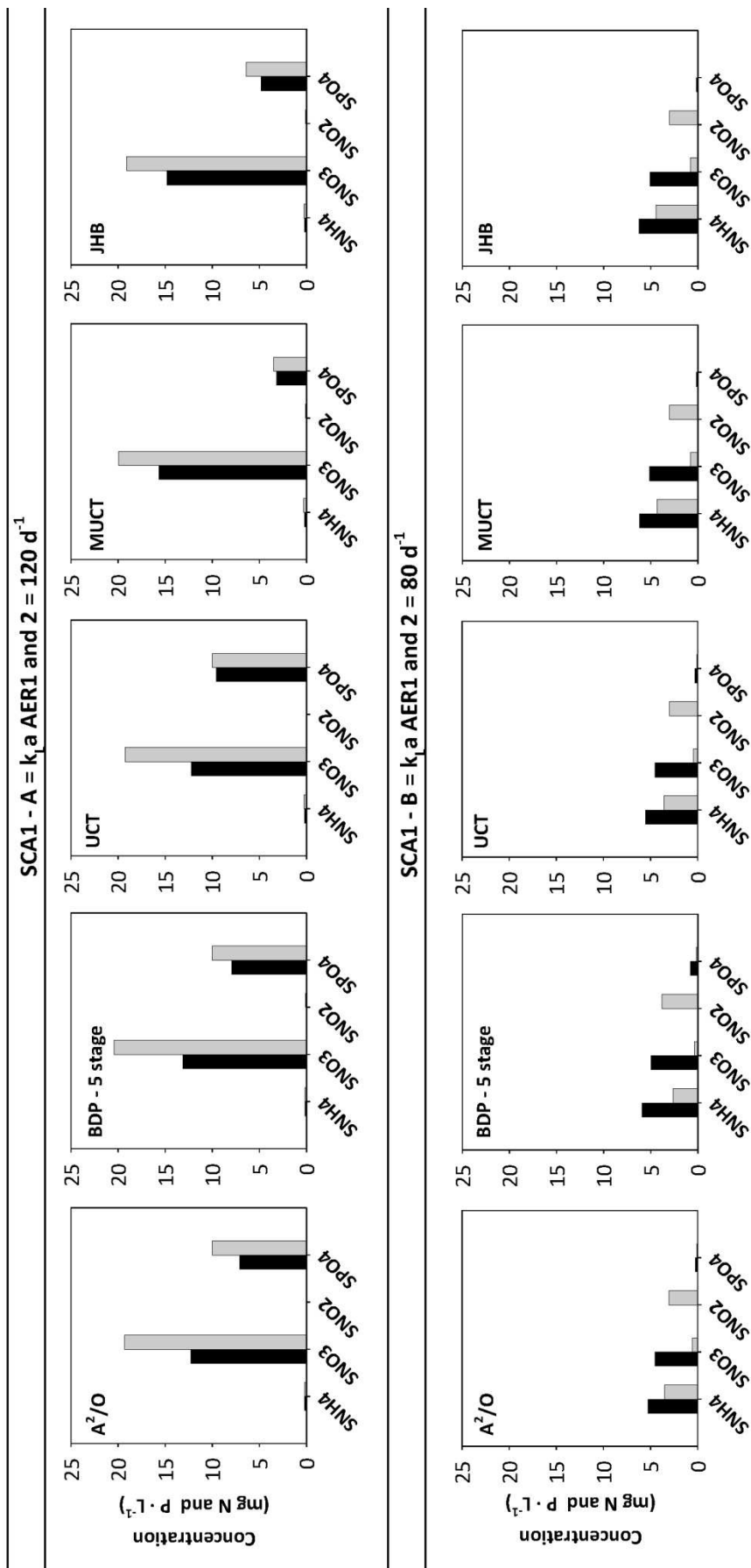


**Figure 7.5** Effluent concentrations obtained for SCA1-A ( $k_{La}$  AER 1 and 2 = 120 d<sup>-1</sup>) and SCA1-B ( $k_{La}$  AER 1 and 2 = 80 d<sup>-1</sup>) when the nitrification/denitrification processes are described as single (approach A1, black) or two step processes (approach A2, grey). SNH<sub>4</sub> corresponds to ammonium nitrogen, SNO<sub>3</sub> to nitrate nitrogen, SNO<sub>2</sub> to nitrite nitrogen and SPO<sub>4</sub> to orthophosphate phosphorus.

As can be observed for SCA1-A, after considering two step nitrification in the ASM2d (grey bars, A2), the effluent nitrate concentration increased again due to the reduction in the denitrification rates when considering the mixed substrates approach to simulate two-step denitrification (see above). When the air supply was reduced (SCA1-B) and nitrite was not considered (black bars, A1), the main nitrification product was nitrate. Contrary, when nitrite was considered in the model (A2), the ammonium concentration in the effluent decreased, in comparison with A1, and nitrite accumulation was observed. These differences are explained due to the oxygen saturation coefficient used when autotrophic biomass was considered i) as a single group ( $K_{O_2, AUT} = 0.5 \text{ mg O}_2 \cdot \text{L}^{-1}$ ) or ii) when it was divided into ammonia oxidising bacteria (AOB) and nitrite oxidising bacteria (NOB) ( $K_{O_2, AOB} = 0.4 \text{ mg O}_2 \cdot \text{L}^{-1}$  and  $K_{O_2, NOB} = 1.0 \text{ mg O}_2 \cdot \text{L}^{-1}$ ) (Wett and Rauch, 2003). The lower value for AOB explains the higher nitrification capacity at lower DO for A2, and as such resulted in a decrease of the ammonium concentration compared to the standard ASM2d (A1). The fact that both AOB and NOB have different oxygen affinities also explains the observed nitrite accumulation in A2. The dissolved oxygen concentration in the aerobic reactors was indeed always below  $0.5 \text{ mg} \cdot \text{L}^{-1}$  in SCA1-B, so nitrification was favoured instead of the denitrification process (i.e. NOB were almost washed out from the system).

The competition between PAO and OHO for the carbon source was also affected by the inclusion of nitrite. It is well-known that denitrification requires less COD (around 40%) than nitrification (Seyfried *et al.*, 2001). Therefore, when nitrite is the main nitrification product, less COD is required in the anaerobic phase to denitrify and then, more COD is available for the EBPR process (i.e. the PAO population in AER3 for SCA1-B increased from  $943 \text{ mg COD} \cdot \text{L}^{-1}$  using A1 to  $1180 \text{ mg COD} \cdot \text{L}^{-1}$  using A2). Similar results were also observed when this scenario was simulated for the other plant configurations (Figure 7.5).

These results demonstrated the importance of including nitrite in the ASM2d to achieve a better description of all the processes where nitrogen species take part and to avoid the simulation of potentially non-realistic behaviour at certain operational conditions (i.e. nitrification failures under low oxygen conditions). Moreover, this nitrite inclusion opens new possibilities in terms of developing operational strategies that can result in costs savings by decreasing the aeration requirements and the COD demand for denitrification.

### 7.3.1.3 Biological reactions in the secondary settler

When a reactive settler was simulated (A3), part of the  $\text{NO}_x$  was denitrified in the bottom of the secondary clarifier leading to a decrease of the  $\text{NO}_x$  present in the  $Q_{\text{REXT}}$  and in the effluent (Figure 7.3). P-removal was obviously improved (A2 versus A3) because less COD was consumed for denitrification in the anaerobic reactor, and thus became available for EBPR. Hence, the impact of considering the reactive settler approach when modelling EBPR processes was proved.

It is important to keep in mind that the reactive capacity will be overestimated with a series of ten CSTRs (i.e. mass transfer/diffusion limitations are not considered) leading to an unrealistic predicted EBPR activity due to the low nitrate concentrations in  $Q_{REXT}$  after denitrification in the settler (Flores-Alsina *et al.*, 2012). Limiting the reaction rates in the reactive settler should result in more realistic results. For this reason, a last test was run (A4), essentially multiplying the biological reaction rates in the settler with a global efficiency factor. Different simulations were conducted with different global efficiency factors (0 for non reactive settler, 0.25, 0.50, 0.75 and 1 for a reactive settler with no transport limitation) in order to simulate a more realistic biological level of activity in the settler. LT conditions (609 days) were simulated in the A<sup>2</sup>/O configuration and the last 364 days were used to evaluate the impact of the global efficiency factor on the reactive settler approach. According to the studies of Siegrist *et al.* (1995) in real decanters, the denitrifying capacity of the settler should be around 15% of the total denitrifying capacity of the system. Based on this value, 0.25 was selected as global efficiency factor since it resulted in a settler denitrifying capacity of 17% (Figure 7.6). This global efficiency factor was therefore kept during all the rest of the simulation study.

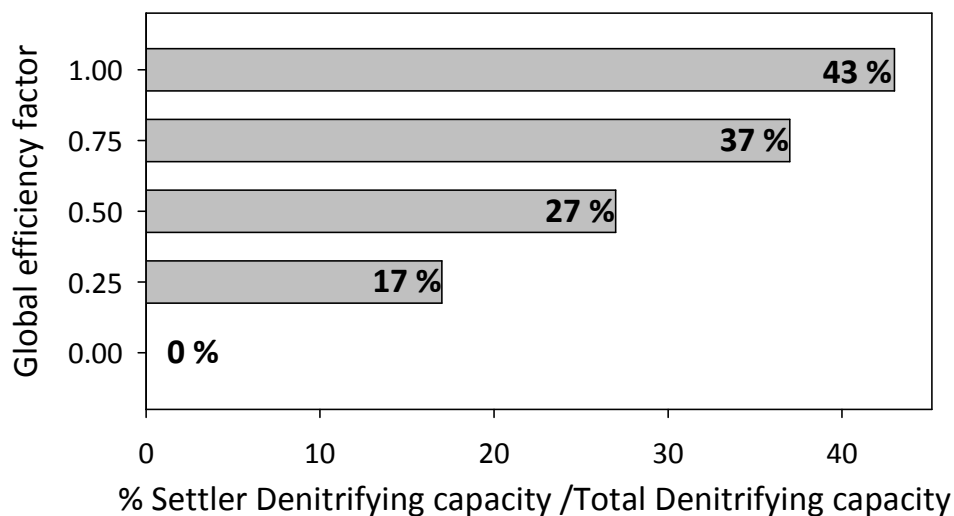


**Figure 7.6** Percentage of settler denitrifying capacity versus total denitrifying capacity in the A<sup>2</sup>/O configuration for different global efficiency factors.

When the approaches A3 and A4 were compared (non-limited and diffusion limited settler, respectively), less optimistic denitrification rates in the bottom of the clarifier were obtained for scenario A4 (Figure 7.3). As a result, there was a higher P concentration in the effluent since the amount of  $NO_x$  entering into the anaerobic phase via  $Q_{REXT}$  was higher. This reduction in the denitrification process efficiency was also evident in the fact that the TN concentration (mainly  $NO_x$ ) also increased in the effluent (Figure 7.3). On the contrary, a slight improvement of P-removal was still observed for A4 compared to A2 (non-reactive settler). Based on these results, it was concluded that it is important to consider the

denitrifying capacity of the settler to properly describe EBPR in BNR. A similar behaviour was observed for the rest of WWTP configurations (Figure 7.3).

#### **7.3.1.4 Importance of considering reactive settler under certain operation conditions**

A new scenario analysis was proposed to study the effect on the BNR processes of reactive settlers (SCA2). Figures 7.7-7.11 present the 10-layer settler model profiles for the five configurations when using the constant influent. As can be observed, no big differences on the removal efficiency were obtained for the different configurations (i.e. layer one corresponds to effluent concentrations) when comparing the reactive (A3 and A4) and the non-reactive (A2) settler approach for the default plant operation (SCA2-A). Only the absence of oxygen in the bottom layers of the settler produced a small decrease of nitrate linked to an increase of nitrite which in turn resulted in a better P-removal. This behaviour became even clearer when no reactive limitations were considered in the settler (A3). The fast oxygen consumption in the lower layers of the settler highly favoured denitrification processes but the low COD available resulted in an incomplete nitrate denitrification and thus, nitrite accumulation. However, the fact of considering each layer as a CSTR resulted in an overestimation of the intensity of the reactions occurring in the settler. For A3, the denitrification capacity of the settler was 43% of the TN denitrified in the system, which is disproportionate when is compared to the 15% reported in the literature for full-scale settlers (Siegrist *et al.*, 1995). As was commented before, the inclusion of a limitation of the reactive settler capacity (i.e. global efficiency factor in A4) resulted in a more realistic denitrification capacity (17%).

A greater effect of the reactive settler (A3 and A4) can be observed in scenarios with a higher loaded WWTP. This new scenario was simulated with an influent increase of 25% (SCA2-B) compared to the default value (from 20648 to 25810  $\text{m}^3 \cdot \text{d}^{-1}$ ). Despite the decrease of the hydraulic retention time in the settler (from 3.5 to 3.1 h), the higher load resulted in an increase of the biomass concentration in the system (the purge flow-rate was not increased) and thus, more reactivity in the settler was observed (Figures 7.7 to 7.11). The limited reactive settler (grey dots, A4) denitrified most of the nitrate in the lower layers, thus providing an extra anoxic volume. In addition, it is important to note that the nitrite inclusion in the model also allowed describing nitrite occurrence in the lower layers of the settler due to an incomplete denitrification process. Despite this nitrite increase, less  $\text{NO}_x$  entered in the anaerobic reactors and thus, more COD was available for PAO, improving EBPR process compared to non-reactive settler results (black dots, A2). This fact was not observed in MUCT and JHB because high P removal was always observed for all the model assumptions (Figure 7.10 and 7.11). Additionally, the anaerobic conditions in the bottom of the settler and the presence of COD due to lysis of biomass and PHA resulted in some P-release by PAO activity when using A3 assumptions.



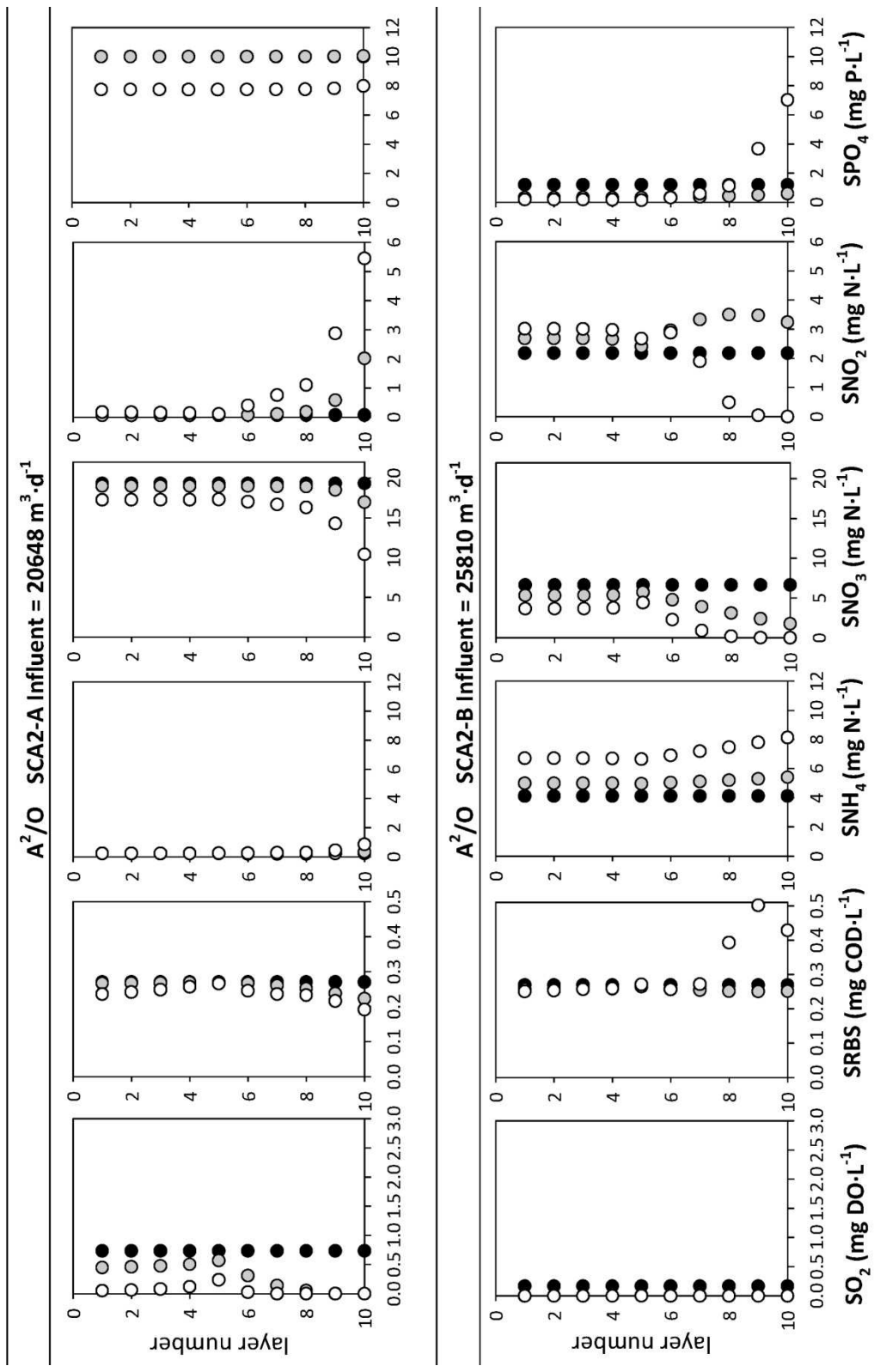


**Figure 7.7** Profiles of DO (SO<sub>2</sub>), readily biodegradable substrates (SRBS = SA + SF), ammonium nitrogen (SNH<sub>4</sub>), nitrate nitrogen (SNO<sub>3</sub>), nitrite nitrogen (SNO<sub>2</sub>), and orthophosphate phosphorus (SPO<sub>4</sub>) in the settler for A<sup>2</sup>O configuration at the default influent flow-rate (SCA2-A) and when it was increased 25% (SCA2-B). The non-reactive secondary settler (black dots, A2) is compared with a reactive settler (white dots, A3) or a diffusion-limited reactive settler (grey dots, A4). Layer 1 corresponds to the top of the settler (effluent) and layer 10 to the bottom (external recycle).

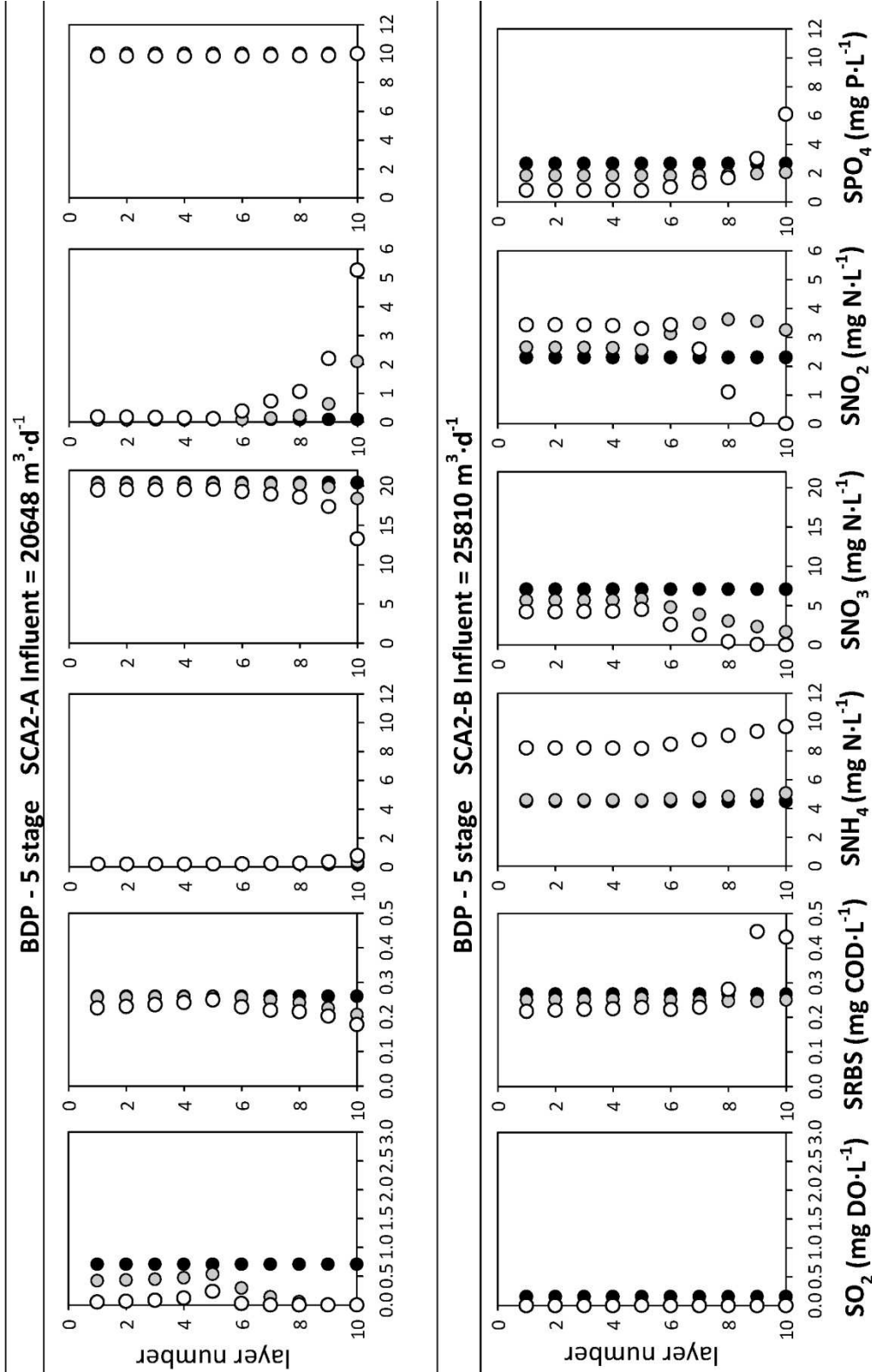


**Figure 7.8** Profiles of DO (SO<sub>2</sub>), readily biodegradable substrates (SRBS = SA+SF), ammonium nitrogen (SNH<sub>4</sub>), nitrate nitrogen (SNO<sub>3</sub>), nitrite nitrogen (SNO<sub>2</sub>), and orthophosphate phosphorus (SPO<sub>4</sub>) in the settler for BDP – 5 stage configuration at the default influent flow-rate (SCA2-A) and when it was increased 25% (SCA2-B). The non-reactive secondary settler (black dots, A2) is compared with a reactive settler (white dots, A3) or a diffusion-limited reactive settler (grey dots, A4). Layer 1 corresponds to the top of the settler (effluent) and layer 10 to the bottom (external recycle).

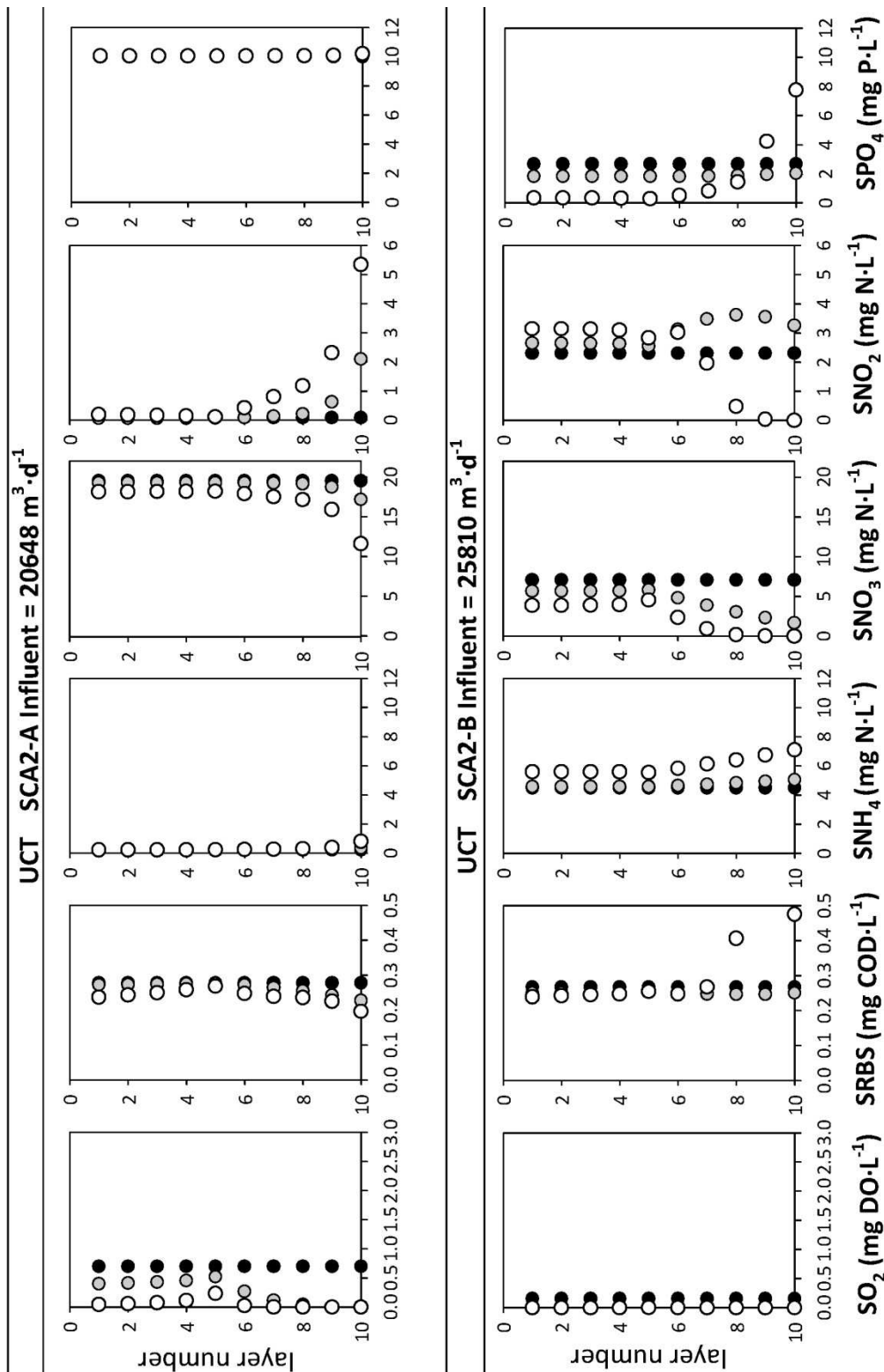


**Figure 7.9** Profiles of DO (SO<sub>2</sub>), readily biodegradable substrates (SRBS = SA+SF), ammonium nitrogen (SNH<sub>4</sub>), nitrate nitrogen (SNO<sub>3</sub>), nitrite nitrogen (SNO<sub>2</sub>), and orthophosphate phosphorus (SPO<sub>4</sub>) in the settler for UCT configuration at the default influent flow-rate (SCA2-A) and when it was increased 25% (SCA2-B). The non-reactive secondary settler (black dots, A2) is compared with a reactive settler (white dots, A3) or a diffusion-limited reactive settler (grey dots, A4). Layer 1 corresponds to the top of the settler (effluent) and layer 10 to the bottom (external recycle).

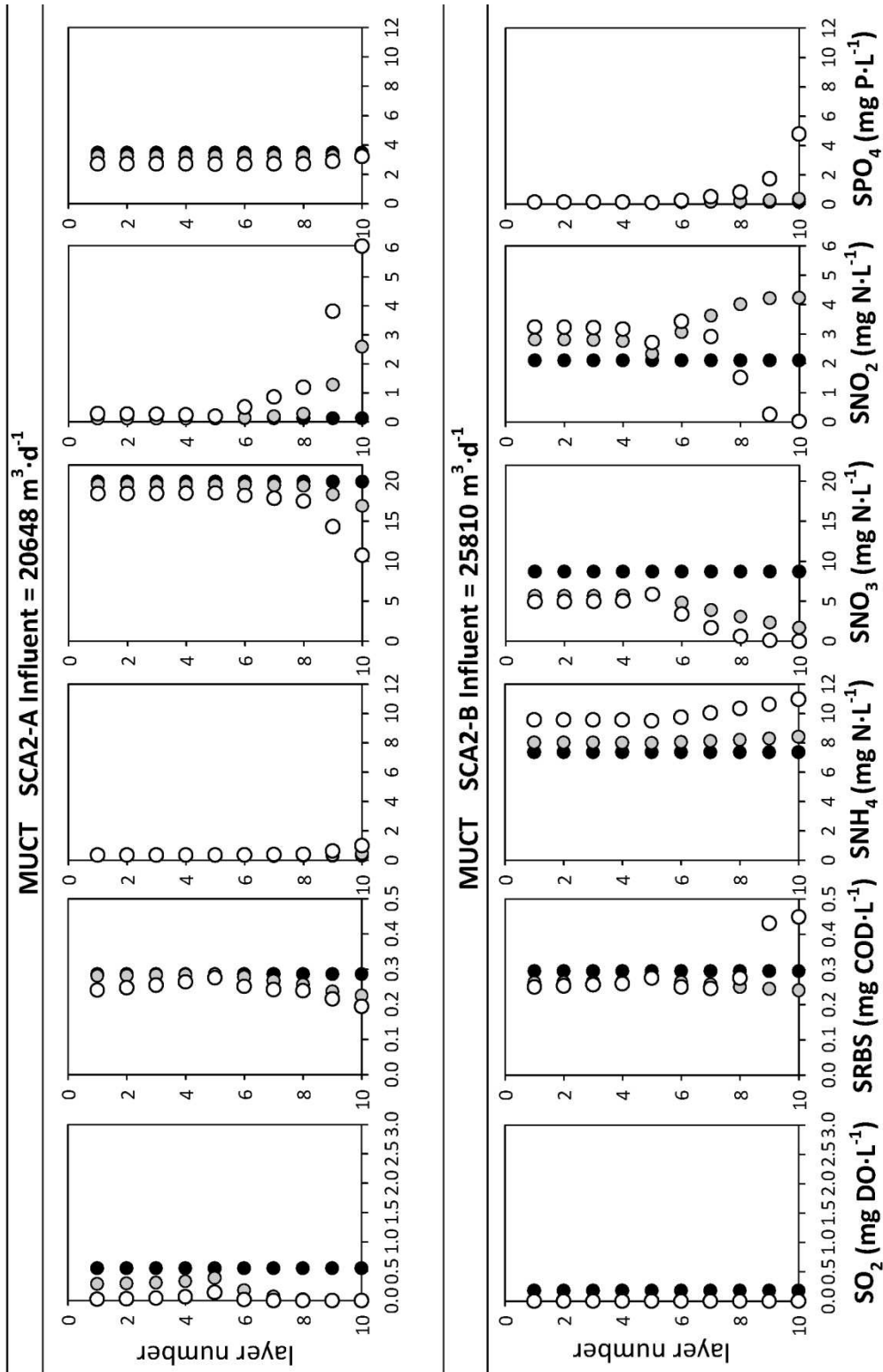


**Figure 7.10** Profiles of DO ( $\text{SO}_2$ ), readily biodegradable substrates ( $\text{SRBS} = \text{SA} + \text{SF}$ ), ammonium nitrogen ( $\text{SNH}_4$ ), nitrate nitrogen ( $\text{SNO}_3$ ), nitrite nitrogen ( $\text{SNO}_2$ ), and orthophosphate phosphorus ( $\text{SPO}_4$ ) in the settler for MUCT configuration at the default influent flow-rate (SCA2-A) and when it was increased 25% (SCA2-B). The non-reactive secondary settler (black dots, A2) is compared with a reactive settler (white dots, A3) or a diffusion-limited reactive settler (grey dots, A4). Layer 1 corresponds to the top of the settler (effluent) and layer 10 to the bottom (external recycle).

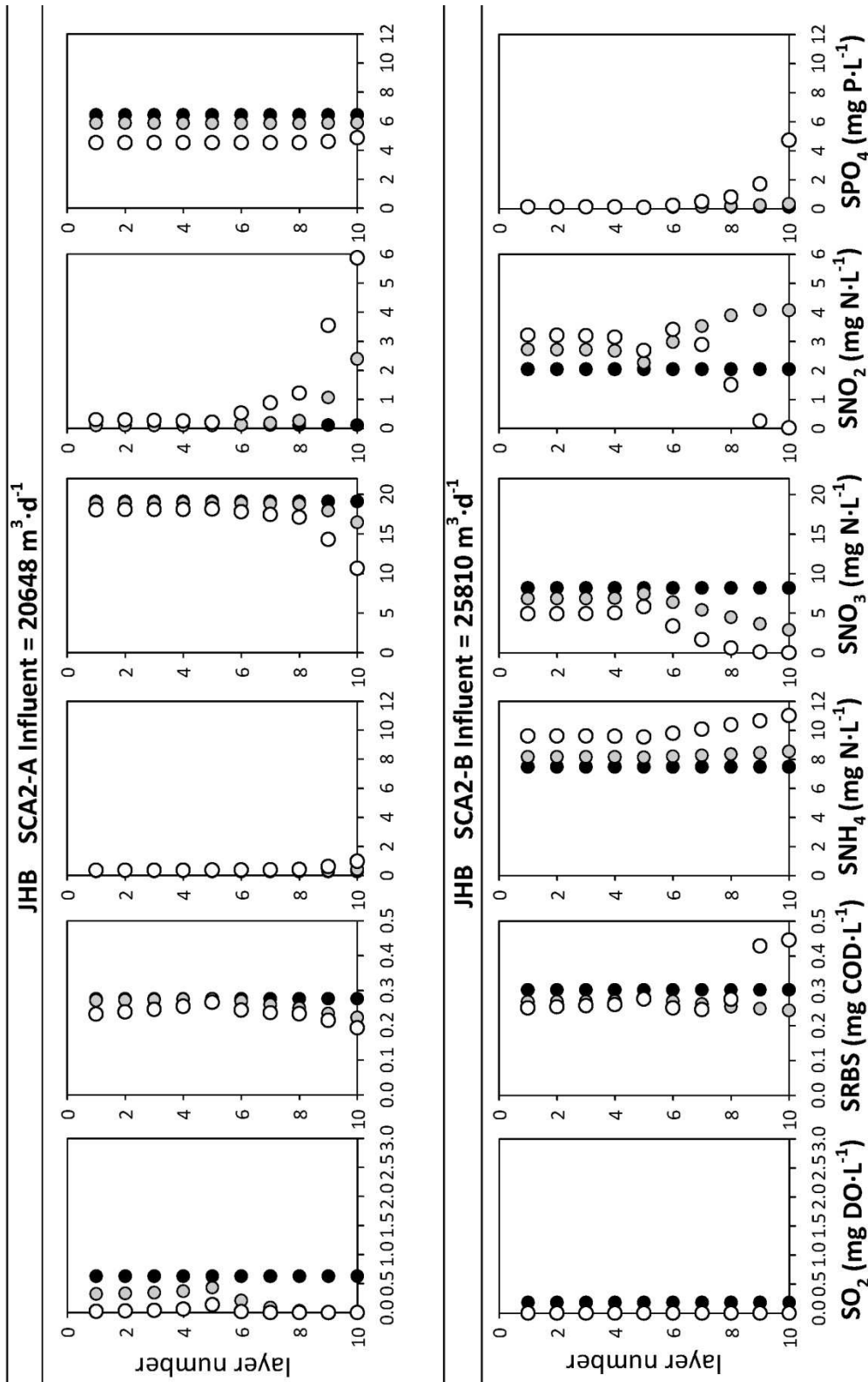


**Figure 7.11** Profiles of DO ( $\text{SO}_2$ ), readily biodegradable substrates (SRBS = SA+SB), ammonium nitrogen ( $\text{SNH}_4$ ), nitrate nitrogen ( $\text{SNO}_3$ ), nitrite nitrogen ( $\text{SNO}_2$ ), and orthophosphate phosphorus ( $\text{SPO}_4$ ) in the settler for JHB configuration at the default influent flow-rate (SCA2-A) and when it was increased 25% (SCA2-B). The non-reactive secondary settler (black dots, A2) is compared with a reactive settler (white dots, A3) or a diffusion-limited reactive settler (grey dots, A4). Layer 1 corresponds to the top of the settler (effluent) and layer 10 to the bottom (external recycle).

Comparing SCA2-A to SCA2-B, the higher flow rate of the second scenario resulted in a lower oxygen concentration in AER3 and thus, in lower oxygen load entering in the settler (Figures 7.7 to 7.11). This fact increased the anoxic conditions in the settler and then, some denitrification activity was observed in upper layers compared to SCA2-A, where total oxygen depletion and denitrification only occurred in the lower layers. Once again, not limiting the reactive capacity in the settler (A3) resulted in an overestimation of the processes occurring in the settler (e.g. total  $\text{NO}_x$  depletion or high ammonium production due to biomass decay in the lower layers).

These results demonstrated the importance of considering a reactive settler approach in systems with high biomass content and a high anoxic degree in the settler (SCA2-B); on the contrary, the traditional assumption of non-reactive settler (Takács *et al.*, 1991) seemed to be enough for describing the settling process in systems with relatively low biomass content. Note as well that the reactive settler here considered was corrected by considering a global efficiency factor to easily simulate diffusion limitations in reaction rates (A4), resulting in more realistic results. This approach could be further extended by considering the effect of other physical parameters (e.g. an increase of settler inflow) on the diffusion limitations. The global efficiency factor estimation could be made depending on effluent flow rate.

### 7.3.2. EBPR BEHAVIOUR UNDER DIFFERENT PLANT CONFIGURATIONS

Taking the conventional  $\text{A}^2/\text{O}$  configuration as a reference, this section compares alternative configurations (BDP-5 stage, JHB, UCT and MUCT, see figure 7.1) that have been proposed to minimise the detrimental effect on EBPR of  $\text{NO}_x$  entering the anaerobic phase. Based on the previous results, the inclusion of nitrite in ASM2d and the assumption of a diffusion-limited reactive settler (approach A4) were proved to be necessary to obtain a more realistic description of the BNR processes and thus, these approaches were used for these simulations. Figure 7.12 shows the main results obtained for the LT plant operation (Figure 7.13). The effluent TN concentrations were below the discharge level ( $18 \text{ mg N}\cdot\text{L}^{-1}$ ) for all the configurations, providing the  $\text{A}^2/\text{O}$  plant the lower TN level ( $12.13 \text{ mg N}\cdot\text{L}^{-1}$ ). On the other hand, the TP effluent concentrations were all above the P discharge limit ( $1.5 \text{ mg P}\cdot\text{L}^{-1}$ ). In this case, MUCT and JHB yielded the lower effluent P concentrations ( $3.69$  and  $4.61 \text{ mg P}\cdot\text{L}^{-1}$ , respectively) at the expense of the highest effluent TN ( $15.24$  and  $14.40 \text{ mg N}\cdot\text{L}^{-1}$ ), as is also pointed out in Van Haandel and Van der Lubbe (2007) and in Henze *et al.* (2008). This is mainly because these configurations minimise the arrival of nitrate to the anaerobic section (and are thus favouring P release by PAO). For the MUCT and JHB plants, the purpose of the ANOX1 compartment is to denitrify the  $\text{NO}_x$  from  $Q_{\text{REXT}}$  before entering the anaerobic tank, while the ANOX2 was only used to denitrify  $\text{NO}_x$  from  $Q_{\text{RINT}}$ . However, on the basis of the simulations, it can be concluded that the denitrifying capacity was not fully exploited since ANOX1 was oversized considering the low  $\text{NO}_x$  load originating from  $Q_{\text{REXT}}$ , whereas ANOX2 was overloaded to denitrify the  $\text{NO}_x$  fed by the  $Q_{\text{RINT}}$ . In the  $\text{A}^2/\text{O}$  configuration, on the contrary, a lower effluent  $\text{NO}_x$  concentration was observed because both ANOX1 and ANOX2

were used to denitrify the  $\text{NO}_x$  from the  $Q_{\text{RINT}}$  instead of only ANOX2. For example the  $\text{NO}_x$  concentration at the end of the JHB-ANOX2 was  $6.68 \text{ mg N}\cdot\text{L}^{-1}$  while it was  $4.46 \text{ mg N}\cdot\text{L}^{-1}$  for  $\text{A}^2/\text{O}$ -ANOX2. Thus, it can be concluded that MUCT and JHB plants give the PAO a competitive advantage compared to denitrifying bacteria, since more of the influent carbon source was channelled into the EBPR processes.

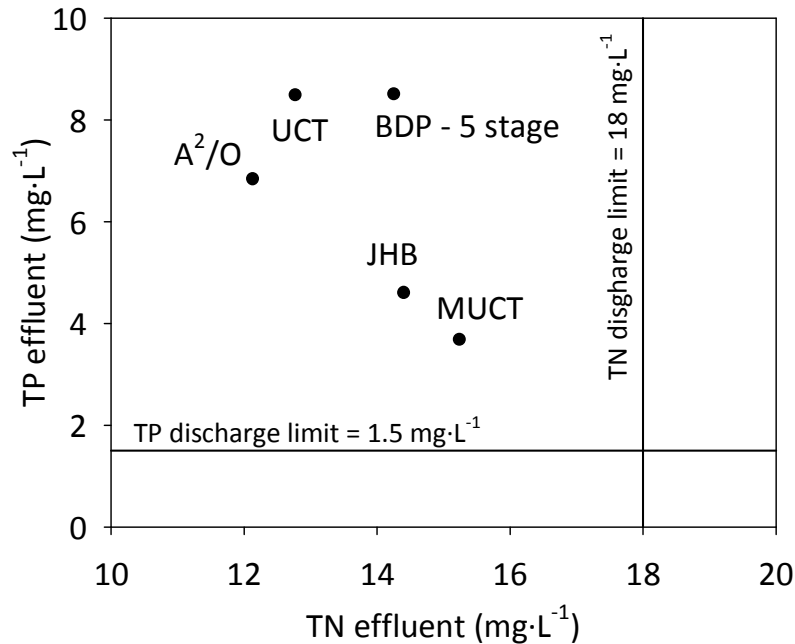


**Figure 7.12** Average effluent concentrations obtained for the different plant configurations under LT conditions compared to effluent discharge limits ( $\text{TN} = 18 \text{ mg}\cdot\text{L}^{-1}$  and  $\text{TP} = 1.5 \text{ mg}\cdot\text{L}^{-1}$ ).

The UCT plant showed a high effluent P concentration (Figure 7.12) contrary to what was expected taking into account that it is one of the most often reported configurations used to prevent  $\text{NO}_x$  presence in the anaerobic reactor (Rabinowitz and Marais, 1980; Henze *et al.*, 2008). UCT plant simulations revealed that total  $\text{NO}_x$  depletion was not achieved at the end of the anoxic phase ( $5.08 \text{ mg N}\cdot\text{L}^{-1}$ ) favouring denitrification instead of P release in the anaerobic reactors. This fact is in agreement with the statements made in some engineering manuals (Henze *et al.*, 2008; Metcalf and Eddy, 2003) that total anoxic  $\text{NO}_x$  denitrification is critical to achieve high biological P removal in the UCT plant. This issue is tackled by the MUCT, which separates the  $Q_{\text{REXT}}$  and  $Q_{\text{RINT}}$  inlet points at the expense of decreasing even more the TN removal capacity.

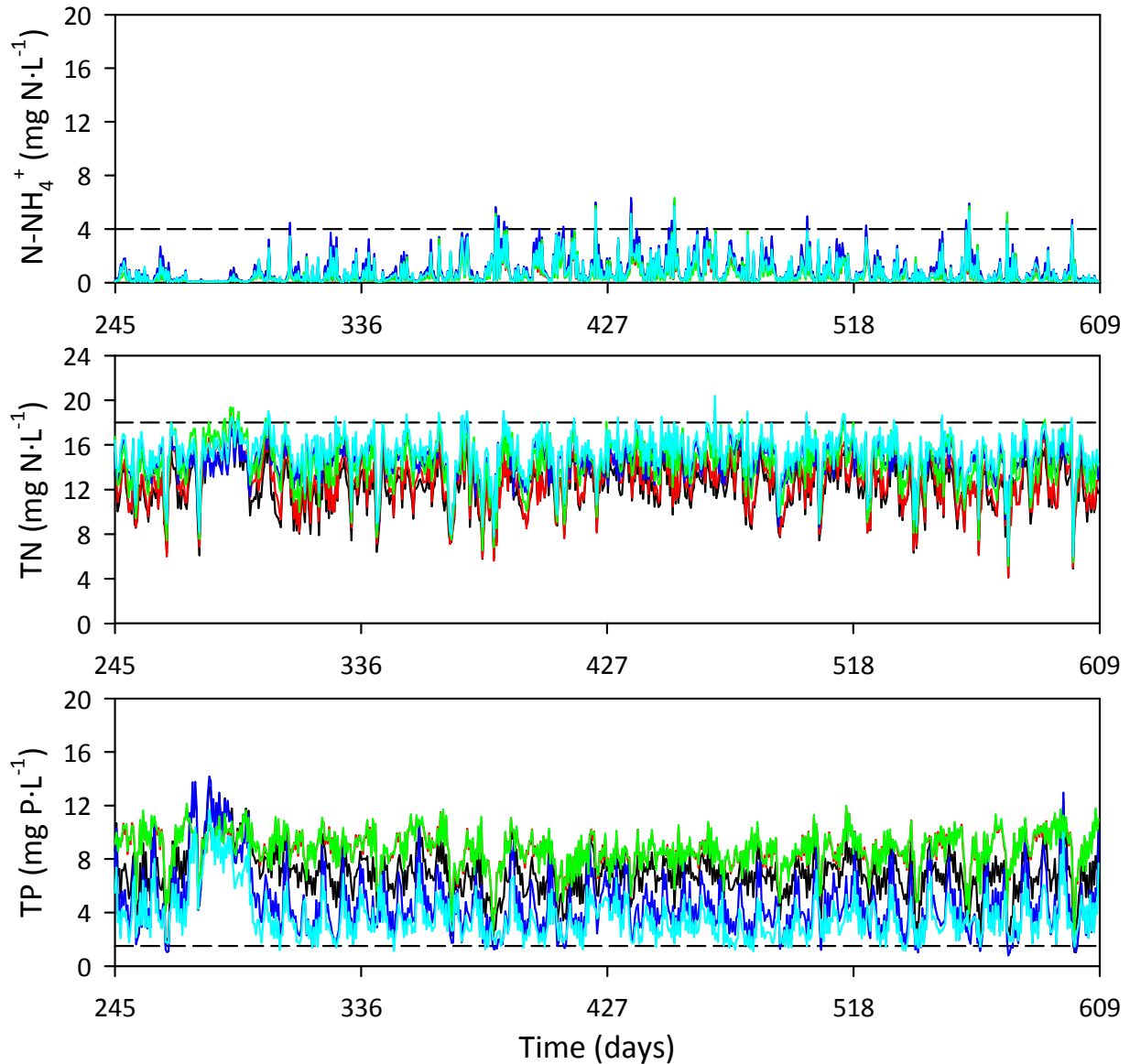


**Figure 7.13** Ammonium nitrogen, TN and TP dynamic evolution for the five plant configurations and considering A4. Black lines corresponds to A<sup>2</sup>/O configuration, red lines to UCT, blue lines to JHB, green lines to BDP-5 stage and cyan lines to MUCT. Dashed lines correspond to the discharge limits of the pollutants.

Finally, the BDP 5-stage resulted in the highest effluent P (Figure 7.12). This could be explained due to the location of ANOX2 in this configuration, which was placed after the AER2 and before AER3 (Figure 7.1). Thus, the  $Q_{RINT}$  only fed the ANOX1, resulting in less denitrifying capacity mainly for two reasons: i) a reduction of the anoxic volume to denitrify  $NO_x$  brought by the  $Q_{RINT}$  (similar to what occurred for JHB and MUCT); and, ii) the low COD available for denitrification that entered into ANOX2 after the aerobic phase (e.g.  $NO_x$  concentration only decreased from 12.77 to 10.29 mg N L<sup>-1</sup> in such a reactor). As reported by Van Haandel and Van der Lubbe (2007), the BDP-5 stage configuration can perform well with high P-removal as long as sufficient denitrification is ensured in the second anoxic reactor.



Otherwise the system is not capable to prevent nitrate to enter in the anaerobic reactor. Barnard (1976) and Osborn and Nicholls (1978) reported some examples of this problem in a BDP-5 stage pilot plant. To solve this problem, external carbon dosage could be introduced in ANOX2 to ensure sufficiently high COD levels to allow such denitrification.

It is important to remark that the design and operation of these five WWTPs configuration were set according to benchmarking guidelines (Nopens *et al.*, 2010) but not optimised. We hypothesise that similar BNR performance would be obtained for all plant configurations if the reactor volumes and recycle streams were optimised to obtain low effluent TN and TP.

Figure 7.14 (black bars) presents the summary of the simulation results for the different plant configurations in terms of benchmarking criteria. The configuration with the best EQI was MUCT (9108 kg PU·d<sup>-1</sup>) and that with the lowest OCI was BDP-5 stage (15986 kg PU d<sup>-1</sup>). As can be observed, these configurations with the best removal capacity presented also the highest operational cost (i.e. a decrease in the EQI leads to an increased OCI) and *vice versa*. These differences were directly related to the sludge production and its processing cost (Figure 7.14 C). The higher BNR efficiencies in the JHB and MUCT plants (15% and 20% less EQI than for A<sup>2</sup>/O) also resulted in a higher solids production (172 kg·d<sup>-1</sup> more for JHB and 271 kg·d<sup>-1</sup> more for MUCT, compared to SP for A<sup>2</sup>/O) and thus, in higher costs associated to solids processing. These results demonstrate clearly that effluent quality and the operating costs need to be traded off against each other. Such an observation has also been made in several studies (Jeppsson *et al.*, 2007; Alex *et al.*, 2008) and in the Chapter IV of this thesis when performing multi-criteria optimisation.

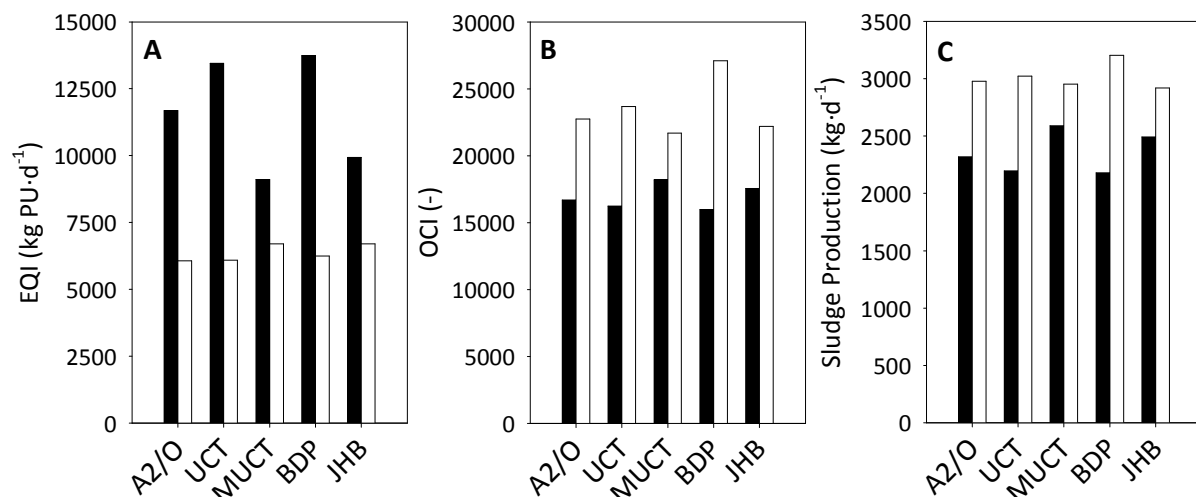


**Figure 7.14** Simulations results for the five plant configurations without carbon source addition (black) and when adding an external carbon source to achieve 1.5 mg·L<sup>-1</sup> P-PO<sub>4</sub><sup>-3</sup> the effluent (white).

### 7.3.3. EFFECT OF CARBON ADDITION FOR THE DIFFERENT WWTP CONFIGURATIONS

Regarding P removal, the simulation results show that none of the plant configurations met the legal effluent P discharge limit of  $1.5 \text{ mg P}\cdot\text{L}^{-1}$  (Figure 7.12). This is because of the low COD content in the wastewater and the competition between PAO and OHO for the electron donor. An extended solution in real WWTP is the addition of an external carbon source in the ANAE1 tank in order to provide a supplementary amount of readily biodegradable organic matter for EBPR and denitrifying processes (Olsson *et al.*, 2005). The last scenario analysis (SCA3) aimed at calculating the required external carbon source quantity (simulated as fermentation products or volatile fatty acids, SA) to obtain an average effluent TP of  $1.50 \pm 0.03 \text{ mg}\cdot\text{L}^{-1}$ . Table 7.4 shows external carbon source needed for each plant configuration as well as the effluent TP and TN concentrations. Sludge production was also calculated because, as was commented before, its processing had a deep impact on the operational costs calculation.

**Table 7.4** External carbon addition to ensure TP discharge limit ( $1.5 \text{ mg}\cdot\text{L}^{-1}$ ) for the different plant configurations.

Plant configuration	External carbon addition ( $\text{kg}\cdot\text{d}^{-1}$ )	Effluent TP ( $\text{mg}\cdot\text{L}^{-1}$ )	Effluent TN ( $\text{mg}\cdot\text{L}^{-1}$ )	Sludge production ( $\text{kg}\cdot\text{d}^{-1}$ )
A <sup>2</sup> /O	920	1.53	8.61	2979
UCT	1100	1.52	8.67	3024
BDP – 5 Stage	2000	1.51	8.33	2953
JHB	780	1.50	11.74	3204
MUCT	612	1.53	12.64	2919

The MUCT configuration required the lowest amount of external carbon source to reduce the effluent TP concentration and to meet P discharge limit, whereas the BDP-5 stage required the highest amount. These results were in agreement with the fact that MUCT favoured the EBPR process and thus, it achieved the highest P removal efficiency. On the contrary, BDP-5 stage favoured OHO denitrification and achieved the worst P removal efficiency (Figure 7.12). The external carbon addition also reduced the effluent pollutant content resulting in similar EQI results for all the plant configurations (Figure 7.14 A). When no carbon source was added, effluent TP played a major role in the EQI calculation favouring the MUCT and JHB configurations (black bars). However, when carbon source was added, the effluent phosphorus concentration was drastically reduced and TN caused the main differences in the EQI values (white bars). Therefore, in SCA3, JHB and MUCT achieved the highest EQI values (Figure 7.14 A) due to a higher effluent TN concentration (11.74 and 12.64

mg N·L<sup>-1</sup>, respectively). When it comes to OCI criteria, using an external carbon source reduced the effluent pollutant loads but at the expense of an increasing OCI (Figure 7.14 B). External carbon dosage implies a cost itself (Equation 7.1) and thus, those configurations that required higher carbon addition obviously also resulted in higher OCI values. In addition, the extra COD also produced an increase of the SP (Figure 7.14 C), which contributed to increase OCI values due to the considerable sludge processing cost. The BDP-5 stage plant resulted in the highest OCI value not only because more external carbon source addition was required to meet the P limit, but also because it resulted in a higher SP.

If EQI and OCI are considered simultaneously, A<sup>2</sup>/O can be considered the most balanced plant configuration. A study of the benefits of using multi-criteria tools to analyse plant performance balancing EQI and OCI is presented in Chapter IV. This configuration did not require any excessive carbon source addition (920 kg·d<sup>-1</sup>) to meet P discharge limits and it presented lower OCI values than BDP-5-stage or UCT plants (Figure 7.14 B, white bars). In addition, the EQI value was one of the lowest obtained (6070 kg PU·d<sup>-1</sup>) due to the low effluent TN obtained (8.61 mg N·L<sup>-1</sup>), in contrast to the MUCT or JHB plants. The latter result gains more importance taking into account that in the last years the TN discharge limit has become stricter, for example 10 mg N·L<sup>-1</sup> according to the Council Directive 91/271/EEC. If this directive was applied, A<sup>2</sup>/O would be considered the best plant configuration because the TN values for MUCT and JHB (11.74 and 12.64 mg N·L<sup>-1</sup>, respectively) would be above the discharge limit.

#### **7.3.4. ANALYSIS OF DESIGN CONFIGURATIONS/CONTROL STRATEGIES USING DISCRIMINANT ANALYSIS**

In this section, the benefits of implementing different control strategies in WWTP BNR performance were studied by using a multivariate statistical method, DA. For this aim, 32 different scenarios were simulated under LT conditions (see Section 7.2.2): open-loop operation and seven control strategies implemented in four of the plant configurations (MUCT was not considered in this part). DA was applied on the simulation results aiming at dividing the original data set into four groups (DA1, plant configurations) and eight groups (DA2, control strategies), respectively. Only the simulation results from the last 364 days were used for criteria evaluation. DA was also applied by using the average effluent concentrations from the last 364 days. Table 7.5 shows the selected criteria with the highest discriminant ability between scenarios and the standardised coefficients of the discriminant functions (DFs). It is important to note that all the information extracted from DA could be directly obtained by the analysis of the simulation data; nevertheless DA allows a fast analysis of correlations of a large data set taking into account many criteria, which are not easy to extract only looking at raw simulation results. In addition, DA is also beneficial for presenting the data in a rather straightforward way.

**Table 7.5** DF coefficients for DA1 and DA2. The most discriminant criteria (highest absolute coefficient values) are presented in bold. eff: Effluent concentration, TIV: Time in violation (i.e. above discharge limit).

Criteria	DA1 – Plant configuration			DA2 – Control strategy		
	DF1	DF2	DF3	DF1	DF2	DF3
N – NH <sub>4</sub> <sup>+</sup> eff	<b>-2,96</b>	0,48	2,54	2,02	0,26	<b>4,69</b>
N – NO <sub>2</sub> <sup>-</sup> eff	<b>11,41</b>	1,25	4,55	0,60	-0,49	0,48
N – NO <sub>3</sub> <sup>-</sup> eff	<b>8,14</b>	<b>8,36</b>	<b>7,59</b>	<b>3,24</b>	<b>-3,42</b>	<b>19,49</b>
P – PO <sub>4</sub> <sup>-3</sup> eff	-0,76	<b>-4,33</b>	<b>11,54</b>	<b>13,55</b>	<b>15,51</b>	<b>-4,16</b>
TN eff				<b>-3,68</b>	<b>4,67</b>	<b>-19,18</b>
TP eff				<b>-13,24</b>	<b>-14,37</b>	<b>3,84</b>
EQI	1,77	2,23	<b>-10,25</b>			
AE	<b>-2,50</b>	1,61	0,44			
ME	0,77	<b>2,40</b>	2,80			
EC	<b>6,63</b>	0,51	3,16			
TIV TP	2,13	<b>-2,41</b>	0,61			

#### 7.3.4.1. Analysis of plant configurations (DA1)

The total variability (100%) could be explained with three DFs. Figure 7.15 (up) shows that DF1 (with a discriminant ability of 75.43%) differentiated the configurations with the higher denitrifying capacity, A<sup>2</sup>/O and UCT, from the others, JHB and BDP-5 stage (Figure 7.12). In a second degree of importance, aeration and the need of carbon source dosage were also discriminant criteria. The higher anoxic volume in A<sup>2</sup>/O and UCT for denitrifying Q<sub>RINT</sub> NO<sub>x</sub> (in JHB and BDP-5stage only one anoxic reactor was used to denitrify the NO<sub>x</sub> from Q<sub>RINT</sub>) favoured the anoxic organic matter removal from the influent resulting in less EC needs (Q<sub>CARB</sub> control strategy in table 7.3) and in lower AE requirement due to less organic matter entered in the aerobic phase. For DF2, with lower discriminant ability (13.65%), the denitrification process was again the most relevant criterion but P removal also had some discriminant capacity. Hence, A<sup>2</sup>/O with a higher denitrification capacity and lower effluent P was separated from UCT. JHB was also well separated from BDP 5-stage, but in this case P removal governed the cluster formation since similar effluent nitrate concentrations were obtained for both configurations. Finally, P removal had the strongest weight on DF3 (discriminant ability 10.92%); however the effect of the implemented control strategy seemed to have an effect on the grouping and thus, the generated clusters were not that well defined (Figure 7.15, down). In other words, N removal processes seemed to be mainly ruled by the plant design/configuration while P removal was mainly ruled by operation (control strategy). Despite this, A<sup>2</sup>/O and JHB, with a better P removal capacity (Figure 7.12), were respectively separated from UCT and BDP.

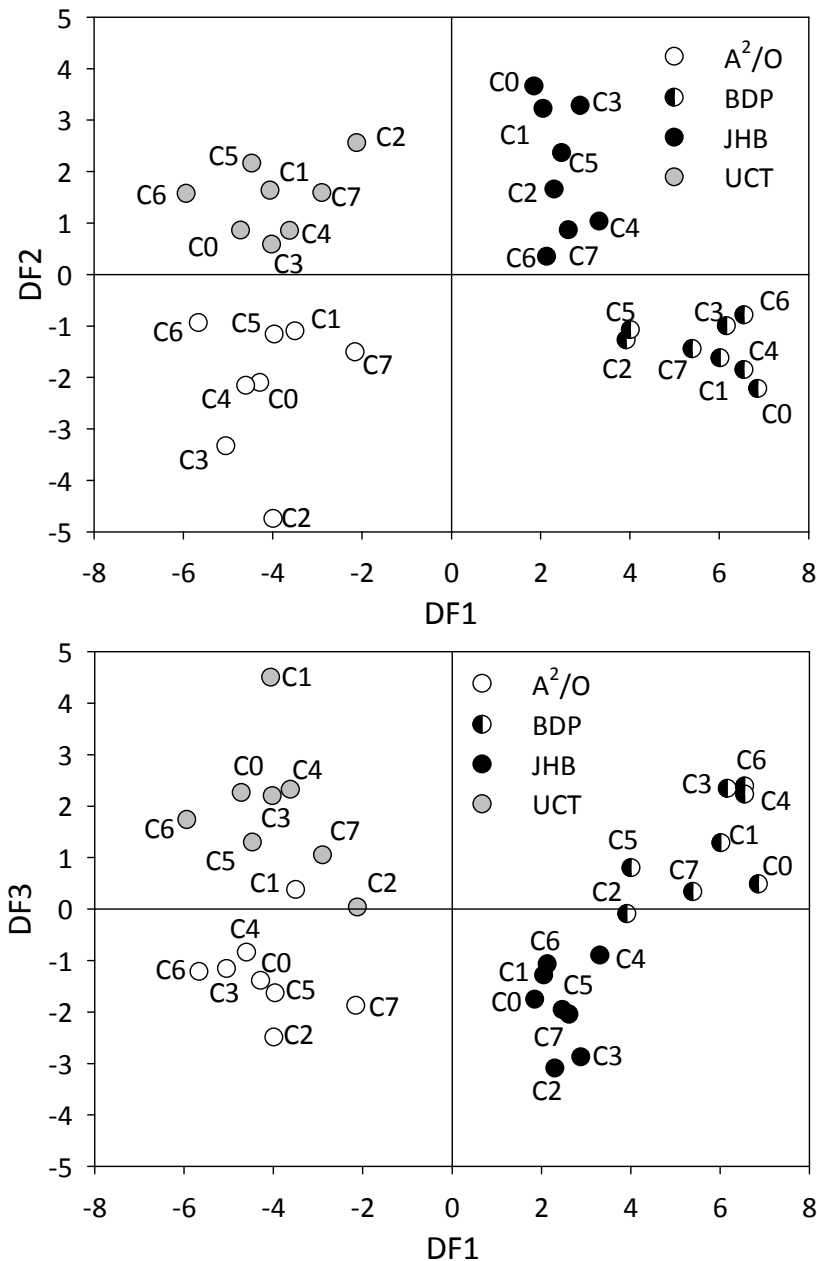


**Figure 7.15** DA of the WWTP plant configurations tested (DA1) for the discriminant functions DF1 vs DF2 (up) and DF1 vs DF3 (down).

### 7.3.4.2. Analysis of control strategies (DA2)

When the DA was focused on discriminating between the implemented control strategies, 99.07% of the total variability was explained with three DFs (Figure 7.16). DF1 (79.44%) grouped the control strategies into two different clusters depending on BNR removal: C6 and C7 with a higher N and P removal efficiency were separated from C0-C5 (Table 7.6). The implementation of ammonium cascade control with high ammonium setpoint (3.0 mg N-NH<sub>4</sub><sup>+</sup>·L<sup>-1</sup>) together with NO<sub>x</sub> control in anoxic reactors (C6 and C7) resulted in the best combination to favour nutrient removal regardless the plant configurations. The ammonium control limited nitrification reducing effluent NO<sub>x</sub> concentration (i.e. ammonium

represented more than 50% of effluent TN) and consequently, its presence under anaerobic conditions. Hence, EBPR was more favoured in comparison with the rest of the control strategies (Table 7.6).

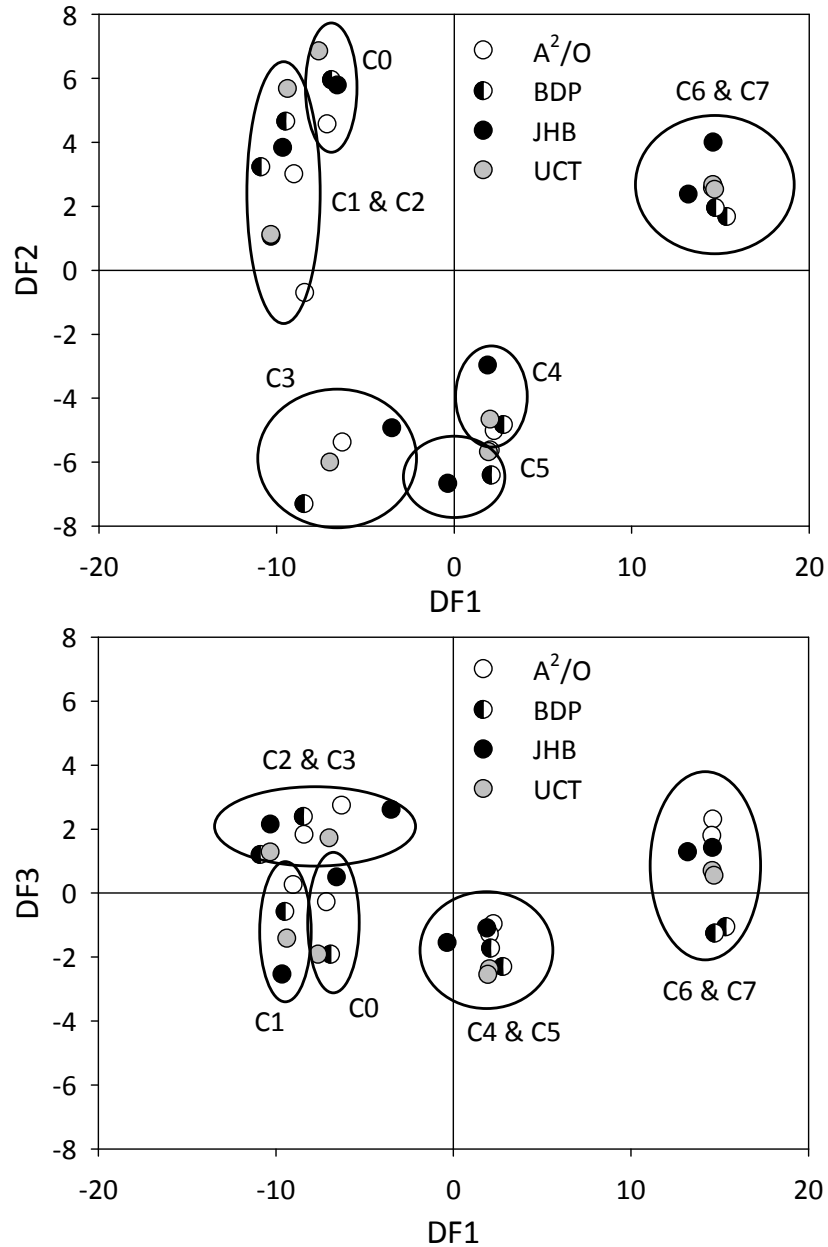


**Figure 7.16** DA of the WWTP control strategies implemented (DA2) for the discriminant function DF1 and DF2 (up) and DF1 and DF3 (down).

N and P removal efficiency were also the most relevant variables for DF2 (17.70%), which allowed differentiating C0-C2 from C3-C5 (Figure 7.16, up). Again, better BNR efficiency was observed when ammonium cascade control was activated (C3-C5) with a lower setpoint (1.5 mg N-NH<sub>4</sub><sup>+</sup>·L<sup>-1</sup>). Nitrification was then not that limited as in C6 or C7 and higher effluent TP was obtained due to more NO<sub>x</sub> arrived to the anaerobic reactor (i.e. NO<sub>x</sub> was around 65% of

effluent TN for C4 and C5). Anyhow, it was proved that ammonium control improved BNR in comparison with those control strategies that did not incorporate it (C0-C2). It is to be noted that C3 was an exception to this observation since only NO<sub>x</sub> control in ANOX2 was activated (i.e. no ammonium cascade control) and similar BNR removal was also observed (Table 7.6). The addition of an external carbon source, as the manipulated variable, in C3 (Table 7.3) ensured high denitrification capacity in the anoxic reactors reducing the NO<sub>x</sub> inlet in the anaerobic phase. Similar control set-up was proposed in C2 by controlling NO<sub>x</sub> concentration with Q<sub>RINT</sub> flow rate, however worse BNR was observed. In this case, the ammonium was almost totally nitrified in aerobic reactors resulting in such amount of NO<sub>x</sub> that Q<sub>RINT</sub> flow rate had to be reduced to meet the anoxic NO<sub>x</sub> setpoint (1 mg NO<sub>x</sub>·L<sup>-1</sup>). Table 7.6 shows that the lowest pumping energy consumption was obtained for C2. As a result, less NO<sub>x</sub> was denitrified increasing NO<sub>x</sub> inlet to the anaerobic reactors and negatively affecting in EBPR process.

**Table 7.6** Example of the evaluation criteria for the seven control strategies in A<sup>2</sup>/O WWTP, including open-loop (C0). eff: Effluent concentration, TIV: Time in violation (i.e. above discharge limit).

Evaluation criteria	Control strategy							
	C0	C1	C2	C3	C4	C5	C6	C7
N-NH <sub>4</sub> <sup>+</sup> eff (mg·L <sup>-1</sup> )	0.82	0.62	0.59	0.71	1.46	1.49	2.93	2.95
N-NO <sub>2</sub> <sup>-</sup> eff (mg·L <sup>-1</sup> )	0.17	0.08	0.10	0.11	0.60	0.58	0.80	0.83
N-NO <sub>3</sub> <sup>-</sup> eff (mg·L <sup>-1</sup> )	9.88	9.86	8.74	6.50	4.32	4.08	2.84	2.93
TN eff (mg·L <sup>-1</sup> )	12.13	11.82	10.60	8.46	7.47	7.28	7.68	7.83
P-PO <sub>4</sub> <sup>-3</sup> eff (mg·L <sup>-1</sup> )	6.36	5.87	4.30	1.55	0.67	0.20	0.33	0.21
TP eff (mg·L <sup>-1</sup> )	6.84	6.39	4.98	2.49	1.72	1.32	1.44	1.35
EQI (kg PU·d <sup>-1</sup> )	11678	11087	9421	6610	6011	5643	6450	6433
SP (kg Sludge·d <sup>-1</sup> )	2320	2369	2487	2854	2898	3006	2976	3025
AE (kWh·d <sup>-1</sup> )	4000	3580	3540	3756	3091	3292	2940	3065
ME (kWh·d <sup>-1</sup> )	660	812	823	802	975	968	1021	1018
PE (kWh·d <sup>-1</sup> )	432	432	330	432	493	432	538	432
EC (kg COD·d <sup>-1</sup> )	0	0	0	705	0	253	0	123
OCI (-)	16694	16670	17129	21376	19048	20480	19379	20009
TIV N-NH <sub>4</sub> <sup>+</sup> (%)	1.30	0.62	0.94	1.22	0.46	1.67	5.71	7.29
TIV TN (%)	0.08	0	0	0	0.04	0.06	0.07	0.08
TIV TP (%)	100	100	100	73	34	9	19	11

Regarding DF3, it presented the lowest discriminant capacity (1.93%) but a proper separation of the control strategies was obtained when combined with DF1 (Figure 7.16, down) showing a correlation between the ammonium cascade control setpoints and the P-removal efficiency: i) C6-C7: setpoint of  $3.0 \text{ mg NH}_4^+ \cdot \text{N} \cdot \text{L}^{-1}$  resulted in the lowest P effluent; ii) C4-C5: setpoint of  $1.5 \text{ mg NH}_4^+ \cdot \text{N} \cdot \text{L}^{-1}$  also favoured EBPR but to a lesser degree and; iii) C0-C3: no ammonium nitrogen control resulted in the highest P effluent content. Looking at the results, they were in agreement with the DA1 observations that suggested that P-removal was more affected by plant operation and not so much by the configuration.

## 7.4. Practical Implications

---

The inclusion of nitrite allows a better description of N removal in systems with low aeration because partial nitrification to nitrite can be predicted. Moreover, inclusion of nitrite allows a better accounting of the organic matter needed to denitrify (i.e. denitrification requires less COD than total denitrification), which enables a better description and understanding of the competition between PAO and OHO for the carbon source, especially in systems with carbon shortage. Moreover, the nitrite inclusion in the model could be very useful at predicting some possible EBPR failures since free nitrous acid (the protonated form of nitrite) is a strong inhibitor of PAO metabolisms (Zhou *et al.*, 2007; Pijuan *et al.* 2010).

The limited reactive settler approach with a global efficiency factor (0.25) allowed a more realistic description of the settling process in terms of biological reaction rates that can be achieved in settlers (around 17% of the total denitrification of the system occurred in the settler). If the assumption of a reactive settler model is not considered, the real denitrifying capacity of the system is not reflected and a false EBPR failure could be predicted (anaerobic  $\text{NO}_x$  load is overestimated). Otherwise, non limiting the reactive settler due to diffusion limitation could result in unrealistically high denitrification rates. In addition, the consideration of reactive settler gains importance in systems with high biomass content because of the higher reactivity of the settler. On the contrary, in systems with low biomass content, only physical processes may be used to simulate settling phenomena.

The  $\text{NO}_x$  presence under anaerobic conditions played an important role on EBPR performance for the different plant configurations. Therefore, those configurations that reduced the  $\text{NO}_x$  in the inlet to the anaerobic reactor resulted in the highest TP removal (MUCT and JHB) while in the rest, OHO denitrification was favoured instead of EBPR.

Finally, the results presented by DA established a comparative basis between plant configurations or control strategies under many different criteria that can be used in future research studies. In this sense, the information extracted from DA can be used for process engineers and other wastewater professionals to quickly analyse a high number of alternatives and select the most efficient ones in view of optimal design/operation of BNR systems. It is important to note that the operational limits of each configuration were not



presented in this study. Hence, the next research step could be conducted to establish the optimal reactor volumes as well as the optimal recycle streams for each configuration or the setpoint optimisation for the different control strategies, since they have been reported as promising alternatives to improve WWTP operation (Rivas *et al.*, 2008; Benedetti *et al.*, 2010; Chen *et al.*, 2014).

## 7.5. Conclusions

---

The improvement provided by the nitrite inclusion in the ASM2d model was clearly demonstrated, avoiding the prediction of N removal failure in systems with low aeration. Diffusion-limited reactive settler model also allowed a more realistic description of the settling process and thus, the settler reactivity was not overestimated. Regarding the effect of the plant configurations on biological C/N/P removal, the highest biological P removal was obtained for JHB and MUCT (65% and 55%, respectively). UCT and BDP-5-stage configurations resulted in the lowest TP removal because high amounts of  $\text{NO}_x$  entered the anaerobic zone, favouring OHO denitrification instead of EBPR. The  $\text{A}^2/\text{O}$  configuration resulted in the best option when an external carbon source was added to meet discharge P limits due to it resulted in low effluent TP and TN (low EQI) without excessive carbon addition (low OCI).

DA was demonstrated to facilitate enormously the interpretation and selection of the best operational scenario among 32 WWTPs (four configurations and eight control strategies) according to 16 criteria. After DA application, it was observed the location of anaerobic/anoxic/aerobic phases and the number/type of recycle streams had a major impact on the plant denitrification capacity (independently of the controller). On the other hand, aeration patterns, recirculation flow rates and the carbon/m ratio in the influent mainly influenced the overall EBPR efficiency (independently of the plant configuration).



## **CHAPTER VIII**

### **A novel control strategy for efficient biological phosphorus removal with carbon-limited wastewaters: Benchmarking studies II**

Part of this chapter has been published as:

Guerrero, J., Guisasola, A., Baeza, J.A., 2014. A novel control strategy for efficient biological phosphorus removal with carbon-limited wastewaters. *Water Science and Technology*. *In press*



---

### **Abstract**

*This chapter shows the development and the in silico evaluation of a novel control strategy aiming at successful biological phosphorus removal in a WWTP operating in an A<sup>2</sup>/O configuration with carbon-limited influent. The principle of this novel approach is that phosphorus in the effluent can be controlled with the nitrate setpoint in the anoxic reactor as manipulated variable. The theoretical background behind this control strategy is that lowering nitrate entrance to the anoxic reactor would result in more organic matter available for biological phosphorus removal. Thus, phosphorus removal would be enhanced at the expense of increasing nitrate in the effluent (but always below legal limits). The work shows the control development, tuning and performance of this novel control strategy in comparison to open-loop conditions and to two other conventional control strategies for phosphorus removal based on organic matter and metal addition. It is shown that the novel proposed strategy achieves positive nutrient removal results with similar operational costs to the other control strategies and open-loop operation.*

---

## **8.1. Motivations**

A deficient volatile fatty acids (VFAs) concentration in some municipal wastewaters hinders accomplishing simultaneous nitrogen (N) and phosphorus (P) removal in wastewater treatment plants (WWTPs). When low VFA content is observed but enough COD is available, the fermentation of complex organic matter in the anaerobic reactor plays an important role in view of achieving enhanced biological phosphorus removal (EBPR). As an example, Tuncal *et al.* (2009) observed that the fermentation of settled particulate COD in anaerobic phase resulted in high N and P removal in a full-scale WWTP where the primary settling was suppressed. If not only the VFA content is deficient but also the total organic substrate, the addition of an extra carbon source or a chemical for P precipitation (Makinia *et al.*, 2012; Bertanza *et al.*, 2013) are widely used technical solutions to cope with successful P removal but at the expenses of increasing the plant operational costs and the carbon footprint of the plant (Yuan *et al.*, 2010). Hence, finding an alternative solution to somehow produce VFA from complex COD fraction in wastewater with carbon-shortage deserves more attention. In this sense, the application of novel control strategies could be a promising alternative to favour P-removal in systems under adverse conditions for PAO growth. However, few studies have reported the development of new control structures with a particular emphasis in controlling effluent P (Gernaey *et al.*, 2002; 2004; Machado *et al.*, 2009b; Ostace *et al.*, 2013).

In this context, this chapter describes a model-based study about a novel control strategy to accomplish P removal legislation for WWTP with carbon limitations. This strategy was designed for its application in a conventional anaerobic/anoxic/aerobic (A<sup>2</sup>/O) WWTP for simultaneous C/N/P removal.

## 8.2. Material and Methods

### 8.2.1. WASTEWATER TREATMENT PLANT CONFIGURATION AND MATHEMATICAL MODEL

A benchmark A<sup>2</sup>/O WWTP was simulated for the theoretical development of the control strategy using an extension of the ASM2d model that also includes nitrite as state variable (see Chapter VII and Annex I). The WWTP consisted of two anaerobic reactors (ANAE1 and ANAE2, 1250 m<sup>3</sup> each), two anoxic reactors (ANOX1 and ANOX2, 1500 m<sup>3</sup> each) and three aerobic reactors (AER1, AER2 and AER3, 3000 m<sup>3</sup> each) with a total volume of 14500 m<sup>3</sup> (Figure 8.1). The settler was modelled using the 10-layer model of Takács *et al.* (1991) but including reactive capacity as in Chapter VII.

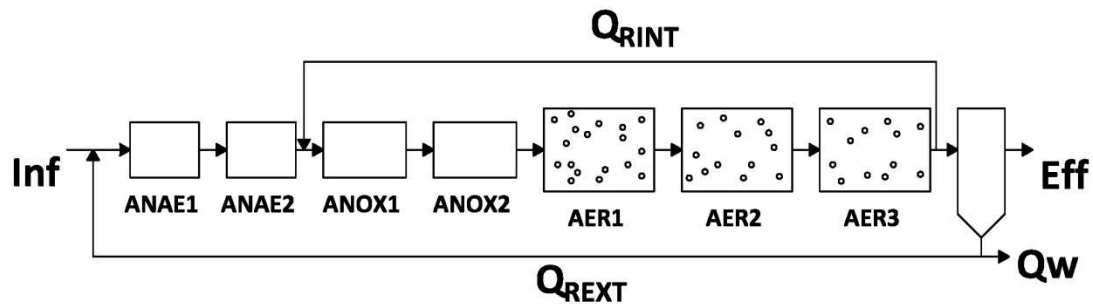


**Figure 8.1.** Simplified scheme of A<sup>2</sup>/O configuration for C/N/P removal. Inf: Influent and Eff: Effluent.

The influent wastewater used mimicked the yearly flow pattern (609 days) of an urban carbon-limited wastewater with low COD/P and low COD/N ratios (average values in mg·L<sup>-1</sup>: 240 COD, 20 N-NH<sub>4</sub><sup>+</sup>, 10 P-PO<sub>4</sub><sup>-3</sup>). The carbon source was considered mainly as X<sub>S</sub> (slowly biodegradable organic matter) in order to simulate the high content of complex organic substrate commonly present in urban wastewaters (Gernaey and Jørgensen, 2004). The influent flow rate average value was 20648 m<sup>3</sup>·d<sup>-1</sup> resulting in a hydraulic retention time (HRT) of 17 hours. In order to assess and compare the goodness of the control strategies, an open-loop scenario was defined where the internal recycle (Q<sub>RINT</sub>) and the external recycle (Q<sub>REXT</sub>) were set to 300% and 100% of the averaged influent flow rate, respectively. In Chapter VII, it was observed that the sludge waste flow rate (Q<sub>W</sub>) recommended in benchmarking for COD and N removal (Q<sub>W</sub> = 385 m<sup>3</sup>·d<sup>-1</sup>) was too low to obtain reasonable biological P removal. Then, Q<sub>W</sub> was fixed at 700 m<sup>3</sup>·d<sup>-1</sup> to maintain a sludge retention time (SRT) of 10 d as recommended to favour EBPR (Carrera *et al.*, 2001). The aeration in this open-loop scenario was assumed to be constant by fixing the global oxygen transfer coefficient in each aerobic reactor (k<sub>LA1</sub>, k<sub>LA2</sub> and k<sub>LA3</sub> values were set to 120, 120 and 60 d<sup>-1</sup>, respectively). For comparison purposes, only the last 364 days were used for evaluation. All simulations were preceded by steady state simulations according to benchmarking guidelines (Jeppsson *et al.*, 2007): 300 days under constant influent conditions with the average pollutant concentrations.

### 8.2.2. DESCRIPTION OF PLANT PERFORMANCE

Operational cost index (OCI) and effluent quality index (EQI) criteria were used, together with effluent nutrient concentrations, to evaluate the performance of the novel control strategy. Both indexes were calculated as described in Chapter VII (Equations 7.1 and 7.11).

### 8.2.3. PRINCIPLE OF THE CASCADE AND OVERRIDE P CONTROL STRATEGY (COPCS)

EBPR fails when the carbon source is more complex than VFA and/or nitrate enters in the anaerobic phase. As commented in Chapter V, the detrimental effect of nitrate was not to inhibit the P-release process itself but to prevent the fermentation for VFA production. Based on this concept, the principle of the proposed control strategy was: the effluent P (i.e. P concentration in the last aerobic reactor) can be controlled below its discharge limit ( $1.5 \text{ mg P-PO}_4^{-3} \cdot \text{L}^{-1}$  according to Gernaey and Jørgensen, 2004) with the nitrate setpoint in the anoxic reactor as the manipulated variable. Then, when effluent P is high, the nitrate setpoint in the anoxic phase should be lowered so that the extra anaerobic conditions allowed more COD fermentation to VFA favouring EBPR at the expense of less denitrification, but always respecting the TN legal limit ( $15 \text{ mg TN} \cdot \text{L}^{-1}$  according to Directive 91/271/EEC). The control strategy (Figures 8.2 and 8.3) was based on a cascade configuration with two proportional integral (PI) feedback control-loops and complemented with an override control to prevent excess of nitrate in the effluent:

- i) **Primary loop:** P was controlled in AER3 by manipulating the nitrate setpoint for ANOX2. The P setpoint chosen in AER3 was  $0.5 \text{ mg PO}_4^{-3} \cdot \text{L}^{-1}$  and nitrate setpoint ranged from 0.1 to  $1.0 \text{ mg N-NO}_3^{-} \cdot \text{L}^{-1}$ .
- ii) **Secondary loop:** Nitrate was controlled in ANOX2 by manipulating the  $Q_{\text{RINT}}$ . The controller parameters were fixed according to Gernaey and Jørgensen (2004).
- iii) **Override loop:** When nitrate concentration in AER3 was higher than  $13 \text{ mg N-NO}_3^{-} \cdot \text{L}^{-1}$ , the primary loop was deactivated and a default setpoint of  $1 \text{ mg N-NO}_3^{-} \cdot \text{L}^{-1}$  for nitrate in ANOX2 was established for the secondary loop.

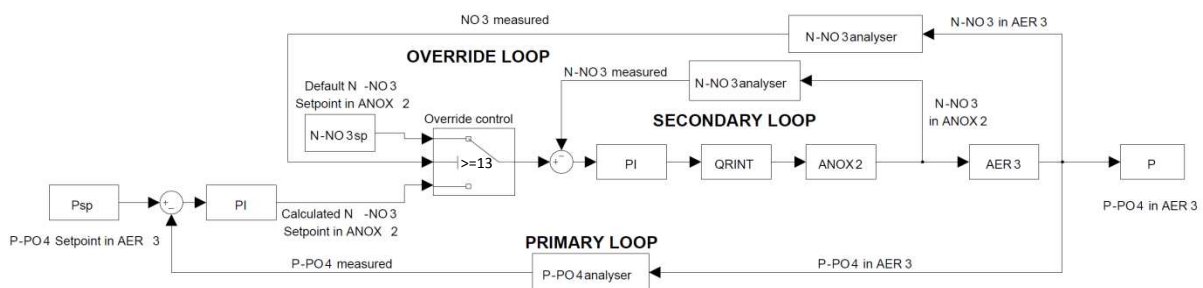


**Figure 8.2** Block diagram of the proposed control strategy for P removal.

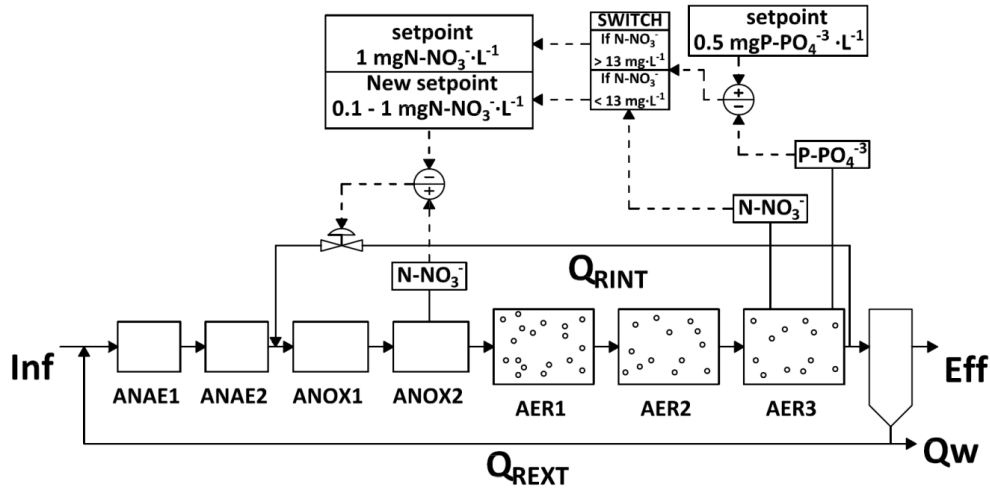


**Figure 8.3** Scheme of the proposed COPCS for P removal. Dashed lines represent the measured variables and control actions involved in the control strategy.

The COPCS strategy aimed at favouring P removal by limiting the nitrate inlet into the anoxic reactors and thus, increasing the anaerobic volume of the plant. However, this decrease on the anoxic volume of the plant could result in higher total nitrogen (TN) levels in the effluent, since less nitrate would be denitrified. Therefore, an override control loop was also considered: the primary loop of the cascade control was disabled when nitrate concentration in the effluent was above  $13 \text{ mg N}\cdot\text{L}^{-3}$ . This value was selected for being a warning level below  $15 \text{ mg TN}\cdot\text{L}^{-1}$ , which is the legal limit for TN. In this scenario, only the secondary control loop was operative with a nitrate setpoint of  $1 \text{ mg N-NO}_3^-\cdot\text{L}^{-1}$ .  $\text{N-NO}_3^-$  was considered in the effluent instead of TN, since most of the effluent nitrogen was nitrate in our case.

The response delay and/or the signal noise were simulated according to principles reported by Rieger *et al.* (2003). Dissolved oxygen (DO) sensors were simulated as ideal, with no delay or noise, while  $\text{N-NO}_x$  sensors had a delay of 10 minutes and white, normally distributed, zero mean noise (standard deviation of  $0.1 \text{ mg}\cdot\text{L}^{-1}$ ). Differently to Chapter VII,  $\text{P-PO}_4^{3-}$  analyzer dynamics were also simulated, with the same characteristics of  $\text{N-NO}_x$  sensor, because it was the controlled variable in COPCS. In this case, a measurement frequency of 5 minutes was considered for P analyser.

#### 8.2.4. CONVENTIONAL CONTROL LOOPS ON BENCHMARKING STUDIES FOR P REMOVAL

Two conventional control loops proposed for controlling phosphate in benchmarking studies (Table 8.1) were also implemented and compared with the COPCS performance and with the open-loop operation: i) CARBCS: External carbon addition ( $Q_{\text{CARB}}$ ) in ANAE1 to favour biological P removal (Olsson *et al.*, 2005) ii) METCS: Metal addition ( $Q_{\text{MET}}$ ) in AER3 to precipitate P (Germaey *et al.*, 2002). For all the control loops tested, DO was also controlled at  $2 \text{ mg DO}\cdot\text{L}^{-1}$  in AER2 by  $k_{\text{La}1}$  and  $k_{\text{La}2}$  manipulation and  $1 \text{ mg DO}\cdot\text{L}^{-1}$  in AER3 by  $k_{\text{La}3}$  manipulation (Nopens *et al.*, 2010).



**Table 8.1** Characteristics of reported control strategies for controlling effluent P concentration.

	CARBCS	METCS
Controlled variable	P-PO <sub>4</sub> <sup>-3</sup> in AER3	P-PO <sub>4</sub> <sup>-3</sup> in AER3
Setpoint	0.5 mg P · L <sup>-1</sup>	0.5 mg P · L <sup>-1</sup>
Manipulated variable	Q <sub>CARB</sub> in ANAE 1	Q <sub>MET</sub> in AER3
Maximum addition	5 m <sup>3</sup> ·d <sup>-1</sup>	3 m <sup>3</sup> ·d <sup>-1</sup>
Control algorithm	PI	PI
Objective	Favouring EBPR activity	P precipitation

## 8.3. Results and Discussion

### 8.3.1. COPCS TUNING

The controller parameters were optimised according to different textbook tuning methods (Stephanopoulos, 1984): Integral Absolute value of Error (IAE), Integral of the Time-weighted Absolute value of Error (ITAE), Integral of the Square Error (ISE) and Integral of the Time-weighted Square Error (ITSE). An influent of 90 days with a constant flow rate (20648 m<sup>3</sup>·d<sup>-1</sup>) but with step changes in ammonium (20 to 25 mg N·L<sup>-1</sup>), phosphate (10 to 13 mg P·L<sup>-1</sup>) and organic matter (240 to 200 mg COD·L<sup>-1</sup>) concentrations was used. As figure 8.4 shows, all tuning methods properly controlled the effluent P concentration around the setpoint value (0.5 mgP-PO<sub>4</sub><sup>-3</sup>·L<sup>-1</sup>). Among all, IAE criterion was selected because it resulted in the most robust control response since i) the setpoint was reached fast after COPCS activation (Figure 8.4B) and ii) the response observed after step changes was the least oscillatory (Figure 8.4C). The optimised controller parameter values were:  $K_c = 0.35 \text{ mg N-NO}_3^- \cdot \text{L}^{-1} \cdot (\text{mg P-PO}_4^{-3} \cdot \text{L}^{-1})^{-1}$  and  $\tau_i = 0.24 \text{ days}$ , where  $K_c$  is the proportional gain and  $\tau_i$  the integral time constant.

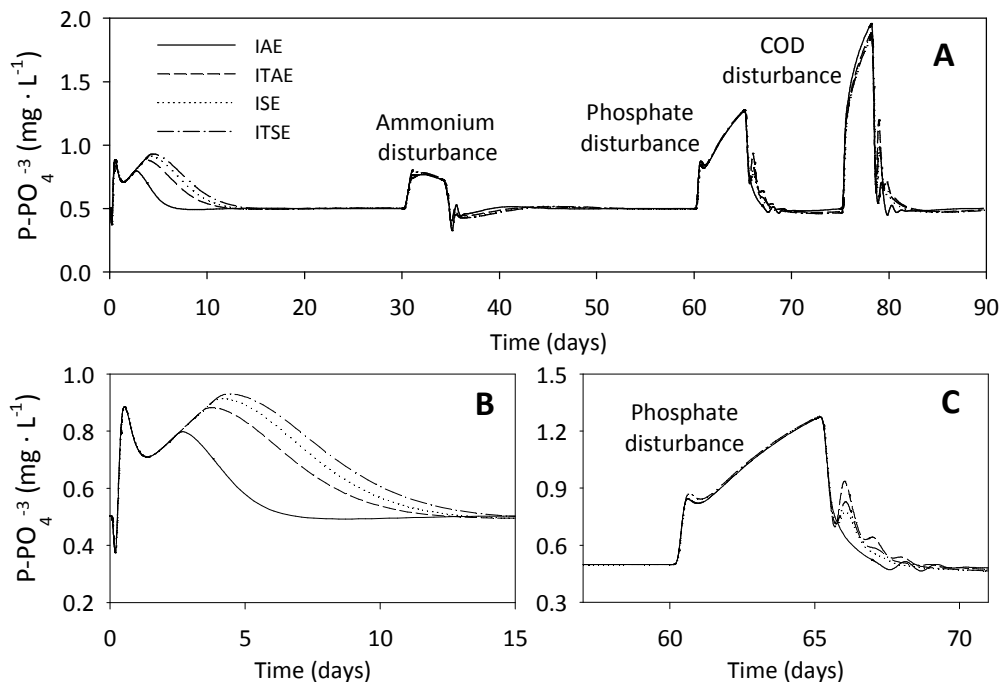


**Figure 8.4** Optimised response of COPCS for the different tuning methods tested. A: P effluent behaviour for the three step changes. B: Zoom for P effluent during COPCS activation. C: Zoom for P effluent during phosphate disturbance.

### 8.3.2. COPCS PERFORMANCE

Figure 8.5 and table 8.2 compare the COPCS performance to the open-loop conditions. P-removal capacity increased when COPCS was implemented (i.e. effluent P decreased around 54%). The higher anaerobic fraction of the plant obtained by reducing  $Q_{RINT}$  flow rate (Figure 8.5D) favoured complex carbon source fermentation to more readily biodegradable components (mainly VFA), which are preferred substrates in the EBPR process. On the contrary, effluent P during open-loop operation was above the discharge limit ( $1.50 \text{ mg P} \cdot \text{L}^{-1}$ ) because the low COD entering to the plant was preferentially oxidised via denitrification with the nitrate brought by the  $Q_{REXT}$  or  $Q_{RINT}$  rather than via EBPR, contrary to COPCS. As an overall result, the EBPR process was highly favoured when implementing COPCS at the expense of increasing the effluent TN concentration (15.6%) but always keeping it below the legal discharge limit ( $15 \text{ mg TN} \cdot \text{L}^{-1}$ ). If stricter discharge limits had been considered, for example  $10 \text{ mg N} \cdot \text{L}^{-1}$  according to the Council Directive 91/271/EEC, COPCS would have also resulted in an effluent TN that would be below the limit most of the time (Figure 8.5B).

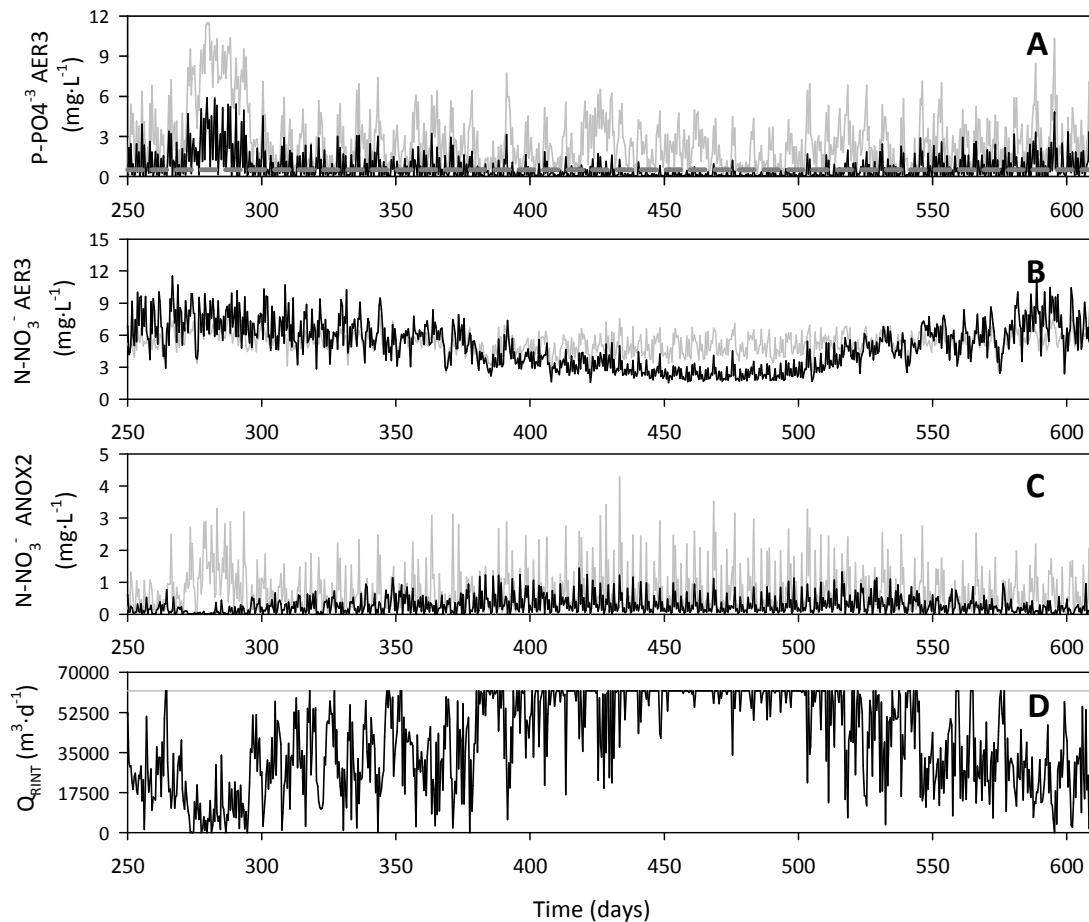


**Figure 8.5** Comparison between open-loop and COPCS performance. Grey lines represent to open-loop results, black lines the COPCS results and dashed line the  $\text{P-PO}_4^{-3}$  setpoint in AER3 for COPCS.

**Table 8.2** Nutrient averaged effluent concentrations (364 days) for the operational scenarios.

	Effluent concentrations (mg·L <sup>-1</sup> )				EQI (kg PU·d <sup>-1</sup> )
	N-NH <sub>4</sub> <sup>+</sup>	TN	P-PO <sub>4</sub> <sup>3-</sup>	TP	
<b>Open-loop</b>	1.32	7.63	2.49	3.27	7101
<b>CARBCS</b>	1.65	7.14	0.34	1.24	5139
<b>METCS</b>	2.23	7.77	0.31	1.25	5498
<b>COPCS</b>	2.06	9.04	0.61	1.51	6241

The COPCS was also compared to two other typical control strategies aiming at improving P removal: addition of external carbon source in the anaerobic reactor (CARBCS) and addition of metal for P precipitation in the aerobic reactor (METCS). Table 8.2 also shows the yearly averaged (364 days) effluent concentrations for these control strategies. When CARBCS or METCS were implemented, phosphate in AER3 rapidly decreased to the setpoint value (0.50 mg P·L<sup>-1</sup>) resulting in effluent P concentrations below the discharge limit for both cases (Table 8.2). However, these control loops were based on external dosages and, thus, they increased operational costs. Figure 8.6 shows the operational cost distribution of each control strategy according to Alex *et al.* (2008). The sludge production costs represented the main contribution to OCI (around 85%) because a high purge flow ( $Q_w$ ) was selected (700 m<sup>3</sup>·d<sup>-1</sup>) to guarantee high P removal. As expected, CARBCS resulted in the highest sludge production because the additional carbon source favoured the PAO growth (it was observed that  $X_{PAO}$  and  $X_{PP}$  values, which represented PAO biomass and poly-P content in the model, increased with the open-loop results). Moreover, not all the extra COD was consumed in the anaerobic or anoxic reactors and it arrived to the aerobic phase increasing the aeration energy invested and the aeration costs.

On the contrary, unexpectedly, METCS did not result in higher sludge production in comparison with open-loop results, although P precipitation was performed. Most of the particulate compounds concentrations were similar in both cases, except for P particulate compounds in the sludge (poly-P or P-precipitates). Hence, the nature of those compounds seems to be the key to explain this fact. For open-loop operation most of P in the sludge was present as poly-P, which can be converted to total suspended solids (TSS) assuming that 1.0 g of poly-P is equivalent to 3.11 g of TSS according to ASM2d stoichiometry (Henze *et al.*, 2000). For METCS, the main P compound in the sludge was metal-P which is equivalent to 0.3 g of TSS per 1.0 g of metal-P. This low value for metal-P is explained because it is considered that the P-precipitates are highly hydrated. Therefore, although less poly-P was obtained during open-loop operation in comparison with metal-P for METCS, both scenarios resulted in similar sludge TSS production.

For COPCS results, the novel control strategy reached the desired effluent P concentration (Table 8.2) without any external mass input, which resulted in lower operational costs than

CARBCS or METCS. As was stated before, the COPCS favoured EBPR at expenses of slightly worsening N removal via denitrification and thus, obtaining higher TN effluent in comparison with CARBCS or METCS. On the other hand, its higher EQI value with respect to CARBCS or METCS led to lower OCI because, among other reasons, less energy was invested in pumping (20% lower) to recycle nitrate to the anoxic reactors (i.e. COPCS manipulated  $Q_{RINT}$  to achieve nitrate setpoint in the anoxic reactors). COPCS also resulted in higher sludge production similarly to CARBCS. The higher amount of PAO and poly-P present in the sludge, due to the EBPR activity, can also explain these results. Compared to the open-loop scenario, similar OCI with lower EQI values were obtained for COPCS proving that the novel control strategy was able to improve P removal capacity of an existing plant (open-loop operation) with a low impact in the costs (< 1%). This was one of the main achievements of this study.

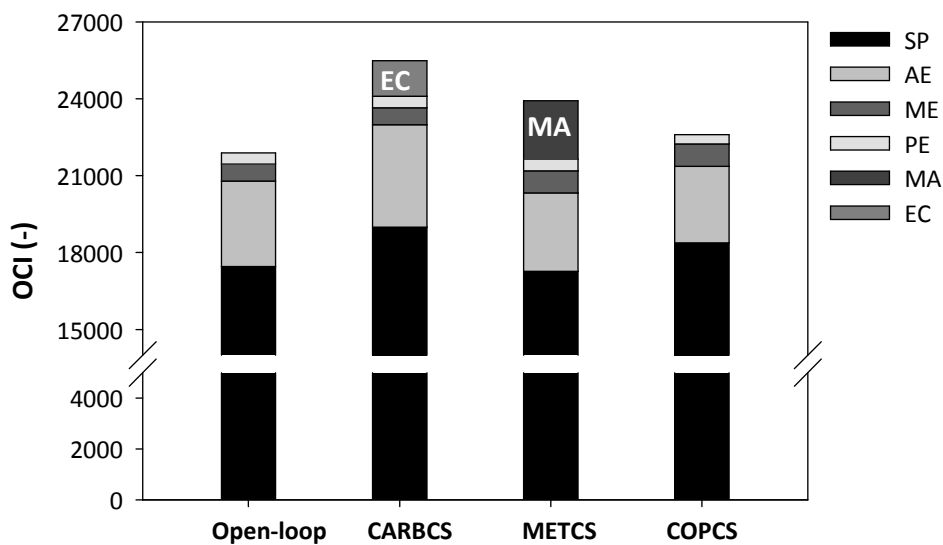


**Figure 8.6** Operational costs index (OCI) for the different control loops implemented. SP: Sludge production; AE: Aeration energy; ME: Mixing energy; PE: Pumping energy; MA: Metal addition; EC: External carbon addition.

Extra simulations were also performed to compare the three control strategies when resulting in similar EQI values (differences lower than 10%). A limitation of maximum external carbon and metal dosage was necessary for CARBCS and METCS, respectively (e.g. maximum carbon addition was reduced from 5.0 to 0.75  $\text{m}^3 \cdot \text{d}^{-1}$  for CARBCS and the metal addition in METCS from 3.0 to 0.75  $\text{m}^3 \cdot \text{d}^{-1}$ ). Table 8.3 shows the EQI values and figure 8.7 the OCI obtained for each control strategy. In this new scenario, similar EQI values resulted in similar OCI results. Hence, it can be concluded that the implementation of COPCS could be as efficient as other conventional control strategies used to control and improve P-removal, but without the need to add external carbon source or metal salts.

**Table 8.3** Nutrient averaged effluent concentrations (364 days) for the operational scenarios when limiting carbon and metal addition.

	Effluent concentration (mg·L <sup>-1</sup> )				
	N-NH <sub>4</sub> <sup>+</sup>	TN	P-PO <sub>4</sub> <sup>3-</sup>	TP	EQI
<b>Open-loop</b>	1.32	7.63	2.49	3.27	7101
<b>CARBCS</b>	2.87	8.02	0.50	1.40	5946
<b>METCS</b>	2.54	8.08	0.61	1.52	5703
<b>COPCS</b>	2.06	9.04	0.61	1.51	6241

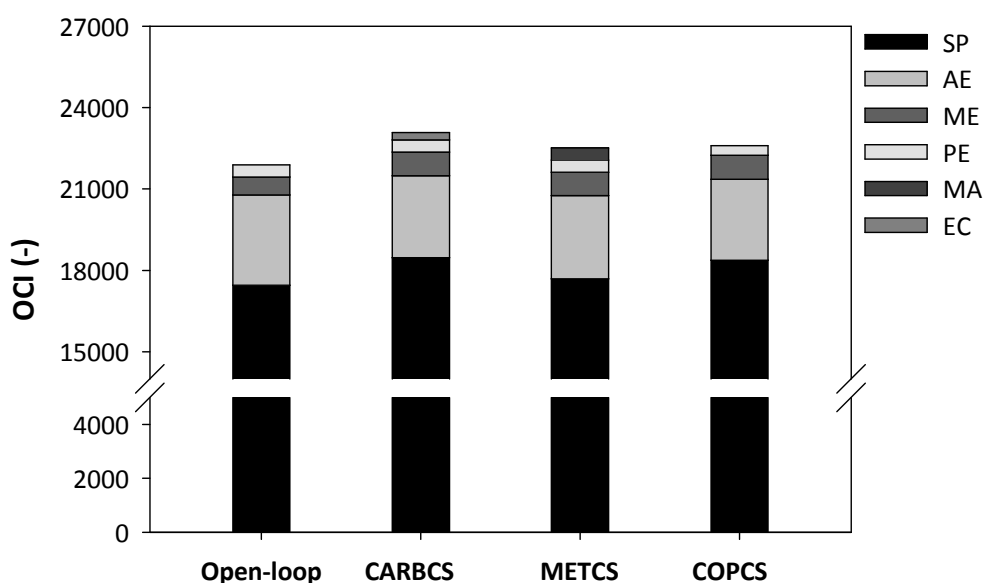


**Figure 8.7** Operational costs index (OCI) for the different control loops implemented when CARBCS and METCS actuation were limited. SP: Sludge production; AE: Aeration energy; ME: Mixing energy; PE: Pumping energy; MA: Metal addition; EC: External carbon addition.

Future research could be conducted on combining COPCS with some other control-loops (e.g. ammonium cascade control loop) and on setpoint optimisation in view of reducing even more the operational costs with lower effluent discharges.

## 8.4. Practical Implications

This study only considers the water line so, before full-scale implementation, further research would be necessary on plant-wide simulations integrating the sludge line. With high EBPR activity, part of the P from the sludge could be resolubilised during anaerobic digestion, which would be then recycled to the activated sludge line increasing the total influent P load. If part of the P-removal came from METCS, less P would be recycled to the plant inlet since P-precipitation products are highly insoluble. On the other hand, CARBCS would have high possibilities to sort out the problem by increasing carbon dosage. Despite

the worth of COPCS is not clear *a priori*, the good results obtained suggest that proper bio-P removal would also be achieved. In this sense, the inclusion of VFA production via pre-fermentation of the sludge settled in the primary decanter (Ribes *et al.*, 2002) should be also considered because it would favour EBPR and, thus, it would reduce the control requirements (i.e. lower carbon or metal addition) in VFA-limited scenarios.

The full-scale implementation of COPCS does not require the addition of chemicals, avoiding some issues such as chemicals purchase or storage of, in some cases, toxic products (ferric chloride for METCS) or corrosive products (acetic acid for CARBCS). In addition, not using an external carbon source in COPCS would also reduce the plant carbon footprint (Yuan *et al.*, 2010) and not using metal dosage would avoid an increase of inorganic compounds in the sludge with the consequent problems during tertiary treatment (e.g. less methane production during anaerobic digestion).

Finally, the benefits of this strategy for low-COD wastewaters could be partially obtained in a non-automated WWTP by manually decreasing the  $Q_{\text{RINT}}$  when high P-effluent concentration is detected. This would decrease the amount of nitrate applied to the anoxic reactor, leading to more VFA production by fermentation of complex carbon sources and then higher PAO activity. However, the on line implementation would allow the adaptation of the WWTP operation to variable influent characteristics obtaining a more stable and reliable operation thanks to the benefits of automatic control.

## 8.5. Conclusions

---

A novel control strategy based on a cascade plus override control structure was proposed to enhance P removal for carbon-limited wastewaters in WWTP aiming at simultaneous C/N/P removal. This strategy allowed diverting the available COD to P removal by modifying the nitrate setpoint in the anoxic reactor of the slave control loop. When effluent P was high, the nitrate setpoint in the anoxic phase was decreased so that more COD was diverted to EBPR at the expense of less denitrification.

This strategy showed very good performance when compared to open-loop conditions and it was proved to be a proper alternative to other control strategies applied to low carbon strength systems as external carbon dosage or metal addition.

# **CHAPTER IX**

## General Conclusions





The overall results obtained in this thesis contributed to achieve their main objectives: a deeper understanding of the EBPR deterioration due to nitrate presence in the anaerobic phase, proposal of new approaches/alternatives to mitigate this issue and experimental assessment in view of real implementation. As an overview, the main achievements and conclusions that can be drawn from this thesis are next summarized:

- ✓ The influent COD content and the nature of the carbon source have been shown to be the key parameters to understand the competition for the carbon source between PAO and denitrifiers when nitrate is present in the anaerobic phase. When the organic substrate was mainly volatile fatty acids, nitrate did not inhibit EBPR and thus, PAO outcompeted ordinary heterotrophic organisms, even when treating wastewaters with carbon shortage. On the other hand, with more complex carbon sources (i.e. sucrose, starch or dairy wastewater), EBPR failed not due to a direct inhibition of P-release process itself by nitrate presence but because denitrification would be favoured against COD fermentation for the VFA production. However, it was also observed that PAO should be firstly acclimated to coexist with nitrate; otherwise nitrate could inhibit EBPR regardless of the nature of the carbon source.
- ✓ The optimisation of the conventional control loops existing in a WWTP can successfully improve the biological nutrient removal performance not only resulting in low operational costs but also ensuring low effluent discharges and low risk of developing microbiology-related failures due to solid separation problems (i.e. rising or bulking sludge). The optimisation procedure was also successful at enhancing P-removal although P measurement was not included in any specific control-loop. The inclusion of effluent P as an optimised criterion resulted in a set of optimum control setpoints (anoxic nitrate and aerobic ammonium concentrations) that decreased the nitrate load recycled to the anaerobic reactor and hence, its deleterious effect on EBPR.
- ✓ The use of multi-criteria and multivariate statistical tools was proved to be very useful when selecting the best plant configurations or control strategies for a specific scenario. The application of these techniques allowed highlighting the most important information from several alternatives taking into account many criteria. For multi-criteria optimisation, it was the first time that biological P-removal was linked to the prediction of microbial-related solids separation problems.
- ✓ The controlled dosage of crude glycerol, from biodiesel production, was demonstrated to be a successful and an economic alternative carbon source when preventing nitrate-driven EBPR failure in two different pilot plants ( $A^2/O$  and JHB). The control design procedure based on four steps (model-calibration, control-loop

construction, simulation of the control strategy performance under different scenarios and experimental validation) was proved to be efficient since it resulted in a simple PI feed-back control that properly controlled effluent P concentration below legal limits, even under high nitrate anaerobic inlet conditions. The developed model was also used to propose and study new modifications of the control structure to correct its weaknesses (e.g. control actuation delay). A feed-forward control or controlling anaerobic P concentration were proved as good alternatives to also reduce anaerobic nitrate presence.

- ✓ A novel control strategy for effluent P, that minimises the interactions between N-removal and EBPR processes, was successfully developed and *in silico* evaluated when treating an influent with carbon limitations. The philosophy of this novel approach was diverting the available COD to P-removal and not to denitrification process (i.e. higher effluent TN), but always below the discharge limits. Avoiding the addition of chemicals (external carbon source or P-precipitators) to control P concentration is one of the main advantages of this novel control strategy when compared with some other reported control strategies. Another advantage is related to the low increase on the running costs of its implementation, only 1% higher, compared to the costs during open-loop operation.
  
- ✓ The inclusion of new model extensions related to nitrification and denitrification processes in WWTP (i.e. two-step nitrification/denitrification or in-settler denitrifying capacity) have to be considered for a better description of the interactions between N removal and EBPR in certain scenarios where nitrite plays a significant role. Otherwise, inaccurate models would be obtained that may predict unrealistic EBPR failures.

## **REFERENCES**



**A**hn, J., Daidou, T., Tsuneda, S., Hirata, A., 2001. Metabolic behavior of denitrifying polyphosphate-accumulating organisms under nitrate and nitrite electron acceptor. *J. Biosci. Bioeng.* 92, 442-446.

Ahn, J.H., Kim, S., Park, H., Rahm, B., Pagilla, K., Chandran, K., 2010. N<sub>2</sub>O emissions from activate sludge processes, 2008-2009: results of a National Monitoring Survey in the United States. *Environ. Sci. Technol.* 44(12), 4505-4511.

Akin, B., Ugurlu, A., 2004. The effect of an anoxic zone on biological phosphorus uptake by a sequential batch reactor. *Bioresource Technol.* 94, 1-7.

Akunna, J.C., Bizeau, C., Moletta, R., 1993. Nitrate and nitrite reductions with anaerobic sludge using various carbon sources: glucose, glycerol, acetic acid, lactic acid and methanol. *Water Res.* 27 (8), 1303-1312.

Alex, J., Benedetti, L., Copp, J., Gernaey, K.V., Jeppsson, U., Nopens, I., Pons, M.N., Rosen C., Steyer, J.P., Vanrolleghem, P., Winkler, S., 2008. Benchmark Simulation Model no.1 (BSM1). Tech. Report no. LUTEDX/(TEIE-7229)/1-62/(2008).

Alley, R., Berntsen, T., Bindoff, N.L., Chen, Z., Chidthaisong, A., Friedlingstein, P., Gregory, J., Hegerl, G., Heimann, M., Hewitson, B., others. 2007. Climate change 2007: The physical science basis. Summary for policy makers. Fourth Assessment Report of the Intergovernment Panel on Climate Change.

Amann, R.I., 1995. *In situ* identification of microorganisms by whole cell hybridization with RNA-targeted nucleic acid probes. In: Ackermans ADL, van Elsas JD, de Bruijn FJ, editors. *Molecular Microbial Ecology Manual*. Dordrecht, Holland: Kluwer Academic Publications.

Anthonisen, A.C., Loehr, R.C., Prakasam, T.B.S., Srinath, E.G., 1976. Inhibition of nitrification by ammonia and nitrous acid. *J. Water Pollut. Con. F.* 48(5), 835-852.

APHA, 1995. Standard methods for the examination of water and wastewater, 19<sup>th</sup> ed., American Publishers Health Association, Washington, DC, USA.

Appeldoorn, K.J., Kortstee, J.J., Zehnder, A.J.B., 1992. Biological phosphate removal by activated sludge under defined conditions. *Water Res.* 26, 453-460.

Arden, E., Lockett, W.T., 1914. Experiments on the oxidation of sewage without the aid of filters. *J. Soc. Chem. Ind-L.* 33, 523-539.

Artan, N., Tasli, R., Örgür N., Orhon, D., 1998. The fate of phosphate under anoxic conditions in biological nutrient removal activated sludge systems. *Biotechnol. Lett.* 20(11), 1085-1090.

Arun, V., Mino, T., Matsuo, T., 1988. Biological mechanism of acetate uptake mediated by carbohydrate consumption in excess phosphorus removal systems. *Water Res.* 22(5), 565-572.

Aslan, S., Dahab, M., 2008. Nitrification and denitrification of ammonium-rich wastewater using fluidized-bed biofilm reactors. *J. Hazard. Mater.* 156(1-3), 56- 63.

Ayasa, E., De la Sota, A., Grau, P., Sagarna, J.M., Salterain, A., Suescun, J., 2006. Supervisory control strategies for the new WWTP of Galindo-Bilbao: the long run from the conceptual design to the full-scale experimental validation. *Water Sci. Technol.* 53(4-5), 193-201.

**B**aeza, J., 1999. Development and implementation of a supervisory system for the management and control of WWTPs (in Spanish). PhD Thesis. UAB. Bellaterra.

- Baeza, J.A., Gabriel, D., Lafuente, J., 1999. An expert supervisory system for pilot WWTP. *Environ. Modell. Softw.* 14, 383-390.
- Baeza, J.A., Gabriel, D., Lafuente, J., 2002. Improving the nitrogen removal efficiency of an A<sup>2</sup>/O based WWTP by using on-line Knowledge Based Expert System. *Water Res.* 36, 2109-2123.
- Barnard, J.L., 1976. Nutrient removal in biological systems. *Water Pollut. Control* 74(2), 143-154.
- Bartoli, A., Perez, J., Carrera, J., 2010. Applying ratio control in a continuous granular reactor to achieve full nitrification under stable operating conditions. *Environ. Sci. Technol.* 44(23), 8930-8935.
- Bassin, J.P., Kleerebezem, R., Dezotti, M., van Loosdrecht, M.C.M., 2012. Simultaneous nitrogen and phosphate removal in aerobic granular sludge reactor operated at different temperatures. *Water Res.* 46, 3805-3816.
- Batchelor, B., Lawrence, A.W., 1978. A kinetic model for autotrophic denitrification using elemental sulfur. *Water Res.* 12, 1075-1084.
- Batstone, D.J., Keller, J., Angelidaki, I., Kalyuzhnyi, S.V., Pavlostathis, S.G., Rozzi, A., Sanders, W.T.M., Siegrist, H., Vavilin, V.A., 2002. The IWA Anaerobic Digestion Model No 1 (ADM1). *Water Sci. Technol.* 45(10), 65-73.
- Battistoni, P., Angelis, A.D., Prisciandaro, M., Boccadoro, R., Bolzonella, D., 2002. P removal from anaerobic supernatants by struvite crystallization: long term validation and process modelling. *Water Res.* 36, 1927-1938.
- Bellmann, R., Zadeh, L.A., 1970. Decision-making in a fuzzy environment. *Manage. Sci.* 17, 141-164.
- Benedetti, L., De Baets, B., Nopens, I., Vanrolleghem, P.A., 2010. Multi-criteria analysis of wastewater treatment plant design and control scenarios under uncertainty. *Environ. Modell. Softw.* 25, 616-621.
- Bertanza, G., Pedrazzani, R., Manili, L., Menoni, L., 2013. Bio-P release in the final clarifiers of a large WWTP with co-precipitation: Key factors and troubleshooting. *Chem. Eng. J.* 230, 195-201.
- Bodík, I., Blstáková, A., Sedláček, S., Hutnan, M., 2009. Biodiesel waste as source of organic carbon for municipal WWTP denitrification. *Bioresource Technol.* 100 (8), 2452-2456.
- Bond, P.L., Hugenholtz, P., Keller, J., Blackall, L.L., 1995. Bacterial community structures of phosphate-removing and non-phosphate-removing activated sludges from sequencing batch reactors. *Appl. Environ. Microb.* 61(5), 1910-1916.
- Bond, P. L., Erhart, R., Wagner, M., Keller, J., Blackall, L.L., Keller, R.G., 1999. Identification of some of the major groups of bacteria in efficient and nonefficient biological phosphorus removal activated sludge systems. *Appl. Environ. Microb.* 65(9), 4077-4084.
- Bougard, D., Bernet, N., Cheneby, D., Delgenes, J.P., 2006. Nitrification of a highstrength wastewater in an inverse turbulent bed reactor: Effect of temperature on nitrite accumulation. *Process Biochem.* 41(1), 106-113.
- Brdjanovic, D., Slamet, A., van Loosdrecht, M.C.M., Hooijmans, C.M., Alaerts, G. J., Heijnen, J.J., 1998. Impact of excessive aeration on Biological phosphorus removal from wastewater. *Water Res.* 32(1), 200-208.
- Broughton, B., Pratt, S., Shilton, A., 2008. Enhanced biological phosphorus removal for high-strength wastewater with a low rBCOD: P ratio. *Bioresource Technol.* 99 (5), 1236-1241.
- Burow, L.C., Kong, Y.H., Nielsen, J.L., Blackall, L.L., Nielsen, P.H., 2007. Abundance and ecophysiology of *Defluviicoccus* spp., glycogen accumulating organisms in full-scale wastewater treatment processes. *Microbiology+* 153(1), 178-185.

- Carrera, J., Sarrà, M., Lafuente, F.J., Vicent, T., 2001. Effect of different operational parameters in the enhanced biological phosphorus removal process. Experimental design and results. *Environ. Technol.* 22, 1439-1446.
- Carrera, J., Baeza, J.A., Vicent, T., Lafuente, J., 2003. Biological nitrogen removal of high-strength ammonium industrial Wastewater with two-sludge system. *Water Res.* 37(7), 4211-4221.
- Carmango, J.A., Alonso, A., 2006. Ecological and toxicological effect of inorganic nitrogen pollution in aquatic ecosystems: A global assessment. *Environ. Int.* 32, 831-849.
- Carvalho, G., Lemos, P.C., Oehmen, A., Reis, A.M., 2007. Denitrifying phosphorus removal: Linking the process performance with the microbial community structure. *Water Res.* 41, 4383-4396.
- Cecil, D., Kozłowska, M. 2010. Software sensors are a real alternative to true sensors. *Environ. Modell. Softw.* 25, 622-625.
- Cech, J.S., Hartman, P., 1993. Competition between polyphosphate and polysaccharide accumulating bacteria in enhanced biological phosphate removal systems. *Water Res.* 27(7), 1219-1225.
- Chen, Y., Randall, A.A., McCue, T., 2004. The efficiency of enhanced biological phosphorus removal from real wastewater affected by different ratios of acetic to propionic acid. *Water Res.* 38(1), 27-36.
- Chen, W., Chonghua, Y., Lu, X., 2014. Optimal design activated sludge process by means of multi-objective optimisation: case study in BSM1. *Water Sci. Technol.* 69(10), 2052-2058.
- Chen, Y., Chen, Y.S., Xu, Q., Zhou, Q., Gu, G., 2005. Comparison between acclimated and unacclimated biomass affecting anaerobic-aerobic transformation in the biological removal of phosphorus. *Process Biochem.* 40(2), 723-732.
- Cho, E., Molof, A.H., 2004. Effect of sequentially combining methanol and acetic acid on the performance of biological nitrogen and phosphorus removal. *J. Environ. Manage.* 73, 183-187.
- Christensson, M., Lie, E., Welander, T., 1994. A comparison between ethanol and methanol as carbon-sources for denitrification. *Water Sci. Technol.*, 30 (6), 83-90.
- Chuang, S.H., Ouyang, C.F., Wang, Y.B., 1996. Kinetic competition between phosphorus release and denitrification on sludge under anoxic conditions. *Water Res.* 30 (12), 2961-2968.
- COM2012/670, 2012. River Basin Management plans. Report of the implementation of the Water Framework Directive (200/60/EC). European Commission. Brussels.
- Comas, J., Rodríguez-Roda, I., Gernaey, K.V., Rosen, C., Jeppsson, U., Poch, M., 2008. Risk assessment modelling of microbiology-related solids separation problems in activated sludge systems. *Environ. Modell. Softw.* 23 (10-11), 1250-1261.
- Comeau, Y., Hall, K.J., Hancock, R.E.W., Oldham, W.K., 1986. Biochemical model for enhanced biological phosphorus removal. *Water Res.* 20(12), 1511-1521.
- Copp, J.B., Spanjers, H., Vanrolleghem, P.A., 2002. *Respirometry in control of the activated sludge process: Benchmark control strategies.* Scientific and Technical Report nº 11; IWA Publishing, United Kingdom.
- Corominas, L., Flores-Alsina, X., Snip, L., Vanrolleghem, P.A., 2012. Comparison of different modelling approaches to better understand greenhouse gas emissions from wastewater treatment plants. *Biotechnol. Bioeng.* 109 (11), 2855-2863.

Crocetti, G.R., Hugenholtz, P., Bond, P.L., Schuler, A., Keller, J., Jenkins, D., Blackall, L.L., 2000. Identification of polyphosphate-accumulating organisms and design of 16S rRNA-directed probes for their detection and quantitation. *Appl. Environ. Microb.* 66(3), 1175-1182.

Crocetti, G.R., Banfield, J.F., Keller, J., Bond, P.L., Blackall, L.L., 2002. Glycogen-accumulating organisms in laboratory-scale and full-scale wastewater treatment processes. *Microbiology+* 148 (11), 3353-3364.

**D**aims, H., Brühl, A., Amann, R., Schleider, K.H., Wagner, M., 1999. The domain-specific probe EUB338 is insufficient for the detection of all bacteria: development and evaluation of a more comprehensive probe set. *Syst. Appl. Microbiol.* 22 (2), 434-444.

Dalmau, J., 2009. Knowledge-based modelling and simulation of operational problems of microbiological origin in wastewater treatment plants. PhD Thesis, Laboratory of Chemical and Environmental Engineering, Universitat de Girona. Girona, Spain.

Desloover, J., De Clippeleir, H., Boeckx, P., Du Laing, G., Colsen, J., Verstraete, W., Vlaeminck, S.E., 2011. Floc-based sequential partial nitrification and anammox at full scale with contrasting N<sub>2</sub>O emissions. *Water Res.* 45(9), 2811-2821.

Dochain, D., Vanrolleghem, P., 2001. *Dynamic modelling and estimation in wastewater treatment processes.* IWA Publishing, London.

Doherty, D., Freeman, M.A., Kumar, R., 2004. Optimization with Matlab and the Genetic Algorithm and Direct Search Toolbox. *MATLAB Digest* September 2004, available for download from <http://www.mathworks.com> (accessed 14<sup>th</sup> July 2009).

**E**lefsiniotis, P., Wareham, D.G., Smith, M.O., 2004. Use of volatile fatty acids from an acid-phase digester for denitrification. *J. Biotechnol.* 114(3), 289-297.

EPA, 1993. *Manual of nitrogen control.* Environmental Protection Agency, Washington D.C. (U.S.).

EPA, 2010. *Nutrient control design manual.* Environmental Protection Agency, Washington D.C. (U.S.).

Etter, B., Tilley, E., Khadka, R., Udert, M., 2011. Low-cost struvite production using source-separated urine in Nepal. *Water Res.* 45(2), 852-862.

**F**ajardo, C., Mosquera-Corral, A., Campos J.L., Méndez, R., 2012. Autotrophic denitrification with sulphide in a sequencing batch reactor. *J. Environ. Manage.* 113, 552-556.

Fang, F., Ni, B.J., Li, W.W., Sheng, G.P., Yu, H.Q. (2011) A simulation-based integrated approach to optimise the biological nutrient removal process in a full-scale wastewater treatment plant. *Chem. Eng. J.* 174(2-3), 635-643.

Fleming, G., van der Merwe, M., McFerren, G., 2007. Fuzzy expert systems and GIS for cholera health risk prediction in southern Africa. *Environ. Modell.Softw.* 22 (4), 442-448.

Flores, X., Comas, J., Roda, I.R., Jiménez, J., Gernaey, K.V., 2007. Application of multivariable statistical techniques in plant-wide WWTP control strategies analysis. *Water Sci. Technol.* 56(6), 75-83.

Flores-Alsina, X., Comas, J., Rodríguez Roda, I., Poch, M., Gernaey, K.V., Jeppsson, U., 2009a. Evaluation of plant-wide WWTP control strategies including the effects of filamentous bulking sludge. *Water Sci. Technol.* 60 (8), 2093-2103.



Flores-Alsina, X., Comas, J., Rodriguez-Roda, I., Gernaey, K.V., Rosen, C., 2009b. Including the effects of filamentous bulking sludge during the simulation of wastewater treatment plants using a risk assessment model. *Water Res.* 43 (18), 4527-4538.

Flores-Alsina, X., Gallego, A., Feijoo, G., Rodriguez-Roda, I., 2010. Multiple-objective evaluation of Wastewater treatment plant control alternatives. *J. Environ. Manage.* 91, 1193-1201.

Flores-Alsina, X., Gernaey, K.V., Jeppsson, U., 2012. Benchmarking biological nutrient removal in wastewater treatment plants: influence of mathematical model assumptions. *Water Sci. Technol.* 65(8), 1496-1505.

Flores-Alsina, X., Arnell, M., Amerlinck, Y., Corominas, L., Gernaey, K.V., Guo, L., Lindblom, E., Nopens, I., Porro, J., Shaw, A., Snip, L., Vanrolleghem, P., Jeppsson, U., 2014. Balancing effluent quality, economic cost and greenhouse gas emissions during the evaluation of (plant-wide) control/operational strategies in WWTPs. *Sci. Total Environ.* 466-467, 616-624.

Flowers, J., He, S., Yilmaz, S., Noguera, D., McMahon, K.D., 2009. Denitrification capabilities of two biological phosphorus removal sludges dominated by different 'Candidatus Accumulibacter' clades. *Environ. Microbiol. Rep.* 1 (6), 583-8.

Fuhs, G.W., Chen, M., 1975. Microbiological basis of phosphate removal in the activated sludge process for the treatment of wastewater. *Microb. Ecol.* 2(2), 119-138.

**G**abriel, D., 2000. Monitoring and modelling applied to the control of a pilot wastewater treatment plant with nutrient removal (in Catalan). PhD Thesis. UAB. Bellaterra.

Ganigué, R., Volcke, E.I.P., Puig, S., Balaguer, M.D., Colprim, J., 2012. Impact of influent characteristics on a partial nitrification SBR treating high nitrogen load wastewater. *Bioresource Technol.* 111, 62-69.

Gerber, A., Mostert, E.S., Winter, C.T., Villiers, R.H., 1986. The effect of acetate and other short-chain carbon compounds on the kinetics of biological nutrient removal. *Water S.A.* 12 (1) 7-12.

Gernaey, K., Mussati, M., Yuan, Z., Nielsen, M.K., Jørgensen, S.B., 2002. Control strategy evaluation for combined N and P removal using a benchmark wastewater treatment plant. In: *Proceedings of 15th IFAC World Congress for Automatic Control*. July 21-26, Barcelona, Spain.

Gernaey, K.V., Jørgensen, S.B., 2004. Benchmarking combined biological phosphorus and nitrogen removal wastewater treatment processes. *Control Eng. Pract.* 12(3), 357-373.

Gernaey, K.V., Jeppsson, U., Batstone, D.J., Ingildsen, P., 2005. Impact of reactive settler models on simulated WWTP performance. *Water Sci. Technol.* 53(1), 159-167.

Gernaey, K.V., Flores-Alsina, X., Rosen, C., Benedetti, L., Jeppsson, U., 2011. Dynamic influent pollutant disturbance scenario generation using a phenomenological modeling approach. *Environ. Modell. Softw.* 26 (11), 1255-1267.

Gernaey, K.V., Jeppsson, U., Vanrolleghem, P.A., Copp, J.B., Steyer, J-P., 2013. *Benchmarking of Control Strategies for Wastewater Treatment Plants*. IWA Scientific and Technical Report, IWA Publishing, London, UK. Publication date: 2013.

Gillot, S., De Clercq, B., Defour, D., Simoens, F., Gernaey, K.V., Vanrolleghem, P.A., 1999. Optimization of wastewater treatment plant design and operation using simulation and cost analysis. In: *Proceedings of 72<sup>nd</sup> Annual WEF Conference and Exposition*, New Orleans, USA, 9-13 October 1999.

- Grabinska-Loniewska, A., Slomczynski, T., Kanska, Z., 1985. Denitrification studies with glycerol as a carbon source. *Water Res.* 19 (12), 1471-1477.
- Grady, C.P.L., Daigger, G.T., Lim, H.C., 1999. *Biological wastewater treatment*. 2<sup>nd</sup> Ed. Marcel Dekker, New York.
- Griffiths, P.C., Stratton, H.M., Seviour, R.J., 2002. Environmental factors contributing to the “G bacteria” population in full-scale EBPR plants. *Water Sci. Technol.* 46(4-5), 185-192.
- Guerrero, J., Tayà, C., Guisasola, A., Baeza, J.A., 2012. Glycerol as a sole carbon source for enhanced biological phosphorus removal. *Water Res.* 46(9), 2983-2991.
- Guisasola, A., 2005. Modelling biological organic matter and nutrient removal processes from wastewater using respirometric and titrimetric techniques. PhD Thesis. UAB. Bellaterra.
- Guisasola, A., Baeza, J.A., Carrera, J., Sin, G., Vanrolleghem, P.A., Lafuente, J., 2006. The influence of the experimental data quality and quantity on parameter estimation accuracy: Andrews inhibition model as a case study. *Educ. Chem. Eng* 1(1), 139–145.
- Guisasola, A., Petzet, S., Baeza, J.A., Carrera, J., Lafuente, J., 2007a. Inorganic carbon limitations on nitrification: experimental assessment and modelling. *Water Res.* 41, 277–286.
- Guisasola, A., Vargas, M., Marcelino, M., Lafuente, J., Casas, C., Baeza, J.A., 2007b. On-line monitoring of the enhanced biological phosphorus removal processes using respirometry and titrimetry. *Biochem. Eng. J.* 35, 371-379.
- Guisasola, A., Qurie, M., Vargas, M.M., Casas, C., Baeza, J.A., 2009. Failure of an enriched nitrite-DPAO population to use nitrate as an electron acceptor. *Process Biochem.* 44, 689-695.
- H**air, J.Fr., Andersen, R.E., Tatham, R.L., Black, W.C., 1998. *Multivariate Data Analysis*, 5th ed. Prentice-Hall, London, UK.
- Hascoet, M.C., Florentz, M., 1985. Influence of nitrates on biological phosphorus removal from wastewater. *Water SA* 11, 1-8.
- Hallin, S., Rothman, M., Pell, M., 1996. Adaptation of denitrifying bacteria to acetate and methanol in activated sludge. *Water Res.* 30, 1445-1450.
- He, S., Gu, A.Z., McMahon, K.D., 2005. “The role of Rhodocyclus-like organisms in biological phosphorus removal: factors influencing population structure and activity” in WEFTEC.
- He, S., Gall, D.L., McMahon, K.D., 2007. “Candidatus Accumulibacter” population structure in enhanced biological phosphorus removal sludge as revealed by polyphosphate kinase genes. *Appl. Environ. Microb.* 73 (18), 5865-5874.
- Hellinga, C., Schellen, A.A.J.C., Mulder, J.W., Van Loosdrecht, M.C.M., Heijnen, J.J., 1998. The SHARON process: An innovative method for nitrogen removal from ammonium-rich waste water. *Water Sci. Technol.* 37(9), 135-142.
- Henze, M., Gujer, W., Mino, T., Matsuo, T., Wentzel, M.C., Marais, G.V.R., van Loosdrecht, M.C.M., 1999. Activated sludge model n<sup>o</sup> 2d, ASM2d. *Water Sci. Technol.* 39(1), 165-182.
- Henze, M., Gujer, W., Mino, T., van Loosdrecht, M.C.M., 2000. *Activated Sludge Models ASM1, ASM2, ASM2d, ASM3*, IWA Publishing, London.

Henze, M., van Loosdrecht, M.C.M., Ekama, G., Brdjanovic, D., 2008. Biological wastewater treatment. IWA Publishing London, 162-169. ISBN: 1843391880.

Hesselmann, R.P., Werlen, C., Hahn, D., van der Meer, J.R., Zehnder, A.J., 1999. Enrichment, phylogenetic analysis and detection of a bacterium that performs enhanced biological phosphate removal in activated sludge. *Syst. Appl. Microbiol.* 22(3), 454–65.

Hirasawa, I., Kaneko, S., Kanai, Y., Hosoya, S., Okuyama, K., Kamahara, T., 2002. Crystallization phenomena of magnesium ammonium phosphate (MAP) in a fluidized-bed-type crystallizer. *J. Cryst. Growth* 237–239, 2183–2187.

Hood, C.R., Randall, A.A., 2001. A biochemical hypothesis explaining the response of enhanced biological phosphorus removal biomass to organic substrates. *Water Res.* 35(11), 2758–66.

Huang, H., Chunlian, X., Zhang, W., 2011. Removal of nutrients from piggery wastewater using struvite precipitation and pyrogenation technology. *Bioresource Technol.* 102(3) 2523-2528.

Hwang, I.S., Min, K.S., Choi, E., Yun, Z., 2005. Nitrogen removal from piggery waste using the combined SHARON and ANAMMOX process. *Water Sci. Technol.* 52(10-11), 487-494.

Ingildsen, P., Rosen, C., Gernaey, K.V., Nielsen, M.K., Guildal, T., Jacobsen, B.N., 2005. Modelling and control strategy testing of biological and chemical removal at Avedore WWTP. *Water Sci. Technol.* 53(4-5), 105-113.

Isaacs, S.H., Henze, M., Sjøberg, H., Kummel, M., 1994. External carbon source addition as a means to control an activated sludge nutrient removal process. *Water Res.* 28, 511-520.

Isaacs, S.H., Henze, M., 1995. Controlled carbon source addition to an alternating nitrification-denitrification wastewater treatment process including biological P removal. *Water Res.* 29 (1), 77-89.

Isanta, E., Figueroa, M., Mosquera-Corral, A., Campos, L., Carrera, J., Pérez, J., 2013. A novel control strategy for enhancing biological N-removal in a granular sequencing batch reactor: A model-based study. *Chem. Eng. J.* 232, 468-477.

Jeemat, Z., Bartrolí, A., Isanta, E., Carrera, J., Suárez-Ojeda, M.E., Perez, J., 2013. Closed-loop control of ammonium concentration in nitritation: Convenient for reactor operation but also for modeling. *Bioresource Technol.* 123, 655-663.

Jenkins, J., Richard, M.G., Lim, H.C., 2003. Manual on the causes and control of activated sludge bulking, foaming & other solids separation problems, 3<sup>rd</sup> ed, IWA Publishing, London, UK.

Jeon, C.O., Park, J.M., 2000. Enhanced biological phosphorus removal in an anaerobic-aerobic sequencing batch reactor: characteristics of carbon metabolism. *Water Environ. Res.* 73(3), 295-300.

Jeppsson, U., 2005. Aeration and mixing energy for BSM1, BSM1\_LT and BSM2. Benchmark Internal Report September 2005, available for download from <http://benchmarkwwtp.org>

Jeppsson, U., Pons, M.N., Nopens, I., Alex, J., Copp, J.B., Gernaey, K.V., Rosen, C., Steyer, J.P., Vanrolleghem, P.A., 2007. Benchmark Simulation Model 2 – general protocol and exploratory case studies. *Water Sci. Technol.* 56 (8), 287-295.

Jianlong, W., Ning, Y., 2004. Partial nitrification under limited dissolved oxygen conditions. *Process Biochem.* 39, 1223-1229.

Johnson, R.A., Wichern, D.A., 1992. Applied Multivariate Statistical Analysis. Prentice-Hall International, Englewood Cliffs, NJ, USA.

Johnson, D.T., Taconi, K.A., 2007. The glycerin glut: options for the value-added conversion of crude glycerol resulting from biodiesel production. *Environ. Prog.* 26, 338-348.

Jones, P.H., Tadwalkar, A.D., Hsu, C.L., 1987. Enhanced uptake of phosphorus by activated sludge: effect of substrate addition. *Water Res.* 21, 301-308.

Jordaan, E.M., Ackerman, J., Cicek, N., 2010. Phosphorus removal from anaerobically digested swine wastewater through struvite precipitation. *Water Sci. Technol.* 61(12), 3228-3234.

Jubany, I., Carrera, J., Lafuente, J., Baeza, J.A., 2008. Start-up of a nitrification system with automatic control to treat highly concentrated ammonium wastewater: Experimental results and modeling. *Chem. Eng. J.* 144 (3), 407-419.

Jubany, I., Lafuente, J., Carrera, J., Baeza, J.A., 2009. Automated thresholding method (ATM) for biomass fraction determination using FISH and confocal microscopy. *J. Chem. Technol. Biot.* 84 (8), 1140-1145.

**K**ernn-Jespersen, J.P., Henze, M., 1993. Biological phosphorus uptake under anoxic and aerobic conditions. *Water Res.* 27, 617-624.

Kim, D.J., Lee, D.I., Kellet, J., 2006. Effect of temperature and free ammonia on nitrification and nitrite accumulation in landfill leachate and analysis of its nitrifying bacterial community by FISH. *Bioresource Technol.* 97(3), 459-468.

Koch, G., Pianta, R., Krebs, P., Siegrist, H., 1999. Potential of denitrification and solids removal in the rectangular clarifier. *Water Res.* 33(2), 309-318.

Kong, Y., Nielsen, J.L., Halkjær, P., Nielsen, P.H., 2004. Microautoradiographic study of Rhodocyclus – related Polyphosphate-Accumulating Bacteria in full-scale enhanced biological phosphorus removal Plants. *Appl. Environ. Microb.* 70(9), 5383–5390.

Kuai, L., Verstraete, W., 1998. Ammonium removal by the oxygen limited autotrophic nitrification-denitrification system. *App. Environ. Microb.* 64, 4500-4506.

Kuba, T., Wachtmeister, A., van Loosdrecht, M.C.M., Heijnen, J.J., 1994. Effect of nitrate on phosphorus release in biological phosphorus removal systems. *Water Sci. Technol.* 30 (6), 263-269.

Kuba, T., van Loosdrecht, M.C.M., Heijnen, J.J., 1996. Phosphorus and nitrogen removal with minimal COD requirement by integration of denitrifying dephosphatation and nitrification in a two-sludge system. *Water Res.* 30 (7), 1702-1710.

**L**ee, J.W., Lee, K.H., Park, K.Y., Maeng, S.K., 2010. Hydrogenotrophic denitrification in a packed bed reactor: Effects of hydrogen-to-water flow rate ratio. *Water Res.* 101(11), 3940-3946.

Lee, K.C., Rittmann, B. E., 2002. Applying a novel autohydrogenotrophic hollow-fiber membrane biofilm reactor for denitrification of drinking water. *Water Res.* 36 (8), 2040-2052.

Liu, W.T., Mino, T., Nakamura, K., Matsuo, T., 1994. Role of glycogen in acetate uptake and polyhydroxyalkanoates synthesis in anaerobic-aerobic activated-sludge with minimized polyphosphate content. *J. Ferment. Bioeng.* 77(5), 535–540.

- Liu, Y., Qin, L., Yang, S.F., 2007. Microbial granulation technology for nutrient removal from wastewater. Nova Science Publisher, New York.
- Liu, S.T., Yang, F.L., Xue, Y., Gong, Z., Chen, H.H., Wang, T., Su, Z.C., 2008a. Evaluation of oxygen adaptation and identification of functional bacteria composition for anammox consortium in non-woven biological rotating contactor. *Bioresource Technol.* 99(17), 8273-8279.
- Liu, Z., Zhao, Q., Lee, D.L., Yang, N., 2008b. Enhancing phosphorus recovery by a new internal recycle seeding MAP reactor. *Bioresource Technol.* 99, 6488-6493.
- Liu, H., Jiang, W., Dongjin, W., Qu, J., 2009. Study of a combined heterotrophic and sulfur autotrophic denitrification technology for removal of nitrate in water. *J. Hazard. Mater.* 169(1-3), 23-28.
- M**a, J., Yang, Q., Wang, S., Wang, L., Takigawa, A., Peng, Y., 2010. Effect of free nitrous acid as inhibitors on nitrate reduction by a biological nutrient removal sludge. *J. Hazard. Mater.* 175 (1-3), 518-523.
- Machado, V.C., Tapia, G., Gabriel, D., Lafuente, J., Baeza, J.A. 2009a. Systematic identifiability study based on the Fisher Information Matrix for reducing the number of parameters in calibration of an activated sludge model. *Environ. Modell. Softw.* 24, 1274-1284.
- Machado, V.C., Gabriel D., Lafuente, J., Baeza J.A., 2009b. Cost and effluent quality controllers design based on the Relative Gain Array for nutrient removal WWTP. *Water Res.* 43 (20), 5129-5141.
- Machado, V.C., 2012. Retrofitting analysis for improving benefits of A/O WWTPs considering process control aspects. PhD Thesis. UAB. Bellaterra.
- Makinia, J., Drewnowski, J., Swinarski, M., Czerwionka, K., Kaszubowska, M., Majtacz, J., 2012. The impact of precipitation and external carbon source addition on biological nutrient removal in activated sludge systems – experimental investigation and mathematical modeling. *Water Pract. Technol.* doi:10.2166/wpt.2012.011.
- Mamdani, E.H., Assilan, S., 1975. An experiment in linguistic synthesis with a fuzzy logic controller. *Int. J. Man. Mach. Stud.* 7, 1–13.
- Mampaey, K.E., Beuckels, B., Kampschreur, M.J., Kleerebezem, R., van Loosdrecht, M.C.M., Volcke, E.I.P., 2013. Modelling nitrous and nitric oxide emissions by autotrophic ammonia-oxidizing bacteria. *Environ. Technol.* 34(12), 1555-1566.
- Marcelino, M., 2009. Biological nutrient removal in advanced SBR systems. Integration of partial nitrification and simultaneous phosphorus and nitrite removal (in Spanish). PhD Thesis. UAB. Bellaterra.
- Marcelino, M., Wallaert, D., Guisasola, A., Baeza, J.A., 2011. A two-sludge system for simultaneous biological C, N and P removal via nitrite pathway. *Water Sci. Technol.* 64(5), 1142–1147.
- Martinez, M., 2006. A dynamic knowledge-based decision support system to handle solids separation problems in activated sludge systems: Development and Validation. PhD Thesis, Laboratory of Chemical and Environmental Engineering, Universitat de Girona. Girona, Spain.
- Mathews, J.H., Fink, K.D., 2004. Numerical methods using Matlab. 4<sup>th</sup> Edition. New Jersey.
- Merzouki, M., Bernet, N., Delgenès, J.P., Benlemlih, M., 2005. Effect of prefermentation on denitrifying phosphorus removal in slaughterhouse wastewater. *Bioresource Technol.* 96 (12), 1317-1322.
- Metcalfe, Eddy, 2003. Wastewater Engineering: Treatment, Disposal and Reuse. McGraw-Hill Inc., New York.

- Meyer, R., Saunders, A.M., Blackall, L.L., 2006. Putative glycogen-accumulating organisms belonging to Alphaproteobacteria identified through rRNA-based stable isotope probing. *Microbiology+* 152, 419-429.
- Michalowski, T., Pietrzyk, A., 2006. A thermodynamic study of struvite + water system. *Talanta* 68, 594–601.
- Mino, T., Arun, V., Tsuzuki, Y., Matsuo, T., 1987. Effect of phosphorus accumulation on acetate metabolism in the biological phosphorus removal. *Advances in Water Pollution Control: Biological phosphate removal from Wastewater*. Ed. R. Ramadori, Pergamon Press, Oxford.
- Mino, T., Liu, W.T., Kurisu, F., Matsuo, T., 1995. Modeling glycogen- storage and denitrification capability of microorganisms in enhanced biological phosphate removal processes. *Water Sci. Technol.* 31(2), 25–34.
- Mino, T., van Loosdrecht, M.C.M., Heijnen, J.J., 1998. Microbiology and biochemistry of enhanced biological phosphate removal process. *Water Res.*, 32(11) 3193–3207.
- Mobarry, B.K., Wagner, M., Urbain, V., Rittmann, B.E., Stahl D.A., 1996. Phylogenetic probes for analyzing abundance and spatial organization of nitrifying bacteria. *Appl. Environ. Microb.* 62, 2156-2162.
- Mora, M., Lopez, R.L., Gamisans, X., Gabriel, D., 2014. Coupling respirometry and titrimetry for the characterization of the biological activity of a SO-NR consortium. *Chem. Eng. J.* 251, 111-115.
- Moser-Engeler, R., Kuhni, M., Bernhard, C., Siegrist, H., 1999. Fermentation of raw sludge on an industrial scale and applications for elutriating its dissolved products and non-sedimentable solids. *Water Res.* 33, 3503–3511.
- N**elson, N.O., Mikkelsen, R.L., Hesterberg, D.L., 2003. Struvite precipitation in anaerobic swine lagoon liquid: effect of pH and Mg:P ratio and determination of rate constant. *Bioresource Technol.* 89, 229–236.
- Nguyen, H.T.T., Le, V.Q., Hansen, A.A., Nielsen, J.L., Nielsen, P.H., 2011. High diversity and abundance of putative polyphosphate-accumulating Tetrasphaera-related bacteria in activated sludge systems. *FEMS Microbiol. Ecol.* 76(2), 256–267.
- Ni, B.J., Yuan, Z., Chandran, K., Vanrolleghem, P.A, Murthy, S., 2013. Evaluating four mathematical models for nitrous oxide production by autotrophic ammonia-oxidizing bacteria. *Biotechnol. Bioeng.* 110(1), 153-163.
- Nielsen, A.T., Liu, W.T., Filipe, C., Grady, L., Molin, S., Stahl, D.A., 1999. Identification of novel group of bacteria in sludge of deteriorated biological phosphorus removal reactor. *Appl. Environ. Microb.* 65(3), 1251–1258.
- Nopens, I., Benedetti, L., Jeppsson, U., Pons, M.N., Alex, J., Copp J.B., Gernaey, K.V., Rosen, C., Steyer, J.P., Vanrolleghem, P.A., 2010. Benchmark Simulation model no 2: finalization of plant layout and default control strategy. *Water Sci. Technol.* 62(9), 1967-1974.
- Nowak, O., Svardal, K., Schweighofer, P., 1995. The dynamic behaviour of nitrifying activated sludge systems influenced by inhibiting wastewater compounds. *Water Sci. Technol.* 31(2), 115-124.
- Nye, J. (2004) Genetic algorithms: Explanation and implementation tradeoff, available for download from <http://www.devmaster.net> (accessed 14 July 2009).
- O**ehmen, A., Vives, T.M., Lu, H., Yuan, Z., Keller, J., 2005. The effect of pH on the competition between polyphosphate-accumulating organisms and glycogen-accumulating organisms. *Water Res.* 39(15), 3727–3737.
- Oehmen, A., Saunder A.M., Vives M.T., Yuan Z., Keller J., 2006. Competition between polyphosphate and glycogen accumulating organisms in enhanced biological phosphorus removal systems with acetate and propionate as carbon source. *J. Biotechnol.* 123, 22-32.

Oehmen, A., Lemos, P.C., Carvalho, G., Yuan, Z., Keller, J., Blackall, L.L., Reis, M.A.M., 2007. Advances in enhanced biological phosphorus removal: from micro to macro scale. *Water Res.* 41, 2271-2300.

Oehmen, A., Lopez-Vazquez, C.M., Carvalho, G., Reis, M.A.M., van Loosdrecht, M.C.M., 2010. Modelling the population dynamic and metabolic diversity of organisms relevant in anaerobic/anoxic/aerobic enhanced biological phosphorus removal processes. *Water Res.* 44, 4473-4486.

Okabe, S., Oshiki, M., Takahashi, Y., Satoh, H., 2011. Development of long-term stable partial nitrification and subsequent anammox process. *Bioresource Technol.* 102,(13), 6801-6807.

Olsson, G., Newell, B., 1999. *Wastewater Treatment System: Modelling, Diagnosis and Control*, first ed. IWA Publishing, London, UK.

Olsson, G., Nielsen, M.K., Yuan, Z., Lynggaard-Jensen, A., Steyer, J.P., 2005. *Instrumentation, Control and Automation in Wastewater Systems*. IWA Publishing, London, UK.

Olsson G., Nielsen M., Yuan Z., Lynggaard-Jensen A., Steyer J.P., 2007. *Instrumentation, Control and Automation in wastewater systems*. Scientific and Technical Report nº15. IWA Publishing. London.

Osborn, D.W., Nicholls, H.A., 1978. Optimisation of the activated sludge process for the biological removal of phosphorus. *Prog. Water Technol.* 10 (1/2), 261-277.

Ostace, G.S., Baeza, J.A., Guerrero, J., Guisasola, A., Cristea, V.M., Agachi, P.S., Lafuente, J., 2013. Development and economic assessment of different WWTP control strategies for optimal simultaneous removal of carbon, nitrogen and phosphorus. *Comput. Chem. Eng.* 53, 164-177.

**P**astor, L., Mangin, D., Barat, R., Seco, A., 2008. A pilot-scale study of struvite precipitation in a stirred tank reactor: Conditions influencing the process. *Bioresource Technol.* 99 (14), 6285-6291.

Patel, J., Nakhla, G., 2006. Interaction of denitrification and P removal in anoxic P removal systems. *Desalination.* 201, 82-99.

Pedrycz, W., 1995. *Fuzzy Sets Engineering*. CRC Press, Boca Raton, Florida, USA.

Peng, Y., Zhu, G., 2006. Biological nitrogen removal with nitrification and denitrification via nitrite pathway. *Appl. Microbiol. Biot.* 73,(1), 15-26.

Pereira, H., Lemos, P.C., Reis, M., Crespo, J., Carrondo, M., Santos, H., 1996. Model carbon metabolism in biological phosphorus removal processes base don in vivo C-NMR labelling experiments. *Water Res.* 30(9), 2128-2138.

Petersen, J.E., Werner, B., 2005. International Workshop on "Where do fertilizers go?". European Environment Agency. ISPRA, Italy.

Pijuan, M., 2004. Effect of different carbon sources and continuous aerobic conditions on the EBPR process. PhD Thesis. UAB. Bellaterra.

Pijuan, M., Saunders, A.M., Guisasola, A., Baeza, J.A., Casas, C., Blackall L.L., 2004. Enhanced biological phosphorus removal in a sequencing batch reactor using propionate as the sole carbon source. *Biotechnol. Bioeng.* 85 (1), 56-67.

Pijuan, M., Baeza, J.A., Casas, C., Lafuente, J., 2004. Response of an EBPR population developed in an SBR with propionate to different carbon sources. *Water Sci. Technol.* 50, 131-138.

- Pijuan, M., Casas, C., Baeza, J.A., 2009. Polyhydroxyalkanoate synthesis using different carbon sources by two enhanced biological phosphorus removal microbial communities. *Process Biochem.* 44(1), 97-105.
- Pijuan, M., Ye, L., Yuan, Z., 2010. Free nitrous acid inhibition on the aerobic metabolisms of poly-phosphate accumulating organisms. *Water Res.* 44(20), 6063-6072.
- Puig, S., Coma, M., Monclús, H., van Loosdrecht, M C M, Colprim, J., Balaguer, M. D., 2008. Selection between alcohols and volatile fatty acids as external carbon sources for EBPR. *Water Res.*, 42(3), 557–66.
- Purtschert, I., Siegrist, H., Gujer, W., 1996. Enhanced denitrification with methanol at WWTP Zürich-Werdhölzli. *Water Sci. Technol.* 33(12), 117-126.
- R**abinowitz, B., Marais, G.v.R., 1980. Chemical and biological phosphorus removal in the activated sludge process. MAsc. Thesis, Univ.Cape Town, S.A., Res.Rep.No. W32.
- Ráduly, B., Tapia, G., Baeza, J.A., Gabriel, D., Capodaglio, A.G., Gernaey, K.V., 2004. Variable-volume sludge blanket reactor – a simple way to model denitrification in secondary settler tanks. *IWA 4<sup>th</sup> World Water Congress and Exhibition, Marrakech, Morocco, 20-24 Sept., 2004.*
- Randall, A.A., Benefield, L.D., Hill, W.E., Nicol, J.P., Boman, G.K., Jing, S.R., 1997. The effect of volatile fatty acids on enhanced biological phosphorus removal and population structure in anaerobic/aerobic sequencing batch reactors. *Water Sci. Technol.* 35(1), 153-160.
- Rezania, B., Oleszkiewicz, J.A., Cicek, N., 2007. Hydrogen-dependent denitrification of water in an anaerobic submerged membrane bioreactor coupled with a novel hydrogen delivery system. *Water Res.* 41(5), 1074-1080.
- Ribes, J., Ferrer, J., Bouzas, A., Seco, A., 2002. Modelling of an activated primary settling tank including the fermentation process and VFA elutriation. *Environ. Technol.* 23(10), 1147-1156.
- Rieger, L., Koch, G., Kuhni, M., Gujer, W., Siegrist, H., 2001. The EAWAG bio-P module for activated sludge model no. 3. *Water Res.* 35 (16), 3887–3903.
- Rieger, L., Alex, J., Winkler, S., Boehler, M., Thomann, M., Siegrist, H., 2003. Progress in sensor technology – progress in process control? Part I: Sensor property investigation and classification. *Water Sci. Tech.* 47(2), 103-112.
- Rivas, A., Irizar, I., Ayesa, E., 2008. Model-based optimisation of wastewater treatment plants design. *Environ. Modell. Softw.* 23, 435-450.
- Rosen, C., Jeppsson, U., Vanrolleghem, P.A., 2004. Towards a common benchmark for long-term process control and monitoring performance evaluation. *Water Sci.Technol.* 50(11), 41–49.
- Ruano, M.V., Ribes, J., Sin, G., Seco, A., Ferrer, J., 2010. A systematic approach for fine-tuning of fuzzy controllers applied to WWTPs. *Environ. Modell. Softw.* 25, 670-676.
- S**aito, T., Brdjanovic, D., van Loosdrecht, M.C.M., 2004. Effect of nitrite on phosphate uptake by phosphate accumulating organisms. *Water Res.* 38, 3760-3768.
- Samuelsson, P., Carlsson, B., 2001. Feedforward control of the external carbon flow rate in a activated sludge process. *Water Sci. Technol.* 43(1), 115-122.



- Satoh, H., Ramey, W.D., Koch, F.A., Oldham, W.K., Mino, T., Matsuo, T., 1996. Anaerobic substrate uptake by the enhanced biological phosphorus removal activated sludge treating real sewage. *Water Sci. Technol.* 34, 9-16.
- Seber, G.A.F., Wild, C.J., 1989. *Nonlinear Regression*. Wiley, New York.
- Seyfried, C.F., Hippen, A., Helmer, C., Kunst, S., Rosenwinkel, K.H. 2001. One-stage deammonification: nitrogen elimination at low costs. *Water Sci. Technol.* 1(1), 71–80.
- Siegrist, H., Krebs, P., Bühler, R., Purtschert, I., Röck, C., Rufer, R., 1995. Denitrification in secondary clarifiers. *Water Sci. Technol.* 31 (2), 205-214.
- Siegrist, H., Brunner, I., Koch, G., Con Phan, L., Van Chieu, L., 1999. Reduction of biomass decay under anoxic and anaerobic conditions. *Water Sci. Technol.* 39(1), 129–137.
- Sierra-Alvarez, R., Beristan-Cardoso, R., Salazar, M., Gómez, J., Razo-Flores, E., Field, J.A. Chemolithotrophic denitrification with elemental sulfur for groundwater treatment. *Water Res.* 41(6), 1253-1262.
- Simpkins, M.J., McLaren, A.R., 1978. Consistent biological phosphate and nitrate removal in an activated sludge plant. *Prog. Water Technol.* 10(5-6), 433-442.
- Sin G., Vanrolleghem, P.A., 2006. Evolution of an ASM2d-like model structure due to operational changes of an SBR process. *Water Sci. Technol.* 53 (12), 237-245.
- Sin, G., Kaelin, D., Kampschreur, M.J., Takács, I., Wett, B., Gernaey, K.V., Rieger, L., Siegrist, H., van Loosdrecht M.C.M., 2008. Modelling nitrite in wastewater treatment systems: A discussion of different modelling concepts. *Water Sci. Technol.* 58 (6), 1155-1171.
- Shen, W., Chen, X., Pons, M.N., Corriou, J.P., 2009. Model predictive control for wastewater treatment process with feedforward compensation. *Chem. Eng. J.* 155 (1-2), 161-174.
- Shu, L., Schneider, P., Jegatheesan, V., Johnson, J., 2006. An economic evaluation of phosphorus recovery as struvite from digester supernatant. *Bioresource Technol.* 97(17), 2211-2216.
- Smith, A., Bindraban, P., Schröder, J., Conjin, J., Van der Meer, H., 2009. Phosphorus in Agriculture: Global Resources, Trends and Developments. Report to the Steering Committee Technology Assessment of the Ministry of Agriculture, The Netherlands.
- Smolders, G.J.F., van der Meij, J., van Loosdrecht M.C.M., Heijnen, J.J., 1994. Model of the anaerobic metabolism of the biological phosphorus removal process: stoichiometry and pH influence. *Biotechnol. Bioeng.* 42, 461–470.
- Soares, A., Kampas, P., Maillard, S., Wood, E., Brigg, J., Tillotson, M., Parsons, S.A., Cartmell, E., 2010. Comparison between disintegrated and fermented sewage sludge for production of a carbon source suitable for biological nutrient removal. *J. Hazard. Mater.* 175, 733-739.
- Stare, A., Vrecko, D., Hvala, N., Strmcnik, S., 2007. Comparison of control strategies for nitrogen removal in an activated sludge process in terms of operating costs. *Water Res.* 41(9), 2004-2014.
- Steffens, M.A., Lant, P.A., 1999. Multivariable control of nutrient-removing activated sludge systems. *Water Res.* 33(12), 2864-2878.
- Stephanopoulos, G., 1984. *Chemical process control: an introduction to theory to practice*. Prentice-Hall, Englewood Cliffs, New Jersey.

Strous, M., Heijnen, J.J., Kuenen, J.G., Jetten, M.S.M., 1998. The sequencing batch reactor as a powerful tool for the study of slowly growing anaerobic ammonium-oxidizing microorganisms. *Appl. Microbiol. Biot.* 50(5), 589-596.

**T**akács, I., Patry, G.G., Nolasco, D., 1991. A dynamic model of the clarification thickening process. *Water Res.* 25 (10), 1263-1271.

Tasli, R., Orhon, D., Artan, N., 1999. The effect of substrate composition on the nutrient removal potential of sequencing batch reactors. *Water S.A.* 25(3), 337-344.

Tayà, C., Guisasola, A., Baeza, J.A., 2011. Assessment of a bioaugmentation strategy with polyphosphate accumulating organisms in a nitrification/denitrification sequencing batch reactor. *Bioresource Technol.* 102(17), 7678-7684.

Tayà, C., 2013. Facing Current Bottlenecks in view of Full-Scale Implementation. PhD Thesis. UAB. Bellaterra.

Tayà, C., Guerrero, J., Vanneste, G., Guisasola, A., Baeza, J.A., 2013. Methanol-driven enhanced biological phosphorus removal with a syntrophic consortium. *Biotechnol. Bioeng.* 110(2), 391-400.

Tayà, C., Garlapati, V.K., Guisasola, A., Baeza, J.A., 2013. The selective role of nitrite in the PAO/GAO competition. *Chemosphere* 93(4), 612-618.

Tchobanoglous, G., Burton, F.L., Stensel, H.D., 2003. *Wastewater Engineering: Treatment, Disposal and Reuse.* McGraw-Hill, New York, USA.

Tong, J., Chen, Y., 2007. Enhanced biological phosphorus removal driven by short-chain fatty acids produced from waste activated sludge alkaline fermentation. *Environ. Sci. Technol.* 41(20), 7126-30.

Torà, J.A., Lafuente, J., Baeza, J.A., Carrera, J., 2010. Combined effect of inorganic carbon limitation and inhibition by free ammonia and free nitrous acid on ammonia oxidizing bacteria. *Bioresource Technol.* 101(15), 6051-6058.

Torà, J.A., Baeza, J.A., Carrera, J., Oleszkiewicz, J.A., 2011. Denitrification of a high-strength nitrite wastewater in a sequencing batch reactor using different organic carbon sources. *Chem. Eng. J.* 172 (2-3), 994-998.

Torà, J.A., Lafuente, J., Carrera, J., Baeza, J.A., 2012. Fast start-up and controlled operation during long-term period of a high-rate partial nitrification activated sludge system. *Environ. Technol.* 33(12), 1361-1366.

Torà, J.A., Lafuente, J., Garcia-Belinchón, C., Bouchy, L., Carrera, J., Baeza, J.A., 2013. High-throughput nitritation of reject water with a novel ammonium control loop: Stable effluent generation for anammox or heterotrophic denitrification. *Chem. Eng. J.* 243(1), 265-271.

Tuncal, T., Pala, A., Uslu, O., 2009. Importance of particulate biodegradable organic compounds in performance of full-scale biological phosphorus removal system. *Water Environ. Res.* 81, 886-895

Turk, O., Mavinic, D.S., 1987. Benefits of using selective inhibition to remove nitrogen from highly nitrogenous wastes. *Environ. Technol. Lett.* 8(9), 419-426.

**U**eno, Y., Fujii, M., 2001. Three years experience of operating and selling recovered struvite from full-scale plant. *Environ. Technol.* 22, 1373-1381.

NESCO, 2006. *Water, a shared responsibility. The United Nations World Water Development Report 2.* Paris, France.

UNESCO, 2012. Drops of water 14: Manual for Saving Water. Water Civilization International Centre, Venice.

**V**an Dongen, U., Jetten, M.S.M., Van Loosdrecht, M.C.M., 2001. The SHARON®-Anammox® process for treatment of ammonium rich wastewater. *Water Sci. Technol.* 44(1), 153-160.

Van Haandel, A., Van der Lubbe, J., 2007. Handbook Biological Waste Water Treatment, Quist Publishing, Leidschendam, Netherlands, ISBN: 978-90-77983-22-5

Van Hulle, S.W.H., Vandeweyer, H.J.P., Meesschaert, B.D., Vanrolleghem, P.A., Dejans, P., Dumoulin, A., 2010. Engineering aspects and practical application of autotrophic nitrogen removal from nitrogen rich streams. *Chem. Eng. J.* 162,(1), 1-20.

Van Niel, E.W.J., Appeldoorn, K.J., Zehnder, A.J.B., Kortstee, G.J.J., 1998. Inhibition of anaerobic phosphate release by nitric oxide in activated sludge. *Appl. Environ. Microbiol.* 64, 2925-2930.

Vanrolleghem, P.A., Jeppsson, U., Carstensen, J., Carlsson, B., Olsson, G., 1996. Integration of wastewater treatment plant design and operation – A systematic approach using cost functions. *Water Sci. Technol.* 34(3-4), 159-171.

Vanrolleghem, P.A., Gillot, S., 2002. Robustness and economic measures as control benchmark performance criteria. *Water Sci. Technol.* 45(4-5), 117-126.

Vargas, M., 2010. Advances in the enhanced biological phosphorus removal process: Use of different electron acceptor and influence of limiting conditions. PhD Thesis. UAB. Bellaterra.

Vargas, M., Guisasola, A., Artigues, A., Casas, C., Baeza, J.A., 2011. Comparison of a nitrite-based anaerobic-anoxic EBPR system with propionate or acetate as electron donors. *Process Biochem.* 46(3), 714-720.

Vázquez-Padín, J.R., Pozo, M.J., Jarpa, M., Figueroa, M., Franco, A., Mosquera-Corral, A., Campos, J.L., Méndez, R., 2009. Treatment of anaerobic sludge digester effluents by the CANON process in an air pulsing SBR. *J. Hazard. Mater.* 166, 336-341.

Vlaeminck, S.E., Terada, A., Smets, B.F., De Clippeleir, H., Schaubroeck, T., Bolca, S., 2010. Aggregate size and architecture determine microbial activity balance for one-stage partial nitrification and anammox. *Appl. Environ. Microbiol.* 76, 900–909.

Vrecko, D., Gernaey, K.V., Rosen, C., Jeppsson U., 2006. Benchmark simulation No 2 in matlab-simulink: towards plant-wide WWTP control strategy evaluation. *Water Sci Technol* 54(8), 65-72.

**W**agner, M., Erhart, R., Manz, W., Amann, R., Lemmer, H., Wedl, D., Schleifer, K. H., 1994. Development of an rRNA-targeted oligonucleotide probe specific for the genus *Acinetobacter* and its application for in situ monitoring in activated sludge. *Appl. Environ. Microbiol.* 60(3), 792–800.

Wagner, M., Rath, G., Koops, H.P., Flood, J., Amann, R., 1996. In situ analysis of nitrifying bacteria in sewage treatment plants. *Water Sci. Technol.* 34, 237-244.

Wang, J.S., Song, Y.H., Yuan, P., Peng, J.F., Fan, M.H., 2006. Modeling the crystallization of magnesium ammonium phosphate for phosphorus recovery. *Chemosphere* 65, 1182–1187.

Wang, X., Zeng, R.J., Dai, Y., Peng, Y., Yuan, Z., 2008. The denitrification capability of cluster 1 *Defluviicoccus vanus*-related glycogen-accumulating organisms. *Biotechnol. Bioeng.* 99(6), 1329-1336.

- Wett, B., Rauch, W., 2002. The role of inorganic carbon limitation in biological nitrogen removal of extremely ammonia concentrated wastewater. *Water Res.* 37, 1100–1110.
- Whang, L.M., Park, J. K., 2006. Competition between polyphosphate and glycogen-accumulating organisms in enhanced-biological-phosphorus-removal systems: effect of temperature and sludge age. *Water Environ. Res.* 78(1), 4–11.
- Wiesmann, U., 1994. Biological nitrogen removal from wastewater. *Adv. Biochem. Eng. Biot.* 51, 113-154.
- Williams, S., 1999. Struvite precipitation in the sludge stream at slough wastewater treatment plant opportunities for phosphorus recovery. *Environ. Technol.* 20, 743–747.
- Winkler, M.K.H., Bassin, J.P., Kleerebezem, R., Bruin, L.M.M., van den Brand, T.P.H., van Loosdrecht, M.C.M., 2011. Selective sludge removal in a segregated aerobic granular biomass system as a strategy to control PAO-GAO competition at high temperature. *Water Res.* 45(11), 3291-3299.
- Winter, C.T., 1989. The role of acetate in denitrification and biological phosphate removal in modified Bardenpho systems. *Water Sci. Technol.* 21, 375-385.
- Wong, M.T., Tan, F.M., Ng, W. J., Liu, W.T., 2004. Identification and occurrence of tetrad-forming *Alphaproteobacteria* in anaerobic-aerobic activated sludge processes. *Microbiology+* 150(11), 3741-3748.
- Wong, M.T., Mino, T., Seviour, R. J., Onuki, M., Liu, W. T., 2005. In situ identification and characterization of the microbial community structure of full-scale enhanced biological phosphorous removal plants in Japan. *Water Res.* 39(13), 2901–14.
- X**avier, J.B., De Kreuk, M.K., Picioreanu, C., Van Loosdrecht, M.C.M., 2007. Multi-scale individual-based model of microbial and byconversion dynamics in aerobic granular sludge. *Environ. Sci. Technol.* 41, 6410-6417.
- Y**agci, N., Artan, N., Cokgör, E.U., Randall, C.W., Orhon, D., 2003. Metabolic model for acetate uptake by a mixed culture of phosphate- and glycogen-accumulating organisms under anaerobic conditions. *Biotechnol. Bioeng.* 84(3), 359-373.
- Ye, Z.L., Chen, S.H., Lu, M., Shi, J.W., Lin, J.W., Wang, S.M., 2011. Recovering phosphorus as struvite from the digested swine wastewater with bittern as magnesium source. *Water Sci. Technol.* 64(2), 334-340.
- Yetilmezsoy, K., Sapci-Zengin, Z., 2009. Recovery of ammonium nitrogen from the effluent of UASB treating poultry manure wastewater by MAP precipitation as a slow release fertilizer. *J. Hazard. Mater.*, 166, 260–269.
- Yilmaz, G., Lemaire, R., Keller, J., Yuan, Z., 2007. Effectiveness of an alternating aerobic, anoxic/anaerobic strategy for maintaining biomass activity of BNR sludge during long-term starvation. *Water Res.* 41(12), 2590-2598.
- Yuan, Q., Sparling, R., Lagasse, P., Lee, Y.M., Taniguchi, D., Oleszkiewicz, J.A., 2010. Enhancing biological phosphorus removal with glycerol. *Water Sci. Technol.* 61 (7), 1837-1843.
- Z**eng, R.J., Saunders, A.M., Yuan, Z., Blackall, L. L., Keller, J., 2003. Identification and comparison of aerobic and denitrifying polyphosphate-accumulating organisms. *Biotechnol. Bioeng.* 83 (2), 140–148.
- Zeng, R.J., Yuan, Z., Keller, J., 2006. Effects of solids concentration, pH and carbon addition on the production rate and composition of volatile fatty acids in prefermenters using primary sewage sludge. *Water Sci. Technol.* 53(8), 263-269.

Zhang, P., Chen, Y., Zhou, Q., 2009. Waste activated sludge hydrolysis and short-chain fatty acids accumulation under mesophilic and thermophilic conditions: Effect of pH. *Water Res.* 43, 3735-3742.

Zhou, Y., Pijuan, Y., Zhiguo, Y., 2007. Free nitrous acid inhibition on anoxic phosphorus uptake and denitrification by poly-phosphate accumulating organisms. *Biotechnol. Bioeng.* 98(4), 903-912.

Zhou, Y., Oehmen, A., Lim, M., Vadivelu, V., Ng, W.J., 2011. The role of nitrite and free nitrous acid (FNA) in wastewater treatment plants. *Water Res.* 45, 4672-4682.

Zilles, J.L., Peccia, J., Kim, M., Hung, C., Noguera, D.R., 2002. Involvement of Rhodocyclus-related organisms in phosphorus removal in full-scale wastewater treatment plants. *Appl. Environ. Microbiol.* 68(6), 2763-2769.

## List of Figures

### Chapter I

**Figure 1.1** Biological transformations in the N cycle. Blue and green arrows represent the conventional nitrification and heterotrophic denitrification process, respectively. The Anammox process is presented in red.

**Figure 1.2** Scheme of Modified Ludzack-Ettinger process.

**Figure 1.3** Schematic representation of PAO metabolism.

**Figure 1.4** Scheme of A<sup>2</sup>/O process.

**Figure 1.5** Alternative plant configurations for reducing nitrate inlet in the anaerobic reactor, including A<sup>2</sup>/O configuration. Q<sub>w</sub>: Sludge for disposal (purge).

**Figure 1.6** Plant layout for BSM2 (Jeppsson *et al.*, 2007).

### Chapter III

**Figure 3.1** Pilot WWTP located in the Departament d'Enginyeria Química labs (UAB).

**Figure 3.2** Scheme of the pilot plant and the instrumentation used for monitoring.

**Figure 3.3** Screenshot of the software (*AddControl*) used for pilot plant monitoring and control.

### Chapter IV

**Figure 4.1** Scheme of the A<sup>2</sup>/O pilot plants I and II simulated for simultaneous C/N/P removal. Dotted lines represent the control actions over the manipulated variables.

**Figure 4.2** Example of the influent data for Dry-2, Rain-2 and Storm-2 scenarios for pilot plant I. Left: Influent flow rate. Right: Dashed lines belong to influent ammonium nitrogen concentration and solid lines belong to influent phosphate phosphorus concentration.

**Figure 4.3** Cost function for effluent fines. Adapted from Stare *et al.*, (2007).

**Figure 4.4** Three dimensional multi-criteria function.

**Figure 4.5** Scheme of the risks assessment model for microbiology-related solids separation problems. Adapted from Comas *et al.* (2008).

**Figure 4.6** Example of membership functions for input and output variables for the risk of bulking due to SRT and readily biodegradable organic substrate (S<sub>s</sub>) influent concentration in the anoxic reactor.

**Figure 4.7** Response surface filamentous bulking risk depending on SRT and readily biodegradable organic substrate.

**Figure 4.8** Example of the rules for the determination of a hypothetical problem development risk. Adapted from Dalmau (2009).

**Figure 4.9** DO concentration in R4 of pilot plant I under RO conditions (dashed lines) and after the implementation of DOC strategy with a setpoint of 4 mg DO·L<sup>-1</sup> (solid line).

**Figure 4.10** A&N-FS control strategy behaviour for Dry-2 influent in pilot plant I. (A) Ammonium R4; (B) Phosphate R4; (C) Total Nitrogen R4; (D) Nitrate R2; (E) TSS R4; (F) DO setpoint R4; (G) Q<sub>RINT</sub>; (H) Q<sub>w</sub>. Dashed lines belong to system measurements, dotted lines belong to the limit of pollutant (4 mg N-NH<sub>4</sub><sup>+</sup>·L<sup>-1</sup>, 18 mg TN·L<sup>-1</sup> and 1.5 mg P-PO<sub>4</sub><sup>-3</sup>·L<sup>-1</sup>) and solid lines to optimised setpoints.

**Figure 4.11** A&N-DVS control strategy behaviour for Dry-2 influent in pilot plant I. (A) Ammonium R4; (B) Phosphate R4; (C) Total Nitrogen R4; (D) Nitrate R2; (E) TSS R4; (F) DO setpoint R4; (G)  $Q_{RINT}$ ; (H)  $Q_W$ . Dashed lines belong to system measurements, dotted lines belong to the limit of pollutant ( $4 \text{ mg N-NH}_4^+ \cdot \text{L}^{-1}$ ,  $18 \text{ mg TN} \cdot \text{L}^{-1}$  and  $1.5 \text{ mg P-PO}_4^{3-} \cdot \text{L}^{-1}$ ) and solid lines to optimised setpoints.

**Figure 4.12** A&N-WVS control strategy behaviour for Dry-2 influent in pilot plant I. (A) Ammonium R4; (B) Phosphate R4; (C) Total Nitrogen R4; (D) Nitrate R2; (E) TSS R4; (F) DO setpoint R4; (G)  $Q_{RINT}$ ; (H)  $Q_W$ . Dashed lines belong to system measurements, dotted lines belong to the limit of pollutant ( $4 \text{ mg N-NH}_4^+ \cdot \text{L}^{-1}$ ,  $18 \text{ mg TN} \cdot \text{L}^{-1}$  and  $1.5 \text{ mg P-PO}_4^{3-} \cdot \text{L}^{-1}$ ) and solid lines to optimised setpoints.

**Figure 4.13** A&N-HVS control strategy behaviour for Dry-2 influent in pilot plant I. (A) Ammonium R4; (B) Phosphate R4; (C) Total Nitrogen R4; (D) Nitrate R2; (E) TSS R4; (F) DO setpoint R4; (G)  $Q_{RINT}$ ; (H)  $Q_W$ . Dashed lines belong to system measurements, dotted lines belong to the limit of pollutant ( $4 \text{ mg N-NH}_4^+ \cdot \text{L}^{-1}$ ,  $18 \text{ mg TN} \cdot \text{L}^{-1}$  and  $1.5 \text{ mg P-PO}_4^{3-} \cdot \text{L}^{-1}$ ) and solid lines to optimised setpoints.

**Figure 4.14** Best setpoints obtained by OCF optimisation in pilot plant II. Dashed lines belong to ammonium (Left) and nitrate (Right) for A&N-FS control strategy and solid lines the setpoints for A&N-DVS control strategy.

**Figure 4.15** Percentage of simulated time (14 days) that microbiological risks probability to develop solid separations problems was above 0.8 in pilot plant II.

**Figure 4.16** Results of the Monte Carlo simulations (1500 random set of setpoints) for A&N-FS control strategy using the MCF for pilot plant II.

**Figure 4.17** Three-dimensional representation of the A&N-FS control strategy for pilot plant II in terms of OC, EQI and MR for 1500 random set of setpoints.

**Figure 4.18** Three-dimensional representation of the A&N-DVS control strategy for pilot plant II in terms of OC, EQI and MR for 1500 random set of daily setpoints.

## Chapter V

**Figure 5.1** Scheme of  $A^2/O$  and MLE pilot plant configurations

**Figure 5.2** Influent and effluent concentrations during the experimental steps 0-III. ▼ COD inlet, ▽ COD outlet, ■ ammonium inlet, □ ammonium outlet, ● phosphorus inlet, ○ phosphorus outlet and ◇  $\text{NO}_x$  outlet.

**Figure 5.3** FISH representative images in confocal laser scanning microscope of the sludge from  $A^2/O$  pilot plant during steps 0 and III and the biomass inoculated in the start-up step, sludge from WWTP of Granollers. Specific probe PAOmix is shown in pink and EUBmix probes in blue.

**Figure 5.4** Pilot plant behaviour under carbon shortage conditions. Step IV: VFA were the main components of the total carbon source inlet. Step IV: sucrose was used as a sole carbon source inlet (Step V). □ represents effluent ammonium, ◆  $\text{NO}_x$  in R1, ◇ effluent  $\text{NO}_x$  and ● effluent phosphorus.

**Figure 5.5** Experimental batch test for model calibration purposes. ▼ COD, ◇  $\text{NO}_x$  and ● phosphorus. Dotted line belongs to the phosphorus behaviour described by the model, solid line to  $\text{NO}_x$  and dashed line to COD.

**Figure 5.6** Model validation. Pilot plant behaviour and model predictions for steps 0 to III. □ ammonium, ◇  $\text{NO}_x$  and ● phosphorus. Dotted line belongs to the phosphorus model prediction, dashed line to ammonium and solid line to  $\text{NO}_x$ .

**Figure 5.7** Effluent composition and model predictions with a low COD inlet (Step IV). □ ammonium, ◇  $\text{NO}_x$  and ● phosphorus. Dotted line belongs to the model prediction for phosphorus, dashed line to ammonium and solid line to  $\text{NO}_x$ .

**Figure 5.8** Simulation results to study the effect of influent COD content (A) and the nature of the carbon source (B) in the EBPR process. ◇  $\text{NO}_x$  and ○ phosphorus. White symbols represent the simulated results of

default ASM2d and black symbols the calibrated model results. Grey symbols correspond to experimental values obtained during pilot plant operation.

**Figure 5.9** Batch tests results obtained with sludge from SBR (up) and A<sup>2</sup>/O (down) by adding different carbon sources (A acetic acid, B propionic acid and C sucrose). Dotted line and  $\triangle$  represent COD, solid line and  $\circ$  P-PO<sub>4</sub><sup>-3</sup> and dash line and  $\square$  N-NO<sub>3</sub><sup>-</sup>. The symbol filling corresponds to the initial nitrate concentration: 0 mg·L<sup>-1</sup> (white), 40 mg·L<sup>-1</sup> (grey) and 60 mg·L<sup>-1</sup> (black).

## Chapter VI

**Figure 6.1** Scheme of the A<sup>2</sup>/O and JHB pilot plant configurations.

**Figure 6.2** Diagram of the feedback PI phosphorus control-loop for crude glycerol dosage in the A<sup>2</sup>/O pilot plant.

**Figure 6.3** Effect of nitrogen disturbances on P-removal efficiency in A<sup>2</sup>/O pilot plant. HAD = High ammonium influent disturbance. HND = High nitrite Q<sub>REXT</sub> disturbance.  $\triangle$  stands for ammonium,  $\square$  nitrate,  $\circ$  nitrite and  $\diamond$  phosphorus. Black colour belongs to influent compounds concentrations, red colour to R1 (anaerobic reactor), white colour to R3 (effluent) and grey colour to Q<sub>REXT</sub> concentrations. Dashed black line represents percentage of P-removal efficiency.

**Figure 6.4** Effect of nitrogen disturbances on P-removal efficiency in the JHB pilot-plant. HAD 1 and 2 = High ammonium influent disturbances 1 and 2. HND = High nitrite Q<sub>REXT</sub> disturbance.  $\triangle$  represents ammonium,  $\square$  nitrate,  $\circ$  nitrite and  $\diamond$  phosphorus. Black colour belongs to influent compounds concentrations, red colour to R1 (anaerobic reactor), white colour to R3 (effluent), grey colour to Q<sub>REXT</sub> concentrations and green colour to R4 (Johannesburg reactor). Dashed black line represents percentage of P-removal efficiency.

**Figure 6.5** Model calibration and validation. A<sup>2</sup>/O pilot plant experimental behaviour and model predictions. Experimental data:  $\square$  stands for nitrate,  $\circ$  nitrite and  $\diamond$  phosphorus. Red colour belongs to R1 (anaerobic reactor) concentrations, white colour to R3 (effluent), grey colour to Q<sub>REXT</sub>. Model predictions: black line belongs to nitrate in R3, grey line to nitrate in Q<sub>REXT</sub>, green line to nitrite in Q<sub>REXT</sub>, red line to phosphate in R1 and black dashed line to phosphate in R3.

**Figure 6.6** Comparison of P-removal capacity for open-loop operation (up) and for optimum ITAE CGCL implementation (down). In black solid lines is presented phosphate concentration in R3, dashed line represents the glycerol addition due to CGCL actuation and the black dotted line the setpoint of P-PO<sub>4</sub><sup>-3</sup> in R3 (1 mg·L<sup>-1</sup>).

**Figure 6.7** Effects of nitrogen disturbances on P-removal efficiency in A<sup>2</sup>/O pilot plant with implemented CGCL.  $\triangle$  represents ammonium,  $\square$  nitrate,  $\circ$  nitrite and  $\diamond$  phosphorus. Black colour belongs to influent compounds concentrations, red colour to R1 (anaerobic reactor), white colour to R3 (effluent) and grey colour to Q<sub>REXT</sub> concentrations. Dashed black line represents P-removal efficiency, dotted line the P setpoint of CGCL (1 mg P-PO<sub>4</sub><sup>-3</sup>·L<sup>-1</sup>) in R3 and red line the glycerol addition.

**Figure 6.8** Effect of nitrogen disturbances on P-removal efficiency in the JHB pilot-plant.  $\triangle$  represents ammonium,  $\square$  nitrate,  $\circ$  nitrite and  $\diamond$  phosphorus. Black colour belongs to influent compounds concentrations, red colour to R1 (anaerobic reactor), white colour to R3 (effluent), grey colour to Q<sub>REXT</sub> concentrations and green colour to R4 concentrations. Black dashed line represents percentage of P-removal efficiency, red dashed line the glycerol addition and black dotted line the P setpoint of CGCL (1 mg P-PO<sub>4</sub><sup>-3</sup>·L<sup>-1</sup>) in R3.

**Figure 6.9** Model calibration. A<sup>2</sup>/O pilot plant behaviour and model predictions when CGCL was implemented. Experimental data:  $\square$  represents nitrate,  $\circ$  nitrite and  $\diamond$  phosphorus. Red filled colour belongs to R1



(anaerobic reactor), white colour to R3 (effluent) and grey colour to  $Q_{REXT}$  concentrations. Model predictions: black line belongs to nitrate in R3, grey line to nitrate in  $Q_{REXT}$ , green line to nitrite in  $Q_{REXT}$ , red line to phosphate in R1 and black dashed line to phosphate in R3.

**Figure 6.10** Model validation. JHB pilot plant behaviour and model predictions when CGCL was implemented.  $\square$  represents nitrate,  $\circ$  nitrite and  $\diamond$  phosphorus. Experimental data: Red filled colour belongs to R1 (anaerobic reactor), white colour to R3 (effluent), grey colour to  $Q_{REXT}$  and cyan colour to R4 concentrations. Model predictions: black line belongs to nitrate in R3, grey line to nitrate in  $Q_{REXT}$ , grey dashed line to nitrite in  $Q_{REXT}$ , red line to phosphate in R1, black dashed line to phosphate in R3, green solid line to nitrite in  $Q_{REXT}$  and cyan line to nitrate concentration in R4 (JHB reactor).

**Figure 6.11** Diagram of the feedback PI control-loop for controlling phosphorus concentration in R1 by adding crude glycerol in the  $A^2/O$  pilot plant.

**Figure 6.12** Comparison of  $CGCL_{P-R1}$  and CGCL performance for  $A^2/O$  and JHB pilot plants when simulating HAD and HND periods. A graphs: Grey solid and dotted lines belong to  $P-PO_4^{-3}$  concentration in R1 for  $CGCL_{P-R1}$  and to  $P-PO_4^{-3}$  setpoint in R1 ( $30 \text{ mg}\cdot\text{L}^{-1}$ ), black dashed and solid lines to P concentration in R3 for CGCL and for  $CGCL_{P-R1}$ , respectively. Black dotted line represents  $P-PO_4^{-3}$  setpoint in R3 ( $1 \text{ mg}\cdot\text{L}^{-1}$ ) for CGCL. B graphs: Glycerol addition. Black dashed line represents CGCL actuation and black solid line  $CGCL_{P-R1}$ .

**Figure 6.13** Diagram of the new feedback + feedforward control structure for P control in R3 by crude glycerol addition in the  $A^2/O$  pilot plant.

**Figure 6.14** Comparison of CGCL and FF-CGCL performance for  $A^2/O$  and JHB pilot plants during HAD. A graphs: Black dashed line belongs to P concentration in R3 as resulted for CGCL actuation and black solid line to FF-CGCL. Black dotted line represents  $P-PO_4^{-3}$  setpoint in R3 ( $1 \text{ mg}\cdot\text{L}^{-1}$ ). B graphs: Black dashed line represents glycerol addition for CGCL and black solid line belongs to glycerol addition for FF-CGCL.

## Chapter VII

**Figure 7.1** Plant configurations for simultaneous C/N/P removal:  $A^2/O$ , BDP-5 stage, UCT, MUCT and JHB. Inf: Influent, Eff: Effluent,  $Q_{RINT}$ : Internal recycle,  $Q_{REXT}$ : External recycle,  $Q_{RANAE}$ : Anaerobic recycle,  $Q_W$ : Waste sludge or purge and IB: Influent bypass.

**Figure 7.2** Examples of discriminant distributions.

**Figure 7.3** Average effluent concentrations compared to discharge limits ( $TN = 18 \text{ mg}\cdot\text{L}^{-1}$  and  $TP = 1.5 \text{ mg}\cdot\text{L}^{-1}$  according to BSM guidelines; Gernaey and Jørgensen, 2004) for the four model assumptions and with the five plant configurations.

**Figure 7.4** Ammonium nitrogen, TN and TP dynamic evolution when the four model approaches studied were tested in the  $A^2/O$  configuration. Green lines corresponds to A1, blue lines to A2, red lines to A3 and black lines to A4. Dashed lines correspond to the discharge limits of the pollutants.

**Figure 7.5** Effluent concentrations obtained for SCA1-A ( $k_La$  AER 1 and 2 =  $120 \text{ d}^{-1}$ ) and SCA1-B ( $k_La$  AER 1 and 2 =  $80 \text{ d}^{-1}$ ) when the nitrification/denitrification processes are described as single (approach A1, black) or two step processes (approach A2, grey).  $SNH_4$  corresponds to ammonium nitrogen,  $SNO_3$  to nitrate nitrogen,  $SNO_2$  to nitrite nitrogen and  $SPO_4$  to orthophosphate phosphorus.

**Figure 7.6** Percentage of settler denitrifying capacity versus total denitrifying capacity in the  $A^2/O$  configuration for different global efficiency factors.

**Figure 7.7** Profiles of  $DO$  ( $SO_2$ ), readily biodegradable substrates ( $SRBS = SA + SF$ ), ammonium nitrogen ( $SNH_4$ ), nitrate nitrogen ( $SNO_3$ ), nitrite nitrogen ( $SNO_2$ ), and orthophosphate phosphorus ( $SPO_4$ ) in the settler for  $A^2/O$  configuration at the default influent flow-rate (SCA2-A) and when it was increased 25% (SCA2-B). The non-reactive secondary settler (black dots, A2) is compared with a reactive settler (white dots, A3) or a diffusion-

limited reactive settler (grey dots, A4). Layer 1 corresponds to the top of the settler (effluent) and layer 10 to the bottom (external recycle).

**Figure 7.8** Profiles of DO ( $\text{SO}_2$ ), readily biodegradable substrates (SRBS = SA+SF), ammonium nitrogen ( $\text{SNH}_4$ ), nitrate nitrogen ( $\text{SNO}_3$ ), nitrite nitrogen ( $\text{SNO}_2$ ), and orthophosphate phosphorus ( $\text{SPO}_4$ ) in the settler for BDP – 5 stage configuration at the default influent flow-rate (SCA2-A) and when it was increased 25% (SCA2-B). The non-reactive secondary settler (black dots, A2) is compared with a reactive settler (white dots, A3) or a diffusion-limited reactive settler (grey dots, A4). Layer 1 corresponds to the top of the settler (effluent) and layer 10 to the bottom (external recycle).

**Figure 7.9** Profiles of DO ( $\text{SO}_2$ ), readily biodegradable substrates (SRBS = SA+SF), ammonium nitrogen ( $\text{SNH}_4$ ), nitrate nitrogen ( $\text{SNO}_3$ ), nitrite nitrogen ( $\text{SNO}_2$ ), and orthophosphate phosphorus ( $\text{SPO}_4$ ) in the settler for UCT configuration at the default influent flow-rate (SCA2-A) and when it was increased 25% (SCA2-B). The non-reactive secondary settler (black dots, A2) is compared with a reactive settler (white dots, A3) or a diffusion-limited reactive settler (grey dots, A4). Layer 1 corresponds to the top of the settler (effluent) and layer 10 to the bottom (external recycle).

**Figure 7.10** Profiles of DO ( $\text{SO}_2$ ), readily biodegradable substrates (SRBS = SA+SF), ammonium nitrogen ( $\text{SNH}_4$ ), nitrate nitrogen ( $\text{SNO}_3$ ), nitrite nitrogen ( $\text{SNO}_2$ ), and orthophosphate phosphorus ( $\text{SPO}_4$ ) in the settler for MUCT configuration at the default influent flow-rate (SCA2-A) and when it was increased 25% (SCA2-B). The non-reactive secondary settler (black dots, A2) is compared with a reactive settler (white dots, A3) or a diffusion-limited reactive settler (grey dots, A4). Layer 1 corresponds to the top of the settler (effluent) and layer 10 to the bottom (external recycle).

**Figure 7.11** Profiles of DO ( $\text{SO}_2$ ), readily biodegradable substrates (SRBS = SA+SB), ammonium nitrogen ( $\text{SNH}_4$ ), nitrate nitrogen ( $\text{SNO}_3$ ), nitrite nitrogen ( $\text{SNO}_2$ ), and orthophosphate phosphorus ( $\text{SPO}_4$ ) in the settler for JHB configuration at the default influent flow-rate (SCA2-A) and when it was increased 25% (SCA2-B). The non-reactive secondary settler (black dots, A2) is compared with a reactive settler (white dots, A3) or a diffusion-limited reactive settler (grey dots, A4). Layer 1 corresponds to the top of the settler (effluent) and layer 10 to the bottom (external recycle).

**Figure 7.12** Average effluent concentrations obtained for the different plant configurations under LT conditions compared to effluent discharge limits (TN =  $18 \text{ mg}\cdot\text{L}^{-1}$  and TP =  $1.5 \text{ mg}\cdot\text{L}^{-1}$ ).

**Figure 7.13** Ammonium nitrogen, TN and TP dynamic evolution for the five plant configurations and considering A4. Black lines corresponds to  $\text{A}^2/\text{O}$  configuration, red lines to UCT, blue lines to JHB, green lines to BDP-5 stage and cyan lines to MUCT. Dashed lines correspond to the discharge limits of the pollutants.

**Figure 7.14** Simulations results for the five plant configurations without carbon source addition (black) and when adding an external carbon source to achieve  $1.5 \text{ mg}\cdot\text{L}^{-1} \text{ P-PO}_4^{-3}$  the effluent (white).

**Figure 7.15** DA of the WWTP plant configurations tested (DA1) for the discriminant functions DF1 vs DF2 (up) and DF1 vs DF3 (down).

**Figure 7.16** DA of the WWTP control strategies implemented (DA2) for the discriminant function DF1 and DF2 (up) and DF1 and DF3 (down).

## Chapter VIII

**Figure 8.1.** Simplified scheme of  $\text{A}^2/\text{O}$  configuration for C/N/P removal. Inf: Influent and Eff: Effluent.

**Figure 8.2** Block diagram of the proposed control strategy for P removal.

**Figure 8.3** Scheme of the proposed COPCS for P removal. Dashed lines represent the measured variables and control actions involved in the control strategy.

**Figure 8.4** Optimised response of COPCS for the different tuning methods tested. A: P effluent behaviour for the three step changes. B: Zoom for P effluent during COPCS activation. C: Zoom for P effluent during phosphate disturbance.

**Figure 8.5** Comparison between open-loop and COPCS performance. Grey lines represent to open-loop results, black lines the COPCS results and dashed line the  $P-PO_4^{-3}$  setpoint in AER3 for COPCS.

**Figure 8.6** Operational costs index (OCI) for the different control loops implemented. SP: Sludge production; AE: Aeration energy; ME: Mixing energy; PE: Pumping energy; MA: Metal addition; EC: External carbon addition.

**Figure 8.7** Operational costs index (OCI) for the different control loops implemented when CARBCS and METCS actuation were limited. SP: Sludge production; AE: Aeration energy; ME: Mixing energy; PE: Pumping energy; MA: Metal addition; EC: External carbon addition.

## List of Tables

### Chapter I

**Table 1.1** Discharge requirements for N and P in urban WWTP to eutrophication sensitive areas by Council Directive 91/271/EEC. One or both parameters may be applied depending on local situation. Total nitrogen = total Kjeldahl nitrogen (organic and ammonium nitrogen), nitrate nitrogen and nitrite nitrogen. \*p.e. population equivalent.

**Table 1.2** Discharge limits for industrial wastewater by Decret 130/2003.

**Table 1.3** Benchmarking criteria to evaluate WWTP performance. I: influent and e: effluent.

### Chapter III

**Table 3.1** Oligonucleotide probes used in this thesis.

### Chapter IV

**Table 4.1** Operational parameters for both pilot plants under reference operation.

**Table 4.2** Parameters used to evaluate the effluent fines.

**Table 4.3** Knowledge bases of the risks assessment model. The extension to include P in the risks assessment model is presented in grey. Adapted from Comas *et al.* (2008).

**Table 4.4** Membership functions for each variable considered in the risk assessment model. The extension to include P in the risks assessment model is presented in grey. Adapted from Comas *et al.* (2008).

**Table 4.5** Initial setpoints and constrains for the evaluation of the different optimisation methods.

**Table 4.6** Results of the optimisation of A&N-FS strategy with different search methods using Dry-2 influent in pilot plant I.

**Table 4.7** Summary of the different control strategies for the Dry-2, Rain-2 and Storm-2 influents and the main results of pilot plant I. CI is the cost improvement with respect to the reference operation.

**Table 4.8** Performance comparison of A&N-WVS with setpoints optimised for each influent or with a general set of optimised setpoints (Dry-2 influent) in pilot plant I.

**Table 4.9** Summary of sensitivity analysis results for different values of effluent fines for pilot plant I. VI is the variation interval of the values when compared to A&N-WVS. APSC is the sum of the Aeration costs, Pumping costs and Sludge production costs. *wd* Week days and *we* Weekend days.

**Table 4.10** Summary of the different control strategies for the Dry-2 influent in pilot plant II. CI is the cost improvement with respect to the reference operation expressed in percentage.

**Table 4.11** Results obtained for two operating points at the edges of the Pareto surface.

### Chapter V

**Table 5.1** Synthetic wastewater composition.

**Table 5.2** Pilot plant conditions for each experimental step.

**Table 5.3** Steady-state effluent composition obtained at the end of each experimental step.

**Table 5.4** Calibrated parameters obtained for the batch experiment with acetate and nitrate.

**Table 5.5** Major transformations obtained in the batch studies with different carbon sources. *Hac* Acetic Acid and *Hprop* Propionic Acid.

**Table 5.6** Biomass quantification using FISH technique. Results expressed in % of total biomass quantified.

## Chapter VI

**Table 6.1** Synthetic wastewater composition.

**Table 6.2** Parameters obtained from model calibration by using the experimental data of normal operation and HAD in A<sup>2</sup>/O configuration. GEF: Global efficiency factor applied to the reactive settler capacity. Confidence interval was calculated by applying FIM approach.

**Table 6.3** Parameters obtained after model calibration by using the experimental data of A<sup>2</sup>/O configuration with implemented CGCL. GEF: Global efficiency factor applied to the reactive settler capacity. Confidence interval was calculated by applying FIM approach.

## Chapter VII

**Table 7.1** Operational parameters for the plant configurations.

**Table 7.2** Summary of the modelling approaches studied in this work.

**Table 7.3** Summary of the control loops studied. DO: Dissolved oxygen; TSS: Total suspended solids; Q<sub>CARB</sub>: Carbon addition.

**Table 7.4** External carbon addition to ensure TP discharge limit (1.5 mg·L<sup>-1</sup>) for the different plant configurations.

**Table 7.5** DF coefficients for DA1 and DA2. The most discriminant criteria (highest absolute coefficient values) are presented in bold. eff: Effluent concentration, TIV: Time in violation (i.e. above discharge limit).

**Table 7.6** Example of the evaluation criteria for the seven control strategies in A<sup>2</sup>/O WWTP, including open-loop (CO). eff: Effluent concentration, TIV: Time in violation (i.e. above discharge limit).

## Chapter VIII

**Table 8.1** Characteristics of reported control strategies for controlling effluent P concentration.

**Table 8.2** Nutrient averaged effluent concentrations (364 days) for the operational scenarios.

**Table 8.3** Nutrient averaged effluent concentrations (364 days) for the operational scenarios when limiting carbon and metal addition.

## List of Acronyms and Abbreviations

A/O	Anaerobic and aerobic (WWTP configuration)
A1-A4	Model assumptions 1 to 4
A <sup>2</sup> /O	Anaerobic, anoxic and aerobic (WWTP configuration)
AE	Aeration energy
AER	Aerobic reactor
ANAE	Anaerobic reactor
ANOX	Anoxic reactor
AOB	Ammonia Oxidising Bacteria
APSC	Sum of aeration energy costs, pumping energy costs and sludge production costs
AS	Activated sludge
ASM	Activated Sludge Models
ASM2d	Activated Sludge Model No. 2d
ASM3	Activated Sludge Model No. 3
ASM3-BioP	Activated sludge Model No. 3 with EBPR extension
ATU	Allylthiourea
A&N-FS	Ammonium and nitrate fixed setpoints (control strategy)
A&N-DVS	Ammonium and nitrate daily variable setpoints (control strategy)
A&N-WVS	Ammonium and nitrate weekly variable setpoints (control strategy)
A&N-HVS	Ammonium and nitrate hourly variable setpoints (control strategy)
BDP-5stage	Bardenpho 5 stage (WWTP configuration)
BNR	Biological Nutrient Removal
BOD	Biological oxygen demand
BSM/s	Benchmark Simulation Model/s
BSM1	Benchmark Simulation Model No. 1
BSM1_LT	Benchmark Simulation Model No. 1. Long term simulations (609 days).
BSM2	Benchmark Simulation Model No. 2
BSM3	Benchmark Simulation Model No. 3
$\beta_x$	Weight factor for component X
C	Carbon / Organic matter
C0-7	Control strategies from 0 (open-loop) to 7
CARBCS	External carbon addition control strategy
CFA	Continuous flow analyser
CGCL	Crude glycerol control loop
CGCL <sub>P-R1</sub>	Crude glycerol control loop (R1 controlled variable)
CI	Cost improvement
CLSM	Confocal laser scanning microscope
COD	Chemical oxygen demand
COPCS	Cascade and override P control strategy
CSTR	Continuously Stirred Tank Reactor
EBPR	Enhanced Biological Phosphorus Removal
EC	External Carbon source addition
EF	Effluent fines
EQ	Effluent quality
EQI	Effluent quality index
DA	Discriminant analysis
DF	Discriminant function
DGAO	Denitrifying GAO
DO	Dissolved oxygen
DOC	Dissolved oxygen control
DPAO	Denitrifying PAO
F/M	Organic loading
FA	Free ammonia
FB	Fermentative bacteria / Feedback controller
FF-CGCL	Feedforward crude glycerol control loop

FID	Flame ionization detector
FIM	Fisher Information Matrix
FISH	Fluorescence in situ hybridisation
FNA	Free nitrous acid
GA	Genetic algorithm (Optimisation method)
GAO	Glycogen accumulating organisms
GC	Gas chromatography
GEF	Global efficiency factor for reactive settler rates
GHG	Green house gases
Hac	Acetic acid
Hprop	Propionic acid
IAE	Integral absolute value of error
IB	Influent bypass
IQI	Influent quality index
ISE	Integral of the square error
ITAE	Integral of the time-weighted absolute value of error
ITSE	Integral of the time-weighted square error
IWA	International Water Association
H <sub>2</sub>	Hydrogen
HAD	High ammonium disturbance
HND	High nitrite disturbance
HRT	Hydraulic retention time
JHB	Johannesburg WWTP configuration
k <sub>L</sub> a	Oxygen transfer coefficient
K <sub>C</sub>	Proportional gain in PI controller
K <sub>O<sub>2</sub>,AUT, AOB or NOB</sub>	Oxygen saturation coefficient for AUT, AOB or NOB
LT	Long Term
MCF	Multi-criteria function
ME	Mixing Energy
METCS	Metal addition control strategy
MLE	Modified Ludzack-Ettinger (WWTP configuration)
MPR	Maximum performance for nutrient removal (control strategy)
MR	Microbial risks
MST	Multivariate statistical techniques
MUCT	Modified UCT WWTP configuration
μ <sub>H</sub>	Maximum growth rate of OHO
μ <sub>PAO</sub>	Maximum growth rate of PAO
μ <sub>AOB</sub>	Maximum growth rate for AOB
N	Nitrogen
N <sub>2</sub>	Nitrogen gas
N <sub>2</sub> O	Nitrous oxide
NH <sub>3</sub>	Ammonia
N-NH <sub>4</sub> <sup>+</sup>	Ammonium nitrogen
NH <sub>4</sub> <sup>+</sup>	Ammonium
NH <sub>2</sub> OH	Hydroxylamine
NM	Nelder-Mead (Optimisation method)
NO	Nitric oxide
N-NO <sub>2</sub> <sup>-</sup>	Nitrite nitrogen
N-NO <sub>3</sub> <sup>-</sup>	Nitrate nitrogen
NOB	Nitrite Oxidising Bacteria
NO <sub>x</sub>	Nitrate and denitrification intermediates (sum of nitrate and nitrite concentration)
NUR	Nitrate uptake rate
η <sub>NO<sub>3</sub>, PAO</sub>	Nitrate reduction for denitrification from nitrate to nitrite of PAO
η <sub>NO<sub>2</sub>, PAO</sub>	Nitrate reduction for denitrification from nitrite to nitrogen gas of PAO
η <sub>NO<sub>3</sub>, OHO</sub>	Nitrate reduction for denitrification from nitrate to nitrite of OHO
η <sub>NO<sub>2</sub>, OHO</sub>	Nitrate reduction for denitrification from nitrite to nitrogen of OHO
OC	Operational costs

OCF	Operating costs function
OCI	Operational costs index
ode	Ordinary differential equation
OHO	Ordinary Heterotrophic Organisms
OTR	Oxygen transfer rate
P	Phosphorus
P-PO <sub>4</sub> <sup>-3</sup>	Phosphate phosphorus
PAO	Polyphosphate Accumulating Organisms
PBS	Phosphate buffered saline
PCA	Principal components analysis
PE	Pumping Energy
PHA	Poly-β-hydroxyalkanoates
PF	Pumping factor
PFA	Paraformaldehyde
PI	Proportional-integral controller
Poly-P	Poly-orthophosphate
PS	Patter search (Optimisation method)
PU	Pollutants units
Q <sub>IN</sub>	Influent flow-rate
Q <sub>CARB</sub>	External carbon addition
Q <sub>MET</sub>	Metal addition for P precipitation
q <sub>PHA</sub>	Maximum rate of PHA storage
q <sub>pp</sub>	Maximum P-uptake rate
Q <sub>RANAe</sub>	Anaerobic recirculation (UCT and Modified UCT)
Q <sub>REXT</sub>	External Recirculation
Q <sub>RINT</sub>	Internal Recirculation
Q <sub>W</sub>	Purge or sludge for disposal stream
RO	Reference operation
SA	Fermentation products
SBR	Sequential batch reactor
SCA	Scenario case analysis
SF	Readily biodegradable substrate
SNO <sub>2</sub>	Nitrite nitrogen
SNO <sub>3</sub>	Nitrate nitrogen
SO <sub>2</sub>	Dissolved oxygen
SP	Sludge production
SPO <sub>4</sub>	Orthophosphate phosphorus
SRBS	Readily biodegradable organic substrates
SS	Organic substrate
SRT	Sludge retention time
TIV	Time in violation
TKN	Total Kjeldahl Nitrogen
TN	Total Nitrogen
TP	Total Phosphorus
TSS	Total suspended solids
τ <sub>I</sub>	Integral time constant in PI controller
UCT	University of Cape Town (WWTP configuration)
VFA	Volatile fatty acids
V <sub>ref</sub>	Reference volume
V <sub>settler</sub>	Settler volume
VSS	Volatile suspended solids
WWTP/s	Wastewater Treatment Plant/s
X <sub>H</sub>	OHO biomass in ASM2d
X <sub>pAO</sub>	PAO biomass in ASM2d
X <sub>pp</sub>	Intracellular Poly-P for PAO in ASM2d



## **ANNEX I**

Activated Sludge Models for simulating  
biological C/N/P removal



## A.1. Biological models description

Here are presented the stoichiometric and kinetic equations of the different models used for simulating biological C/N/P removal along the thesis. The Activated Sludge Model 2d (ASM2d) proposed by the International Water Association (IWA, Henze *et al.*, 2000) was used as the starting point, where the different extensions or calibrations were performed. The most important model extension proposed in this thesis by far was the inclusion of nitrite as a new state variable and thus, nitrification was simulated as a two-step process including ammonia oxidizing bacteria (AOB) and nitrite oxidizing bacteria (NOB) as autotrophic biomass. The denitrification process was also modelled in two steps to include the denitrifying capacity of PAO to use either nitrate and/or nitrite as electron acceptor.

The default ASM2d model is composed by 19 state variables and 21 processes. For the nitrite inclusion, three new state variables (AOB, NOB and nitrite) and new processes were required. Different model approaches have been used along the thesis and hence, seven new processes were included in Chapter IV, V and VI (from 21 to 28 processes) and six in Chapters VII and VIII (from 21 to 27 processes). Table A.1 presents the state variables used. The stoichiometry and the kinetic equations for BNR simulation are shown in tables A.2-A.9.

**Table A.1** State variables of ASM2d extended model. The new state variables are marked in grey.

<b>Dissolved Components</b>	
$S_{O_2}$	Dissolved oxygen, DO
$S_F$	Readily biodegradable substrate
$S_A$	Fermentation products
$S_{NH_4}$	Ammonium nitrogen
$S_{NO_2}$	Nitrite nitrogen
$S_{NO_3}$	Nitrate nitrogen
$S_{NOX}$	Sum of nitrogen oxides ( $S_{NO_2}+S_{NO_3}$ )
$S_{N_2}$	Nitrogen gas
$S_{PO_4}$	Orthophosphate phosphorus
$S_I$	Inert, non-biodegradable organic compounds
$S_{ALK}$	Bicarbonate alkalinity
<b>Particulate Components</b>	
$X_I$	Inert, non-biodegradable organic compounds
$X_S$	Slowly biodegradable substrate
$X_H$	Heterotrophic biomass
$X_{PAO}$	Polyphosphate accumulating organisms, PAO
$X_{PP}$	Stored poly-phosphate of PAO
$X_{PHA}$	Organic storage products of PAO
$X_{AOB}$	Ammonia oxidizing bacteria, AOB
$X_{NOB}$	Nitrite oxidizing bacteria, NOB
$X_{MeP}$	Ferric-phosphate
$X_{MeOH}$	Ferric-hydroxide
$X_{TSS}$	Particulate material as model compound

**Table A.2** Process stoichiometry for nitrite inclusion in ASM2d (Dissolved components) in Chapters IV, V and VI. In grey are presented the new processes for nitrite inclusion.

Process	Compounds									
	$S_{O_2}$ mg O <sub>2</sub> · L <sup>-1</sup>	$S_F$ mg COD · L <sup>-1</sup>	$S_A$ mg COD · L <sup>-1</sup>	$S_{NH_4}$ mg N · L <sup>-1</sup>	$S_{NO_2}$ mg N · L <sup>-1</sup>	$S_{NO_3}$ mg N · L <sup>-1</sup>	$S_{N_2}$ mg N · L <sup>-1</sup>	$S_{PO_4}$ mg P · L <sup>-1</sup>	$S_i$ mg COD · L <sup>-1</sup>	$S_{ALK}$ mM HCO <sub>3</sub> <sup>-</sup>
<i>Hydrolysis processes</i>										
1. Aerobic hydrolysis		1 · f <sub>S</sub>		V <sub>1,NH4</sub>					f <sub>S</sub>	V <sub>1,ALK</sub>
2. Anoxic hydrolysis (NO <sub>2</sub> )		1 · f <sub>S</sub>		V <sub>2,NH4</sub>					f <sub>S</sub>	V <sub>2,ALK</sub>
3. Anoxic hydrolysis (NO <sub>3</sub> )		1 · f <sub>S</sub>		V <sub>3,NH4</sub>					f <sub>S</sub>	V <sub>3,ALK</sub>
4. Anaerobic hydrolysis		1 · f <sub>S</sub>		V <sub>4,NH4</sub>					f <sub>S</sub>	V <sub>4,ALK</sub>
<i>Heterotrophic organisms, X<sub>H</sub></i>										
5. Aerobic growth on S <sub>F</sub>	1 · 1/Y <sub>H</sub>	-1/Y <sub>H</sub>		V <sub>5,NH4</sub>						V <sub>5,ALK</sub>
6. Aerobic growth on S <sub>A</sub>	1 · 1/Y <sub>H</sub>	-1/Y <sub>H</sub>		-i <sub>NH4</sub>						V <sub>6,ALK</sub>
7. Anoxic growth on S <sub>F</sub> (Denitrification NO <sub>3</sub> - NO <sub>2</sub> )		-1/Y <sub>H</sub>		V <sub>7,NH4</sub>	$\left(\frac{1-Y_H}{8/7 \cdot Y_H}\right)$	$-\left(\frac{1-Y_H}{8/7 \cdot Y_H}\right)$				V <sub>7,ALK</sub>
8. Anoxic growth on S <sub>F</sub> (Denitrification NO <sub>2</sub> - N <sub>2</sub> )		-1/Y <sub>H</sub>		V <sub>8,NH4</sub>	$-\left(\frac{1-Y_H}{12/7 \cdot Y_H}\right)$	$-\left(\frac{1-Y_H}{12/7 \cdot Y_H}\right)$				V <sub>8,ALK</sub>
9. Anoxic growth on S <sub>A</sub> (Denitrification NO <sub>3</sub> - NO <sub>2</sub> )		-1/Y <sub>H</sub>		-i <sub>NH4</sub>	$\left(\frac{1-Y_H}{8/7 \cdot Y_H}\right)$	$-\left(\frac{1-Y_H}{8/7 \cdot Y_H}\right)$				V <sub>9,ALK</sub>
10. Anoxic growth on S <sub>A</sub> (Denitrification NO <sub>2</sub> - N <sub>2</sub> )		-1/Y <sub>H</sub>		-i <sub>NH4</sub>	$-\left(\frac{1-Y_H}{12/7 \cdot Y_H}\right)$	$-\left(\frac{1-Y_H}{12/7 \cdot Y_H}\right)$				V <sub>10,ALK</sub>
11. Fermentation		-1	1	-i <sub>SF</sub>						V <sub>11,ALK</sub>
12. Lysis of X <sub>H</sub>				V <sub>12,NH4</sub>						V <sub>12,ALK</sub>
<i>Accumulating phosphorus organisms, X<sub>PAO</sub></i>										
13. Storage of X <sub>PHA</sub>			-1					Y <sub>PO4</sub>		V <sub>13,ALK</sub>
14. Aerobic storage of X <sub>PHA</sub>			-Y <sub>PHA}</sub>					-1		V <sub>14,ALK</sub>
15. Anoxic storage of X <sub>PHA</sub> (Denitrification NO <sub>3</sub> - NO <sub>2</sub> )					$\frac{Y_{PHA}}{8/7}$	$-\frac{Y_{PHA}}{8/7}$				V <sub>15,ALK</sub>
16. Anoxic storage of X <sub>PHA</sub> (Denitrification NO <sub>2</sub> - N <sub>2</sub> )					$-\frac{Y_{PHA}}{12/7}$	$-\frac{Y_{PHA}}{12/7}$				V <sub>16,ALK</sub>
17. Aerobic growth	1 · 1/Y <sub>PAO</sub>			-i <sub>NH4</sub>						V <sub>17,ALK</sub>
18. Anoxic growth (Denitrification NO <sub>3</sub> - NO <sub>2</sub> )				-i <sub>NH4</sub>	$\left(\frac{1-Y_{PAO}}{8/7 \cdot Y_{PAO}}\right)$	$-\left(\frac{1-Y_{PAO}}{8/7 \cdot Y_{PAO}}\right)$				V <sub>18,ALK</sub>
19. Anoxic growth (Denitrification NO <sub>2</sub> - N <sub>2</sub> )				-i <sub>NH4</sub>	$-\left(\frac{1-Y_{PAO}}{12/7 \cdot Y_{PAO}}\right)$	$-\left(\frac{1-Y_{PAO}}{12/7 \cdot Y_{PAO}}\right)$				V <sub>19,ALK</sub>
20. Lysis of X <sub>PAO</sub>				V <sub>20,NH4</sub>						V <sub>20,ALK</sub>
21. Lysis of X <sub>PHA</sub>			1					1		V <sub>21,ALK</sub>
22. Lysis of X <sub>NH4</sub>										V <sub>22,ALK</sub>
<i>Nitrifying organisms, X<sub>AOB</sub> and X<sub>NCB</sub></i>										
23. Aerobic growth of X <sub>AOB</sub>	$\frac{24/7 \cdot Y_{AOB}}{Y_{AOB}}$			-i <sub>NH4} - 1/Y_{AOB}</sub>						V <sub>23,ALK</sub>
24. Aerobic growth of X <sub>NH4</sub>	$\frac{8/7 \cdot Y_{NCB}}{Y_{AOB}}$			-i <sub>NH4}</sub>						V <sub>24,ALK</sub>
25. Lysis of X <sub>AOB</sub>				V <sub>25,NH4</sub>						V <sub>25,ALK</sub>
26. Lysis of X <sub>NCB</sub>				V <sub>26,NH4</sub>						V <sub>26,ALK</sub>
<i>Phosphorus precipitation and redissolution</i>										
27. Precipitation									-1	V <sub>27,ALK</sub>
28. Redissolution									1	V <sub>28,ALK</sub>

**Table A.3** Process stoichiometry for nitrite inclusion in ASM2d (Particulate components) in Chapters IV, V and VI. In grey are presented the new processes for nitrite inclusion.

Process	Compounds										
	$X_i$ mg COD · L <sup>-1</sup>	$X_S$ mg COD · L <sup>-1</sup>	$X_H$ mg COD · L <sup>-1</sup>	$X_{PAO}$ mg COD · L <sup>-1</sup>	$X_{PP}$ mg P · L <sup>-1</sup>	$X_{PHA}$ mg COD · L <sup>-1</sup>	$X_{AOB}$ mg COD · L <sup>-1</sup>	$X_{NOB}$ mg COD · L <sup>-1</sup>	$X_{TSS}$ mg TSS · L <sup>-1</sup>	$X_{MeOH}$ mg TSS · L <sup>-1</sup>	$X_{MEP}$ mg TSS · L <sup>-1</sup>
<i>Hydrolysis processes</i>											
1. Aerobic hydrolysis		-1							$V_{1,TSS}$		
2. Anoxic hydrolysis (NO <sub>2</sub> )		-1							$V_{3,TSS}$		
3. Anoxic hydrolysis (NO <sub>3</sub> )		-1									
4. Anaerobic hydrolysis		-1							$V_{4,TSS}$		
<i>Heterotrophic organisms, <math>X_H</math></i>											
5. Aerobic growth on $S_F$			1						$V_{5,TSS}$		
6. Aerobic growth on $S_A$			1						$V_{6,TSS}$		
7. Anoxic growth on $S_F$ (Denitrification NO <sub>3</sub> - NO <sub>2</sub> )			1						$V_{7,TSS}$		
8. Anoxic growth on $S_F$ (Denitrification NO <sub>2</sub> - N <sub>2</sub> )			1						$V_{8,TSS}$		
9. Anoxic growth on $S_A$ (Denitrification NO <sub>3</sub> - NO <sub>2</sub> )			1						$V_{9,TSS}$		
10. Anoxic growth on $S_A$ (Denitrification NO <sub>2</sub> - N <sub>2</sub> )			1						$V_{10,TSS}$		
11. Fermentation									$V_{11,TSS}$		
12. Lysis of $X_H$	$f_{lyt,H}$	$1 - f_{lyt,H}$	-1						$V_{12,TSS}$		
<i>Accumulating phosphorus organisms, <math>X_{PAO}</math></i>											
13. Storage of $X_{PHA}$					$-Y_{PO4}$	1			$V_{13,TSS}$		
14. Aerobic storage of $X_{PP}$					1				$V_{14,TSS}$		
15. Anoxic storage of $X_{PP}$ (Denitrification NO <sub>3</sub> - NO <sub>2</sub> )					1				$V_{15,TSS}$		
16. Anoxic storage of $X_{PP}$ (Denitrification NO <sub>2</sub> - N <sub>2</sub> )					1				$V_{16,TSS}$		
17. Aerobic growth				1					$V_{17,TSS}$		
18. Anoxic growth (Denitrification NO <sub>3</sub> - NO <sub>2</sub> )				1					$V_{18,TSS}$		
19. Anoxic growth (Denitrification NO <sub>2</sub> - N <sub>2</sub> )				1					$V_{19,TSS}$		
20. Lysis of $X_{PAO}$	$f_{lyt,PAO}$	$1 - f_{lyt,PAO}$		-1					$V_{20,TSS}$		
21. Lysis of $X_{PP}$					-1				$V_{21,TSS}$		
22. Lysis of $X_{PHA}$									$V_{22,TSS}$		
<i>Nitrifying organisms, <math>X_{AOB}</math> and <math>X_{NOB}</math></i>											
23. Aerobic growth of $X_{AOB}$							1		$V_{23,TSS}$		
24. Aerobic growth of $X_{NOB}$								1	$V_{24,TSS}$		
25. Lysis of $X_{AOB}$	$f_{lyt,AOB}$	$1 - f_{lyt,AOB}$							$V_{25,TSS}$		
26. Lysis of $X_{NOB}$	$f_{lyt,NOB}$	$1 - f_{lyt,NOB}$							$V_{26,TSS}$		
<i>Phosphorus precipitation and redissolution</i>											
27. Precipitation									1.42	-3.45	4.87
28. Redissolution									-1.42	3.45	-4.87

**Table A.4** Process stoichiometry for nitrite inclusion in ASM2d (Dissolved components) in Chapters VII and VIII. In grey are presented the new processes for nitrite inclusion.

Process	Compounds									
	$S_{O_2}$ mg O <sub>2</sub> · L <sup>-1</sup>	$S_F$ mg COD · L <sup>-1</sup>	$S_A$ mg COD · L <sup>-1</sup>	$S_{NH_4}$ mg N · L <sup>-1</sup>	$S_{NO_2}$ mg N · L <sup>-1</sup>	$S_{NO_3}$ mg N · L <sup>-1</sup>	$S_{N_2}$ mg N · L <sup>-1</sup>	$S_{PO_4}$ mg P · L <sup>-1</sup>	$S_I$ mg COD · L <sup>-1</sup>	$S_{ALK}$ mM HCO <sub>3</sub> <sup>-</sup>
<b>Hydrolysis processes</b>										
1. Aerobic hydrolysis		1 · f <sub>S</sub>		V <sub>1,NH4</sub>				f <sub>S1</sub>		V <sub>1,ALK</sub>
2. Anoxic hydrolysis (NO <sub>x</sub> )		1 · f <sub>S</sub>		V <sub>2,NH4</sub>				f <sub>S1</sub>		V <sub>2,ALK</sub>
3. Anaerobic hydrolysis		1 · f <sub>S</sub>		V <sub>3,NH4</sub>				f <sub>S1</sub>		V <sub>3,ALK</sub>
<b>Heterotrophic organisms, X<sub>r</sub></b>										
4. Aerobic growth on S <sub>F</sub>	1 · 1/Y <sub>H</sub>	-1/Y <sub>H</sub>		V <sub>5,NH4</sub>						V <sub>5,ALK</sub>
5. Aerobic growth on S <sub>A</sub>	1 · 1/Y <sub>H</sub>	-1/Y <sub>H</sub>	-1/Y <sub>H</sub>	-i <sub>NBM</sub>						V <sub>6,ALK</sub>
6. Anoxic growth on S <sub>F</sub> (Denitrification NO <sub>3</sub> <sup>-</sup> - NO <sub>2</sub> <sup>-</sup> )		-1/Y <sub>H</sub>		V <sub>7,NH4</sub>	$\left(\frac{1-Y_H}{8/7 \cdot Y_H}\right) - \left(\frac{1-Y_H}{8/7 \cdot Y_H}\right)$					V <sub>7,ALK</sub>
7. Anoxic growth on S <sub>F</sub> (Denitrification NO <sub>2</sub> <sup>-</sup> - N <sub>2</sub> )		-1/Y <sub>H</sub>		V <sub>8,NH4</sub>	$-\left(\frac{1-Y_H}{12/7 \cdot Y_H}\right)$				$\left(\frac{1-Y_H}{12/7 \cdot Y_H}\right)$	V <sub>8,ALK</sub>
8. Anoxic growth on S <sub>A</sub> (Denitrification NO <sub>3</sub> <sup>-</sup> - NO <sub>2</sub> <sup>-</sup> )			-1/Y <sub>H</sub>	-i <sub>NBM</sub>	$\left(\frac{1-Y_H}{8/7 \cdot Y_H}\right) - \left(\frac{1-Y_H}{8/7 \cdot Y_H}\right)$					V <sub>9,ALK</sub>
9. Anoxic growth on S <sub>A</sub> (Denitrification NO <sub>2</sub> <sup>-</sup> - N <sub>2</sub> )			-1/Y <sub>H</sub>	-i <sub>NBM</sub>	$-\left(\frac{1-Y_H}{12/7 \cdot Y_H}\right)$				$\left(\frac{1-Y_H}{12/7 \cdot Y_H}\right)$	V <sub>10,ALK</sub>
10. Fermentation		-1	1	-i <sub>NSF</sub>					-i <sub>FSF</sub>	V <sub>11,ALK</sub>
11. Lysis of X <sub>II</sub>				V <sub>11,NH4</sub>					V <sub>11,PO4</sub>	V <sub>11,ALK</sub>
<b>Accumulating phosphorus organisms, X<sub>PAO</sub></b>										
12. Storage of X <sub>PHA</sub>			-1						Y <sub>PO4</sub>	V <sub>13,ALK</sub>
13. Aerobic storage of X <sub>PP</sub>		-Y <sub>PHA</sub>							-1	V <sub>14,ALK</sub>
14. Anoxic storage of X <sub>PP</sub> (Denitrification NO <sub>3</sub> <sup>-</sup> - NO <sub>2</sub> <sup>-</sup> )					$\frac{Y_{PHA}}{8/7}$	$\frac{Y_{PHA}}{8/7}$			-1	V <sub>15,ALK</sub>
15. Anoxic storage of X <sub>PP</sub> (Denitrification NO <sub>2</sub> <sup>-</sup> - N <sub>2</sub> )					$-\frac{Y_{PHA}}{12/7}$	$-\frac{Y_{PHA}}{12/7}$			-1	V <sub>16,ALK</sub>
16. Aerobic growth	1 · 1/Y <sub>PAO</sub>			-i <sub>NBM</sub>						V <sub>17,ALK</sub>
17. Anoxic growth (Denitrification NO <sub>3</sub> <sup>-</sup> - NO <sub>2</sub> <sup>-</sup> )				-i <sub>NBM</sub>	$\left(\frac{1-Y_{PAO}}{8/7 \cdot Y_{PAO}}\right) - \left(\frac{1-Y_{PAO}}{8/7 \cdot Y_{PAO}}\right)$					V <sub>18,ALK</sub>
18. Anoxic growth (Denitrification NO <sub>2</sub> <sup>-</sup> - N <sub>2</sub> )				-i <sub>NBM</sub>	$-\left(\frac{1-Y_{PAO}}{12/7 \cdot Y_{PAO}}\right)$				$\left(\frac{1-Y_{PAO}}{12/7 \cdot Y_{PAO}}\right)$	V <sub>19,ALK</sub>
19. Lysis of X <sub>PAO</sub>				V <sub>19,NH4</sub>					V <sub>20,PO4</sub>	V <sub>20,ALK</sub>
20. Lysis of X <sub>PP</sub>									1	V <sub>21,ALK</sub>
21. Lysis of X <sub>PHA</sub>			1							V <sub>22,ALK</sub>
<b>Nitrifying organisms, X<sub>AOB</sub> and X<sub>NOB</sub></b>										
22. Aerobic growth of X <sub>AOB</sub>	$\frac{24/7 \cdot Y_{AOB}}{Y_{AOB}}$			-i <sub>NBM} - 1/Y_{ACB}</sub>						V <sub>23,ALK</sub>
23. Aerobic growth of X <sub>NOB</sub>	$\frac{8/7 \cdot Y_{NOB}}{Y_{NOB}}$			-i <sub>NBM}</sub>						V <sub>24,ALK</sub>
24. Lysis of X <sub>AOB</sub>				V <sub>25,NH4</sub>					V <sub>25,PO4</sub>	V <sub>25,ALK</sub>
25. Lysis of X <sub>NOB</sub>				V <sub>26,NH4</sub>					V <sub>26,PO4</sub>	V <sub>26,ALK</sub>
<b>Phosphorus precipitation and redissolution</b>										
26. Precipitation									-1	V <sub>27,ALK</sub>
27. Redissolution									1	V <sub>28,ALK</sub>

**Table A.5** Process stoichiometry for nitrite inclusion in ASM2d (Particulate components) in Chapters VII and VIII. In grey are presented the new processes for nitrite inclusion.

Process	Compounds										
	$X_I$ mg COD · L <sup>-1</sup>	$X_S$ mg COD · L <sup>-1</sup>	$X_H$ mg COD · L <sup>-1</sup>	$X_{PAO}$ mg COD · L <sup>-1</sup>	$X_{PP}$ mg P · L <sup>-1</sup>	$X_{PHIA}$ mg COD · L <sup>-1</sup>	$X_{AOB}$ mg COD · L <sup>-1</sup>	$X_{NOB}$ mg COD · L <sup>-1</sup>	$X_{TSS}$ mg TSS · L <sup>-1</sup>	$X_{MeOH}$ mg TSS · L <sup>-1</sup>	$X_{MeP}$ mg TSS · L <sup>-1</sup>
<i>Hydrolysis processes</i>											
1. Aerobic hydrolysis	-1										$V_{1,TSS}$
2. Anoxic hydrolysis (NO <sub>2</sub> )	-1										$V_{2,TSS}$
3. Anaerobic hydrolysis	-1										$V_{4,TSS}$
<i>Heterotrophic organisms, X<sub>H</sub></i>											
4. Aerobic growth on S <sub>F</sub>			1								$V_{5,TSS}$
5. Aerobic growth on S <sub>A</sub>			1								$V_{6,TSS}$
6. Anoxic growth on S <sub>1</sub> (Denitrification NO <sub>3</sub> - NO <sub>2</sub> )			1								$V_{7,TSS}$
7. Anoxic growth on S <sub>1</sub> (Denitrification NO <sub>2</sub> - N <sub>2</sub> )			1								$V_{8,TSS}$
8. Anoxic growth on S <sub>1</sub> (Denitrification NO <sub>3</sub> - NO <sub>2</sub> )			1								$V_{9,TSS}$
9. Anoxic growth on S <sub>1</sub> (Denitrification NO <sub>2</sub> - N <sub>2</sub> )			1								$V_{10,TSS}$
10. Fermentation											$V_{11,TSS}$
11. Lysis of X <sub>H</sub>	$f_{X_{HBM}}$	$1 - f_{X_{HBM}}$	-1								$V_{12,TSS}$
<i>Accumulating phosphorus organisms, X<sub>PAO</sub></i>											
12. Storage of X <sub>PHIA</sub>					$-Y_{PO4}$	1					$V_{13,TSS}$
13. Aerobic storage of X <sub>PP</sub> (Denitrification NO <sub>3</sub> - NO <sub>2</sub> )					1	$-Y_{PHIA}$					$V_{14,TSS}$
14. Anoxic storage of X <sub>PP</sub> (Denitrification NO <sub>3</sub> - NO <sub>2</sub> )					1	$-Y_{PHIA}$					$V_{15,TSS}$
15. Anoxic storage of X <sub>PP</sub> (Denitrification NO <sub>2</sub> - N <sub>2</sub> )					1	$-Y_{PHIA}$					$V_{16,TSS}$
16. Aerobic growth				1							$V_{17,TSS}$
17. Anoxic growth (Denitrification NO <sub>3</sub> - NO <sub>2</sub> )				1							$V_{18,TSS}$
18. Anoxic growth (Denitrification NO <sub>2</sub> - N <sub>2</sub> )				1							$V_{19,TSS}$
19. Lysis of X <sub>PAO</sub>	$f_{X_{HBM}}$	$1 - f_{X_{HBM}}$	-1								$V_{20,TSS}$
20. Lysis of X <sub>PP</sub>											$V_{21,TSS}$
21. Lysis of X <sub>PHIA</sub>											$V_{22,TSS}$
<i>Nitrifying organisms, X<sub>AOB</sub> and X<sub>NOB</sub></i>											
22. Aerobic growth of X <sub>AOB</sub>							1				$V_{23,TSS}$
23. Aerobic growth of X <sub>NOB</sub>							1				$V_{24,TSS}$
24. Lysis of X <sub>AOB</sub>	$f_{X_{HBM}}$	$1 - f_{X_{HBM}}$	-1								$V_{25,TSS}$
25. Lysis of X <sub>NOB</sub>	$f_{X_{HBM}}$	$1 - f_{X_{HBM}}$	-1								$V_{26,TSS}$
<i>Phosphorus precipitation and redissolution</i>											
26. Precipitation											1.42
27. Redissolution											-1.42
											-3.45
											3.45
											4.87
											-4.87

**Table A.6** Process kinetic for nitrite inclusion in ASM2d for Chapters IV, V and VI. In grey are presented the new processes for nitrite inclusion.

Process (i)	Process Rate (d <sup>-1</sup> ) $\rho_i$
<b>Hydrolysis processes</b>	
1. Aerobic hydrolysis	$K_H \cdot \frac{S_{O_2}}{K_{O_2} + S_{O_2}} \cdot \frac{X_S/X_H}{K_X + X_S/X_H} \cdot X_H$
2. Anoxic hydrolysis (NO <sub>2</sub> <sup>-</sup> )	$\eta_{NO_2} \cdot K_H \cdot \frac{K_{O_2}}{K_{O_2} + S_{O_2}} \cdot \frac{S_{NO_2}}{K_{NO_2} + S_{NO_2}} \cdot \frac{X_S/X_H}{K_X + X_S/X_H} \cdot X_H$
3. Anoxic hydrolysis (NO <sub>3</sub> <sup>-</sup> )	$\eta_{NO_3} \cdot K_H \cdot \frac{K_{O_2}}{K_{O_2} + S_{O_2}} \cdot \frac{S_{NO_3}}{K_{NO_3} + S_{NO_3}} \cdot \frac{X_S/X_H}{K_X + X_S/X_H} \cdot X_H$
4. Anaerobic hydrolysis	$\eta_{FE} \cdot K_H \cdot \frac{K_{O_2}}{K_{O_2} + S_{O_2}} \cdot \frac{K_{NO_x}}{K_{NO_x} + S_{NO_2} + S_{NO_3}} \cdot \frac{X_S/X_H}{K_X + X_S/X_H} \cdot X_H$
<b>Heterotrophic organisms, X<sub>H</sub></b>	
5. Aerobic growth on S <sub>F</sub>	$\mu_H \cdot \frac{S_{O_2}}{K_{O_2} + S_{O_2}} \cdot \frac{S_F}{K_F + S_F} \cdot \frac{S_F}{S_A + S_F} \cdot \frac{S_{NH_4}}{K_{NH_4} + S_{NH_4}} \cdot \frac{S_{PO_4}}{K_{PO_4} + S_{PO_4}} \cdot \frac{S_{ALK}}{K_{ALK} + S_{ALK}} \cdot X_H$
6. Aerobic growth on S <sub>A</sub>	$\mu_H \cdot \frac{S_{O_2}}{K_{O_2} + S_{O_2}} \cdot \frac{S_A}{K_A + S_A} \cdot \frac{S_A}{S_A + S_F} \cdot \frac{S_{NH_4}}{K_{NH_4} + S_{NH_4}} \cdot \frac{S_{PO_4}}{K_{PO_4} + S_{PO_4}} \cdot \frac{S_{ALK}}{K_{ALK} + S_{ALK}} \cdot X_H$
7. Anoxic growth on S <sub>F</sub> (Denitrification NO <sub>3</sub> <sup>-</sup> - NO <sub>2</sub> <sup>-</sup> )	$\eta_{NO_3} \cdot \mu_H \cdot \frac{K_{O_2}}{K_{O_2} + S_{O_2}} \cdot \frac{S_{NO_3}}{K_{NO_3} + S_{NO_3}} \cdot \frac{S_{NO_3}}{S_{NO_3} + S_{NO_2}} \cdot \frac{S_F}{K_F + S_F} \cdot \frac{S_F}{S_A + S_F} \cdot \frac{S_{NH_4}}{K_{NH_4} + S_{NH_4}} \cdot \frac{S_{PO_4}}{K_{PO_4} + S_{PO_4}} \cdot \frac{S_{ALK}}{K_{ALK} + S_{ALK}} \cdot X_H$
8. Anoxic growth on S <sub>F</sub> (Denitrification NO <sub>2</sub> <sup>-</sup> - N <sub>2</sub> )	$\eta_{NO_2} \cdot \mu_H \cdot \frac{K_{O_2}}{K_{O_2} + S_{O_2}} \cdot \frac{S_{NO_2}}{K_{NO_2} + S_{NO_2}} \cdot \frac{S_{NO_2}}{S_{NO_3} + S_{NO_2}} \cdot \frac{S_F}{K_F + S_F} \cdot \frac{S_F}{S_A + S_F} \cdot \frac{S_{NH_4}}{K_{NH_4} + S_{NH_4}} \cdot \frac{S_{PO_4}}{K_{PO_4} + S_{PO_4}} \cdot \frac{S_{ALK}}{K_{ALK} + S_{ALK}} \cdot X_H$
9. Anoxic growth on S <sub>A</sub> (Denitrification NO <sub>3</sub> <sup>-</sup> - NO <sub>2</sub> <sup>-</sup> )	$\eta_{NO_3} \cdot \mu_H \cdot \frac{K_{O_2}}{K_{O_2} + S_{O_2}} \cdot \frac{S_{NO_3}}{K_{NO_3} + S_{NO_3}} \cdot \frac{S_{NO_3}}{S_{NO_3} + S_{NO_2}} \cdot \frac{S_A}{K_A + S_A} \cdot \frac{S_A}{S_A + S_F} \cdot \frac{S_{NH_4}}{K_{NH_4} + S_{NH_4}} \cdot \frac{S_{PO_4}}{K_{PO_4} + S_{PO_4}} \cdot \frac{S_{ALK}}{K_{ALK} + S_{ALK}} \cdot X_H$
10. Anoxic growth on S <sub>A</sub> (Denitrification NO <sub>2</sub> <sup>-</sup> - N <sub>2</sub> )	$\eta_{NO_2} \cdot \mu_H \cdot \frac{K_{O_2}}{K_{O_2} + S_{O_2}} \cdot \frac{S_{NO_2}}{K_{NO_2} + S_{NO_2}} \cdot \frac{S_{NO_2}}{S_{NO_3} + S_{NO_2}} \cdot \frac{S_A}{K_A + S_A} \cdot \frac{S_A}{S_A + S_F} \cdot \frac{S_{NH_4}}{K_{NH_4} + S_{NH_4}} \cdot \frac{S_{PO_4}}{K_{PO_4} + S_{PO_4}} \cdot \frac{S_{ALK}}{K_{ALK} + S_{ALK}} \cdot X_H$
11. Fermentation	$q_{Fe} \cdot \frac{K_{O_2}}{K_{O_2} + S_{O_2}} \cdot \frac{K_{NO_x}}{K_{NO_x} + S_{NO_2} + S_{NO_3}} \cdot \frac{S_F}{K_{FeH} + S_F} \cdot \frac{S_{ALK}}{K_{ALK} + S_{ALK}} \cdot X_H$
12. Lysis of X <sub>H</sub>	$b_H \cdot X_H$
<b>Poly-phosphorus organisms, X<sub>PAO</sub></b>	
13. Storage of X <sub>PHA</sub>	$q_{PHA} \cdot \frac{S_A}{K_A + S_A} \cdot \frac{S_{ALK}}{K_{ALK} + S_{ALK}} \cdot \frac{X_{PP}/X_{PAO}}{K_{PP} + X_{PP}/X_{PAO}} \cdot X_{PAO}$
14. Aerobic storage of X <sub>PP</sub>	$q_{PP} \cdot \frac{S_{O_2}}{K_{O_2} + S_{O_2}} \cdot \frac{S_{PO_4}}{K_{PS} + S_{PO_4}} \cdot \frac{S_{ALK}}{K_{ALK} + S_{ALK}} \cdot \frac{X_{PHA}/X_{PAO}}{K_{PHA} + X_{PHA}/X_{PAO}} \cdot \frac{K_{MAX} \cdot X_{PP}/X_{PAO}}{K_{IPP} + K_{MAX} \cdot X_{PP}/X_{PAO}} \cdot X_{PAO}$
15. Anoxic storage of X <sub>PP</sub> (Denitrification NO <sub>3</sub> <sup>-</sup> - NO <sub>2</sub> <sup>-</sup> )	$\eta_{NO_3} \cdot q_{PP} \cdot \frac{K_{O_2}}{K_{O_2} + S_{O_2}} \cdot \frac{S_{NO_3}}{K_{NO_3} + S_{NO_3}} \cdot \frac{S_{NO_3}}{S_{NO_3} + S_{NO_2}} \cdot \frac{S_{PO_4}}{K_{PS} + S_{PO_4}} \cdot \frac{S_{ALK}}{K_{ALK} + S_{ALK}} \cdot \frac{X_{PHA}/X_{PAO}}{K_{PHA} + X_{PHA}/X_{PAO}} \cdot \frac{K_{MAX} \cdot X_{PP}/X_{PAO}}{K_{IPP} + K_{MAX} \cdot X_{PP}/X_{PAO}} \cdot X_{PAO}$
16. Anoxic storage of X <sub>PP</sub> (Denitrification NO <sub>2</sub> <sup>-</sup> - N <sub>2</sub> )	$\eta_{NO_2} \cdot q_{PP} \cdot \frac{K_{O_2}}{K_{O_2} + S_{O_2}} \cdot \frac{S_{NO_2}}{K_{NO_2} + S_{NO_2}} \cdot \frac{S_{NO_2}}{S_{NO_3} + S_{NO_2}} \cdot \frac{S_{PO_4}}{K_{PS} + S_{PO_4}} \cdot \frac{S_{ALK}}{K_{ALK} + S_{ALK}} \cdot \frac{X_{PHA}/X_{PAO}}{K_{PHA} + X_{PHA}/X_{PAO}} \cdot \frac{K_{MAX} \cdot X_{PP}/X_{PAO}}{K_{IPP} + K_{MAX} \cdot X_{PP}/X_{PAO}} \cdot X_{PAO}$
17. Aerobic growth	$\mu_{PAO} \cdot \frac{S_{O_2}}{K_{O_2} + S_{O_2}} \cdot \frac{S_{NH_4}}{K_{NH_4} + S_{NH_4}} \cdot \frac{S_{PO_4}}{K_{PO_4} + S_{PO_4}} \cdot \frac{X_{PHA}/X_{PAO}}{K_{PHA} + X_{PHA}/X_{PAO}} \cdot \frac{S_{ALK}}{K_{ALK} + S_{ALK}} \cdot X_{PAO}$
18. Anoxic growth (Denitrification NO <sub>3</sub> <sup>-</sup> - NO <sub>2</sub> <sup>-</sup> )	$\eta_{NO_3} \cdot \mu_{PAO} \cdot \frac{K_{O_2}}{K_{O_2} + S_{O_2}} \cdot \frac{S_{NO_3}}{K_{NO_3} + S_{NO_3}} \cdot \frac{S_{NO_3}}{S_{NO_3} + S_{NO_2}} \cdot \frac{S_{NH_4}}{K_{NH_4} + S_{NH_4}} \cdot \frac{S_{PO_4}}{K_{PO_4} + S_{PO_4}} \cdot \frac{S_{ALK}}{K_{ALK} + S_{ALK}} \cdot \frac{X_{PHA}/X_{PAO}}{K_{PHA} + X_{PHA}/X_{PAO}} \cdot X_{PAO}$



19. Anoxic growth (Denitrification $\text{NO}_2^- - \text{N}_2$ )	$\eta_{\text{NO}_2} \cdot \mu_{\text{PAO}} \cdot \frac{K_{\text{O}_2}}{K_{\text{O}_2} + S_{\text{O}_2}} \cdot \frac{S_{\text{NO}_2}}{K_{\text{NO}_2} + S_{\text{NO}_2}} \cdot \frac{S_{\text{NO}_2}}{S_{\text{NO}_3} + S_{\text{NO}_2}} \cdot \frac{S_{\text{NH}_4}}{K_{\text{NH}_4} + S_{\text{NH}_4}} \cdot \frac{S_{\text{PO}_4}}{K_{\text{PO}_4} + S_{\text{PO}_4}} \cdot \frac{S_{\text{ALK}}}{K_{\text{ALK}} + S_{\text{ALK}}} \cdot \frac{X_{\text{PHA}}/X_{\text{PAO}}}{K_{\text{PHA}} + X_{\text{PHA}}/X_{\text{PAO}}} \cdot X_{\text{PAO}}$
20. Lysis of $X_{\text{PAO}}$	$b_{\text{PAO}} \cdot \frac{S_{\text{ALK}}}{K_{\text{ALK}} + S_{\text{ALK}}} \cdot X_{\text{PAO}}$
21. Lysis of $X_{\text{PP}}$	$b_{\text{PP}} \cdot \frac{S_{\text{ALK}}}{K_{\text{ALK}} + S_{\text{ALK}}} \cdot X_{\text{PP}}$
22. Lysis of $X_{\text{PHA}}$	$b_{\text{PHA}} \cdot \frac{S_{\text{ALK}}}{K_{\text{ALK}} + S_{\text{ALK}}} \cdot X_{\text{PHA}}$
<b>Nitrifying organisms, <math>X_{\text{AOB}}</math> and <math>X_{\text{NOB}}</math></b>	
23. Aerobic growth of $X_{\text{AOB}}$	$\mu_{\text{AOB}} \cdot \frac{S_{\text{O}_2}}{K_{\text{O}_2} + S_{\text{O}_2}} \cdot \frac{S_{\text{NH}_4}}{K_{\text{NH}_4} + S_{\text{NH}_4}} \cdot \frac{S_{\text{PO}_4}}{K_{\text{PO}_4} + S_{\text{PO}_4}} \cdot \frac{S_{\text{ALK}}}{K_{\text{ALK}} + S_{\text{ALK}}} \cdot X_{\text{AOB}}$
24. Aerobic growth of $X_{\text{NOB}}$	$\mu_{\text{NOB}} \cdot \frac{S_{\text{O}_2}}{K_{\text{O}_2} + S_{\text{O}_2}} \cdot \frac{S_{\text{NO}_2}}{K_{\text{NO}_2} + S_{\text{NO}_2}} \cdot \frac{S_{\text{PO}_4}}{K_{\text{PO}_4} + S_{\text{PO}_4}} \cdot \frac{S_{\text{ALK}}}{K_{\text{ALK}} + S_{\text{ALK}}} \cdot X_{\text{NOB}}$
25. Lysis of $X_{\text{AOB}}$	$b_{\text{AOB}} \cdot X_{\text{AOB}}$
26. Lysis of $X_{\text{NOB}}$	$b_{\text{NOB}} \cdot X_{\text{NOB}}$
<b>Phosphorus precipitation and redissolution</b>	
27. Precipitation	$k_{\text{PRE}} \cdot S_{\text{PO}_4} \cdot X_{\text{MeOH}}$
28. Redissolution	$k_{\text{RED}} \cdot X_{\text{MeP}} \cdot \frac{S_{\text{ALK}}}{K_{\text{ALK}} + S_{\text{ALK}}}$

**Table A.7** Kinetic parameters for the nitrite inclusion in ASM2d at T = 20°C and pH = 7.5 in Chapters IV, V and VI. The calibrated parameters in Chapters IV and VI are not showed here but they are shown in the respective Chapters. \*Values from Jubany *et al.*, (2008).

Parameter	ASM2d value	Extended model	Units	Description
<b>Hydrolysis processes</b>				
$K_H$	3.00	3.00	$d^{-1}$	Hydrolysis rate constant
$\eta_{NO_3}$	0.60	0.60		Anoxic hydrolysis reduction factor for nitrate
$\eta_{NO_2}$		0.60		Anoxic hydrolysis reduction factor for nitrite
$\eta_{FE}$	0.40	0.40		Anaerobic hydrolysis reduction factor
$K_{O_2}$	0.20	0.20	$mg\ O_2 \cdot L^{-1}$	Saturation/inhibition coefficient for oxygen
$K_{NO_3}$	0.50	0.50	$mg\ N \cdot L^{-1}$	Saturation/inhibition coefficient for nitrate
$K_{NO_2}$		0.50	$mg\ N \cdot L^{-1}$	Saturation/inhibition coefficient for nitrite
$K_{NOX}$		0.50	$mg\ N \cdot L^{-1}$	Saturation/inhibition coefficient for nitrogen oxides
$K_X$	0.10	0.10	$mg\ X_S \cdot mg\ X_H^{-1}$	Saturation coefficient for particulate COD
<b>Heterotrophic organisms, <math>X_H</math></b>				
$\mu_H$	6.00	6.00	$d^{-1}$	Maximum growth rate on substrate
$q_{fe}$	3.00	3.00	$d^{-1}$	Maximum rate for fermentation
$\eta_{NO_3}$	0.80	0.80		Reduction factor for denitrification ( $NO_3^- - NO_2^-$ )
$\eta_{NO_2}$		0.80		Reduction factor for denitrification ( $NO_2^- - N_2$ )
$b_H$	0.40	0.40	$d^{-1}$	Decay rate of heterotrophic organisms
$K_{O_2}$	0.20	0.20	$mg\ O_2 \cdot L^{-1}$	Saturation/inhibition coefficient for oxygen
$K_F$	4.00	4.00	$mg\ COD \cdot L^{-1}$	Saturation coefficient for growth on $S_F$
$K_{fe}$	4.00	4.00	$mg\ COD \cdot L^{-1}$	Saturation coefficient for fermentation of $S_F$
$K_A$	4.00	4.00	$mg\ COD \cdot L^{-1}$	Saturation coefficient for growth on $S_A$
$K_{NO_3}$	0.50	0.50	$mg\ N \cdot L^{-1}$	Saturation/inhibition coefficient for nitrate
$K_{NO_2}$		0.50	$mg\ N \cdot L^{-1}$	Saturation/inhibition coefficient for nitrite
$K_{NOx}$		0.50	$mg\ N \cdot L^{-1}$	Saturation/inhibition coefficient for nitrogen oxides
$K_{NH_4}$	0.05	0.05	$mg\ N \cdot L^{-1}$	Saturation/inhibition coefficient for ammonium (nutrient)
$K_{PO_4}$	0.01	0.01	$mg\ P \cdot L^{-1}$	Saturation/inhibition coefficient for phosphate (nutrient)
$K_{ALK}$	0.10	0.10	$mmol\ HCO_3^- \cdot L^{-1}$	Saturation coefficient for alkalinity
$Y_H$	0.625	0.625	$g\ COD \cdot g\ COD^{-1}$	Yield coefficient for heterotrophic biomass XH
<b>Polyphosphate accumulating organisms, <math>X_{PAO}</math></b>				
$q_{PHA}$	3.00	3.00	$d^{-1}$	Rate constant for storage of $X_{PHA}$
$q_{PP}$	1.50	1.50	$d^{-1}$	Rate constant for storage of $X_{PP}$
$\mu_{PAO}$	1.00	1.00	$d^{-1}$	Maximum growth rate of PAO
$\eta_{NO_3}$	0.60	0.60		Reduction factor for denitrification ( $NO_3^- - NO_2^-$ )
$\eta_{NO_2}$		0.60		Reduction factor for denitrification ( $NO_2^- - N_2$ )
$b_{PAO}$	0.20	0.20	$d^{-1}$	Decay rate of PAO
$b_{PP}$	0.20	0.20	$d^{-1}$	Lysis rate of PP
$b_{PHA}$	0.20	0.20	$d^{-1}$	Lysis rate of PHA
$K_{O_2}$	0.20	0.20	$mg\ O_2 \cdot L^{-1}$	Saturation/inhibition coefficient for oxygen
$K_{NO_3}$	0.50		$mg\ N \cdot L^{-1}$	Saturation/inhibition coefficient for nitrate
$K_{NO_2}$		0.50	$mg\ N \cdot L^{-1}$	Saturation/inhibition coefficient for nitrite
$K_A$	4.00	4.00	$mg\ COD \cdot L^{-1}$	Saturation coefficient for growth on $S_A$
$K_{NH_4}$	0.05	0.05	$mg\ N \cdot L^{-1}$	Saturation/inhibition coefficient for ammonium (nutrient)
$K_{PS}$	0.20	0.20	$mg\ P \cdot L^{-1}$	Saturation coefficient for phosphorus in storage PP
$K_{PO_4}$	0.01	0.01	$mg\ P \cdot L^{-1}$	Saturation/inhibition coefficient for phosphate (nutrient)
$K_{ALK}$	0.10	0.10	$mmol\ HCO_3^- \cdot L^{-1}$	Saturation coefficient for alkalinity
$K_{PP}$	0.01	0.01	$mgX_{PP} \cdot mgX_{PAO}^{-1}$	Saturation coefficient for poly-phosphate
$K_{MAX}$	0.34	0.34	$mgX_{PP} \cdot mgX_{PAO}^{-1}$	Maximum ratio $X_{PP}/X_{PAO}$

Improving EBPR stability in WWTPs aiming at simultaneous carbon and nutrient removal:  
From modeling studies to experimental validation

$K_{IPP}$	0.02	0.02	$\text{mg}X_{PP} \cdot \text{mg}X_{PAO}^{-1}$	Inhibition coefficient for PP storage
$K_{PHA}$	0.01	0.01	$\text{mg}X_{PHA} \cdot \text{mg}X_{PAO}^{-1}$	Saturation coefficient for PHA
$Y_{PAO}$	0.625	0.625	$\text{g COD} \cdot \text{g COD}^{-1}$	Yield coefficient for PAO biomass ( $X_{PAO}$ )
$Y_{PO_4}$	0.40	0.40	$\text{g P} \cdot \text{g COD}^{-1}$	PP requirement ( $PO_4$ release) per PHA stored
$Y_{PHA}$	0.20	0.20	$\text{g COD} \cdot \text{g P}^{-1}$	PHA requirement for PP storage
<b>Nitrifying organisms, <math>X_{AOB}</math> and <math>X_{NOB}</math></b>				
$\mu_{AUT}$	1.00		$\text{d}^{-1}$	Maximum growth rate of autotrophic biomass
$\mu_{AOB}$		1.21*	$\text{d}^{-1}$	Maximum growth rate of AOB
$\mu_{NOB}$		1.02*	$\text{d}^{-1}$	Maximum growth rate of NOB
$b_{AUT}$	0.15		$\text{d}^{-1}$	Decay rate of autotrophic biomass of autotrophic biomass
$b_{AOB}$		0.20*	$\text{d}^{-1}$	Decay rate of AOB
$b_{NOB}$		0.17*	$\text{d}^{-1}$	Decay rate of NOB
$K_{O_2, AUT}$	0.50		$\text{mg O}_2 \cdot \text{L}^{-1}$	Saturation/inhibition coefficient for oxygen of autotrophic biomass
$K_{O_2, AOB}$		0.74*	$\text{mg O}_2 \cdot \text{L}^{-1}$	Saturation/inhibition coefficient for oxygen of AOB
$K_{O_2, NOB}$		1.75*	$\text{mg O}_2 \cdot \text{L}^{-1}$	Saturation/inhibition coefficient for oxygen of NOB
$K_{NH_4, AUT}$	1.00		$\text{mg N} \cdot \text{L}^{-1}$	Saturation coefficient for ammonium (nutrient) of autotrophic biomass
$K_{NH_4, AOB}$		0.50	$\text{mg N} \cdot \text{L}^{-1}$	Saturation coefficient for ammonium of AOB (nutrient)
$K_{NO_2, NOB}$		0.50	$\text{mg N} \cdot \text{L}^{-1}$	Saturation coefficient for nitrite of NOB
$K_{ALK, AUT}$	0.10		$\text{mmol HCO}_3^- \cdot \text{L}^{-1}$	Saturation coefficient for alkalinity of autotrophic biomass
$K_{ALK, AOB}$		0.10	$\text{mmol HCO}_3^- \cdot \text{L}^{-1}$	Saturation coefficient for alkalinity of AOB
$K_{ALK, NOB}$		0.10	$\text{mmol HCO}_3^- \cdot \text{L}^{-1}$	Saturation coefficient for alkalinity of NOB
$K_{PO_4, AUT}$	0.01		$\text{mg P} \cdot \text{L}^{-1}$	Saturation coefficient for phosphate of autotrophic biomass
$K_{PO_4, AOB}$		0.01	$\text{mg P} \cdot \text{L}^{-1}$	Saturation coefficient for phosphate of AOB
$K_{PO_4, NOB}$		0.01	$\text{mg P} \cdot \text{L}^{-1}$	Saturation coefficient for phosphate of NOB
$Y_{AUT}$	0.24		$\text{mg COD} \cdot \text{g N}^{-1}$	Yield coefficient of autotrophic biomass
$Y_{AOB}$		0.18*	$\text{mg COD} \cdot \text{g N}^{-1}$	Yield coefficient for AOB
$Y_{NOB}$		0.08*	$\text{mg COD} \cdot \text{g N}^{-1}$	Yield coefficient for NOB
<b>Other parameters</b>				
$i_{NSI}$	0.01	0.01	$\text{g N} \cdot \text{g COD}^{-1}$	N content of inert COD $S_i$
$i_{NSF}$	0.00	0.00	$\text{g N} \cdot \text{g COD}^{-1}$	N content of fermentable substrates $S_F$
$i_{NXI}$	0.02	0.02	$\text{g N} \cdot \text{g COD}^{-1}$	N content of inert particulate COD $X_i$
$i_{NXS}$	0.04	0.04	$\text{g N} \cdot \text{g COD}^{-1}$	N content of slowly biodegradable substrates $X_S$
$i_{NBM}$	0.07	0.07	$\text{g N} \cdot \text{g COD}^{-1}$	N content of biomass: $X_H$ , $X_{PAO}$ , $X_{AOB}$ and $X_{NOB}$
$i_{PSI}$	0.00	0.00	$\text{g P} \cdot \text{g COD}^{-1}$	P content of inert COD $S_i$
$i_{PSF}$	0.00	0.00	$\text{g P} \cdot \text{g COD}^{-1}$	P content of fermentable substrates $S_F$
$i_{PXI}$	0.01	0.01	$\text{g P} \cdot \text{g COD}^{-1}$	P content of inert particulate COD $X_i$
$i_{PXS}$	0.01	0.01	$\text{g P} \cdot \text{g COD}^{-1}$	P content of slowly biodegradable substrates $X_S$
$i_{PBM}$	0.02	0.02	$\text{g P} \cdot \text{g COD}^{-1}$	P content of biomass: $X_H$ , $X_{PAO}$ , $X_{AOB}$ and $X_{NOB}$
$i_{TSSXI}$	0.75	0.75	$\text{g TSS} \cdot \text{g COD}^{-1}$	TSS to COD ratio for $X_i$
$i_{TSSXS}$	0.75	0.75	$\text{g TSS} \cdot \text{g COD}^{-1}$	TSS to COD ratio for $X_S$
$i_{TSSBM}$	0.90	0.90	$\text{g TSS} \cdot \text{g COD}^{-1}$	TSS to COD ratio for biomass: $X_H$ , $X_{PAO}$ , $X_{AOB}$ and $X_{NOB}$
$f_{SI}$	0.00	0.00	$\text{g COD} \cdot \text{g COD}^{-1}$	Production of $S_i$ in hydrolysis
$f_{XIBM}$	0.10	0.10	$\text{g COD} \cdot \text{g COD}^{-1}$	Fraction of inert COD generated in biomass lysis

**Table A.8** Process kinetic for nitrite inclusion in ASM2d for Chapters VII and VIII. In grey are presented the new processes for nitrite inclusion.

Process (i)	Process Rate (d <sup>-1</sup> ) $\rho_i$
<b>Hydrolysis processes</b>	
1. Aerobic hydrolysis	$K_H \cdot \frac{S_{O_2}}{K_{O_2} + S_{O_2}} \cdot \frac{X_S/X_H}{K_X + X_S/X_H} \cdot X_H$
2. Anoxic hydrolysis (NO <sub>3</sub> <sup>-</sup> )	$\eta_{NO_3} \cdot K_H \cdot \frac{K_{O_2}}{K_{O_2} + S_{O_2}} \cdot \frac{S_{NO_3} + S_{NO_2}}{K_{NO_3} + S_{NO_3} + S_{NO_2}} \cdot \frac{X_S/X_H}{K_X + X_S/X_H} \cdot X_H$
3. Anaerobic hydrolysis	$\eta_{FE} \cdot K_H \cdot \frac{K_{O_2}}{K_{O_2} + S_{O_2}} \cdot \frac{K_{NO_x}}{K_{NO_x} + S_{NO_3} + S_{NO_2}} \cdot \frac{X_S/X_H}{K_X + X_S/X_H} \cdot X_H$
<b>Heterotrophic organisms, X<sub>H</sub></b>	
4. Aerobic growth on S <sub>F</sub>	$\mu_H \cdot \frac{S_{O_2}}{K_{O_2} + S_{O_2}} \cdot \frac{S_F}{K_F + S_F} \cdot \frac{S_F}{S_A + S_F} \cdot \frac{S_{NH_4}}{K_{NH_4} + S_{NH_4}} \cdot \frac{S_{PO_4}}{K_{PO_4} + S_{PO_4}} \cdot \frac{S_{ALK}}{K_{ALK} + S_{ALK}} \cdot X_H$
5. Aerobic growth on S <sub>A</sub>	$\mu_H \cdot \frac{S_{O_2}}{K_{O_2} + S_{O_2}} \cdot \frac{S_A}{K_A + S_A} \cdot \frac{S_A}{S_A + S_F} \cdot \frac{S_{NH_4}}{K_{NH_4} + S_{NH_4}} \cdot \frac{S_{PO_4}}{K_{PO_4} + S_{PO_4}} \cdot \frac{S_{ALK}}{K_{ALK} + S_{ALK}} \cdot X_H$
6. Anoxic growth on S <sub>F</sub> (Denitrification NO <sub>3</sub> <sup>-</sup> - NO <sub>2</sub> <sup>-</sup> )	$\eta_{NO_3} \cdot \mu_H \cdot \frac{K_{O_2}}{K_{O_2} + S_{O_2}} \cdot \frac{S_{NO_3}}{K_{NO_3} + S_{NO_3}} \cdot \frac{S_{NO_3}}{S_{NO_3} + S_{NO_2}} \cdot \frac{S_F}{K_F + S_F} \cdot \frac{S_F}{S_A + S_F} \cdot \frac{S_{NH_4}}{K_{NH_4} + S_{NH_4}} \cdot \frac{S_{PO_4}}{K_{PO_4} + S_{PO_4}} \cdot \frac{S_{ALK}}{K_{ALK} + S_{ALK}} \cdot X_H$
7. Anoxic growth on S <sub>F</sub> (Denitrification NO <sub>2</sub> <sup>-</sup> - N <sub>2</sub> )	$\eta_{NO_2} \cdot \mu_H \cdot \frac{K_{O_2}}{K_{O_2} + S_{O_2}} \cdot \frac{S_{NO_2}}{K_{NO_2} + S_{NO_2}} \cdot \frac{S_{NO_2}}{S_{NO_3} + S_{NO_2}} \cdot \frac{S_F}{K_F + S_F} \cdot \frac{S_F}{S_A + S_F} \cdot \frac{S_{NH_4}}{K_{NH_4} + S_{NH_4}} \cdot \frac{S_{PO_4}}{K_{PO_4} + S_{PO_4}} \cdot \frac{S_{ALK}}{K_{ALK} + S_{ALK}} \cdot X_H$
8. Anoxic growth on S <sub>A</sub> (Denitrification NO <sub>3</sub> <sup>-</sup> - NO <sub>2</sub> <sup>-</sup> )	$\eta_{NO_3} \cdot \mu_H \cdot \frac{K_{O_2}}{K_{O_2} + S_{O_2}} \cdot \frac{S_{NO_3}}{K_{NO_3} + S_{NO_3}} \cdot \frac{S_{NO_3}}{S_{NO_3} + S_{NO_2}} \cdot \frac{S_A}{K_A + S_A} \cdot \frac{S_A}{S_A + S_F} \cdot \frac{S_{NH_4}}{K_{NH_4} + S_{NH_4}} \cdot \frac{S_{PO_4}}{K_{PO_4} + S_{PO_4}} \cdot \frac{S_{ALK}}{K_{ALK} + S_{ALK}} \cdot X_H$
9. Anoxic growth on S <sub>A</sub> (Denitrification NO <sub>2</sub> <sup>-</sup> - N <sub>2</sub> )	$\eta_{NO_2} \cdot \mu_H \cdot \frac{K_{O_2}}{K_{O_2} + S_{O_2}} \cdot \frac{S_{NO_2}}{K_{NO_2} + S_{NO_2}} \cdot \frac{S_{NO_2}}{S_{NO_3} + S_{NO_2}} \cdot \frac{S_A}{K_A + S_A} \cdot \frac{S_A}{S_A + S_F} \cdot \frac{S_{NH_4}}{K_{NH_4} + S_{NH_4}} \cdot \frac{S_{PO_4}}{K_{PO_4} + S_{PO_4}} \cdot \frac{S_{ALK}}{K_{ALK} + S_{ALK}} \cdot X_H$
10. Fermentation	$q_{Fe} \cdot \frac{K_{O_2}}{K_{O_2} + S_{O_2}} \cdot \frac{K_{NO_x}}{K_{NO_x} + S_{NO_2} + S_{NO_3}} \cdot \frac{S_F}{K_{FeH} + S_F} \cdot \frac{S_{ALK}}{K_{ALK} + S_{ALK}} \cdot X_H$
11. Lysis of X <sub>H</sub>	$b_H \cdot \left( \frac{S_{O_2}}{K_{O_2} + S_{O_2}} + \eta_{NO_x end} \cdot \frac{K_{O_2}}{K_{O_2} + S_{O_2}} \cdot \frac{S_{NO_3} + S_{NO_2}}{K_{NO_x} + S_{NO_3} + S_{NO_2}} \right) X_H$
<b>Polyphosphate accumulating organisms, X<sub>PAO</sub></b>	
12. Storage of X <sub>PHA</sub>	$q_{PHA} \cdot \frac{S_A}{K_A + S_A} \cdot \frac{S_{ALK}}{K_{ALK} + S_{ALK}} \cdot \frac{X_{PP}/X_{PAO}}{K_{PP} + X_{PP}/X_{PAO}} \cdot X_{PAO}$
13. Aerobic storage of X <sub>PP</sub>	$q_{PP} \cdot \frac{S_{O_2}}{K_{O_2} + S_{O_2}} \cdot \frac{S_{PO_4}}{K_{PS} + S_{PO_4}} \cdot \frac{S_{ALK}}{K_{ALK} + S_{ALK}} \cdot \frac{X_{PHA}/X_{PAO}}{K_{PHA} + X_{PHA}/X_{PAO}} \cdot \frac{K_{MAX} - X_{PP}/X_{PAO}}{K_{IPP} + K_{MAX} - X_{PP}/X_{PAO}} \cdot X_{PAO}$
14. Anoxic storage of X <sub>PP</sub> (Denitrification NO <sub>3</sub> <sup>-</sup> - NO <sub>2</sub> <sup>-</sup> )	$\eta_{NO_3} \cdot q_{PP} \cdot \frac{K_{O_2}}{K_{O_2} + S_{O_2}} \cdot \frac{S_{NO_3}}{K_{NO_3} + S_{NO_3}} \cdot \frac{S_{NO_3}}{S_{NO_3} + S_{NO_2}} \cdot \frac{S_{PO_4}}{K_{PS} + S_{PO_4}} \cdot \frac{S_{ALK}}{K_{ALK} + S_{ALK}} \cdot \frac{X_{PHA}/X_{PAO}}{K_{PHA} + X_{PHA}/X_{PAO}} \cdot \frac{K_{MAX} - X_{PP}/X_{PAO}}{K_{IPP} + K_{MAX} - X_{PP}/X_{PAO}} \cdot X_{PAO}$
15. Anoxic storage of X <sub>PP</sub> (Denitrification NO <sub>2</sub> <sup>-</sup> - N <sub>2</sub> )	$\eta_{NO_2} \cdot q_{PP} \cdot \frac{K_{O_2}}{K_{O_2} + S_{O_2}} \cdot \frac{S_{NO_2}}{K_{NO_2} + S_{NO_2}} \cdot \frac{S_{NO_2}}{S_{NO_3} + S_{NO_2}} \cdot \frac{S_{PO_4}}{K_{PS} + S_{PO_4}} \cdot \frac{S_{ALK}}{K_{ALK} + S_{ALK}} \cdot \frac{X_{PHA}/X_{PAO}}{K_{PHA} + X_{PHA}/X_{PAO}} \cdot \frac{K_{MAX} - X_{PP}/X_{PAO}}{K_{IPP} + K_{MAX} - X_{PP}/X_{PAO}} \cdot X_{PAO}$
16. Aerobic growth	$\mu_{PAO} \cdot \frac{S_{O_2}}{K_{O_2} + S_{O_2}} \cdot \frac{S_{NH_4}}{K_{NH_4} + S_{NH_4}} \cdot \frac{S_{PO_4}}{K_{PO_4} + S_{PO_4}} \cdot \frac{X_{PHA}/X_{PAO}}{K_{PHA} + X_{PHA}/X_{PAO}} \cdot \frac{S_{ALK}}{K_{ALK} + S_{ALK}} \cdot X_{PAO}$
17. Anoxic growth (Denitrification NO <sub>3</sub> <sup>-</sup> - NO <sub>2</sub> <sup>-</sup> )	$\eta_{NO_3} \cdot \mu_{PAO} \cdot \frac{K_{O_2}}{K_{O_2} + S_{O_2}} \cdot \frac{S_{NO_3}}{K_{NO_3} + S_{NO_3}} \cdot \frac{S_{NO_3}}{S_{NO_3} + S_{NO_2}} \cdot \frac{S_{NH_4}}{K_{NH_4} + S_{NH_4}} \cdot \frac{S_{PO_4}}{K_{PO_4} + S_{PO_4}} \cdot \frac{S_{ALK}}{K_{ALK} + S_{ALK}} \cdot \frac{X_{PHA}/X_{PAO}}{K_{PHA} + X_{PHA}/X_{PAO}} \cdot X_{PAO}$
18. Anoxic growth (Denitrification NO <sub>2</sub> <sup>-</sup> - N <sub>2</sub> )	$\eta_{NO_2} \cdot \mu_{PAO} \cdot \frac{K_{O_2}}{K_{O_2} + S_{O_2}} \cdot \frac{S_{NO_2}}{K_{NO_2} + S_{NO_2}} \cdot \frac{S_{NO_2}}{S_{NO_3} + S_{NO_2}} \cdot \frac{S_{NH_4}}{K_{NH_4} + S_{NH_4}} \cdot \frac{S_{PO_4}}{K_{PO_4} + S_{PO_4}} \cdot \frac{S_{ALK}}{K_{ALK} + S_{ALK}} \cdot \frac{X_{PHA}/X_{PAO}}{K_{PHA} + X_{PHA}/X_{PAO}} \cdot X_{PAO}$

19. Lysis of $X_{PAO}$	$b_{PAO} \cdot \frac{S_{ALK}}{K_{ALK} + S_{ALK}} \cdot \left( \frac{S_{O_2}}{K_{O_2} + S_{O_2}} + \eta_{NO_x \text{end}} \cdot \frac{K_{O_2}}{K_{O_2} + S_{O_2}} \cdot \frac{S_{NO_3} + S_{NO_2}}{K_{NO_x} + S_{NO_3} + S_{NO_2}} \right) \cdot X_{PAO}$
20. Lysis of $X_{PP}$	$b_{PP} \cdot \frac{S_{ALK}}{K_{ALK} + S_{ALK}} \cdot \left( \frac{S_{O_2}}{K_{O_2} + S_{O_2}} + \eta_{PP \text{ NO}_x \text{end}} \cdot \frac{K_{O_2}}{K_{O_2} + S_{O_2}} \cdot \frac{S_{NO_3} + S_{NO_2}}{K_{NO_x} + S_{NO_3} + S_{NO_2}} \right) \cdot X_{PP}$
21. Lysis of $X_{PHA}$	$b_{PHA} \cdot \frac{S_{ALK}}{K_{ALK} + S_{ALK}} \cdot \left( \frac{S_{O_2}}{K_{O_2} + S_{O_2}} + \eta_{PHA \text{ NO}_x \text{end}} \cdot \frac{K_{O_2}}{K_{O_2} + S_{O_2}} \cdot \frac{S_{NO_3} + S_{NO_2}}{K_{NO_x} + S_{NO_3} + S_{NO_2}} \right) \cdot X_{PHA}$
<b>Nitrifying organisms, <math>X_{AOB}</math> and <math>X_{NOB}</math></b>	
22. Aerobic growth of $X_{AOB}$	$\mu_{AOB} \cdot \frac{S_{O_2}}{K_{O_2} + S_{O_2}} \cdot \frac{S_{NH_4}}{K_{NH_4} + S_{NH_4}} \cdot \frac{S_{PO_4}}{K_{PO_4} + S_{PO_4}} \cdot \frac{S_{ALK}}{K_{ALK} + S_{ALK}} \cdot X_{AOB}$
23. Aerobic growth of $X_{NOB}$	$\mu_{NOB} \cdot \frac{S_{O_2}}{K_{O_2} + S_{O_2}} \cdot \frac{S_{NO_2}}{K_{NO_2} + S_{NO_2}} \cdot \frac{S_{PO_4}}{K_{PO_4} + S_{PO_4}} \cdot \frac{S_{ALK}}{K_{ALK} + S_{ALK}} \cdot X_{NOB}$
24. Lysis of $X_{AOB}$	$b_{AOB} \cdot \left( \frac{S_{O_2}}{K_{O_2} + S_{O_2}} + \eta_{AOB \text{ NO}_x \text{end}} \cdot \frac{K_{O_2}}{K_{O_2} + S_{O_2}} \cdot \frac{S_{NO_3} + S_{NO_2}}{K_{NO_x} + S_{NO_3} + S_{NO_2}} \right) \cdot X_{AOB}$
25. Lysis of $X_{NOB}$	$b_{NOB} \cdot \left( \frac{S_{O_2}}{K_{O_2} + S_{O_2}} + \eta_{NOB \text{ NO}_x \text{end}} \cdot \frac{K_{O_2}}{K_{O_2} + S_{O_2}} \cdot \frac{S_{NO_3} + S_{NO_2}}{K_{NO_x} + S_{NO_3} + S_{NO_2}} \right) \cdot X_{NOB}$
<b>Phosphorus precipitation and redissolution</b>	
26. Precipitation	$k_{PRE} \cdot S_{PO_4} \cdot X_{MeOH}$
27. Redissolution	$k_{RED} \cdot X_{MeP} \cdot \frac{S_{ALK}}{K_{ALK} + S_{ALK}}$

**Table A.9** Kinetic parameters for the nitrite inclusion in ASM2d at T = 20°C and pH = 7.5 in Chapter VII and VIII.

Parameter	ASM2d value	Extended model value	Units	Description	Reference
<b>Hydrolysis processes</b>					
$K_H$	3.00	3.00	$d^{-1}$	Hydrolysis rate constant	Henze (2000)
$\eta_{NO_3}$	0.60			Anoxic hydrolysis reduction factor for nitrate	Henze (2000)
$\eta_{NOX}$		0.60		Anoxic hydrolysis reduction factor for nitrogen oxides	This model
$\eta_{FE}$	0.40	0.40		Anaerobic hydrolysis reduction factor	Henze (2000)
$K_{O_2}$	0.20	0.20	$mg\ O_2 \cdot L^{-1}$	Saturation/inhibition coefficient for oxygen	Henze (2000)
$K_X$	0.10	0.10	$mg\ X_s \cdot mg\ X_H^{-1}$	Saturation coefficient for particulate COD	Henze (2000)
$K_{NO_3}$	0.50		$g\ N \cdot m^{-3}$	Saturation/inhibition coefficient for nitrate	Henze (2000)
$K_{NOX}$		0.50	$g\ N \cdot m^{-3}$	Saturation/inhibition coefficient for nitrogen oxides	This model
<b>Heterotrophic organisms, <math>X_H</math></b>					
$\mu_H$	6.00	6.00	$d^{-1}$	Maximum growth rate on substrate	Henze (2000)
$q_{fe}$	3.00	3.00	$d^{-1}$	Maximum rate for fermentation	Henze (2000)
$\eta_{NO_3}$	0.80	0.80		Reduction factor for denitrification ( $NO_3^- - NO_2^-$ )	Henze (2000)
$\eta_{NO_2}$		0.80		Reduction factor for denitrification ( $NO_2^- - N_2$ )	Sin (2006)
$b_H$	0.40	0.40	$d^{-1}$	Decay rate of heterotrophic organisms	Henze (2000)
$\eta_{NO_3\ end}$	0.50			Reduction factor for endogenous respiration	Gujer (1999)
$\eta_{NOX\ end}$		0.50		Reduction factor for endogenous respiration	This model
$K_{O_2}$	0.20	0.20	$mg\ O_2 \cdot L^{-1}$	Saturation/inhibition coefficient for oxygen	Henze (2000)
$K_F$	4.00	4.00	$mg\ COD \cdot L^{-1}$	Saturation coefficient for growth on $S_F$	Henze (2000)
$K_{fe}$	4.00	4.00	$mg\ COD \cdot L^{-1}$	Saturation coefficient for fermentation of $S_F$	Henze (2000)
$K_A$	4.00	4.00	$mg\ COD \cdot L^{-1}$	Saturation coefficient for growth on $S_A$	Henze (2000)
$K_{NH_4}$	0.05	0.05	$mg\ N \cdot L^{-1}$	Saturation/inhibition coefficient for ammonium (nutrient)	Henze (2000)
$K_{PO_4}$	0.01	0.01	$mg\ P \cdot L^{-1}$	Saturation/inhibition coefficient for phosphate (nutrient)	Henze (2000)
$K_{ALK}$	0.10	0.10	$mmolHCO_3^- \cdot L^{-1}$	Saturation coefficient for alkalinity	Henze (2000)
$K_{NO_3}$	0.50	0.50	$g\ N \cdot m^{-3}$	Saturation/inhibition coefficient for nitrate	Henze (2000)
$K_{NO_2}$		0.50	$g\ N \cdot m^{-3}$	Saturation/inhibition coefficient for nitrite	Sin (2006)
$K_{NOx}$		0.50	$g\ N \cdot m^{-3}$	Saturation/inhibition coefficient for nitrogen oxides	This model
$Y_H$	0.625	0.625	$gCOD \cdot gCOD^{-1}$	Yield coefficient for heterotrophic biomass $X_H$	Henze (2000)
<b>Polyphosphate accumulating organisms, <math>X_{PAO}</math></b>					
$q_{PHA}$	3.00	3.00	$d^{-1}$	Rate constant for storage of $X_{PHA}$	Henze (2000)
$q_{PP}$	1.50	1.50	$d^{-1}$	Rate constant for storage of $X_{PP}$	Henze (2000)
$\mu_{PAO}$	1.00	1.00	$d^{-1}$	Maximum growth rate of PAO	Henze (2000)
$\eta_{NO_3}$	0.60	0.60		Reduction factor for denitrification ( $NO_3^- - NO_2^-$ )	Henze (2000)
$\eta_{NO_2}$		0.60		Reduction factor for denitrification ( $NO_2^- - N_2$ )	This model
$b_{PAO}$	0.20	0.20	$d^{-1}$	Decay rate of PAO	Henze (2000)
$b_{PP}$	0.20	0.20	$d^{-1}$	Lysis rate of PP	Henze (2000)
$b_{PHA}$	0.20	0.20	$d^{-1}$	Lysis rate of PHA	Henze (2000)
$\eta_{NO_3\ end}$	0.33			Reduction factor for endogenous respiration	Rieger (2001)
$\eta_{NOX\ end}$		0.33		Reduction factor for endogenous respiration	This model
$\eta_{PP\ NO_3\ end}$	0.33			Reduction factor for endogenous respiration for PP	Rieger (2001)
$\eta_{PP\ NOX\ end}$		0.33		Reduction factor for endogenous respiration for PP	This model
$\eta_{PHA\ NO_3\ end}$	0.33			Reduction factor for endogenous respiration for PHA	Rieger (2001)
$\eta_{PHA\ NOX\ end}$		0.33		Reduction factor for endogenous respiration for PHA	This model
$K_{O_2}$	0.20	0.20	$mg\ O_2 \cdot L^{-1}$	Saturation/inhibition coefficient for oxygen	Henze (2000)
$K_{NO_3}$	0.50	0.50	$g\ N \cdot m^{-3}$	Saturation/inhibition coefficient for nitrate	Henze (2000)
$K_{NO_2}$		0.50	$g\ N \cdot m^{-3}$	Saturation/inhibition coefficient for nitrite	Sin (2006)
$K_{NOx}$		0.50	$g\ N \cdot m^{-3}$	Saturation/inhibition coefficient for nitrogen oxides	This model
$K_A$	4.00	4.00	$mg\ COD \cdot L^{-1}$	Saturation coefficient for growth on $S_A$	Henze (2000)

Improving EBPR stability in WWTPs aiming at simultaneous carbon and nutrient removal:  
From modeling studies to experimental validation

$K_{NH4}$	0.05	0.05	$mg\ N \cdot L^{-1}$	Saturation/inhibition coefficient for ammonium (nutrient)	Henze (2000)
$K_{PS}$	0.20	0.20	$mg\ P \cdot L^{-1}$	Saturation coefficient for phosphorus in storage PP	Henze (2000)
$K_{PO4}$	0.01	0.01	$mg\ P \cdot L^{-1}$	Saturation/inhibition coefficient for phosphate (nutrient)	Henze (2000)
$K_{ALK}$	0.10	0.10	$mmolHCO_3^- \cdot L^{-1}$	Saturation coefficient for alkalinity	Henze (2000)
$K_{PP}$	0.01	0.01	$mgX_{PP} \cdot mgX_{PAO}^{-1}$	Saturation coefficient for poly-phosphate	Henze (2000)
$K_{MAX}$	0.34	0.34	$mgX_{PP} \cdot mgX_{PAO}^{-1}$	Maximum ratio $X_{PP}/X_{PAO}$	Henze (2000)
$K_{IPP}$	0.02	0.02	$mgX_{PP} \cdot mgX_{PAO}^{-1}$	Inhibition coefficient for PP storage	Henze (2000)
$K_{PHA}$	0.01	0.01	$mgX_{PHA} \cdot mgX_{PAO}^{-1}$	Saturation coefficient for PHA	Henze (2000)
$Y_{PAO}$	0.625	0.625	$g\ COD \cdot g\ COD^{-1}$	Yield coefficient for PAO biomass ( $X_{PAO}$ )	Henze (2000)
$Y_{PO4}$	0.40	0.40	$g\ P \cdot g\ COD^{-1}$	PP requirement ( $PO_4$ release) per PHA stored	Henze (2000)
$Y_{PHA}$	0.20	0.20	$g\ COD \cdot g\ P^{-1}$	PHA requirement for PP storage	Henze (2000)

**Nitrifying organisms,  $X_{AOB}$  and  $X_{NOB}$**

$\mu_{AUT}$	1.00		$d^{-1}$	Maximum growth rate of autotrophic biomass	Henze (2000)
$\mu_{AOB}$		0.97	$d^{-1}$	Maximum growth rate of AOB	Wett (2003)
$\mu_{NOB}$		1.71	$d^{-1}$	Maximum growth rate of NOB	Wett (2003)
$b_{AUT}$	0.15		$d^{-1}$	Decay rate of autotrophic biomass of autotrophic biomass	Henze (2000)
$b_{AOB}$		0.23	$d^{-1}$	Decay rate of AOB	Wett (2003)
$b_{NOB}$		0.20	$d^{-1}$	Decay rate of NOB	Wett (2003)
$\eta_{AOB\ NO3\ end}$	0.33			Reduction factor for endogenous respiration of AOB	Gujer (1999)
$\eta_{AOB\ NOX\ end}$		0.33		Reduction factor for endogenous respiration of AOB	This model
$\eta_{NOB\ NO3\ end}$	0.33			Reduction factor for endogenous respiration of NOB	Gujer (1999)
$\eta_{NOB\ NOX\ end}$		0.33		Reduction factor for endogenous respiration of NOB	This model
$K_{O2, AUT}$	0.50		$g\ O_2 \cdot m^{-3}$	Saturation/inhibition coefficient for oxygen of autotrophic biomass	Henze (2000)
$K_{O2, AOB}$		0.40	$g\ O_2 \cdot m^{-3}$	Saturation/inhibition coefficient for oxygen of AOB	Wett (2003)
$K_{O2, NOB}$		1.00	$g\ O_2 \cdot m^{-3}$	Saturation/inhibition coefficient for oxygen of NOB	Wett (2003)
$K_{NH4, AUT}$	1.00		$g\ N \cdot m^{-3}$	Saturation coefficient for ammonium (nutrient) of autotrophic biomass	Henze (2000)
$K_{NH4, AOB}$		0.55	$g\ N \cdot m^{-3}$	Saturation coefficient for ammonium of AOB (nutrient)	Wett (2003)
$K_{NO2, NOB}$		0.30	$g\ N \cdot m^{-3}$	Saturation coefficient for nitrite of NOB	Wett (2003)
$K_{NO3}$	0.50			Saturation/inhibition coefficient for nitrate of autotrophic biomass	Gernaey (2004)
$K_{NOX, AOB}$		0.50		Saturation/inhibition coefficient for nitrogen oxides of AOB	This model
$K_{NOX, NOB}$		0.50		Saturation/inhibition coefficient for nitrogen oxides of NOB	This model
$K_{ALK, AUT}$	0.50		$mol\ HCO_3^- \cdot m^{-3}$	Saturation coefficient for alkalinity of autotrophic biomass	Henze (2000)
$K_{ALK, AOB}$		0.50	$mol\ HCO_3^- \cdot m^{-3}$	Saturation coefficient for alkalinity of AOB	This model
$K_{ALK, NOB}$		0.50	$mol\ HCO_3^- \cdot m^{-3}$	Saturation coefficient for alkalinity of NOB	This model
$K_{PO4, AUT}$	0.01		$g\ P \cdot m^{-3}$	Saturation coefficient for phosphate of autotrophic biomass	Henze (2000)
$K_{PO4, AOB}$		0.01	$g\ P \cdot m^{-3}$	Saturation coefficient for phosphate of AOB	This model
$K_{PO4, NOB}$		0.01	$g\ P \cdot m^{-3}$	Saturation coefficient for phosphate of NOB	This model
$Y_{AUT}$	0.24		$g\ COD \cdot g\ N^{-1}$	Yield coefficient of autotrophic biomass	Henze (2000)
$Y_{AOB}$		0.18	$g\ COD \cdot g\ N^{-1}$	Yield coefficient for AOB	Jubany(2008)
$Y_{NOB}$		0.08	$g\ COD \cdot g\ N^{-1}$	Yield coefficient for NOB	Jubany(2008)

**Other parameters**

$i_{NSI}$	0.01	0.01	$g\ N \cdot g\ COD^{-1}$	N content of inert COD $S_i$	Henze (2000)
$i_{NSF}$	0.03	0.03	$g\ N \cdot g\ COD^{-1}$	N content of fermentable substrates $S_F$	Henze (2000)
$i_{NXI}$	0.02	0.02	$g\ N \cdot g\ COD^{-1}$	N content of inert particulate COD $X_i$	Henze (2000)
$i_{NXS}$	0.04	0.04	$g\ N \cdot g\ COD^{-1}$	N content of slowly biodegradable substrates $X_S$	Henze (2000)
$i_{NBM}$	0.07	0.07	$g\ N \cdot g\ COD^{-1}$	N content of biomass: $X_H$ , $X_{PAO}$ , $X_{AOB}$ and $X_{NOB}$	Henze (2000)
$i_{PSI}$	0.00	0.00	$g\ P \cdot g\ COD^{-1}$	P content of inert COD $S_i$	Henze (2000)

Improving EBPR stability in WWTPs aiming at simultaneous carbon and nutrient removal:  
From modeling studies to experimental validation

$i_{PSF}$	0.01	0.01	$g P \cdot g COD^{-1}$	P content of fermentable substrates $S_F$	Henze (2000)
$i_{PXI}$	0.01	0.01	$g P \cdot g COD^{-1}$	P content of inert particulate COD $X_I$	Henze (2000)
$i_{PXS}$	0.01	0.01	$g P \cdot g COD^{-1}$	P content of slowly biodegradable substrates $X_S$	Henze (2000)
$i_{PBM}$	0.02	0.02	$g P \cdot g COD^{-1}$	P content of biomass: $X_H$ , $X_{PAO}$ , $X_{AOB}$ and $X_{NOB}$	Henze (2000)
$i_{TSSXI}$	0.75	0.75	$g TSS \cdot g COD^{-1}$	TSS to COD ratio for $X_I$	Henze (2000)
$i_{TSSXS}$	0.75	0.75	$g TSS \cdot g COD^{-1}$	TSS to COD ratio for $X_S$	Henze (2000)
$i_{TSSBM}$	0.90	0.90	$g TSS \cdot g COD^{-1}$	TSS to COD ratio for biomass: $X_H$ , $X_{PAO}$ , $X_{AOB}$ and $X_{NOB}$	Henze (2000)
$f_{SI}$	0.00	0.00	$g COD \cdot g COD^{-1}$	Production of $S_i$ in hydrolysis	Henze (2000)
$f_{XIBM}$	0.10	0.10	$g COD \cdot g COD^{-1}$	Fraction of inert COD generated in biomass lysis	Henze (2000)



## A.2. Matlab-Simulink® simulation environment

In Chapter VII and VIII, the water line of the simulated WWTP configurations was implemented in Matlab-Simulink® software. Figure A.1 shows an example of the main screen for A<sup>2</sup>/O configuration.

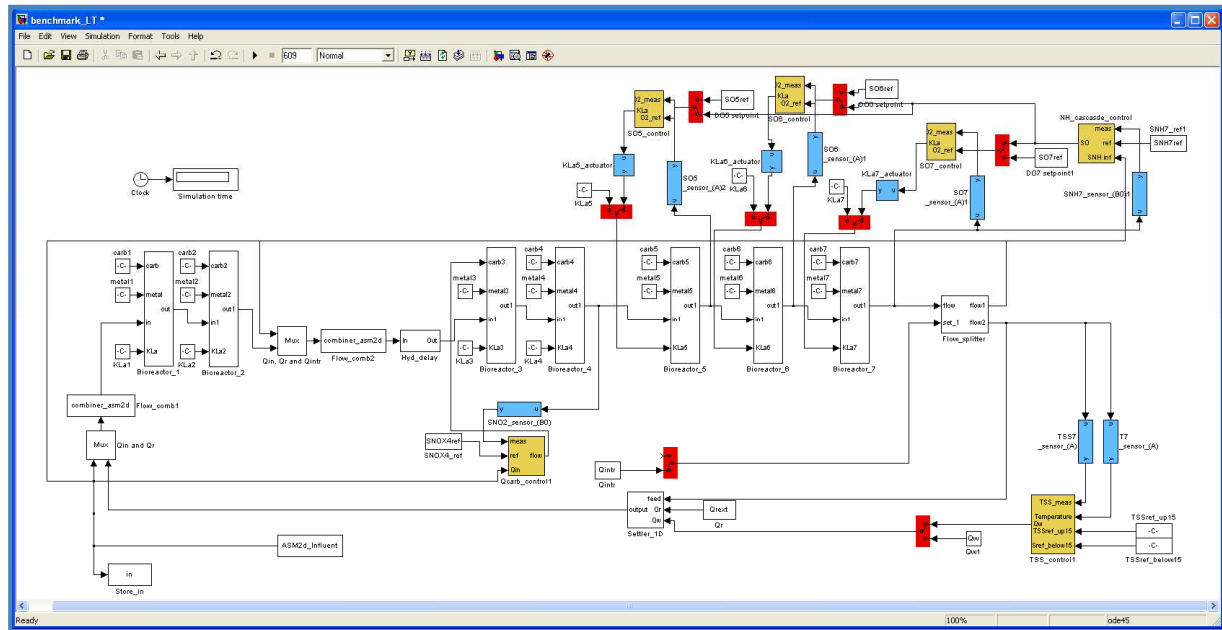


**Figure A.1** Main screen from Matlab-Simulink® software to simulate benchmarking A<sup>2</sup>/O configuration in Chapters VII and VIII.

Apart from the process blocks, which represent the anaerobic, anoxic and aerobic reactors and the settler, the screenshot also shows the process controllers (yellow blocks), the sensors for plant performance monitoring (blue blocks) and different switches (red blocks) to activate/deactivate the different control strategies. The hydraulic and kinetic equations to describe BNR process as well as the optimisation algorithm have been implemented in C-MEX files and they were compiled by the software itself.

In Chapters IV, V and VI, the equations for describing BNR processes and the optimisation algorithms have been directly implemented in Matlab® scripts (.m files).

For complete information about the implementation of the simulated WWTP configurations, please send an e-mail to [javier.guerrero.camacho@gmail.com](mailto:javier.guerrero.camacho@gmail.com).



## **ANNEX II**

# Glycerol as a sole carbon source for EBPR

This Annex has been published as:

Guerrero, J., Tayà, C., Guisasola, A., Baeza, J.A., 2012. Glycerol as a sole carbon source for enhanced biological phosphorus removal. *Water Research* 46(9), 2983-2991.

<http://www.sciencedirect.com/science/article/pii/S0043135412001467>



## **Glycerol as a sole carbon source for enhanced biological phosphorus removal**

Javier Guerrero, Carlota Tayà, Albert Guisasola\* and Juan A. Baeza

\*Corresponding author: Albert Guisasola

Departament d'Enginyeria Química. Escola d'Enginyeria  
Universitat Autònoma de Barcelona, 08193, Bellaterra (Barcelona). Spain.

Tel: +34 93 581 1879

Fax: +34 93 581 2013

email: [albert.guisasola@uab.cat](mailto:albert.guisasola@uab.cat)

Javier Guerrero

Departament d'Enginyeria Química. Escola d'Enginyeria.

Universitat Autònoma de Barcelona, 08193, Bellaterra (Barcelona). Spain.

Tel: +34 93 581 4798

Fax: +34 93 581 2013

email: [franciscojavier.guerrero@uab.cat](mailto:franciscojavier.guerrero@uab.cat)

Carlota Tayà

Departament d'Enginyeria Química. Escola d'Enginyeria.

Universitat Autònoma de Barcelona, 08193, Bellaterra (Barcelona). Spain.

Tel: +34 93 581 4795

Fax: +34 93 581 2013

email: [carlota.taya@uab.cat](mailto:carlota.taya@uab.cat)

Juan A. Baeza

Departament d'Enginyeria Química. Escola d'Enginyeria.

Universitat Autònoma de Barcelona, 08193, Bellaterra (Barcelona). Spain.

Tel: +34 93 581 1587

Fax: +34 93 581 2013

email: [juanantonio.baeza@uab.cat](mailto:juanantonio.baeza@uab.cat)

## ABSTRACT

Wastewaters with low organic matter content are one of the major causes of EBPR failures in full-scale WWTP. This carbon source deficit can be solved by external carbon addition and glycerol is a perfect candidate since it is nowadays obtained in excess from biodiesel production. This work shows for the first time that glycerol-driven EBPR with a single-sludge SBR configuration is feasible (i.e. anaerobic glycerol degradation linked to P-release and aerobic P-uptake). Two different strategies were studied: direct replacement of the usual carbon source for glycerol and a two-step consortium development with glycerol anaerobic degraders and PAO. The first strategy provided the best results. The implementation of glycerol as external carbon source in full-scale WWTP would require a suitable anaerobic hydraulic retention time. An example with dairy wastewater with a low COD:P ratio confirms the feasibility of using glycerol as an external carbon source to increase P-removal activity. The approach used in this work opens a new range of possibilities and, similarly, other fermentable substrates can be used as electron donors for EBPR.

## KEYWORDS

Enhanced biological phosphorus removal (EBPR), consortium, glycerol, polyphosphate accumulating organisms (PAO), volatile fatty acids (VFA)

## 1. INTRODUCTION

Enhanced biological phosphorus removal (EBPR) is considered the most economical and sustainable technology to meet the increasingly stricter discharge requirements of wastewater treatment plants (WWTP) (Broughton *et al.*, 2008). EBPR is based on the enrichment of activated sludge with polyphosphate accumulating organisms (PAO). In contrast to other microorganisms, PAO can take up carbon sources under anaerobic conditions and store them as poly- $\beta$ -hydroxyalkanoates (PHA) for posterior utilisation under the presence of an electron acceptor. During this part of the process, PAO are able to accumulate phosphorus (P) in excess, which is then removed through the waste.

However, the effectiveness of EBPR highly depends on the nature of the carbon source that plays the electron donor role, being the presence of volatile fatty acids (VFA) a key factor to obtain a high P-removal capacity (Chu *et al.*, 1994; Randall *et al.*, 1997; Merzouki *et al.*, 2005; Guerrero *et al.*, 2011). This selective carbon utilisation by PAO hinders EBPR obtainment with influents with low organic content. Two different solutions are proposed to increase the VFA content of these wastewaters: i) an external VFA addition, which is usually not cost-effective and it increases the overall plant carbon footprint (Isaacs and Henze, 1993; Yuan *et al.*, 2010) and ii) the utilization of sludge pre-fermentation to produce these compounds (Tong and Chen, 2010; Feng *et al.*, 2009). Thus, the utilisation of waste materials that could be converted somehow to VFA is a very attractive alternative to overcome such VFA deficiency.

Glycerol is a by-product of biodiesel fuel production: about 1L of glycerol is generated for every 10L of biodiesel fuel produced (Johnson and Taconi, 2007). The glycerol derived from

biodiesel production has many impurities that together with the increase of its production have resulted in a drop of glycerol prices. As a consequence, glycerol has become a waste material with associated disposal costs (Yazdani and Gonzales, 2007; Escapa *et al.*, 2009). Nowadays, glycerol demand only constitutes a 22% of the annual production capacity (Johnson and Taconi, 2007) and thus, has grabbed the attention of the engineering community. Regarding the wastewater treatment field, it has been reported its use as a proper external carbon source for denitrification in WWTP (Grabinska-Loniewska *et al.*, 1985; Akunna *et al.*, 1993; Bodík *et al.*, 2009, Torà *et al.*, 2011). As abovementioned, EBPR is another biological process that may require external carbon addition and hence, it would be very practical to find an inexpensive carbon source suitable for both processes. Although the utilisation of glycerol for these purposes seems promising, few studies on its use as carbon source for EBPR have been reported. Yuan *et al.*, 2010 investigated glycerol as a possible carbon source in EBPR with two configurations: 1) direct application of glycerol as a sole carbon source and 2) supplementing a VFA-enriched supernatant from glycerol co-fermentation with waste activated sludge. Despite the latter was successful, the authors reported that EBPR activity was not achieved when glycerol was used as a sole carbon source. Anaerobic degradation of glycerol under certain conditions can yield significant propionate production (Barbirato *et al.*, 1997; Himmi *et al.*, 2000; Zhang and Yang, 2009), which is a good carbon source for EBPR (Oehmen *et al.*, 2005 and 2007). In fact, Pijuan *et al.* (2004) proved that PAO could selectively consume propionate against glycogen accumulating organisms (GAO, the competitors of PAO). Hence, an *in-situ* generation of propionate or other VFA (i.e. acetic acid) from glycerol would be a possible solution to achieve EBPR with glycerol as a sole carbon source.

The aim of this work was to study the feasibility of using glycerol as a sole carbon source on EBPR. For this purpose, a syntrophic consortium of conventional anaerobic biomass and PAO was needed. Then, anaerobic biomass would degrade glycerol and PAO would live off the fermentation products (mainly VFA) enabling thus EBPR. Two different strategies were tested: i) direct utilisation of glycerol by propionic fed-PAO and ii) two-step development (i.e. starting from conventional anaerobic sludge and then bioaugmenting with PAO). If glycerol-driven EBPR is attained, this would open a new range of possibilities for EBPR systems since not only glycerol but other fermentable substrates could be used following the approach presented in this work.

## 2. MATERIALS AND METHODS

### 2.1. Equipments

Three different sequencing batch reactors (SBR) were used in this study. All of them were fully monitored for oxygen (Hamilton, Oxyferm 120 probe), pH (Hamilton, polilyte Pro120 probe), ORP and temperature. SBR-A (10L) contained a PAO-enriched sludge for the bioaugmentation steps and it was operated with 4 cycles each day with a controlled temperature of  $25 \pm 1^\circ\text{C}$ . HCl (1M) and NaOH (1M) were added to control the pH at  $7.50 \pm 0.05$ . Each cycle consisted of 2 h anaerobic phase (AN), 3.5 h aerobic phase (O), 25 min of settling (S) and 5 min to extract 5 L of the supernatant. A fixed nitrogen gas flow was sparged during the anaerobic phase to maintain strict anaerobic conditions. Dissolved oxygen (DO)

was maintained from 3.5 to 4.5 mg·L<sup>-1</sup> in the aerobic phase to avoid oxygen limitations. A volume of 5 L (synthetic wastewater + concentrated carbon solution) was added during the first 5 minutes of the cycle, resulting in a HRT of 12 h. The synthetic wastewater solution (4.97 L) consisted of (mg·L<sup>-1</sup> in reverse osmosis water): 110.5 KH<sub>2</sub>PO<sub>4</sub>, 83.7 K<sub>2</sub>HPO<sub>4</sub>, 100 NH<sub>4</sub>Cl, 43.9 MgSO<sub>4</sub>·7H<sub>2</sub>O, 160 MgCl<sub>2</sub>·6H<sub>2</sub>O, 42 CaCl<sub>2</sub>·2H<sub>2</sub>O, 50 allylthiourea (ATU) to inhibit nitrification and 30 mL of trace element solution. The initial phosphorus concentration was 20 mg P-PO<sub>4</sub><sup>3-</sup>·L<sup>-1</sup>. The trace element solution (g·L<sup>-1</sup>) used consisted of: 1.5g FeCl<sub>3</sub>·6H<sub>2</sub>O, 0.15g H<sub>3</sub>BO<sub>3</sub>, 0.03g CuSO<sub>4</sub>·5H<sub>2</sub>O, 0.18g KI, 0.12g MnCl<sub>2</sub>·4H<sub>2</sub>O, 0.06g Na<sub>2</sub>MoO<sub>4</sub>·4H<sub>2</sub>O, 0.12g ZnSO<sub>4</sub>·7H<sub>2</sub>O, 0.15g CoCl<sub>2</sub>·6H<sub>2</sub>O and 68.5 mL EDTA 0.5M. 0.03 L of propionic (as propionic acid) was added from a separate concentrated solution to obtain the desired concentration in the reactor. The sludge residence time was maintained at 20 days with periodic wastage at the end of the aerobic phase.

SBR-B (10L) was operated as SBR-A to test the feasibility of a direct replacement of propionate for glycerol in propionate-acclimated PAO (withdrawn from SBR-A). The cycle configuration was modified in different periods, according to the data reported in Table 1. SBR-C was used to grow the syntrophic consortium for simultaneous glycerol and phosphorus removal using a two-step procedure. SBR-C (13 L) had only minor differences with respect to SBR-A or SBR-B. Initial anaerobic sludge inoculum was obtained from the anaerobic digester of a municipal WWTP (Granollers, Spain). A volume of 4 L of synthetic wastewater was added during the first 5 min of each cycle. Settling took place at the end of each cycle, followed by 5 min to extract 4 L of the supernatant. SBR-C was operated under different cycle configuration during this work, as summarized in Table 1.

Finally, the feasibility of using glycerol as external carbon source for wastewaters with a low COD:P content was studied. For this aim, dairy processing wastewater (Table 2) was used with a COD:P ratio that ranged between 13:1 to 10:1. SBR-B was inoculated with 5 L of PAO-enriched sludge from SBR-A and it was operated under the same conditions as period III (Table 1). Dairy wastewater was fed during the first week and afterwards a concentrated solution of glycerol was added together with the dairy wastewater (around 200 mg·L<sup>-1</sup> of glycerol expressed as COD were added in each cycle).

## 2.2. Batch experiments

Off-line batch experiments were performed in a magnetically stirred vessel (2 L). Each batch experiment mimicked a SBR-A cycle with a first anaerobic phase (by nitrogen sparging) and a subsequent aerobic phase (by oxygen sparging). pH (WTW Sentix 81) and DO (WTW Cellox 325) probes were connected to a multiparametric terminal (WTW INOLAB 3). It was in turn connected via RS232 to a PC with a specific software allowing for data monitoring and manipulation of a high precision microdispenser (Crison Multiburette 2S) for pH control with acid/base addition. Biomass (2 L) was withdrawn at the end of the aerobic phase of a SBR and was placed in the stirred vessel under anaerobic conditions. The experiment started with a pulse of concentrated feed with the desired propionate and P concentration.



### 2.3. Chemical and microbiological analyses

Glycerol concentration in 0.22 $\mu$ m filtered samples was determined by HPLC (Dionex Ultimate 3000) analysis using an ionic exchange column (ICSep ICE-COREGEL 87H3, Transgenomic). The mobile phase was 6mM sulphuric acid. The injection volume was 20 $\mu$ L and the chromatogram was quantified with the CROMELEON software (Dionex). Propionic and acetic acid concentrations in 0.22  $\mu$ m filtered samples were analysed by using a Agilent Technologies 7820 A GC equipped with a BP21 SGE column (30m x 0.25mm x 0.25 $\mu$ m; length x internal diameter x film thickness) and a flame ionisation detector (FID). A sample of 1  $\mu$ L was injected at a temperature of 275°C under pulsed split conditions (29 psi). The carrier gas was helium with a split ratio of 10:1 at 2.9 ml/min, the column temperature was set at 85°C for 1 minute, followed by an increase of 3°C·min<sup>-1</sup> to reach 130°C. A second ramp of 35°C/min was maintained to reach 220°C. A cleaning step at 230°C during 5 min was used to remove any residue in the column. The run time was 20 min and the detector temperature was set at 275°C. Phosphorus concentration in 0.22  $\mu$ m filtered samples was measured by a phosphate analyser (115 VAC PHOSPHAX sc, Hach-Lange) based on the Vanadomolybdate yellow method, where a two-beam photometer with LEDS measured the phosphate specific yellow colour. Organic matter, mixed liquor total suspended solids (TSS) and mixed liquor volatile suspended solids (VSS) were analysed according to APHA (1995).

PHA and glycogen were measured by triplicate. PHA was measured according to Oehmen *et al.* (2005b) in a GC system operated with a Hewlett Packard 5890 column (30m length x 0.53 mm I.D. x 1.00  $\mu$ m film). 40 mg of lyophilised sludge samples were digested and methylated with 4 ml of acidulated methanol (10% H<sub>2</sub>SO<sub>4</sub>) and 4 ml of chloroform during 20 h at 100 °C. Benzoic acid was used as internal standard. The calibration of the method was performed using a 3-hydroxybutyric acid and 3-hydroxyvaleric acid copolymer (7:3) as standards for PHB and PHV (Fluka, Buchs SG, Switzerland) and 2-hydroxycaproic acid as standard for PH2MV (Aldrich). Glycogen was determined with a modification of Smolders *et al.* (1994). A volume of 5 mL of 0.6 M HCl was added to each 20 mg of lyophilised sludge sample, and then heated at 100 °C for 6 h. After cooling and filtering through a 0.22  $\mu$ m filter (Millipore), the concentration of glucose was measured using a Yellow Spring Instrument (2700 Select). Fluorescence *in situ* hybridization (FISH) technique (Amann *et al.*, 1995) coupled with confocal microscopy was used to quantify the biomass distribution as in Jubany *et al.* (2009). Hybridizations were performed with Cy3-labelled specific probes and Cy5-labelled EUBMIX for most bacteria (Daims *et al.*, 1999). PAO were hybridized with PAOMIX probes and glycogen accumulating organisms (GAO) with GAOMIX, DF1MIX and DF2MIX probes as described in Guisasola *et al.* (2009).

## 3. RESULTS AND DISCUSSION

### 3.1. Direct replacement strategy

Our first strategy to achieve glycerol-based EBPR was to feed a PAO-enriched sludge with glycerol as a sole carbon source. SBR-B was inoculated with PAO-enriched sludge withdrawn from SBR-A, which had been fed for several months with propionate as sole carbon source under conventional anaerobic-aerobic conditions. The major characteristics of this sludge were: 61 $\pm$ 6 % PAO, a P/C ratio of 0.44 mol P/mol C<sub>PROP</sub> (typical of propionic-fed

PAO, Oehmen *et al.*, 2005a), a P-release rate of  $31.4 \text{ mg P}\cdot\text{g}^{-1} \text{ VSS h}^{-1}$ ,  $2.7 \text{ g VSS}\cdot\text{L}^{-1}$  and a VSS/TSS ratio at the end of the aerobic phase of 0.71. All these values were indicative of a sludge highly enriched in PAO.

Three periods (I, II, III) with different SBR configurations were used (Table 1). Figures 1 and 2 summarise the results of this strategy. Period I consisted of a direct replacement of propionate for glycerol with the standard cycle configuration used with propionate in SBR-A. The initial glycerol concentration was set to a low value of  $60 \text{ mg}\cdot\text{L}^{-1}$  to avoid its presence under aerobic conditions. From the first day on, most of the glycerol was consumed under anaerobic conditions (Figure 2). However, this anaerobic COD consumption was not linked to any EBPR activity as neither P release nor P uptake was observed (Figure 1). During this period, PAO activity was periodically assessed through batch experiments with propionate as carbon source and PAO activity was progressively lost. Figure 3 (left) displays four of these batch tests conducted during all the direct replacement strategy experiment. The comparison of the batch tests at the start and at the end of period I (i.e. black vs white triangles) clearly shows this EBPR activity loss. These results were in agreement with the results of Yuan *et al.* (2010), who introduced glycerol in an acetate-fed PAO-enriched sludge and the process failed.

The initial amount of glycerol in period I was very low and, given the fact that it was not totally converted to PAO-utilisable products (see discussion below), the system might have been carbon limited. Then, it was decided to increase the amount of the initial glycerol up to  $200 \text{ mg}\cdot\text{L}^{-1}$  and, consequently, increase the length of the anaerobic phase to 5 hours (Table 1) so all glycerol could be anaerobically consumed (the total cycle length was in consequence extended to 8 hours in period II). Due to the decrease of PAO activity during period I (Table I), SBR-B was bioaugmented with 5 L of PAO-enriched sludge from SBR-A to have a similar initial PAO population as period I. This glycerol load increase was beneficial and, after two weeks, P release was already observed (Figure 1). Despite the periodic increase of the P released, net-P removal was never achieved in period II, which prevented successful PAO enrichment (Figure 1). Initial glycerol was increased (Figure 2) so that P uptake rate also increased as a consequence of higher PHA storage. However, EBPR activity did not improve in period II. Periodical batch tests with propionate indicated a certain recovery of EBPR activity with respect to period I (Figure 3 left). However, the experimental glycerol and P profiles of the cycles (results not shown) indicated that, whereas the anaerobic phase was longer than needed to take up all the initial COD, the aerobic phase was too short for complete P removal. Then, it was decided to test a last cycle configuration (period III) with longer aerobic phase (Table 1).

The configuration in period III was proved to be very successful and net-P removal was rapidly achieved (Figure 1). Consequently, PAO growth was favoured and EBPR activity was clearly observed. It was decided to push the system to its limits and the amount of initial glycerol was step-wise increased up to  $500 \text{ mg}\cdot\text{L}^{-1}$  (Figure 2). Figure 3 (left) shows that the EBPR activity (tested with propionate) improved after period III. Moreover, figure 3 (right) illustrates a typical EBPR test with glycerol as a sole carbon source during this period,

demonstrating for the first time glycerol-driven EBPR in a single sludge system. The major causes of the success were that the SBR phases were sufficiently long for anaerobic glycerol uptake and posterior aerobic P uptake.

Two extra indications of the PAO increase during this period are the FISH measurements and the P/C ratio evolution (i.e. amount of P released per mol of carbon-glycerol taken up). The percentage of PAO was estimated at the end of each period using the FISH methodology (Table 1). The obtained results, i.e. sharp increase of % PAO in period III, are in clear agreement with the experimental P profiles obtained. Figure 2 displays the P/C ratio evolution throughout the experiment. As can be observed, the ratio tends to 0.2 mol P/mol  $C_{\text{GLYCEROL}}$ . At first glance, this value may seem very low, particularly when compared to P/C ratios for conventional PAO electron donors: acetate (0.5 mol P/mol  $C_{\text{AC}}$ , Smolders et al., 1994) or propionate (0.42 mol P/mol  $C_{\text{PROP}}$ , Oehmen et al., 2005a), however an explanation could be given: we hypothesise that glycerol was not directly used by PAO but it was firstly anaerobically degraded to products that could be used by PAO, essentially propionate. This would explain why glycerol was not directly used for PAO in the period I and also the long time required for EBPR obtainment in our system, i.e. the time required for anaerobic-glycerol degraders or fermenters to grow. The anaerobic glycerol metabolism is widely described in the literature and propionate is known as the major fermentation product of its metabolism with respect to other compounds such as acetate, butyrate or propanol (Barbirato et al., 1997; Himmi et al., 2000; Yuan et al., 2010). The ratio of propionate to glycerol depends on the microbial culture used, being 0.6-0.8 mol/mol an average yield found in the literature with pure cultures, for example, *Propionibacterium freudenreichii* or *Propionibacterium acidipropionici* (Barbirato et al., 1997; Himmi et al., 2000; Zhang and Yang, 2009). However, this yield may be lower with mixed cultures. The real value is difficult to predict since the selectivity of fermentation products from a single substrate in mixed culture fermentations is, nowadays, a research issue (Temudo et al., 2008; Forrest et al., 2010). Hence, the maximum P/C ratio that could be obtained from glycerol could be calculated assuming i) the abovementioned propionic to glycerol yields and ii) that only PAO used the fermentation products. This would result in theoretical maximum P/C ratios around 0.25-0.33 mol P/mol  $C_{\text{GLYCEROL}}$ , which are closer to the ones experimentally observed (Figure 2). The lower values obtained could be probably linked to the fact that the propionate yield from glycerol was lower. In fact, the results obtained in the next section with a mixed culture (Figure 4) show a yield around 0.5 mol of propionate per mol of consumed glycerol (see discussion below) that would result in a theoretical P/C ratio of 0.21 mol P/mol  $C_{\text{GLYCEROL}}$ , which agrees with the experimental P/C ratio obtained (Figure 2). Another reason for this low P/C ratio could be the simultaneous consumption of part of glycerol or propionate by other microorganisms as for example GAO. Table 1 shows the percentage of GAO after periods II and III. Figures S1-S4 show an example of the FISH images obtained after period III. A significant amount of GAO, mostly DF1MIX-binding GAOs were present. These microorganisms were already present in the initial inoculum (SBR A) and are commonly observed in propionate-fed EBPR systems (Oehmen et al., 2009). Thus, the fact that DF1MIX-binding bacteria were not removed during this period can also be an indicator of propionate-based EBPR metabolism.

Moreover, PHA and glycogen evolution was monitored in a batch experiment at the end of period III. The results obtained were in agreement with the discussion above. The ratio of glycogen degraded to glycerol consumed in the anaerobic phase was around 0.25 mol  $C_{\text{GLYCOGEN}}/\text{mol } C_{\text{GLYCEROL}}$  which is lower than the theoretical value reported in the propionate metabolism of PAO (0.33 Oehmen *et al.*, 2005a). This is in agreement with the fact that only a fraction of glycerol turns into PAO-utilisable products. Regarding PHA, its distribution at the end of the anaerobic phase was also distinctive of propionate-fed EBPR systems with a high presence of PHV and PH2MV (Pijuan *et al.*, 2009). In our case, the average distribution of the PHA at the end of the anaerobic phase was 25 % PHB, 45 % PHV and 30 % PH2MV. The ratio of PHA produced per glycerol taken up in molar basis ( $\text{PHA}/C_{\text{GLYCEROL}}$ ) was 0.31, which is also lower than the theoretical value of 1.22 reported in Oehmen *et al.* 2005a.

Assuming that a fermentation step was required in order to obtain glycerol-based EBPR, a new strategy was designed for a faster obtainment of the consortium sludge (i.e. anaerobic glycerol degraders + PAO). This two-step strategy consisted on bioaugmenting a glycerol-fed anaerobic sludge with PAO. The anaerobes (essentially, acidogens) would anaerobically degrade glycerol and PAO would live off the fermentation products enabling thus, simultaneous glycerol and phosphorus removal.

### 3.2. Two-step consortium development strategy

This strategy aimed at obtaining simultaneous glycerol and P removal using a syntrophic consortium between glycerol-degrading anaerobes and PAO in a two-step basis. The first should degrade glycerol to fermentation products, which in turn would be used by PAO for biological phosphorus removal purposes. This syntrophic consortium was obtained using a two-step procedure. In a first step (see Table 1, periods A-C), anaerobic sludge inoculated in SBR-C was subjected to conditions so that anaerobic glycerol was favoured against methanogenesis. Then, in a second step (periods D-E from Table 1), SBR-C was bioaugmented with PAO-enriched sludge so that PAO live off the anaerobic glycerol degradation products.

Period A corresponded to the acclimatization period where a conventional anaerobic community was subjected to glycerol under strict anaerobic conditions (SBR C). Figure 4 left shows the glycerol profiles of two cycles from this period. As can be observed, anaerobic glycerol utilization was obtained from the very first day. During this period, glycerol was likely converted to methane since fermentation products were scarcely present at the end of the reactive phase. In period B, a short aerobic phase (30 min) was introduced to suppress the possible methanogenic activity. Figure 4 right shows three monitored cycles during period B. As can be observed, the introduction of intermittent aeration (0.5 h of every 6 hours) resulted in propionate production due to the expected suppression of methanogenic activity, which is in agreement with textbook knowledge (Hungate, 1969; Martin and Savage, 1988; Whitman *et al.*, 1992). Glycerol was mostly degraded to propionate with an average ratio of  $0.50 \pm 0.05$  (n=5) mol propionate / mol glycerol. As abovementioned, this value was lower than the ones reported in the literature for pure cultures and seems to be in agreement with the experimental results found in the previous section. The aerobic phase was extended two hours during

period C to assess whether long aerobic phases (typical of EBPR systems) were detrimental to anaerobic glycerol-degraders. The results (not shown) were very similar to the ones obtained in period B, indicating that the conventional EBPR configuration was not harmful for this anaerobic sludge and that PAO bioaugmentation was feasible.

The system was bioaugmented with PAO at the start of period D (Figures 5 and 6) and EBPR linked to glycerol degradation was observed from the first day on. However, the extent of P release and P uptake was not as high as expected and the amount of net P removed was very low. Similarly to the direct replacement strategy, the experimental P profiles indicated that EBPR activity was hindered by an aerobic phase that was too short. Then, aerobic phase was extended in period E (Table 1) resulting in the same configuration as in period III of SBR B. The results obtained in period E were more satisfactory than in period D; however, the EBPR activity observed with the direct replacement strategy was never achieved. The major cause of this difference can be found in the experimental ratios that indicate that part of the initial glycerol was not used for EBPR purposes:  $P/C_{\text{GLYCEROL}}$  ratio (always lower than 0.15),  $\text{Gly}_{\text{DEG}}/C_{\text{GLYCEROL}}$  (0.27 in a batch experiment at the end of period E) and  $\text{PHA}/C_{\text{GLYCEROL}}$  (0.47 in a batch experiment at the end of period E). These values, lower than the theoretical values proposed for propionate-fed PAO (Oehmen *et al.*, 2005b). The PHA distribution in these experiments was 8 % PHB, 35 % PHV and 57 % PH2MV, distinctive again of propionate-based EBPR metabolism. The growth of some glycerol degraders (inoculated with the anaerobic sludge) that did not produce VFA and the promotion of anaerobic VFA scavengers other than PAO (as for example GAO, see Table 1) could be a possible explanation for this fact. Figures S5-S7 show an example of the FISH images obtained after period E, where a significant fraction of DF1MIX-binding GAO can be observed. In any case, it should be noted that this strategy also resulted in a significant PAO growth (Table 1) achieving PAO percentages similar to the direct replacement strategy. As a conclusion, despite the fact that glycerol-based EBPR was obtained, this strategy failed to be faster (or even better) than the previous strategy and, hence, according to our experimental results, the direct replacement strategy is recommended.

Using long anaerobic retention times, the growth of anaerobic-glycerol degraders which produce PAO-utilisable products are favoured due to the presence of a highly active EBPR sludge that rapidly uses these fermentation products. However, if anaerobic glycerol-degraders are previously selected without PAO, different anaerobic glycerol degradation routes could be favoured, including bacteria (other than PAO) able to use fermentation products.

### 3.3 Practical implications

This is the first work where glycerol-driven EBPR in a single-sludge system is proved. In particular, the best results were obtained when using the 4(AN) +3.5(O) +0.5(S) cycle configuration in a SBR rather than a two-step strategy.

These results have two major implications:

- Glycerol can be an alternative external carbon source for WWTP facing carbon source shortages. A possible solution is to add external carbon sources to achieve complete P removal and avoid EBPR failures. Glycerol could be applied in full-scale WWTP if enough anaerobic hydraulic retention time was provided.
- The development of a microbial community able to use glycerol for EBPR opens a new range of possibilities. With a similar approach, other fermentable substrates could also be used as carbon sources for EBPR.

Figure 7 illustrates the latter two statements. A SBR was run using dairy wastewater as sole carbon source which led to a low COD:P ratio (between 10:1 and 13:1). According to Broughton *et al.* (2009), 13:1 is the minimum ratio in order to have successful P-removal in similar wastewaters. As can be observed, both net-P removal and the percentage of P-removal were very low during the first days. Then, from day 7 on, a concentrated solution of glycerol was added together with dairy wastewater resulting in a COD:P ratio increase up to 15:1 – 17:1. This modification led to successful results since both net-P removal and the percentage of P-removal were significantly increased.

This study completes previous works where glycerol was shown as a good carbon source for denitrification. Consequently, glycerol could be recommended as an external carbon source for both nitrogen and phosphorus removal. This would simplify WWTP management avoiding the utilization of more dangerous carbon sources as methanol, which must be diluted to reduce its fire hazard and would also allow the utilization of a waste material with a disposal associated costs. However, the interaction between denitrifiers and PAO and their competition for the carbon source must be further studied in view of its utilisation in biological nutrient removal systems. These studies, which were out of the scope of the present work, are nowadays being conducted as a continuation of this research line.

#### 4. CONCLUSIONS

This work demonstrates the feasibility of using glycerol as a sole carbon source for EBPR. The best results were obtained with the direct replacement strategy with a longer anaerobic phase than the default configuration. Using long anaerobic retention times, anaerobic glycerol degradation to PAO-utilisable products are favoured due to the presence of a highly active EBPR sludge. The single-sludge SBR with 4 h anaerobic, 3.5 h aerobic and 0.5 settling was shown as a proper configuration to achieve net P removal using only this carbon source. Therefore, glycerol is a promising external carbon source in full-scale WWTP facing carbon source shortages when enough anaerobic hydraulic retention time is provided.

#### 5. ACKNOWLEDGMENTS

This work was supported by the Spanish *Ministerio de Ciencia y Tecnología* (CTQ2007-61756/PPQ). The authors are members of the GENOCOV group (Grup de Recerca Consolidat de la Generalitat de Catalunya, 2009 SGR 815). The authors would like to thank Marta Ferreres for her support in the laboratory.

## 6. REFERENCES

- Amann, R.I., Ludwig, W., Schleifer, K.H., 1995. Phylogenetic identification and in situ detection of individual microbial cells without cultivation. *Microbiology Reviews*. 59 (1), 143-169.
- APHA, 1995. Standard methods for the examination of water and wastewater, 19th ed., American Publishers Health Association, Washington, DC, USA.
- Akunna, J. C., Bizeaua, C., Moletta, R., 1993. Nitrate and nitrite reductions with anaerobic sludge using various carbon sources: Glucose, glycerol, acetic acid, lactic acid and methanol. *Water Research* 27(8), 1303–1312.
- Barbirato, F., Chedaille, D., Bories, A., 1997. Propionic acid fermentation from glycerol: comparison with conventional substrates. *Applied Microbiology and Biotechnology* 47 (4), 441-446.
- Bodík, I., Blštáková, A., Sedláček, S., Hutnan, M., 2009. Biodiesel waste as source of organic carbon for municipal WWTP denitrification. *Bioresource Technology* 100(8), 2452-2456.
- Broughton, B., Pratt, S., Shilton, A., 2008. Enhanced biological phosphorus removal for high-strength wastewater with a low rbCOD:P ratio. *Bioresource Technology* 99(5), 1236-1241.
- Chu, A., Mavinic, D. S., Kelly, H. G., Ramey, W. D., 1994. Volatile fatty acid production in thermophilic aerobic digestion of sludge. *Water Research* 28(7), 1513–1522.
- Daims, H., Brühl, A., Amann, R., Schleifer, K.H., Wagner, M., 1999. The domain-specific probe EUB338 is insufficient for the detection of all bacteria: Development and evaluation of a more comprehensive probe set. *System Applied Microbiology* 22(3), 434-444.
- Escapa, A., Manuel, M.F., Morant, A., Gomez, X., Guiot, S.R., Tartakovsky, B., 2009 Hydrogen production from glycerol in a membraneless microbial electrolysis cell. *Energy and Fuels* 23 (9), 4612-4618.
- Feng, L., Chen, Y., Zheng, X., 2009. Enhancement of waste activated sludge protein conversion and volatile fatty acids accumulation during waste activated sludge anaerobic fermentation by carbohydrate substrate addition: The effect of pH. *Environmental Science and Technology* 43 (12), 4473-4380.
- Forrest, A.K., Sierra R., Holtzapple, M. T., 2010. Effect of biodiesel type and fermentor configuration on mixed-acid fermentations. *Bioresource Technology* 101 (23), 9185-9189.
- Grabinska-Loniewska, A., Slomczynski, T., Kanska, Z., 1985. Denitrification studies with glycerol as a carbon source. *Water Research* 19(12), 1471–1477.
- Guerrero, J., Guisasola, A., Baeza, J.A., 2011. The nature of the carbon source rules the competition between PAO and denitrifiers in systems for simultaneous biological nitrogen and phosphorus removal. *Water Research* 45(16), 4793-4802.
- Guisasola, A., Qurie, M., Vargas, M. M., Casas, C., Baeza, J. A., 2009 Failure of an enriched nitrite-DPAO population to use nitrate as an electron acceptor. *Process Biochemistry* 44(7), 689-695.
- Himmi, E.H., Bories, A., Boussaid, A., Hassani, L., 2000. Propionic acid fermentation of glycerol and glucose by *Propionibacterium acidipropionici* and *Propionibacterium freudenreichii ssp. shermanii*. *Applied Microbiology and Biotechnology* 53 (4), 435-440.
- Hungate, R. E., 1969. A roll tube method for cultivation of strict anaerobes. In *Methods in Microbiology*, vol. 3B. Norris, J. R. and Ribbons D.W.; Eds.; Academic Press, New York. 1969; pp. 117-132.

- Isaacs, S.H., Henze, M., 1995. Controlled carbon source addition to an alternating nitrification–denitrification wastewater treatment process including biological P removal. *Water Research* 29(1), 77–89.
- Johnson D.T., Taconi K.A., 2007. The glycerin glut: options for the value-added conversion of crude glycerol resulting from biodiesel production. *Environment Progress* 26, 338–348.
- Jubany, I., Lafuente, J., Carrera, J., Baeza, J.A., 2009. Automated thresholding method (ATM) for biomass fraction determination using FISH and confocal microscopy. *Journal of Chemical Technology and Biotechnology* 84, 1140-1145.
- Martin, J.H., Savage, D.C., 1988. Degradation of DNA in cells and extracts of the obligately anaerobic bacterium *Roseburia cecicola* upon exposure to air. *Applied and Environmental Microbiology* 54(6), 1619-1621.
- Merzouki, M., Bernet, N., Delgenès, J.P., Benlemlih, M., 2005. Effect of prefermentation on denitrifying phosphorus removal in slaughterhouse wastewater. *Bioresource Technology* 96(12), 1317-1322.
- Oehmen, A., Zeng, R. J., Yuan, Z G., Keller, J., 2005a. Anaerobic metabolism of propionate by polyphosphate-accumulating organisms in enhanced biological phosphorus removal systems. *Biotechnology Bioengineering*. 91(1), 43–53.
- Oehmen, A., Lehmann, B.K., Zeng, R.J., Yuan, Z., Keller, J. 2005b. Optimisation of poly- $\beta$ -hydroxyalkanoate analysis using gas chromatography for enhanced biological removal systems. *Journal of Chromatography A*, 1070(1-2), 131-6.
- Oehmen, A., Lemos, P.C., Carvalho, G., Yuan, Z., Kelley J., Blackhall L.L., Reis M.A.M., 2007. Advances in enhanced biological phosphorus removal: From micro to macro scale. *Water Research* 41 (11), 2271-2300.
- Oehmen A., Lopez-Vazquez C.M., Carvalho G., M.A.M. Reis M.A.M., Van Loosdrecht M.A.M., 2009. Modelling the population dynamics and metabolic diversity of organisms relevant in anaerobic/anoxic/aerobic enhanced biological phosphorus removal processes. *Water research* 44(15), 4473-4486.
- Pijuan, M., Saunders, A. M., Guisasola, A., Baeza, J. A., Casas, C., Blackall, L. L., 2004. Enhanced biological phosphorus removal in a sequencing batch reactor using propionate as the sole carbon source. *Biotechnology Bioengineering* 85(1), 56–67.
- Pijuan M., Casas C., Baeza J.A., 2009. Polyhydroxyalkanoate synthesis using different carbon sources by two enhanced biological phosphorus removal microbial communities. *Process Biochemistry* 44(1), 97-105.
- Randall A.A., Benefield, L.D., Hill, W.E., Nicol, J.P., Boman, G.K., Jing, S.R., 1997. The effect of volatile fatty acids on enhanced biological phosphorus removal and population structure in anaerobic/aerobic sequencing batch reactors. *Water Science and Technology* 35(1), 153-160.
- Smolders, G.J.F., van der Meij, J., van Loosdrecht, M.C.M., Heijnen, J.J. 1994. Model of the anaerobic metabolism of the biological phosphorus removal process: Stoichiometry and pH influence. *Biotechnology Bioengineering* 43, 461-70.
- Temudo, M.F., Poldermans, R., Kleerebezem, R., van Loosdrecht, M.C.M., 2008. Glycerol fermentation by (open) mixed cultures: A chemostat study. *Biotechnology and Bioengineering* 100 (6), 188-1098.



- Tong, J.A., Chen, Y.G., 2007. Enhanced biological phosphorus removal driven by short-chain fatty acids produced from waste activated sludge alkaline fermentation. *Environmental Science and Technology* 41(20), 7126-7130.
- Torà, J.A., Baeza, J.A., Carrera, J., Oleszkiewicz, J.A., 2011. Denitritation of a high-strength nitrite wastewater in a sequencing batch reactor using different organic carbon sources. *Chemical Engineering Journal* 172 (2-3), 994-998.
- Whitman, W.B., Bowen, T.C., Boone, D.R., 1992. In: *The Prokaryotes*, Vol. I. Balows, A., TruÈ per, H.G., Dworkin, M., Harder, W., Schleifer, K.H.; Eds.; Springer Verlag, New York. 1992; pp. 719-767.
- Yazdani, S.S., Gonzales, R., 2007. Anaerobic fermentation of glycerol: a path to economic viability for the biofuels industry. *Current Opinion in Biotechnology* 18 (3), 213–219.
- Yuan, Q., Sparling, R., Lagasse, P., Lee, Y.M., Taniguchi, D., Oleszkiewicz, J. A., 2010. Enhancing biological phosphorus removal with glycerol. *Water Science and Technology* 61(7), 1837-1843.
- Zhang, A., Yang, S.T., 2009. Propionic acid production from glycerol by metabolically engineered *Propionibacterium acidipropionici*. *Process Biochemistry* 44 (12) 1346-1351.

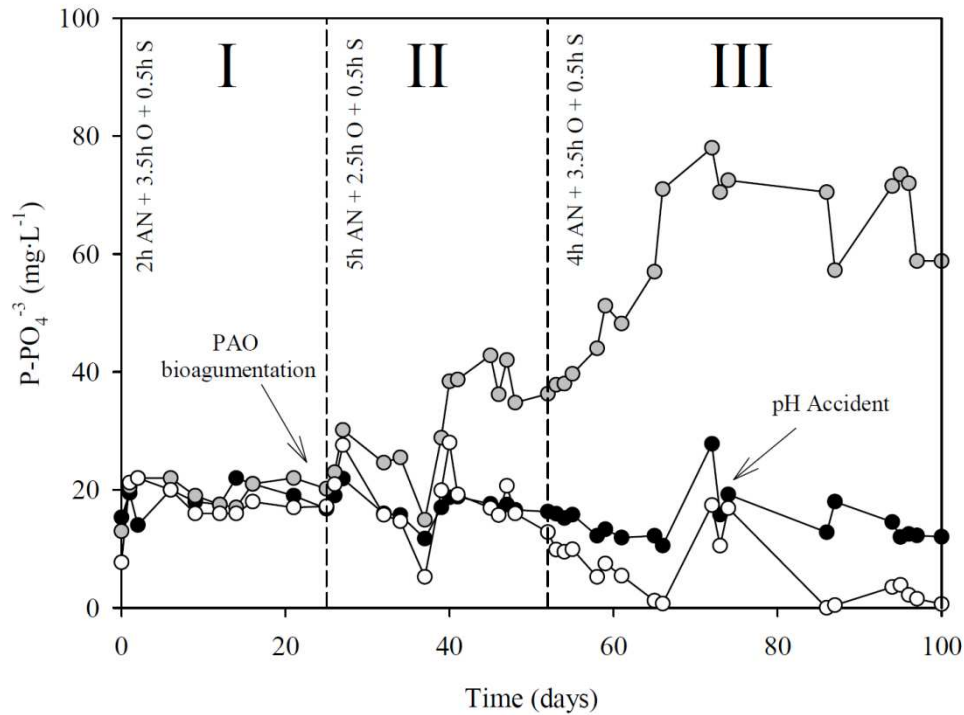


**Figure 1** Profiles during the direct replacement of propionic acid for glycerol strategy. Initial (black), end anaerobic phase (grey), end aerobic phase (white).

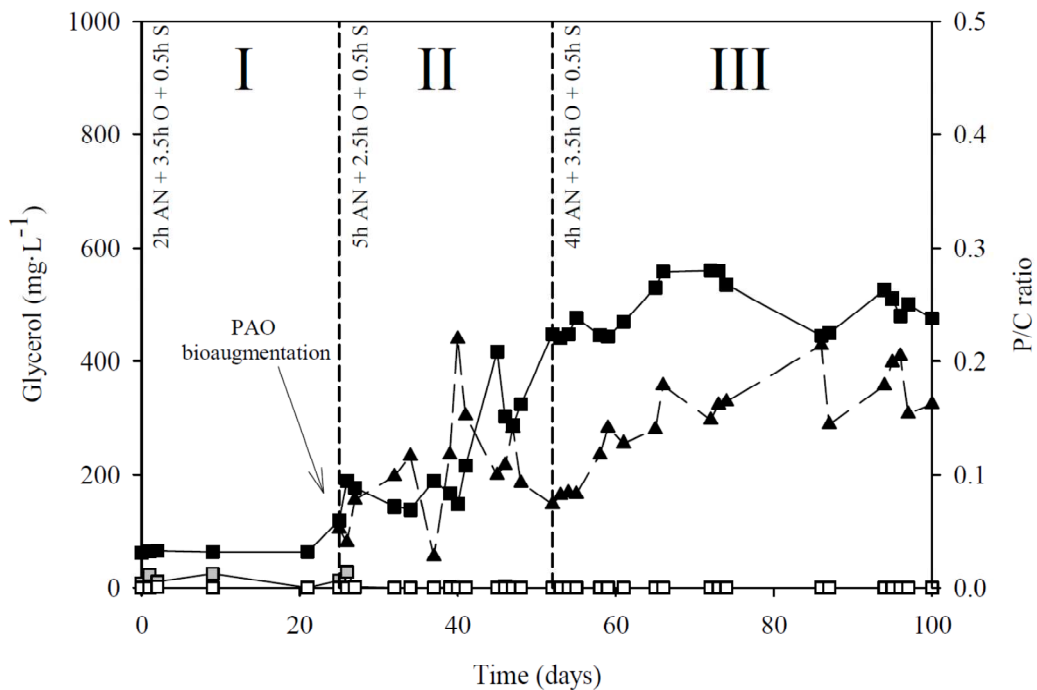


**Figure 2** Glycerol (■) and P/C ratio (▲) during the direct replacement of propionic acid for glycerol strategy. Concentration of glycerol: Initial (black), end anaerobic phase (grey), end aerobic phase (white).

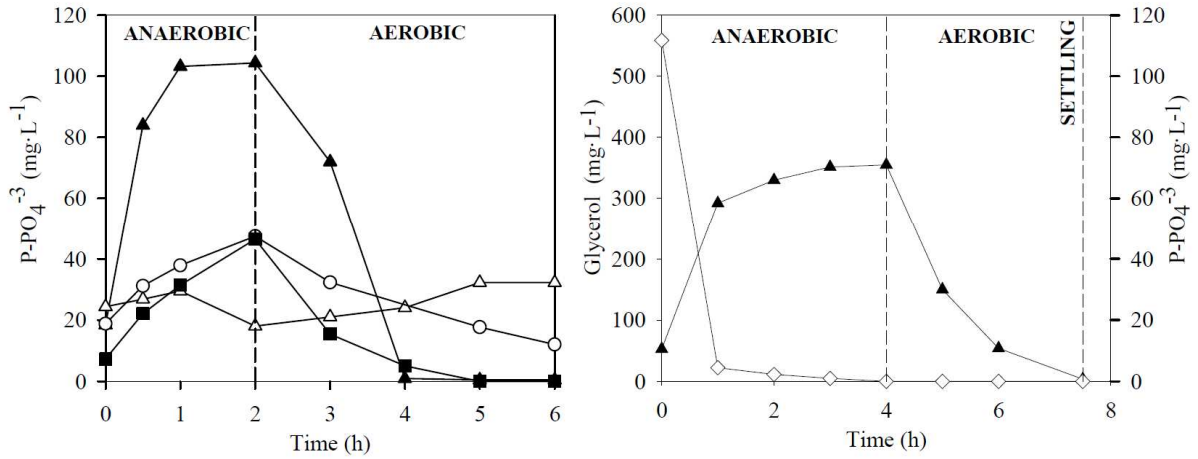


**Figure 3** LEFT: P profiles in four different batch tests with propionic acid during the direct replacement strategy: ▲ (start of period I), △ (end of period I) ○ (end of period II) ■ (mid period III). RIGHT Experimental P (▲) and glycerol (◇) profiles from the last cycle of period III.

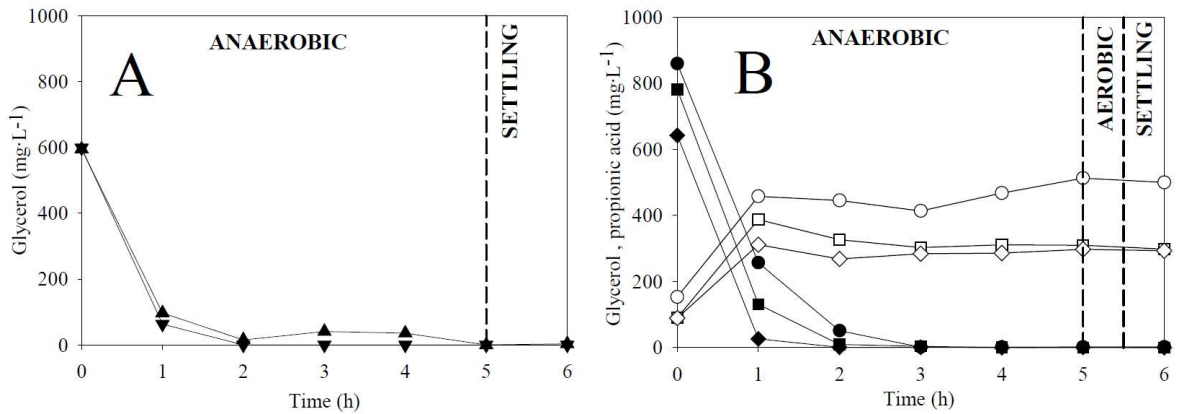


**Figure 4** Glycerol profiles for two cycles of period A of the consortium development strategy: ▲ day 1 ▼ day 5. RIGHT: Glycerol (black) and propionic acid (white) profiles for three different cycles during period B of the consortium development strategy: ● day 13 ■ day 21 ◆ day 26.

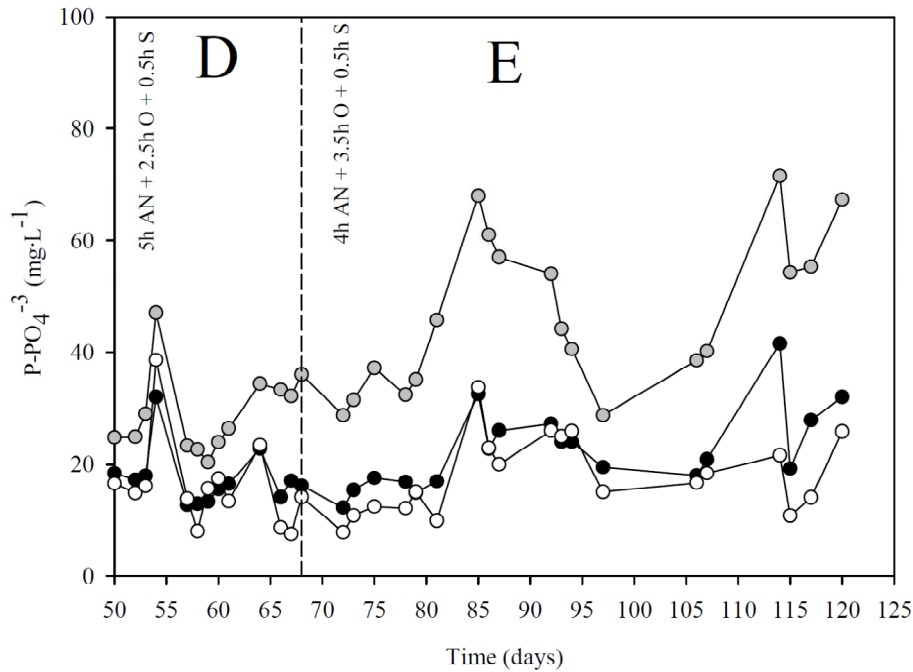


**Figure 5** P profiles during the periods D and E of the consortium development strategy. Initial (black), end anaerobic phase (grey), end aerobic phase (white).

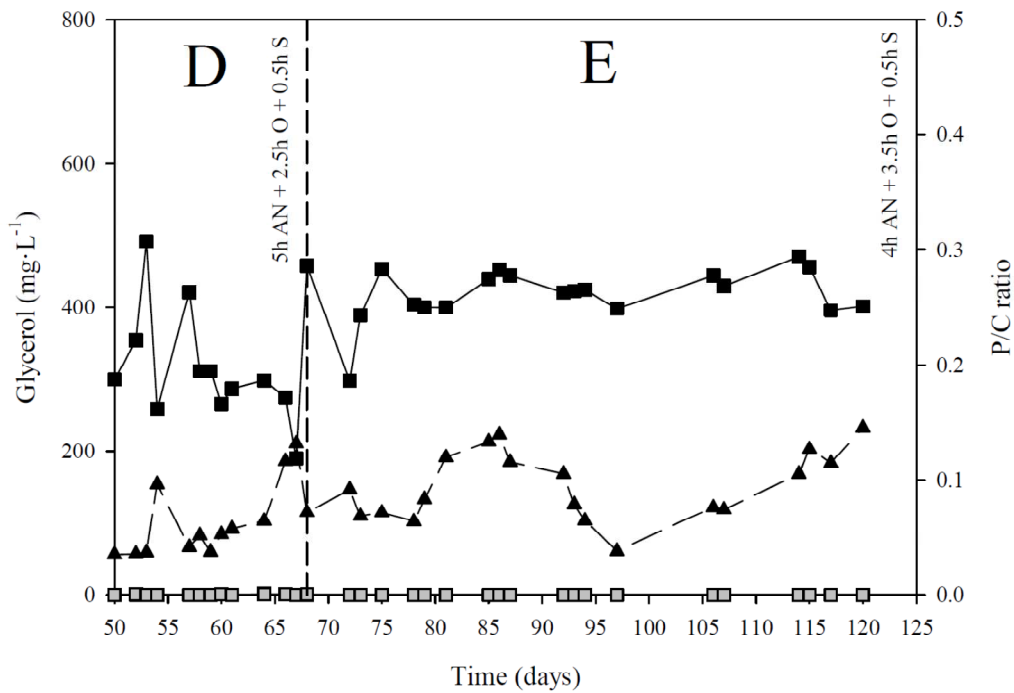


**Figure 6** Glycerol (■) and P/C ratio (▲) profiles during the periods D and E of the consortium development strategy. Concentration of glycerol: Initial (black), end anaerobic phase (grey).

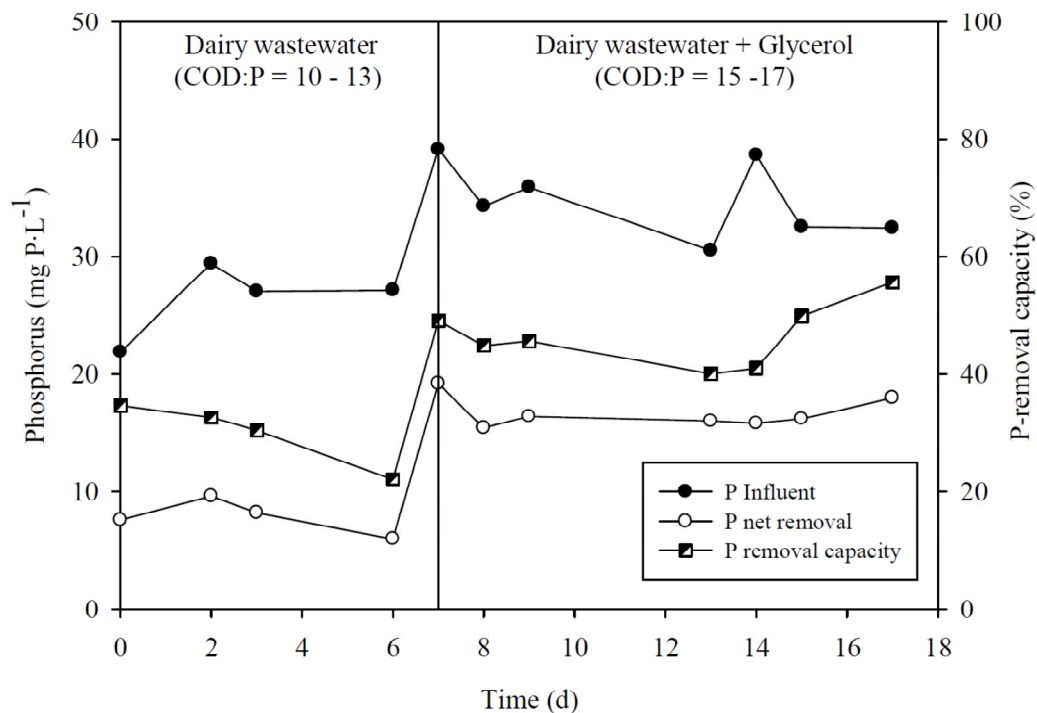


**Figure 7** Experimental net-P removal activity variation when glycerol is supplemented to a dairy wastewater feed.

**Table 1** Description of the different periods for the proposed strategies

	Period	Days	Cycle configuration (h) <sup>1</sup>	VSS (mg·L <sup>-1</sup> ) <sup>2</sup>	VSS/TSS <sup>2</sup>	% PAO <sup>2,3</sup>	%GAO <sup>2,4</sup>
DIRECT REPLACEMENT	I	0-25	2+3.5+0.5	1130	0.84	< 5 %	N.A.
	II	26-52	5+2.5+0.5	1890	0.89	35±6	41±4 (39±4: 1±0.5:1±0.5)
	III	53-100	4+3.5+0.5	4670	0.71	46±4	37±7 (34±7:1.7±0.3:1.1±0.5)
TWO-STEP DEVELOPMENT	A	0-7	5 +0+1	3026	0.82	N.A.	N.A.
	B	8-40	5+0.5+0.5	3255	0.98	N.A.	N.A.
	C	41-50	5+2.5+0.5	6152	0.86	N.A.	N.A.
	D	51-68	5+2.5+0.5	6450	0.85	8±3	23±3 (20±3:1.3±0.2:1.9±0.4)
	E	69-125	4+3.5+0.5	5530	0.88	43±4	31±4 (30±4:0.7±0.2:N.D)

N.A.: not available, <sup>1</sup>Anaerobic(AN)+Aerobic(O)+Settling(S); <sup>2</sup> values at the end of the period; <sup>3</sup>percentage of PAOMIX –binding bacteria; <sup>4</sup>percentages of total GAO and DF1MIX:DF2MIX:GAOMIX –binding bacteria

**Table 2** Dairy processing wastewater characteristics without glycerol addition

<b>Composition</b>	<b>Concentration (mg·L<sup>-1</sup>)</b>
Total COD	355-455
N-NH <sub>4</sub> <sup>+</sup>	20
P-PO <sub>4</sub> <sup>-3</sup>	35
TSS	127
pH	5.0-7.6

## Fco. Javier Guerrero Camacho – Curriculum Vitae

### Personal Data

---

Name: Francisco Javier Guerrero Camacho  
DNI: 47175315 S  
Place and born date: Sabadell, Spain 23/01/1985  
Address: C/Malta 72, 5<sup>º</sup>2<sup>a</sup>, 08205, Sabadell. Barcelona, Spain.  
Telephone: +34 695 430 985  
Email: javier.guerrero.camacho@gmail.com



### Education

---

- |                 |  |
|-----------------|--|
| 2010 - Present  | PhD Student in Environmental Science and Technology,<br>Universitat Autònoma de Barcelona<br>Title: "Improving EBPR stability in WWTPs aiming at simultaneous carbon and nutrient removal: From modelling studies to experimental validation." |
| Sept – Dec 2011 | Research staying at Centre for process engineering and technology,<br>Technical University of Denmark  |
| 2008-2009       | Master in Environmental Studies. Environmental Technology,<br>Universitat Autònoma de Barcelona<br>Title: "Improving WWTP control strategies for simultaneous C/N/P removal by setpoint optimisation".   |
| 2003-2008       | Chemical Engineering (University degree),<br>Universitat Autònoma de Barcelona   |

### Former Scientific Activities and Present Professional Status

---

- |                             |   |
|-----------------------------|---|
| 2009-2011                   | Teaching assistant in the Departament d'Enginyeria Química (Universitat Autònoma de Barcelona).<br>Control and Instrumentation of chemical processes, chemical engineering lab-experimentation and chemical reaction engineering. |
| 2010-2013                   | PhD grant (FPU – Ministerio de educación, cultura y deporte).   |
| August 2013 –<br>March 2014 | Chemical Engineer at the Projects Department in Ahidra, Agua y Energía.   |

### Languages and Computer skills

---

English: Speaking (medium level) and technical writing (high)  
Spanish: Speaking and writing (Native)  
Catalan: Speaking and writing (Native)

Sigmaplot (Advanced level), Windows and Office (Advanced level), Linux (Medium level), C++ (Medium level), MATLAB-Simulink® (Advanced level), AutoCAD® and Plant 3D (Medium level) and Processes simulator HYSYS® (Medium level).

## **Rewards**

---

Idea Award 2012 by the Catalan Biotechnology Reference Network (XRB) to the study entitled: "Flotació in-situ al sedimentador, un mètode novell per a minimitzar el bulking filamentós a les EDARS biològiques".

## **Public research projects**

---

Operación y control óptimo de EDAR: desarrollo e implementación de nuevas estrategias de operación y control para la eliminación de nutrientes diseñadas con técnicas de modelización y benchmarking. October 2007-September, 2010. Scientific in charge: Juan Antonio Baeza Labat.

Estudio mediante herramientas de simulación para la optimización del funcionamiento de la EDAR de Manresa, para mejorar la eliminación de nitrógeno y fósforo con los mínimos requerimientos energéticos necesarios. January, 2008 - January, 2010. Scientific in charge: Juan Antonio Baeza Labat.

Grupo de tratamiento biológico de efluentes líquidos y gaseosos. Eliminación de Nutrientes, Olores y Compuestos Orgánicos Volátiles (GENOCOV). Grupo de investigación de calidad. Pla de Recerca de Catalunya. October 2009 - October 2013. Scientific in charge: Javier Lafuente Sancho.

Descifrando los mecanismos subyacentes al deterioro de EBPR por presencia de nitrato en la zona anaerobia de EDAR con eliminación biológica simultánea de nitrógeno y fósforo. October, 2010 - December, 2013. Scientific in charge: Juan Antonio Baeza Labat.

## **Publications in Journals**

---

Guerrero, J., Guisasola, A., Vilanova, R., Baeza, J.A., 2011. Improving the performance of a WWTP control system by model-based setpoint optimization, *Environmental Modelling Software*. 26 492-497.

Guerrero, J., Guisasola, A., Baeza, J.A., 2011. The nature of the carbon source rules the competition between PAO and denitrifiers in systems for simultaneous biological nitrogen and phosphorus removal. *Water Research* 45(16), 4793-4802.

Guerrero, J., Guisasola, A., Comas, J., Rodríguez-Roda, I., Baeza, J.A., 2012. Multi-criteria selection of optimum WWTP control setpoints based on microbiology-related failures, effluent quality and operating costs. *Chemical Engineering Journal* 188, 23-29.

Guerrero, J., Tayà, C., Guisasola, A., Baeza, J.A., 2012. Glycerol as a sole carbon source for enhanced phosphorus removal. *Water research* 46 (9), 2983-2991.

Guerrero, J., Tayà, C., Guisasola, A., Baeza, J.A., 2012. Understanding the detrimental effect of nitrate presence on EBPR systems: effect of the plant configuration. *Journal of Chemical Technology and Biotechnology* 87 (10), 1508-1511.



Tayà, C., Guerrero, J., Guisasola, A., Baeza, J.A., 2013. Methanol-driven enhanced biological phosphorus removal with a syntrophic consortium. *Biotechnology and bioengineering* 110 (2), 391-400.

Ostace, G.S., Baeza, J.A., Guerrero, J., Guisasola, A., Cristea, V.M., Agachi, P.S., Lafuente, J., 2013. Development and economic assessment of different WWTP control strategies for optimal simultaneous removal of carbon, nitrogen and phosphorus. *Computers and Chemical Engineering* 53, 164-177.

Guerrero, J., Flores-Alsina, X., Guisasola, A., Baeza, J.A., Gernaey, K.V., 2013. Effect of nitrite, limited reactive settler and plant design configuration on the predicted performance of a simultaneous C/N/P removal WWTP. *Bioresource Technology* 136, 680-688.

Guerrero, J., Tayà, C., Guisasola, A., Baeza, J.A., 2014. Eliminación biológica de fósforo: avances en el estudio de su deterioro por recirculación de nitrato. *TecnoAqua* 6, 58-65.

Guerrero, J., Guisasola, A., Baeza, J.A., 2014. A novel control strategy for an efficient biological phosphorus removal with carbon-limited wastewaters. *Water Science and Technology*, *In press*.

### **Publications in Preparation**

---

Guerrero, J., Guisasola, A., Baeza, J.A., 2014. Controlled crude glycerol dosage to prevent EBPR failures due to nitrate external recycle. *In preparation*.

Tayà, C., Guerrero, J., Guisasola, A., Suárez-Ojeda, M.E., Baeza, J.A., 2014. Assessment of crude glycerol for enhanced biological phosphorus removal: Stability and role of LCFA. *In preparation*.

### **Conferences**

---

Guerrero, J., Guisasola, A., Machado, V.C., Baeza, J.A. Improving WWTP control strategies for simultaneous C/N/P removal by setpoint optimisation. 10<sup>th</sup> IWA Conference on Instrumentation Control and Automation 2009. Cairns, Australia. Oral presentation.

Tayà, C., Guerrero, J., Guisasola, A., Baeza, J.A. Estudio de la interacción de nitrato en la eliminación biológica de fósforo. Mesa Española de Tratamiento de Aguas 2010. Bilbao, Spain. Poster presentation.

Guerrero, J., Guisasola, A., Baeza, J.A. Managing an A<sup>2</sup>/O pilot WWTP: a control strategy to reduce the impact of a severe influent ammonium increase. Spain Young Water Professional Conference - IWA 2010, Barcelona, Spain. Poster presentation.

Guerrero, J., Guisasola, A., Comas, J., Rodríguez-Roda, I., Baeza, J.A. Model-based selection of the optimum control strategy based on microbiology-related failures, effluent quality and operating costs. WaterMatex 2011, San Sebastian, Spain. Oral presentation.

Guerrero, J., Tayà, C., Guisasola, A., Baeza, J.A. Understanding the detrimental effect of nitrate presence under anaerobic conditions in an EBPR system. Small Sustainable Solutions (SS4 Water). Venice, Italy. Oral presentation.

Guerrero, J., Tayà, C., Guisasola, A., Baeza, J.A. Descifrando los mecanismos subyacentes al deterioro de EBPR por presencia de nitrato en la zona anaerobia de EDAR con eliminación biológica simultánea

de nitrógeno y fósforo. Mesa Española de Tratamiento de Agua 2012, Almeria, Spain. Oral presentation.

Baeza, J.A., Guerrero, J., Guisasola, A. When is it worth the inclusion of partial nitrification in a C/N/P removal system? IWA Nutrient Removal and Recovery 2012: Trends in NRR. 2012, Harbin, China. Oral presentation.

Tayà, C., Guerrero, J., Guisasola, A., Baeza, J.A. Opening up new possibilities in EBPR: a syntrophic consortium for the utilisation of a wider range of carbon sources. IWA Nutrient Removal and Recovery 2012: Trends in NRR. 2012, Harbin, China. Oral presentation.

Flores-Alsina, X., Guerrero, J., Vangsgaard, A.K., Guisasola, A., Baeza, J.A., Jeppsson, U., Smets, B.F., Sin, G., Gernaey, K.V. Recent trends in modelling and simulation of biological nutrient removal systems. IWA Nutrient Removal and Recovery 2012: Trends in NRR. 2012, Harbin, China. Poster presentation.

Guerrero, J., Guisasola, Flores-Alsina, X., Guisasola, A., Gernaey, K.V., Baeza, J.A. Analysis of design configurations/control strategies in biological nutrient removal processes using discriminant analysis. 11<sup>st</sup> IWA Conference on Instrumentation Control and Automation 2013. Cairns, Narbonne, France. Poster presentation.

Guerrero, J., Guisasola, A., Baeza, J.A. A novel control strategy for an efficient EBPR removal in WWTP with carbon-shortage: in-silico optimisation. 11<sup>st</sup> IWA Conference on Instrumentation Control and Automation 2013. Cairns, Narbonne, France. Oral presentation.

Guerrero, J., Guisasola, A., Baeza, J.A. A control-based approach to achieve efficient biological phosphorus removal in WWTPs: design, simulation, optimisation and experimental. 4th IWA/WEF Wastewater Treatment Modelling Seminar 2014 Spa, Belgium. Poster presentation.

Tayà, C., Guerrero, J., Suárez-Ojeda, M.E., Guisasola, A., Baeza, J.A. Assessment of crude glycerol for enhanced biological phosphorus removal: Stability and role of LCFA. 2nd IWA Specialist Conference on EcoTechnologies for Sewage Treatment Plants 2014"EcoSTP2014". Verona, Italy. Oral presentation.



## Notes

---



## Notes

---